

## **Lincoln University Digital Thesis**

### **Copyright Statement**

The digital copy of this thesis is protected by the Copyright Act 1994 (New Zealand).

This thesis may be consulted by you, provided you comply with the provisions of the Act and the following conditions of use:

- you will use the copy only for the purposes of research or private study
- you will recognise the author's right to be identified as the author of the thesis and due acknowledgement will be made to the author where appropriate
- you will obtain the author's permission before publishing any material from the thesis.

**Chemical and toxicological investigation of the toxic  
dinoflagellate, *Karenia brevisulcata***

---

A thesis  
submitted in partial fulfilment  
of the requirements for the Degree of  
Doctor of Philosophy

at  
Lincoln University

by  
Feng Shi

---

Lincoln University  
2012

Abstract of a thesis submitted in partial fulfilment of the  
requirements for the Degree of Ph.D.

**Chemical and toxicological investigation of the toxic  
dinoflagellate, *Karenia brevisulcata***

by  
Feng Shi

A severe harmful algal bloom (HAB) devastated marine life in the Wellington Harbour in the late summer 1998. A novel species of *Karenia* dinoflagellates was isolated from this HAB and named *Karenia brevisulcata* (Chang). Toxins produced by this alga were categorised into i) brevisulcatic acids (BSXs), a group of six polycyclic ethers with molecular weights 800-950; ii) brevisulcenals (acronym KBTs from a previous name), a complex of 6-8 lipophilic compounds with molecular weights 1900-2200.

This PhD thesis reports the isolation, purification and chemical investigation of BSXs, analytical and toxicological studies of BSXs and KBTs, and the toxicity evaluation of three *Karenia* species. LC-MS provides a powerful micro-analytical technology to detect novel toxins, determine structural characteristics, guide chemical isolation and provide quantitative data on levels of toxins in cultures. An LC-MS (SIR method) with six channels for BSXs and one channel for brevetoxin-2 (calibrant) was developed to guide BSX isolation. A more sensitive method based on solid phase extraction (SPE) and LC-MS (MRM) was validated for determination of 6 BSXs and 4 KBTs in cultures with LOQs for each toxin of ca 0.15  $\mu\text{g L}^{-1}$  in seawater.

Barrels, carboys and a photobioreactor were used to optimise cell growth and toxin production of a *K. brevisulcata* isolate collected by Cawthron Institute in 1998. Carboys were the most efficient in batch culture mode with the highest growth rate ( $\mu=0.086 \text{ day}^{-1}$  versus 0.050-0.057  $\text{day}^{-1}$  for barrels or photobioreactor) and the highest cell yield for total BSXs (0.77  $\text{pg cell}^{-1}$  versus 0.29-0.38  $\text{pg cell}^{-1}$  for barrel or photobioreactor). However, the large volume automated photobioreactor operated in continuous culture mode was more suited to large-scale toxin production from dinoflagellates.

*K. brevisulcata* cultures (total 936 litres unlabelled; 492 litres  $^{13}\text{C}$ -labelled using added  $\text{NaH}^{13}\text{CO}_3$ ) were grown at Cawthron Institute. The toxins were extracted from the bulk cultures by cell disruption and absorption using HP20 polymeric resin followed by acetone extraction. Solvent partitioning of crude acetone extracts was used to prepare neutral fractions containing KBTs and acidic fractions containing BSXs. Semi-purification of BSXs from the acidic fractions used desalting by reverse phase SPE and defatting by normal phase SPE. BSX-1 ( $\text{C}_{49}\text{H}_{72}\text{O}_{16}$ ,  $[\text{M}+\text{H}]^+$  917.5) and BSX-2 ( $\text{C}_{47}\text{H}_{68}\text{O}_{15}$ ,  $[\text{M}+\text{H}]^+$  873.5) were separated by normal phase column chromatography and were purified in mg quantities using preparative C18 high performance liquid chromatography (HPLC). BSX-4 ( $\text{C}_{49}\text{H}_{70}\text{O}_{15}$ ,  $[\text{M}+\text{H}]^+$  899.5) and BSX-5 ( $\text{C}_{47}\text{H}_{66}\text{O}_{14}$ ,  $[\text{M}+\text{H}]^+$  855.5) are the lactones which were produced from BSX-1 and BSX-2 respectively by acid-catalysed ring closure for analytical, structural and toxicological studies. The neutral fractions of crude extracts were sent to the University of Tokyo (Prof. Masayuki Satake) where four KBTs (-F, -G, -H & -I) were isolated.

The chemical structures of BSXs and KBTs were characterised by spectroscopic (UV, MS-MS) and micro-derivatisation techniques (methylation, acetylation, hydrolysis). BSXs are ladder-frame polycyclic ethers with close similarities to brevetoxins. A probable structure for BSX-4 has been determined based on partial NMR spectra obtained from Massey University. BSX-4 has structural similarities to brevetoxin-1 but with some differences in the polyether rings and a longer, carboxylated side chain. However, the full structures of BSXs have not been completely elucidated because of missing NMR peaks due to conformation changes in the time frame of the NMR pulse sequences. Missing signals, even at low temperatures, probably involve three flexible 7-, 8- and 9-membered ether rings in the central part of the molecule with one double bond and a tertiary methyl group. NMR studies are continuing at the University of Tokyo.

The complex structure of KBT-F ( $\text{C}_{107}\text{H}_{160}\text{O}_{38}$ ,  $[\text{M}+\text{H}]^+$  2054.1) has been elucidated at the University of Tokyo using NMR and TOF-TOF MS. KBT-F is a novel ladder frame polycyclic ether compound with a 2-methyl-2-butenal side chain that is the same as that in gymnocin-A. It has the most contiguous ethers rings amongst the known polycyclic ethers.

Acute toxicity, haemolytic activity and cytotoxicity of BSXs and KBTs were studied by mouse bioassay, Bignami assay, and *in vitro* mammalian cell bioassays respectively. BSXs are weakly toxic to mice with intraperitoneal (i.p.)  $\text{LD}_{50}$  of  $> 1500 \mu\text{g kg}^{-1}$  body weight (bw), and weakly haemolytic. Neuro2a cell assays revealed that BSXs are brevetoxin-like voltage gated Na channel (VGSC) agonists but with lower activity. KBT-F and KBT-G are strongly toxic to mice (i.p.  $\text{LD}_{50}$  of  $32\text{--}40 \mu\text{g kg}^{-1}$  bw), strongly haemolytic, and highly cytotoxic to

P388, Vero and Neuro2a cells, but are unlikely to be VGSC agonists. Further cytotoxicity assays using multiple end-points e.g. LDH/MTS and LDH/caspase-3/7 revealed that damage to P388 cells by KBT-F involved effects on membranes but apoptotic mechanisms were not involved.

*In vivo* bioassays using marine biota (two fish species and larvae of six marine invertebrate species) were used to investigate the toxicity and potential modes-of-action of three toxic *Karenia* species. The bioassays confirmed field observations on the very high ecotoxic risks posed by blooms of *K. brevisulcata*. A provisional trigger of  $1 \times 10^4$  cells L<sup>-1</sup> is recommended to provide an early warning of a *K. brevisulcata* bloom. The mechanism for fish and invertebrate kills by *K. brevisulcata* is likely to depend on release of toxins from algal cells into seawater with KBTs being the main toxic agents.

**Keywords:** Wellington Harbour toxin, Toxic dinoflagellate, *Karenia brevisulcata*, Brevisulcatic acid, Brevisulcenal, Brevetoxins, BSX, KBT, LC-MS

## Acknowledgements

Wow, I did it! I still cannot believe that I have finished all my experiments and the writing of my PhD thesis in three years. It was a difficult three years, but also inspiring, exciting and a challenging experience. This wonderful journey was made possible by many people who supported, guided and helped me. I wish to convey my deep gratitude to all of them.

First and foremost, I would like to acknowledge Lincoln University and Cawthron Institute who gave me an opportunity to carry out this research. I would like to thank the Ministry for Science and Innovation (MSI) and Lincoln University for supporting my studies at Cawthron Institute.

My sincere thanks go to my supervisor Associate Professor Dr Ravi Gooneratne, Lincoln University for introducing me to the field of toxicology. His constant source of guidance, encouragement and criticism helped me to stay persistent, focused and motivated. His persistence, faith and kindness were essential to my success.

I would like to take this opportunity to especially thank my co-supervisor Dr Patrick Holland, Cawthron Institute, for assistance during every step of my research project. His constant guidance, support, and criticism made this work possible.

I would like to thank my associate supervisor Dr Sue Mason, Lincoln University, for her encouragement and valuable advice.

I would like to thank my scientific collaborators: Professor Masayuki Satake (the University of Tokyo) for further isolation and chemical studies of KBTs as well as assistance with interpretation of NMR spectra for BSXs, Dr Rex Munday (AgResearch) for toxicological studies using mouse bioassay, Dr Penny Truman (ESR) for Neuro2a assays and invaluable guidance on establishment of *in vitro* cell bioassays, Dr Lynn Briggs (AgResearch) who carried out Bignami assays, and Dr Patrick Edwards (Massey University) for NMR studies of BSXs.

I would like to thank the Cawthron Institute, Nelson for welcoming me and allowing me to conduct all my research there. Particular thanks go to all the staff in the R & D team: Paul McNabb, Dr Patrick Holland, Dr Tim Harwood, Andy Selwood, Roel van Ginkel, David White, Donato Romanazzi and Anne Cargill. Their support and making me feel a valuable member of the team really was essential to me. Special appreciation goes to Paul McNabb

who, as team manager, made this study possible, Dr Tim Harwood who helped with my thesis writing, and Andy Selwood and Roel van Ginkel for technical guidance and assistance.

I would also like to thank the collaborators in the Biosecurity Division, Cawthron Institute. Special thanks go to Veronica Beuzenberg for her invaluable instructions and assistance on algal culturing and harvesting. I would also like to thank Lincoln Mackenzie for his help and advice on my research, Dr Lesley Rhodes for assistance with fish and invertebrate larvae bioassays, and invaluable advice on my experiments and thesis, Janet Adamson and Dr Krystyna Ponikla for their specific advice and assistance on algal culturing, and Dr Doug Mountfort for useful advice.

I would also like to thank staff in the Natural Toxin Lab, Cawthron Institute. Thanks to Catherine Moison, Bernadette Butler, Julie Westrupp, Phaedra Terezaki, Lisa Page, Lisa Wells and Manday Edgar for providing a jovial, supportive, and memorable laboratory environment to work in. Special thanks go to Holly D'Souza who assisted me establish the *in vitro* cell bioassays, and to Michael Boundy for technical advice on LC-MS.

To Wenfeng Song, Bella Zhang, Luke Li, Serena Wang, Alex Li, Lydia Liu, Lary Gan and Clint Lin, thank you for your friendship, care and also comforting me during my studies in New Zealand.

Finally, I would like to thank my family, especially my mom and dad who have been an invaluable source of inspiration, love, support and encouragement. They gave me their support whenever I needed. Their encouragement kept me going in this beautiful foreign land. I owe my all achievements to them.

# Publications

## Manuscripts:

Beuzenberg, V., Mountfort, D., Holland, P. T., **Shi, F.**, & MacKenzie, A. L. (2012). Optimization of growth and production of toxins by three dinoflagellates in photobioreactor cultures. *J. Appl. Phycol.*, *Accepted for publication*, doi: 10.1007/s10811-011-9726-8

(My contribution to this manuscript included the culturing of *Karenia brevisulcata* in the systems studies, associated LC-MS analyses of BSXs and data analysis)

Hamamoto, Y., Tachibana, K., Satake, M., Holland, P. T., **Shi, F.**, & Beuzenberg, V. (2012). Brevisulcenal-F, a polycyclic ether toxin associated with massive fish-kills in New Zealand. *Journal of American Chemical Society*, *134*(10), 4963-4968.

(My contribution to the manuscript included the bulk culturing of *Karenia brevisulcata*, preparation of crude extracts and preliminary separation of KBTs from BSXs)

Holland, P. T., **Shi, F.**, Satake, M., Hamamoto, Y., Ito, E., Beuzenberg, V., McNabb, P., Munday, R., Briggs, L., Truman, P., Gooneratne, R., Edwards, P., & Pascal, S. M. (2012). Novel toxins produced by the dinoflagellate *Karenia brevisulcata*. *Harmful Algae*, *13*(1), 47-57.

(My contribution to this manuscript included the culturing of *Karenia brevisulcata*, development of a method to isolate BSXs by chromatography, provision of isolated toxins for bioassay and toxicology studies, structural elucidation of BSXs using LC-MS and LC-UVD, preparation of chemical derivatives and hydrolysis studies)

**Shi, F.**, McNabb, P., Rhodes, L., Holland, P., Webb, S., Adamson, J., Immers, A., Gooneratne, R., & Holland, J. (2012). The toxic effects of three dinoflagellate species from the genus *Karenia* on invertebrate larvae and finfish. *New Zealand Journal of Marine and Freshwater Research*, *Publication online*, doi: 10.1080/00288330.2011.616210

(My contribution to this manuscript included culturing of three *Karenia* species, LC-MS analysis of the toxins produced, development of fish (snapper and salmon) and invertebrate larvae (brine shrimp, Greenshell<sup>TM</sup> mussel, Pacific oyster, paua, sea slug, and sea urchin) bioassays to determine the ecotoxic risks of microalgal cultures, preparing drafts and guiding through the publication process.)



### Conference proceedings:

Holland, P. T., **Shi, F.**, Satake, M., Hamamoto, Y., Beuzenberg, V., Rhodes, L., McNabb, P., Edwards, P., Munday, R., & Truman, P. (2010, 1-5 November). *Production of novel toxins by dinoflagellate Karenia brevisulcata*. Paper presented at the 14th International Conference on Harmful Algae, Crete, Greece.

**Shi, F.**, Holland, P. T., Satake, M., Beuzenberg, V., Mountfort, D., Rhodes, L. R., McNabb, P., Gooneratne, R., & Munday, R. (2010, October 8-12). *Production of novel toxins by the dinoflagellate Karenia brevisulcata*. Paper presented at the 9th International Marine Biotechnology Conference, Qingdao, China.

**Shi, F.**, McNabb, P., Rhodes, L., Webb, S., Holland, P. T., Holland, J., & Gooneratne, R. (2011, 25th January). *In vivo fish and invertebrate bioassays of Karenia cultures*. Paper presented at the International workshop of Kareniaceae and other fish-killing flagellates, Cawthron Institute, Nelson, New Zealand.

# Table of Contents

<b>Abstract .....</b>	<b>ii</b>
<b>Acknowledgements .....</b>	<b>v</b>
<b>Publications .....</b>	<b>vii</b>
<b>Table of Contents .....</b>	<b>ix</b>
<b>List of Tables .....</b>	<b>xiii</b>
<b>List of Figures .....</b>	<b>xv</b>
<b>List of Figures .....</b>	<b>xv</b>
<b>Abbreviations .....</b>	<b>xviii</b>
<b>Chapter 1 Introduction.....</b>	<b>1</b>
1.1 Harmful algal blooms and the effects on humans	1
1.2 <i>Karenia</i> dinoflagellates and Wellington Harbour bloom, 1998	2
1.3 Toxins produced by <i>K. brevisulcata</i>	3
1.4 Research Aims, objectives and hypothesis	5
1.4.1 Research Aims	5
1.4.2 Research Objectives	5
1.4.3 Hypotheses	6
<b>Chapter 2 Literature review .....</b>	<b>7</b>
2.1 Harmful algal blooms and algal toxins	7
2.1.1 Phytoplankton and their natural products	7
2.1.2 Harmful algal blooms	9
2.1.3 Marine algal toxins in bivalve molluscs.	12
2.2 Conventional methods to identify, investigate and quantify marine algal toxins	14
2.2.1 General overview	14
2.2.2 Mouse bioassay and other <i>in vivo</i> bioassays	16
2.2.3 <i>In vitro</i> cell assays for investigations of cytotoxicity and mode of action	18
2.2.3.1 Overview - <i>in vitro</i> cell assays	18
2.2.3.2 Mammalian cell lines	20
2.2.3.3 Cytotoxicity measurements and mode-of-action investigations	24
2.2.4 Physico-chemical methods	28
2.2.4.1 LC-MS	28
2.2.4.2 Nuclear magnetic resonance (NMR)	30
2.3 <i>Karenia</i> dinoflagellate and their biotoxins	31
2.3.1 <i>Karenia</i> species in New Zealand	31
2.3.2 <i>K. brevis</i> and NSP toxins	34
2.3.3 <i>K. mikimotoi</i> and its complex toxins	38
2.3.4 <i>K. selliformis</i> and gymnodimines	41
2.3.5 <i>K. brevisulcata</i> and its biotoxins	42
<b>Chapter 3 Laboratory culturing of <i>Karenia brevisulcata</i>.....</b>	<b>45</b>
3.1 Introduction	45
3.2 Materials and methods	46
3.2.1 Microalgae and batch cultures	46
3.2.2 Photobioreactor system cultures	47
3.2.3 Extraction of toxins from <i>K. brevisulcata</i> culture for LC-MS monitoring	49

3.2.4	LC-MS analysis of toxins	49
3.2.5	Harvesting of bulk cultures	50
3.3	Results and discussion	50
3.3.1	Batch culturing of <i>K. brevisulcata</i> in different culturing systems	50
3.3.2	Bioreactor culturing of <i>K. brevisulcata</i> under continuous mode	52
3.3.3	Performance of large bioreactor for <i>K. brevisulcata</i> culturing	56
3.3.4	Production of <sup>13</sup> C-labelled compounds for <sup>13</sup> C-NMR research	56
3.3.5	Culture harvesting	57
3.4	Summary	58
<b>Chapter 4 LC-MS analysis of toxins produced by <i>Karenia</i> species.....</b>		<b>60</b>
4.1	Introduction	60
4.2	Materials and methods	61
4.2.1	Microalgae investigated and standard materials	61
4.2.2	Extraction of toxins from <i>Karenia</i> culture for LC-MS monitoring	63
4.2.3	LC-MS analysis	63
4.2.3.1	uPLC-Premier MS	64
4.2.3.2	HPLC-Ultima MS	65
4.3	Results and Discussion	67
4.3.1	Novel toxins produced by <i>K. brevisulcata</i>	67
4.3.1.1	BSXs identification	67
4.3.1.2	Identification of new BSX toxins (BSX-3 and BSX-6)	68
4.3.1.3	Identification of KBTs in <i>K. brevisulcata</i>	69
4.3.2	LC-MS method development for <i>K. brevisulcata</i> studies	74
4.3.2.1	LC-MS (SIR) method for BSX toxins (Method 1)	74
4.3.2.2	Establishment of a MRM method (Method 4) for quantitation of BSXs and KBTs	76
4.3.3	Determination of brevetoxin profile in <i>K. brevis</i> extract	85
4.3.4	Detection of novel compounds produced by <i>K. mikimotoi</i>	87
4.4	Summary	90
<b>Chapter 5 Chemical investigations of BSXs and KBTs.....</b>		<b>91</b>
5.1	Introduction	91
5.2	Materials and methods	92
5.2.1	Crude extracts of <i>K. brevisulcata</i> cultures	92
5.2.2	Isolation and purification of toxins	93
5.2.2.1	Separation of BSX toxins from neutral KBTs	93
5.2.2.2	Isolation and purification of KBT-F & -G (collaboration with Prof. Satake at the University of Tokyo)	93
5.2.2.3	Isolation and purification of BSX-1 and BSX-2 (ring-opened)	93
5.2.2.4	Acidic catalysed lactone ring-closed of BSXs	94
5.2.3	LC-UV, LC-MS and HRMS	95
5.2.3.1	LC-UV plus Premier MS (SIR, scanning, MS/MS)	95
5.2.3.2	HRMS	95
5.2.4	Micro-chemistry of BSXs and KBT-F	95
5.2.4.1	Base hydrolysis assay	95
5.2.4.2	Methylation and acetylation of BSXs	96
5.2.4.3	Preparation of a KBT-F benzene sulfonate derivative	97
5.2.5	NMR spectroscopy (collaborations with Prof Satake and Dr Patrick Edwards)	97
5.3	Results and discussion	98
5.3.1	Separation of crude toxins (solvent partitioning)	98
5.3.2	Isolation and purification of BSX	100
5.3.2.1	Semi-purification BSXs	100

5.3.2.2	Final isolation and purification of BSX-1 and BSX-2	102
5.3.2.3	Production of ring-closed BSX-4 & -5 from ring-opened BSX-1 & -2	104
5.3.2.4	Isolation and purification of <sup>13</sup> C-labelled BSX-4 and BSX-5	105
5.3.3	Structural characterisation of BSXs	105
5.3.3.1	UV- and mass spectrometry of BSXs	105
5.3.3.2	Kinetics of hydrolysis of BSX-4 and BSX-5	108
5.3.3.3	Microchemistry of BSXs (methylation; acetylation)	109
5.3.3.4	Daughter ion spectra of BSXs and their analogues	111
5.3.3.5	Probable structures of BSX toxins (collaboration with Prof Satake and Dr Patrick Edwards)	116
5.3.4	Chemical investigations of KBTs	119
5.3.4.1	Isolation of KBT-F and KBT-G	119
5.3.4.2	Structural characterisation of KBT-F	120
5.4	Summary	123
<b>Chapter 6 Toxicological investigations of novel biotoxins isolated from the dinoflagellate <i>Karenia brevisulcata</i> .....</b>		<b>125</b>
6.1	Introduction	125
6.2	Materials and methods	126
6.2.1	Pure biotoxins	126
6.2.2	Mammalian Toxicology	126
6.2.3	P388 and Vero cell culturing	127
6.2.4	Cell viability assay (MTS reduction)	128
6.2.5	Cell membrane integrity assay (LDH)	129
6.2.6	Caspase-3 colorimetric assay	130
6.2.7	Caspase-3/7 fluorescent activity assay	132
6.2.8	Haemolysis assay	133
6.2.9	Neuro2a cytotoxicity assay	133
6.3	Results and discussion	134
6.3.1	Mouse bioassay	134
6.3.2	Culturing and harvesting of P388 and Vero cells	135
6.3.3	Determination of the initial cell population for cell viability assay	136
6.3.4	Cytotoxicity of novel algal toxins using P388 and Vero cell viability assays	138
6.3.5	Cell membrane integrity assay	141
6.3.6	Caspase-3 colorimetric assay	144
6.3.7	Fluorescent caspase-3/7 activity assay	145
6.3.8	Haemolytic and Neuro2a cell assays	148
6.4	Summary	150
<b>Chapter 7 Toxic effects of <i>Karenia</i> species on fish, invertebrate larvae and mammalian cells.....</b>		<b>151</b>
7.1	Introduction	151
7.2	Materials and methods	152
7.2.1	Microalgae cultures and growth conditions	152
7.2.2	Algal toxin extraction for LC-MS analysis and invertebrate bioassay	153
7.2.3	Preparation of algal extracts and cell-free culture supernatants for cell bioassays	153
7.2.4	Chemical analyses	154
7.2.5	Fish acute toxicity tests	154
7.2.6	Invertebrate larvae bioassays	155
7.2.7	P388 and Vero cell bioassays	156
7.2.8	Cytotoxicity assay for direct exposure to dinoflagellates	156

7.3	Results	156
7.3.1	Algal cultures and toxin production	156
7.3.2	Ichthyotoxicity of <i>Karenia</i> microalgae	158
7.3.3	Toxicity of <i>Karenia</i> to marine invertebrate larvae	161
7.3.4	Toxicity of BSXs and SPE extracts of <i>Karenia</i> cultures, against Greenshell <sup>TM</sup> mussel larvae	166
7.3.5	Cytotoxicity of <i>Karenia</i> extracts	167
7.3.6	Resistance of two mammalian cell lines two seawater media	169
7.3.7	Comparison of cytotoxic potentials of <i>Karenia</i> species by the direct exposure bioassay using Vero cells	171
7.4	Summary	174
<b>Chapter 8 Discussion, future directions and summary .....</b>		<b>175</b>
8.1	LC-MS analysis of biotoxins produced by <i>Karenia</i> dinoflagellates	176
8.2	Development of LC-MS methods for quantitative analysis of BSXs and KBTs	177
8.3	Laboratory culturing of <i>K. brevisulcata</i>	180
8.4	Chemical and toxicological studies of BSXs	181
8.5	Chemical and toxicological studies of KBTs	186
8.6	<i>In vitro</i> cell bioassays for algal toxin research	189
8.7	Effects of <i>Karenia</i> species on marine biota and implications for ecotoxicology	191
8.8	Future directions	196
8.9	Summary of findings	198
<b>References .....</b>		<b>201</b>

## List of Tables

Table 2-1	Secondary metabolites produced by marine dinoflagellates .....	9
Table 2-2	Toxins, causative organisms, clinical symptoms and treatments of shellfish poisoning syndromes .....	13
Table 2-3	Symptoms in mice after i.p. injection of marine algal toxins .....	17
Table 2-4	Cytotoxicities of marine algal toxins against three American Type Cell collection cell lines .....	22
Table 3-1	Comparison of <i>K. brevisulcata</i> growth and toxin production in three culture systems operated in batch mode .....	54
Table 3-2	Cell growth and toxin production of <i>K. brevisulcata</i> in a photobioreactor (5.4 L) operated in continuous mode .....	55
Table 3-3	Yields of each batch culture after harvesting .....	58
Table 4-1	<i>Karenia</i> species tested by LC-MS .....	62
Table 4-2	Analytes, retention times, mass ions monitored and quantitative standards for SIR quantitation of BSXs using LC-MS Method 1 .....	64
Table 4-3	Analytes, retention times, parent mass ions, MRM transitions, collision energies and quantitative standards for MRM quantitation of BSXs and KBTs using LC-MS Method 4 .....	66
Table 4-4	Novel compounds identified in SPE extracts of unlabelled <i>K. brevisulcata</i> cultures by LC-MS (Method 2) scanning at $m/z$ 1900-2200.....	71
Table 4-5	Novel compounds identified in SPE extracts of both unlabelled and $^{13}\text{C}$ -labelled <i>K. brevisulcata</i> cultures by LC-MS (Method 3) scanning at $m/z$ 1000-2300 .....	72
Table 4-6	Recovery of BSXs and KBTs from the culture media fortified with pure toxin or algal extract containing all toxins.....	82
Table 4-7	Precision of LC-MS MRM quantitation (Method 4, MRM) using samples from a <i>K. brevisulcata</i> batch carboy culture (1 x 50 mL SPE extract at three sampling dates, 5 x injections of each sample extract).....	84
Table 4-8	Toxins detected in a <i>K. brevis</i> (CAWD 122) extract using LC-MS (Method 3, scanning) .....	86
Table 4-9	Novel compounds detected in <i>K. mikimotoi</i> extracts by LC-MS (Method 3, scanning) .....	89
Table 5-1	The isolation and purification of BSX toxins.....	103
Table 5-2	Products observed from methylation of BSXs with diazomethane.....	110
Table 5-3	Significant MS/MS fragment ions ( $\text{ESI}^+$ ) for four BSX toxins and their methyl esters .....	114
Table 6-1	Buffer compositions for caspase-3 colorimetric assay (based on the instruction of Sigma CASP-3-C kit) .....	131
Table 6-2	Pipetting scheme for caspase-3 colorimetric assay (96 well-plate, triplicate wells).....	131
Table 6-3	Toxicity of toxins from <i>K. brevisulcata</i> to mice by i.p. administration .....	135
Table 6-4	Determination of initial cell populations for P388 and Vero cell bioassays for different experimental periods.....	138
Table 6-5	Cytotoxicities of novel toxins against P388 and Vero cells.....	141
Table 6-6	Cytotoxicities of BSX and KBT toxins based on Bignami and Neuro2a cell assays .....	149
Table 7-1	Ichthyotoxicity of <i>Karenia</i> species against juvenile Chinook salmon ( <i>Oncorhynchus tshawytscha</i> ) and juvenile New Zealand snapper ( <i>Pagrus auratus</i> ) (For all experiments, n=4 fish).....	160

Table 7-2	Toxic effects of fresh cultures and SPE extracts of <i>Karenia</i> species and of BSX toxins, on invertebrate larvae (6 day old) over 24 hr observation period..	162
Table 7-3	Toxicity of cultures of <i>Karenia</i> species to invertebrate larvae .....	165
Table 7-4	Cytotoxicities of <i>Karenia</i> extracts evaluated using P388 and Vero cell bioassays after 72 hr exposure.....	169

## List of Figures

Figure 1-1	Scanning electron photomicrograph of <i>K. brevisulcata</i> .....	3
Figure 2-1	Polygenic relationships of microalgae .....	8
Figure 2-2	The global increase of reported HABs and incidents of algal toxin events (1970s compared to 1999).....	11
Figure 2-3	Flow chart indicating the general principles of toxin isolation through integration of multiple separating and assay techniques .....	16
Figure 2-4	Flow diagram of potential bioassay methods for marine algal toxins research ...	19
Figure 2-5	Structures of MTS and Formazan.....	25
Figure 2-6	The principle of the fluorescence bioassay for LDH.....	26
Figure 2-7	Internal structure of triple quadrupole mass spectrometer (TSQ) for MS/MS ..	30
Figure 2-8	Photomicrographs of six <i>Karenia</i> species hold at Cawthron Institute, Nelson, New Zealand .....	32
Figure 2-9	Structures and molecular masses of brevetoxins.....	35
Figure 2-10	The metabolism of brevetoxins in shellfish .....	36
Figure 2-11	Neurotoxin receptor sites on voltage-gated sodium channel (VGSC).....	38
Figure 2-12	Structures of gymnocin-A, -B and -C.....	40
Figure 2-13	Structures of gymnodimines .....	42
Figure 2-14	The effect of saxitoxin (STX) in antagonising Wellington Harbour toxin (WHT) in the Neuro2a assay.....	44
Figure 3-1	Schematic diagram showing automated photobioreactor system with electronic process control for pH and optical density.....	48
Figure 3-2	<i>K. brevisulcata</i> growth vs. time and BSX production vs. time in three culture systems operated in batch mode .....	53
Figure 3-3	Mass spectra (ESI <sup>+</sup> ) of <sup>13</sup> C-labelled BSX-1 (top) and unlabelled BSX-1 (bottom).....	57
Figure 4-1	TIC from 7-11 min for LC-MS of an SPE extract of <i>K. brevisulcata</i> culture .....	67
Figure 4-2	Mass spectra (ESI <sup>+</sup> ) of (A) <sup>13</sup> C-labelled BSX-3, (B) unlabelled BSX-3, (C) <sup>13</sup> C-labelled BSX-6, and (D) unlabelled BSX-6 .....	68
Figure 4-3	A) LC-UVD (230 nm) and B) LC-MS (Method 2, scanning <i>m/z</i> 1800-2200) chromatograms for the crude HP20 extract of a bulk culture of <i>K. brevisulcata</i> . 70	
Figure 4-4	Mass spectra (ESI <sup>+</sup> ) of (A) KBT-F, [M+H] <sup>+</sup> <i>m/z</i> 2055; (B) KBT-G, [M+H] <sup>+</sup> <i>m/z</i> 2085 .....	73
Figure 4-5	Mass spectra (ESI <sup>+</sup> ) of (A) unlabelled and (B) <sup>13</sup> C-labelled KBT-H .....	73
Figure 4-6	Mass spectra (ESI <sup>+</sup> ) of (A) M2135, (B) M2165 and (C) M2181 .....	74
Figure 4-7	Linearity of LC-MS (SIR) response for determination of BSX-1 and BSX-2 ....	76
Figure 4-8	LC-MS/MS MRM chromatographs for an SPE extract of a batch carboy <i>K. brevisulcata</i> culture .....	78
Figure 4-9	Flow diagram of toxin recovery experiment .....	80
Figure 4-10	TIC from 8 to 12 min (Method 3, scanning) of an SPE extract of a <i>K. brevis</i> culture at <i>m/z</i> 500-1000.....	86
Figure 4-11	TIC from 7.2 to 10.5 min (Method 3, ESI <sup>+</sup> , scanning) of extracts of <i>K.</i> <i>mikimotoi</i> cultures at <i>m/z</i> 900-2150.....	88
Figure 4-12	Mass spectra (ESI <sup>+</sup> ) of (A) gymnocin-A, (B) gymnocin-B?, (C) gymnocin-C?, and (D) M927 .....	89
Figure 5-1	Chromatographic isolation procedures for KBT and BSX toxins from cultures of <i>K. brevisulcata</i> . .....	94
Figure 5-2	Apparatus for preparation of diazomethane .....	97
Figure 5-3	Determination of optimal conditions for solvent partitioning.....	99



Figure 5-4	The elution profile of BSX toxins from a reserve phase SPE (1g/20 mL Strata-X, 50 mL fractions) preconditioned with methanol and MQ water .....	101
Figure 5-5	Elution profile of BSX-1 and BSX-2 from a silica gel column (20 cm x 10 mm i.d., 10 mL fractions) with methanol in dichloromethane.....	103
Figure 5-6	LC chromatograms of purified BSXs using MS and UV detection .....	103
Figure 5-7	Inter-conversions of ring-opened and lactone BSX toxins .....	104
Figure 5-8	The efficiency of ring-closed BSX compounds (BSX-4 & -5) formation in different solvents with added trifluoroacetic acid .....	105
Figure 5-9	UV spectra of BSX-1 (left) and BSX-2 (right) .....	106
Figure 5-10	Mass spectra (ESI <sup>+</sup> ) of (A) BSX-1, (B) BSX-2, (C) BSX-4, and (D) BSX-5 ...	107
Figure 5-11	Mass spectra (ESI <sup>-</sup> ) of (A) BSX-1, (B) BSX-2, (C) BSX-4, and (D) BSX-5 ....	107
Figure 5-12	Base hydrolysis of BSX-4 to BSX-1 in 80% methanol at different concentrations of NaOH (30 min at room temperature).....	108
Figure 5-13	First order reaction plots of hydrolysis of BSX-4 and BSX-5 (9 µg each in 1 mM NaOH in 80% methanol at 50 °C).....	109
Figure 5-14	LC-MS chromatograms of methylation products of BSX-1 and BSX-2 by diazomethane (scanning TIC plus selected masses).....	111
Figure 5-15	Daughter ion spectra (ESI <sup>+</sup> ) for [M+H] <sup>+</sup> of (A) BSX-1 917, (B) BSX-2 873, (C) BSX-4 899, and (D) BSX-5 855 at collision energy 30 eV .....	113
Figure 5-16	Daughter ion spectra (ESI <sup>+</sup> ) for [M+H] <sup>+</sup> of (A) BSX-3 857 and (B) BSX-6 839 at collision energy 30 eV. ....	113
Figure 5-17	Daughter ion spectra (ESI <sup>+</sup> ) for [M+H] <sup>+</sup> of methylated BSX compounds: (A) BSX-1 Me <sub>2</sub> , (B) BSX-4 Me, and (C) BSX-5 Me at collision energy 27 eV .....	114
Figure 5-18	Daughter ion spectra (ESI <sup>-</sup> ) for [M-H] <sup>-</sup> of BSX-1 at collision energy 25 eV (A) and 45 eV (B) .....	115
Figure 5-19	Daughter ion mass spectra (ESI <sup>-</sup> ) for [M-H] <sup>-</sup> of (A) BSX-4 897 and (B) BSX-5 853 at collision energy 45 eV .....	115
Figure 5-20	The probable structures of BSX-1 and BSX-4 elucidated by NMR (at Massey University and University of Tokyo).....	117
Figure 5-21	<sup>1</sup> H- <sup>13</sup> C HSQC spectrum (part) of BSX-1 .....	118
Figure 5-22	<sup>1</sup> H- <sup>13</sup> C HSQC spectrum (part) of <sup>13</sup> C-labelled BSX-4.....	119
Figure 5-23	MALDI Spiral TOF-TOF MS/MS spectrum of KBT-F BSD .....	121
Figure 5-24	Structure and TSQ (ESI <sup>+</sup> ) daughter ion spectrum of KBT-F (C <sub>107</sub> H <sub>160</sub> O <sub>38</sub> ) at collision energy 50 eV .....	122
Figure 6-1	Effect of initial P388 (A) and Vero (B) cell population on cell viability measured using the MTS assay (absorbance at 492 nm) .....	137
Figure 6-2	Dose-response curves of KBT-F (A, D), KBT-G (B, E) and C402 (C, F) against P388 (A-C) and Vero cells (D-F) bioassays after 24 hr and 72 hr exposure .....	140
Figure 6-3	Dose-response curves of okadaic acid against Vero cell bioassays after 24 hr and 72 hr exposure.....	141
Figure 6-4	Time-response curves of (A) KBT-F 5 nM, (B) C402 5 nM and (C) staurosporine 1 µM for the cell membrane integrity (♦, LDH release) and cell viability (□, MTS) assays.....	143
Figure 6-5	Effects of KBT-F 5 nM, C402 5 nM and staurosporine (St) 1 µM on caspase-3 activity in treated P388 cells after 12 and 24 hr exposure.....	145
Figure 6-6	Time-response curves of KBT-F 5 nM, C402 5 nM and staurosporine 1 µM for the fluorescent caspase-3/7 activity and cell membrane integrity (LDH) assays.....	147
Figure 6-7	Dose response curves of toxins from <i>K. brevisulcata</i> in the Neuro2a cell assay potentiated for VGSC activity with ouabain/veratridine. ....	149
Figure 7-1	Biotoxins produced by (A) <i>K. brevis</i> and (B) <i>K. brevisulcata</i> .....	158

Figure 7-2	Responses of juvenile salmon ( <i>Oncorhynchus tshawytscha</i> ) to two <i>Karenia</i> species versus time .....	161
Figure 7-3	Responses of marine invertebrate larvae to <i>Karenia</i> cultures over 24 hr .....	164
Figure 7-4	Photomicrographs of Greenshell™ mussel ( <i>Perna canaliculus</i> ) larvae affected by <i>K. brevisulcata</i> during exposure over 24 hr to $8.4 \times 10^6$ cells L <sup>-1</sup> .....	166
Figure 7-5	Responses of Greenshell™ mussel ( <i>Perna canaliculus</i> ) larvae against a 56 d <i>K. brevisulcata</i> mass culture without living cells (■) and SPE extracts of 20-30 d <i>Karenia</i> mass cultures .....	167
Figure 7-6	Viability of P388 (A) and Vero (B) cells in control (MEM or DMEM) and seawater media (100% GP+Se or 50% GP) after the indicated periods of times .....	170
Figure 7-7	Viability of Vero cells after direct exposure to algal cultures of three <i>Karenia</i> species .....	172
Figure 7-8	Viability of Vero cells after direct exposure to algal cultures (♦) and cell-free supernatants (■) of (A) <i>K. brevisulcata</i> (CAWD 82) and (B) <i>K. mikimotoi</i> (CAWD 05) .....	173
Figure 8-1	Hypothesised inter-relationships of six BSXs .....	186
Figure 8-2	Possible metabolism of the side-chain of KBTs in <i>Karenia brevisulcata</i> cells .	189

## Abbreviations

APCI	atmospheric pressure chemical ionisation
APPI	atmospheric pressure photo-ionisation
ARfD	acute reference doses
ASP	amnesic shellfish poisoning
ATCC	American Type Culture Collection
AZA	azaspiracid
AZP	azaspiracid poisoning
bw	body weight
BSD	benezene sulfonate derivative
BSX	brevisulcatic acid (former acronym KbTx)
BTX	brevetoxin
CE	capillary electrophoresis
CER	contiguous ether ring
CFP	ciguatera fish poisoning
CICCM	Cawthron Institute Culture Collection of Microalgae
CRM	certified reference material
CTX	ciguatoxin
Da	dalton
DA	domoic acid
DSP	diarrhoeic shellfish poisoning
DTX	dinophysistoxin
dw	dry weight
EC <sub>50</sub>	the half maximal effective concentration
EC <sub>99</sub>	the maximal effective concentration
ECACC	European Collection of Cell Cultures
ED <sub>50</sub>	the half maximal effective dose
EDR	effective detection range
EFSA	European Food Safety Authority
ELISA	enzyme-linked immunosorbent assay
ESI	electrospray ionisation
ESR	Environmental Science Research
FA	formic acid
FAB	fast atom bombardment

FDA	Food and Drug Administration (USA)
FL	fluorescence
GC	gas chromatography
G <sub>max</sub>	the maximum growth
GYM	gymnodimine
HAB	harmful algal bloom
HBSS	3-(hydrazinecarbonyl)-benzene sulfonate sodium salt
HPLC	high performance liquid chromatography
IC <sub>50</sub>	the half maximal inhibitory concentration
i.p.	intraperitoneal
IT	ion trap
KBT	brevissulcatal (former name Karenia brevisulcata toxin)
LC	liquid chromatography
LC <sub>50</sub>	lethal concentration for 50% of fish
LD <sub>50</sub>	lethal dose 50%
LFIC	lateral flow immunochromatography
LOD	limit of detection
LOQ	limit of quantitation
LOAEL	the lowest observed adverse effect level
LSU rRNA	large subunit ribosomal RNA
LT50	the time for 50% of fish to become moribund
MAc <sup>-</sup>	acetate adduct molecular ion
MALDI	matrix-assisted laser desorption ionisation
MATs	marine algal toxins
MBA	mouse bioassay
[M+H] <sup>+</sup>	protonated molecular ion
[M+2H] <sup>2+</sup>	doubly charged molecular ion
[M-H] <sup>-</sup>	proton abstracted molecular ion
[M+H-H <sub>2</sub> O] <sup>+</sup>	water loss protonated molecular ion
[M+H-SO <sub>3</sub> ] <sup>+</sup>	sulphate abstracted protonated molecular ion
MLC <sub>50</sub>	median concentration for 50% of larvae being moribund
MLT <sub>50</sub>	median time for 50% of larvae being moribund
[M+Na] <sup>+</sup>	sodium adduct molecular ion
[M+NH <sub>4</sub> ] <sup>+</sup>	ammonium adduct molecular ion
MQ	Milli-Q water

MRM	multiple reaction monitoring
MS	mass spectrometry
MTS	3-(4,5-dimethylthiazol-2-yl)-5-(3-carboxymethoxyphenyl)-2-(4-sulfophenyl)-2H-tetrazolium
MTT	3-(4,5-Dimethyl-2-thiazolyl)-2,5-diphenyl-2H-tetrazolium bromide
MTX	maitotoxin
m.w.	molecular weight
<i>m/z</i>	mass-to-charge ratio
NMR	Nuclear magnetic resonance
<sup>1</sup> H NMR	Proton ( <sup>1</sup> H) NMR
<sup>13</sup> C NMR	Carbon-13 ( <sup>13</sup> C) NMR
NSP	neurotoxic shellfish poisoning
OA	okadaic acid
PP2A	phosphatases 2A
PSP	paralytic shellfish poisoning
rcf	relative centrifuge force
RSM	research standard material
SIR	Selected Ion Recording
SOA	State Oceanic Administration, China
ROS	reactive oxygen species
R <sub>t</sub>	retention time
SPE	solid phase extraction
STX	saxitoxin
TFA	trifluoroacetic acid
TIC	total ion chromatogram
TLC	thin-layer chromatography
TOF	time of flight
TSQ	triple stage quadrupole
uPLC	ultra-performance liquid chromatography
UV	ultraviolet
VGSC	voltage gated sodium channel
WHT	Wellington Harbour toxin

# Chapter 1

## Introduction

### 1.1 Harmful algal blooms and the effects on humans

Microalgal blooms are natural marine events usually accompanied by discolouration of seawater (red tide – from the high mass of pigmented cells), excessive accumulation of sea foam and unpleasant odours (Roberts *et al.*, 2004). In a typical bloom, algae multiply rapidly to reach  $10^5$  - $10^6$  cells per liter seawater (Smith *et al.*, 1993). Most algal blooms are harmless. However, about 60-80 species of algae can cause HABs (van Dolah, 2000). Effects of HABs include damage to marine ecosystems, economic losses to fisheries and aquaculture, and human illness caused by food-borne marine algal toxins (MATs) (Hallegraeff, 1995). HABs are increasing in frequency, intensity and geographic distribution and these changes are strongly linked to human activities (Daranas *et al.*, 2001).

There are six main human poisoning syndromes caused by contamination of seafood with MATs including amnesic shellfish poisoning (ASP), neurotoxic shellfish poisoning (NSP), paralytic shellfish poisoning (PSP), diarrhoeic shellfish poisoning (DSP), azaspiracid poisoning (AZP), and ciguatera fish poisoning (CFP) (Garthwaite, 2000). These syndromes, mostly gastrointestinal and/or nervous disorders mainly occur following consumption of shellfish or fish that have become contaminated by feeding on toxic algae. Respiratory illness has also been reported through direct exposure to seawater aerosols of toxic microalgae such as *Karenia brevis* and *Ostreopsis ovata* (Backer et al., 2003; Ciminiello et al., 2008; Fleming et al., 2007). Mouse bioassays (MBA) and *in vitro* cell assays have been the main tools for toxin detection, seafood safety monitoring, and mechanism investigation of these MATs. There is now an increasing emphasis on instrumental analysis of individual toxins. Associated with this, there have been changes in the regulation of toxin groups in recognition that the syndromes have overlapping symptoms. Many known MATs act on ion channels in mammalian cells by allowing ions (sodium or calcium) to enter cells in an uncontrolled manner. For instance, brevetoxins, ciguatoxins (CTX) and saxitoxin (STX) are voltage gated Na channel (VGSC)-dependent toxins (Na channel blockers or openers), which disrupt Na ion transport and thus affect cellular homeostasis (Canete & Diogene, 2008; Wang, 2008).

## 1.2 *Karenia* dinoflagellates and Wellington Harbour bloom, 1998

The dinoflagellate genus *Karenia* (Kareniaceae) contains a number of toxic species. *K. brevis* is responsible for NSP and produces brevetoxins. This species was predominant in the annual blooms that have occurred during summer in the past 30 years along the Florida coast (Benson *et al.*, 2005; van Dolah, 2000). *K. cf. brevis* (cf. = ‘looks like’) was identified in a severe outbreak of HAB during 1992-1993 on the northeastern coast of the North Island, New Zealand (Chang, 1995). The species isolated appeared similar to *K. brevis* in morphology and produced ‘brevetoxin-like’ lipid soluble toxins (MacKenzie *et al.*, 1995). Shellfish contamination and a large number of human intoxication cases (>100) were reported following the bloom (Chang, 1995; MacKenzie *et al.*, 1995). Another two toxic species from the *Karenia* genus, *K. mikimotoi* and *K. selliformis*, have also been detected in New Zealand’s coastal waters. They were responsible for mass mortalities of farmed fish, and wild and commercial shellfish during HABs in 1994, 2002 and 2007 (Chang *et al.*, 2002; MacKenzie *et al.*, 1996; Smith *et al.*, 2007). However, the mechanisms of toxicity of these two species are different. *K. mikimotoi* kills fish by gill damage or anoxia due to high cell populations (Hallegraeff, 1995; Haywood *et al.*, 2004; Landsberg, 2002), while *K. selliformis* causes shellfish mortality through neurotoxin production (gymnodimines) (da Silva *et al.*, 2008; MacKenzie *et al.*, 1996; Munday *et al.*, 2004; Seki *et al.*, 1995, 1996).

The central and southern east coast of the North Island of New Zealand experienced a severe HAB during the summer months of January to March, 1998 which devastated almost all marine life in the Wellington Harbour (Chang, 1999a, b; Chang *et al.*, 2001). A new dinoflagellate species of genus *Karenia* was isolated and named *Karenia brevisulcata* (Chang) (Figure 1-1). This species is similar to *K. brevis* and *K. mikimotoi* in morphology, but the cell size is smaller (13-25 µm long) and the groove on the ventral surface of the epicone is shorter (etymology: Latin *brevis* = short, *sulcatum* = groove) (Chang, 1999a). *K. brevisulcata* is extremely toxic to a wide range of marine organisms including fish, sea slugs, shellfish, micro- and macroalgae (Chang, 1999b).



**Figure 1-1.** Scanning electron photomicrograph of *K. brevisulcata* (courtesy Dr Allison Haywood).

Over 100 cases of human respiratory illness were reported during the bloom from late January to early March, 1998, with symptoms including dry cough, severe sore throat (like swallowing razor blades), runny nose, skin and eye irritations, severe headaches, and a facial sun-burn sensation (Chang, 1999a, b). The respiratory distress resembled that caused by aerosolised brevetoxins and was believed to be caused by direct exposure to contaminated seawater and/or sea-spray aerosols that contained live toxic algal cells or biotoxins (Chang *et al.*, 2001; Cheng *et al.*, 2005).

### **1.3 Toxins produced by *K. brevisulcata***

The toxic effects of *K. brevisulcata* appear to be mediated by a range of toxins. This toxin complex was designated Wellington Harbour toxin (WHT) (Keyzers, pers, comm.; Truman, 2007; Truman *et al.*, 2005). WHT contains an acidic group such as carboxylic or sulfamic acid, phenol etc, but no basic groups in the molecule (Keyzers, pers, comm.). WHT is less stable in the presence of bases but is not affected by neutral and acidic conditions. The thermal and oxidative stabilities of WHT were tested by Chang (1999b). Heating *K. brevisulcata* cultures at 100 °C for 30 min did not completely eliminate toxicity. Ozonation treatments were found to be the most effective and efficient way to eliminate WHT toxicity. During the 1998 outbreak in the Wellington Harbour, ozone was used to protect the hatchery facilities of the National Institute of Water and Atmospheric (NIWA) from HAB (Chang, 1999b).



Wellington Harbour toxin produced a unique, distinctive and reproducible dose-response curve in the Neuro2a cytotoxicity assay (with/without ouabain and veratridine), which suggested that it differed from other known VGSC-dependent brevetoxins, CTX and STX (Keyzers, pers, comm.; Truman *et al.*, 2005). Truman (2007) revealed at least partial toxicity of WHT on the effects on Na channel (like brevetoxins, VGSC agonist). Mouse bioassays (MBA) conducted at two independent laboratories suggested that WHT contained nephrotoxins and gymnodimine-like fast acting toxins (Chang, 1999b; Keyzers, pers, comm.). However, the isolation of WHT was incomplete, although the Neuro2a cytotoxicity assay did assist in the isolation of some chemical fractions containing WHT activity (Keyzers, pers, comm.).

Researchers at Tohoku University led by Professor Yasukatsu Oshima identified 6-8 cytotoxic compounds with molecular weight (m.w.) ranging from 1900 to 2200 from the lipophilic extract of *K. brevisulcata* cultures produced at Cawthron Institute (Oshima, 2007). These lipophilic toxins were named brevisulcenals (Hamamoto *et al.*, 2012), which were initially called *Karenia brevisulcata* toxins in the references (Beuzenberg *et al.*, 2012; Holland *et al.*, 2012; Shi *et al.*, 2012), but the acronym KBT was still retained. These KBTs were presumed to comprise the major component of the WHT complex. The complete structures of the complex compounds remain to be determined and are the subject of a continuing collaboration between Cawthron Institute and Professor Masayuki Satake (University of Tokyo, Japan).

In addition to these large lipid soluble toxins, preliminary research at Cawthron has shown that *K. brevisulcata* cultures also produced at least two water-soluble polycyclic ether compounds, brevisulcatic acid 1 (BSX-1 [former acronym KbTx-1], m.w. 916) and brevisulcatic acid 2 (BSX-2, m.w. 872). Their size makes them suitable for determination by liquid chromatography - mass spectrometry (LC-MS) techniques and they could be developed as marker compounds for *K. brevisulcata* blooms and contamination. For example, the BSXs could be readily monitored by LC-MS in seawater or shellfish samples. However, studies on *K. brevisulcata* and its toxins are still at an early stage due to the lack of purified toxins. Co-existence of complex toxins and lack of effective detection method increased the difficulties of isolating and purifying individual toxins. LC-MS was confirmed as one of the most effective methods to detect algae-produced polyether compounds. Reliable LC-MS methods are required to detect KBTs and BSXs during toxin isolation and purification. Purified BSXs and KBTs in milligram quantities will facilitate their full structural elucidation by NMR (proton, <sup>13</sup>carbon and 2D- experiments). The toxicological investigation of fresh

*K. brevisulcata* cultures and individual and pure KBTs and BSXs will contribute to toxicity evaluations, establishment of structure-toxicity relationships, investigation of mode-of-action of individual toxin, and assessment of harmful effects on marine organisms. Such a study would be also useful to protect cage fisheries, mussel aquaculture and human health from *K. brevisulcata* blooms in the future.

## **1.4 Research Aims, objectives and hypothesis**

### **1.4.1 Research Aims**

1. To develop a detailed understanding of the toxins produced by *K. brevisulcata* including their structures, toxicology and modes-of-action.
2. To improve understanding of the threats to the marine ecosystem and aquaculture through bioassays with *K. brevisulcata* cultures against selected marine species.

### **1.4.2 Research Objectives**

1. Optimise *K. brevisulcata* growth conditions (bulk or continuous cultures) to maximise toxin production.
2. Develop methods based on LC-MS to measure BSXs and KBTs in *K. brevisulcata* cultures.
3. Develop efficient procedures for extraction and preliminary purification of *K. brevisulcata* cultures to provide two semi-purified fractions containing i) the main high molecular weight toxins (KBTs); and ii) two medium m.w. polyethers (BSXs). The KBT fraction will be sent to Prof. Masayuki Satake (University of Tokyo, Japan) for isolation, purification and chemical characterisation of individual KBTs.
4. Separate and purify BSXs using chromatographic techniques.
5. Study the chemical structures of BSXs using spectroscopic techniques (UV, MS, HRMS and NMR), and investigate chemical inter-conversions and derivatisations.
6. Perform a preliminary toxicological evaluation on these toxins by mouse bioassay (with Dr Rex Munday, AgResearch), fish acute toxicology tests, and invertebrate larvae survival bioassays.

7. Establish *in vitro* cytotoxicity bioassays based on two cell lines (ECACC P388 and Vero cells) at Cawthron Institute.
8. Investigate cytotoxicity of KBTs and BSXs using Bignami assay (with Dr Lyn Briggs, AgResearch), Neuro2a cell bioassay (with Dr Penny Truman, Environmental Science Research [ESR]), P388 and Vero cell bioassays.

### **1.4.3 Hypotheses**

1. *K. brevisulcata* produces BSXs and KBTs that can be isolated and purified from culture extracts by chromatographic techniques.
2. The chemical structures of BSXs and KBTs can be elucidated by spectroscopic techniques (UV, MS, HRMS and NMR).
3. The toxicity of *K. brevisulcata* cells, BSXs and KBTs can be investigated using both *in vivo* and *in vitro* bioassays.

## Chapter 2

### Literature review

This literature review is organised in three main sections; (1) review of harmful algae, HABs and major algal toxins (2) an introduction to conventional methods for detection, investigation and monitoring of algal toxins, and (3) an overview of toxic *Karenia* dinoflagellates and their biotoxins.

## 2.1 Harmful algal blooms and algal toxins

### 2.1.1 Phytoplankton and their natural products

Phytoplankton are the main producers of biomass and organic compounds in aquatic ecosystems and play a key role at the base of the food chains in oceans and freshwaters (Daranas *et al.*, 2001). More than 10,000 species of these microscopic organisms are known, and can be classified into five major divisions (Shimizu, 1993):

- *Chlorophyta* (green algae)
- *Chrysophyta* (golden-brown, yellow algae and diatoms)
- *Pyrrhophyta* (dinoflagellates)
- *Euglenophyta*
- *Cyanophyta* (blue-green algae).

The phylogenic relationships between these divisions are shown in Figure 2-1. However, there are anomalies in the naming of some microalgal species and their positions on the taxonomic map. Therefore taxonomists are continually revising the classification largely based on new genetic sequence data (Daranas *et al.*, 2001). Blue-green algae, also called cyanobacteria, are photosynthetic bacteria classified based on their structure as prokaryotes rather than true algae (eukaryotes) (Shimizu, 1993). Cyanobacteria are found in both marine and freshwater environments.

The secondary metabolites produced by phytoplankton often have unique chemical structures with unusual biological activities. Their roles in aquatic ecosystems are poorly understood but probably include chemical defence, allelopathy and intercell communication (MacKenzie, 2008). These natural products have attracted attention in the past two decades for two main reasons; 1) as the toxins involved in HABs, and 2) as potential new drug

candidates (Shimizu, 2003). However, most marine metabolites have very complex structures, so only a few compounds have been developed as pharmaceuticals.

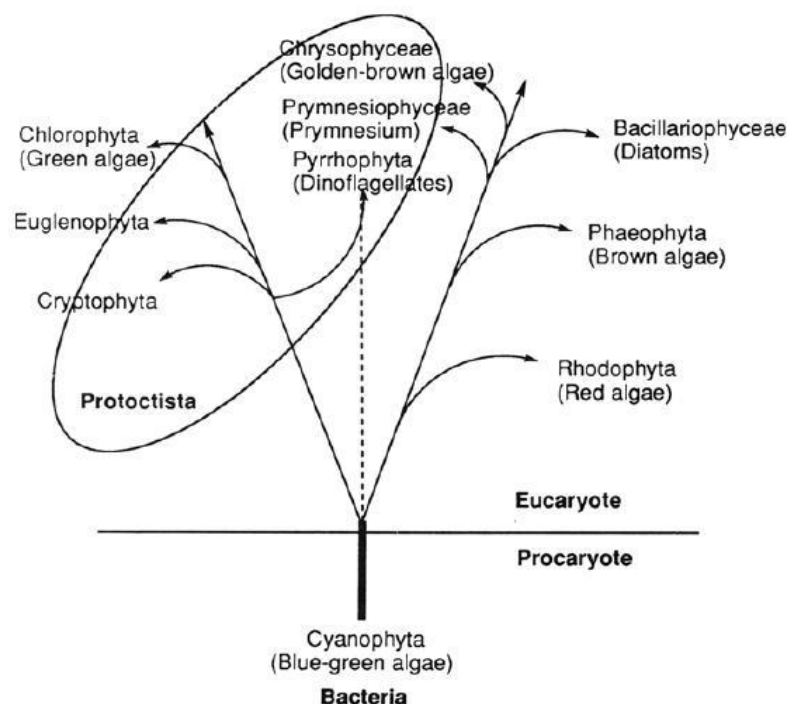


**Figure 2-1.** Polygenic relationships of microalgae (Shimizu, 1993).

The main producers of these novel compounds are dinoflagellates and cyanobacteria, although a few important compounds are produced by diatoms, green algae, brown algae and red algae (Faulkner, 1996; Shimizu, 2003). Bioactive metabolites produced by cyanobacteria include lyngabya toxins, tolytoxin, anatoxins and cyclic peptides such as microcystins (Shimizu, 1993). Pyrrophyta (dinoflagellate) are flagellated eukaryotes, both photosynthetic and heterotrophic. More than 5000 species of dinoflagellates are known and some species are producers of novel compounds with interesting biological and pharmaceutical properties (Shimizu, 1993). These metabolites are diverse in chemical structures, including heterocycles, macrolides and highly oxygenated alkyl compounds (Shimizu, 2003). Table 2-1 lists representative novel marine compounds produced by dinoflagellates. Many of them are lethal to marine invertebrates, vertebrates and humans and can cause intoxications, usually through the food-chain. A brief introduction to these algal toxins is provided in section 2.1.3.

**Table 2-1.** Secondary metabolites produced by marine dinoflagellates (Shimizu, 1993).

Organisms	Type of metabolites
<i>Amphidinium spp.</i>	Macrolides: amphidinolides, amphidinols
<i>Alexandrium tamarense</i> <i>A. catenellum</i> <i>A. catenella</i> <i>Pyrodinium bahamense</i> var. <i>compressa</i> <i>Gymnodinium catenatum</i>	Heterocycles: saxitoxin, gonyautoxin derivatives
<i>Alexandrium ostenfeldii</i>	Spiroimines: spirolides
<i>Dinophysis spp.</i>	Polycyclic ethers: okadaic acid
<i>Gambierdiscus spp.</i>	Polycyclic ethers: ciguatoxin derivatives, maitotoxin
<i>Goniodoma spp.</i>	Macrolides: gonyodomin
<i>Ostreopsis spp.</i>	Complex polyethers: palytoxin
<i>Prorocentrum concavum</i>	Polycyclic ethers: okadaic acid and the derivatives
<i>Karenia brevis</i>	polycyclic ethers: brevetoxins, hemibrevetoxins, brevenal, brevisin, brevisamide
<i>Karenia selliformis</i>	Spiromines: gymnodimine
<i>Protoceratium reticulatum</i> <i>Gonyaulax spinifera</i>	Yessotoxins

### 2.1.2 Harmful algal blooms

Microalgal blooms are natural marine phenomena, usually accompanied by discolouration of seawater (red or brown tides), excessive accumulations of sea foam and unpleasant odours (Roberts *et al.*, 2004). In a typical algal bloom, the algal cells continue growing exponentially and usually reach as high as  $10^5$  -  $10^6$  cells L<sup>-1</sup> in seawater (Smith *et al.*, 1993). Approximately 400 species of microalgae have been found that can cause red or brown tides. Most of them are harmless, but 60-80 species are harmful or toxic, and can cause HABs (van Dolah, 2000). HABs can be classified into three major groups depending on the problems they cause (Hallegraeff, 1995):

1. HABs are historically formed in a particular region and mostly caused by non-toxic phytoplankton, resulting in red tides or brown tides. Oxygen consumption speeds up due to high algal populations, which generates anoxic conditions especially under some conditions (at night or in dim day light during the day) and indiscriminately kills

both vertebrates and invertebrates. The HABs caused by dinoflagellates of *Gonyaulax*, *Noctiluca* and *Scrippsiella* belong to this group (Hallegraeff, 1995).

2. Some species can damage delicate organs of fish via either physical damage or through production of haemolytic substances. HABs caused by these species are more threatening to caged fish than wild fish which are able to avoid such dangerous cell concentrations. *K. mikimotoi* can produce two haemolytic glycolipids, monogalactosyl diacylglycerol and digalactosyl diacylglycerol, which damage fish gills and were responsible for fish kills in Japan and Norway (Haywood *et al.*, 2004; Parrish *et al.*, 1998). Other algal species within this group are diatoms e.g. *Chaetoceros convolutus*, dinoflagellates e.g. *Gymnodinium aureolum*, prymnesiophytes e.g. *Chrysochromulina polylepis*, *Prymnesium patelliferum* and raphidophytes e.g. *Heterosigma carterae*, *Chattonella antiqua* (Daranas *et al.*, 2001).
3. HABs causing both human illness and mass mortalities of fish and invertebrates through production of potent marine toxins (Garthwaite, 2000).

HABs are growing in frequency, intensity, duration and geographic distribution, and have become a very serious global issue since the 1970s (van Dolah, 2000). Figure 2-2 illustrates the global increase of HABs by comparing the incidence of algal toxins reported in 1970s and 1999. Several factors have been responsible for the increase in the HABs:

1. During the past two decades, known toxic algal species have increased from approximately 40 to 60-80 species (Sournia *et al.*, 1991; van Dolah, 2000). For example, *Azadinium spinosum* is a small peridinin-containing photosynthetic dinoflagellate newly isolated from the east coast of Scotland, which has been identified as a producer of azaspiracid toxins (Tillmann *et al.*, 2009).
2. Eutrophication. The global increase of HABs is strongly linked to anthropogenic eutrophication caused by intensive agriculture, industrial activities and human waste. For example, increased global inputs of nutrients such as phosphorus and nitrogen have arisen from widespread use of agricultural fertilizers and sewage disposal to oceans (Pitois *et al.*, 2001). There are many examples demonstrating that such increased inputs are significant factors in triggering phytoplankton production in fresh and in marine waters (Anderson *et al.*, 2002). However, it is difficult to establish a direct relationship between eutrophication and HABs (Glibert *et al.*, 2005). Not all

eutrophic waters will experience HABs, and HABs may also occur in waters that are not significantly enriched with nutrients.

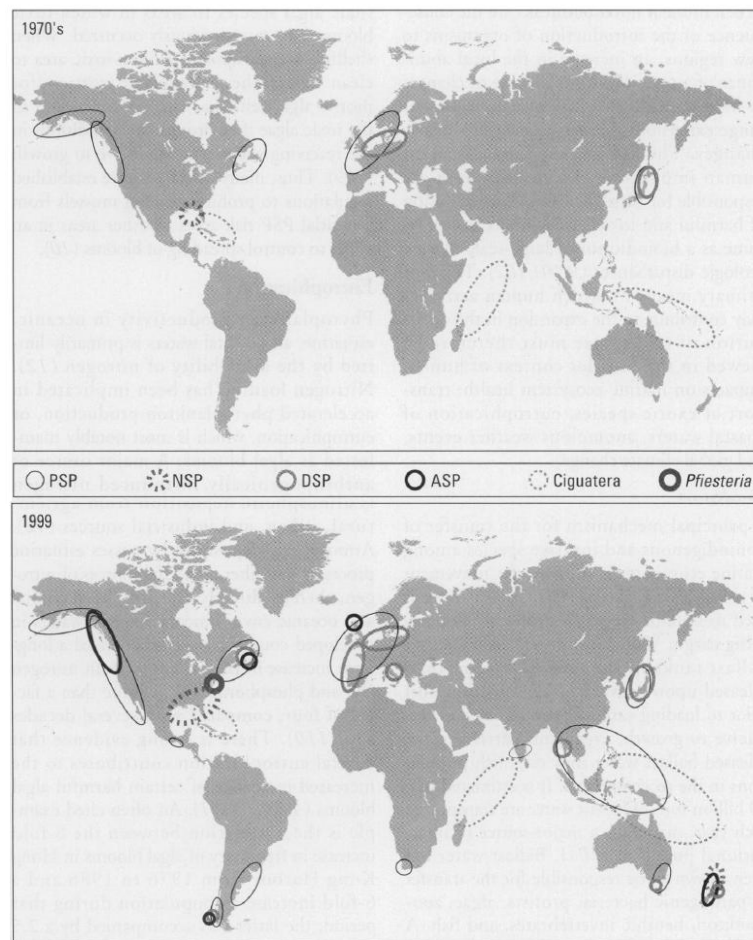


**Figure 2-2.** The global increase of reported HABs and incidents of algal toxin events (1970s compared to 1999). Encircled areas indicate where outbreaks have occurred or toxins have been detected at levels sufficient to impact human or environmental health (van Dolah, 2000).

3. Some HABs occur only in particular regions due to unique geographic conditions, such as in the Arabian Gulf (Heil *et al.*, 2001). Some HABs are triggered by climatic factors such as unusual rainfall, greenhouse effect and formation of stable, warm surface water layers. Some tropical toxic dinoflagellates have extended their distribution to colder waters. For example, *Pyrodinium bahamense*, was initially found in the mangrove-fringed coastal waters of the Atlantic and Indo-West Pacific. However, this species has been found as far south as Sydney and as far north as British waters (Hallegraeff, 1995).
4. Increased utilisation of coastal waters for aquaculture. Aquaculture provides a sensitive bioassay system for harmful algal species, and results in more reports of shellfish poisoning events (Hallegraeff, 1995). Finfish aquaculture in enclosed areas



can be particularly sensitive to blooms of some species such as *Heterosigma carterae*, *K. mikimoti* and *K. selliformis*.

5. Transport of dinoflagellate cysts in ballast water released by ships or translocation of shellfish stock. The ballast water of cargo vessels transports non-indigenous marine planktons. Hallegraeff and Bolch (1992) provided the first evidence that non-indigenous toxic microalgae were introduced to Australia via cargo vessel ballast water, causing widespread losses to a commercial shellfish industry. Microalgae can also disperse via translocation of shellfish stock because living cells and resistant resting cysts of toxic dinoflagellates may reside in the faeces and/or digestive tracts of bivalves.
6. Increased monitoring and reporting of HAB incidents which has been aided by improvements in techniques for detection of harmful algae e.g. r-RNA gene probes and their toxins e.g. LC-MS.

### **2.1.3 Marine algal toxins in bivalve molluscs.**

Marine algal toxins (MATs) are natural metabolites produced by a few species of marine phytoplankton (60-80 in more than 10,000 species) (van Dolah, 2000). Some MATs are lethal to normal, healthy adult humans at very low doses, while others may be less toxic but can accumulate in seafood and cause harm after consumption of contaminated seafood (Aune, 2008). The incidence of seafood-borne human intoxication has increased over the past two decades. On a global basis, MATs are responsible for 50,000-500,000 cases of human poisoning annually and result in approximately 1.5% mortality (Wang, 2008). Approximately 90% of all known intoxication incidents occurred after consumption of molluscs, mainly bivalves, thus most MATs are collectively named as shellfish toxins (Ciminiello & Fattorusso, 2006). Five different shellfish poisoning syndromes (ASP, AZP, DSP, NSP and PSP) caused by particular toxin groups are recognized (Table 2-2).

These syndromes are often not very specific and the preferred classification of shellfish contamination is now based on the chemical class of toxin (Aune, 2008; Toyofuku, 2006). Shellfish toxins are classified by the FAO/WHO into eight groups (Aune, 2008): azapiracids (AZA), brevetoxins, cyclic imines, domoic acid (DA), okadaic acids (OA), pectenotoxins, STXs, and the yessotoxins. Some toxins such as the yessotoxins, pectenotoxins and cyclic imine toxins have not yet been proven to be orally toxic to humans.

**Table 2-2.** Toxins, causative organisms, clinical symptoms and treatments of shellfish poisoning syndromes (Aune, 2008; Ciminiello & Fattorusso, 2006; Hallegraeff, 1995; Sobel & Painter, 2005; Tillmann *et al.*, 2009).

Shellfish poisoning syndrome	Paralytic shellfish poisoning (PSP)	Diarrhoeic shellfish poisoning (DSP)	Amenesic shellfish poisoning (ASP)	Neurological shellfish poisoning (NSP)	Azaspiracid poisoning (AZP)
Toxin Group	saxitoxin (STX)	okadaic acid (OA)	domoic acid (DA)	brevetoxin (BTX)	azaspiracid (AZA)
Causative organism	<i>Alexandrium (A.) catenella</i> ; <i>A. minutum</i> ; <i>A. tamarense</i> ; <i>Gymnodinium catenatum</i> ; <i>Pyrodinium bahamense</i> ; <i>Alteromonas tetraodonis</i> ; <i>Moraxella</i> species	<i>Dinophysis (D.) acuminata</i> ; <i>D. acuta</i> ; <i>D. fortii</i> ; <i>D. norvegica</i> ; <i>Prorocentrum lima</i>	<i>Pseudo-nitzschia</i> spp. e.g. <i>P. multiseriata</i> & <i>P. australis</i>	<i>Karenia brevis</i> (USA); <i>Karenia</i> cf. <i>brevis</i> (NZ)	<i>Protoperdinium crassipes</i> ; <i>Azadinium spinosum</i> gen. et sp. nov
Mechanism of toxin action	VGSC* blockers	Protein phosphatases inhibitors	Glutamate receptors stimulators	VGSC* openers	
Symptoms	<b>Mild case</b> Within 30 min: Tingling sensation or numbness around lips, gradually spreading to face and neck; prickly sensation in fingertips and toes; headache, dizziness, nausea, vomiting, diarrhoea. <b>Extreme Case</b> Muscular paralysis; pronounced respiratory difficulty; choking sensation; death through respiratory paralysis may occur within 2-24 hrs after ingestion.	<b>Mild case</b> After 30 min to a few hrs (seldom more than 12 hrs): diarrhea, nausea, vomiting, abdominal pain. <b>Extreme Case</b> Chronic exposure may promote tumour formation in the digestive system.	<b>Mild case</b> After 3-5 hrs: nausea, vomiting, diarrhoea, abdominal cramps. <b>Extreme Case</b> Decreased reaction to deep pain; dizziness, hallucinations, confusion; short-term memory loss; seizures.	<b>Mild case</b> After 3-6 hrs: chills, headache, diarrhoea, muscle weakness, muscle and joint pain; nausea and vomiting <b>Extreme Case</b> Paraesthesia; altered perception of hot and cold; difficulty in breathing, double vision, trouble in talking and swallowing	<b>Mild case</b> Nausea, vomiting, severe diarrhea, and stomach cramps, similar to DSP and NSP <b>Extreme Case</b> Suspected carcinogen
Treatment	Gastric lavage; artificial respiration. No lasting effects.	Recovery after 3 days, irrespective of medical treatment.	Supportive care	Supportive care	Supportive care

\*VGSC = Voltage gated Sodium Channel.

## 2.2 Conventional methods to identify, investigate and quantify marine algal toxins

### 2.2.1 General overview

Mouse bioassays (MBA) were the only internationally recognized reference methods for most MATs (or shellfish toxins) before 2004 (Riobó *et al.*, 2008). Many countries established shellfish toxins monitoring programme based on MBA. As a reference test, MBA has been used in toxicology and pharmacology for more than a century. It has specific advantages such as being inexpensive, utilises simple technology and can be standardized. However, MBA is unsatisfactory for toxin management in shellfish due to its inherent and operational deficiencies (Cembella *et al.*, 1995; McNabb *et al.*, 2005) including:

- Low correlation of i.p. toxicity with oral toxicity
- Low sensitivity: regulatory limits for some toxin groups cannot be met e.g. AZAs
- Low selectivity: false positive/negative results occur regularly
- Low specificity: little information on toxin composition is provided
- Lack of inter laboratory validation studies
- Animal ethics concerns: the sacrifice of animals for routine quality assurance of food is now ethically unacceptable

The European Food Safety Authority (EFSA) recently stated that MBA was not an appropriate tool for shellfish toxin control in the EU. The expert panel recommended that non-animal assays be adopted (EFSA, 2009). With the rapid advance of technologies, a number of alternative non-animal assays have been developed and classified into four categories (Holland, 2008):

- 1) *In vitro* cell assays — cytotoxicity, red blood cell haemolysis.
- 2) *In vitro* functional assays — receptor binding, enzyme inhibition/induction.
- 3) Immunoassays — enzyme-linked immunosorbent assay (ELISA), lateral flow immunochromatography (LFIC test strips).
- 4) Physico-chemical methods — high performance liquid chromatography (HPLC) coupled with ultraviolet (UV), fluorescence (FL) or mass spectrometry (MS) detection.

Each technique has its own specific advantages and disadvantages. For example, ELISA tests developed for marine toxins including PSP, DSP and NSP toxins are highly sensitive and selective, are based on specific antibodies, and can be used to analyse a large number of samples (Cembella *et al.*, 1995; Garthwaite, 2000). ELISA is more accurate than MBA.

However, several reasons have limited use of ELISA in shellfish testing: (1) narrow detection range that may underestimate total toxin amount, (2) and uncertain relationship between ELISA response and regulated limits for shellfish toxins in foods particularly for mixtures of toxins (Garthwaite, 2000; Holland, 2008). *In vitro* functional assays have also been developed and used for marine toxin testing in recent years such as protein phosphatase 2A (PP2A) inhibition assay for DSP toxins (Prassopoulou *et al.*, 2009) and STX radio-receptor binding assay (Cembella *et al.*, 1995). Functional assays have the advantages of integrating effects for evaluation of mixtures of toxins with the same mode of action. However, their accuracy, precision and inter-laboratory validation have generally not met standards required for regulatory methods.

There is a growing emphasis on use of instrumental methods (physico-chemical methods) based on HPLC-UV, HPLC-FL, LC-MS. These methods have advantages in high sensitivity and high specificity but require higher capital costs and are more complex to set-up and maintain. Analytical standards are required for calibration of each toxin. These methods are discussed in more details in section 2.2.4.

Generally, a typical investigation of new marine toxins includes toxin identification, isolation and purification of unknown toxins, chemical structural elucidation and toxicological analysis. This procedure involves an integration of many different techniques (Figure 2-3).

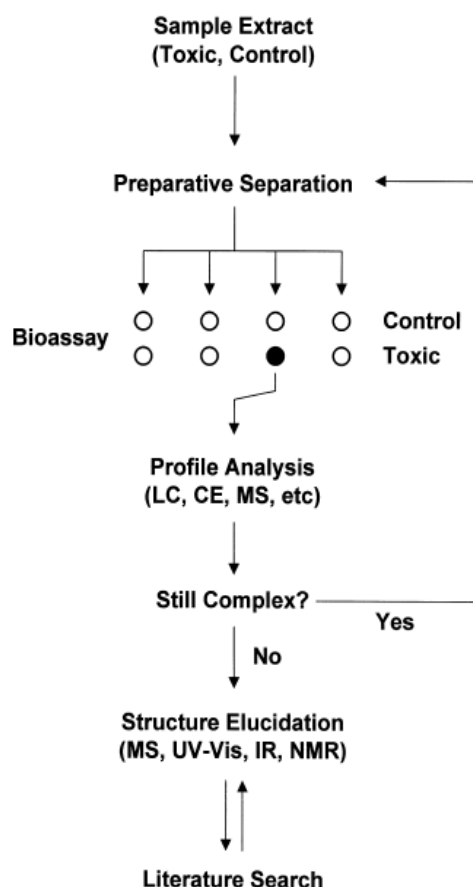


**Figure 2-3.** Flow chart indicating the general principles of toxin isolation through integration of multiple separation and assay techniques (Quilliam, 2003b).

### 2.2.2 Mouse bioassay and other *in vivo* bioassays

Currently, MBA protocols are widely used to detect PSP, DSP and NSP toxins in routine shellfish toxins monitoring programmes. In 1937, the MBA was used for detection of PSP contaminated shellfish before PSP toxins were identified (Cembella *et al.*, 1995). It was used in the isolation of the first PSP toxin, STX, from toxic shellfish in 1960 and to further investigate more than 20 analogues of STX (Quilliam, 2003b). Yasumoto *et al.* (1978) developed a standardized procedure for DSP toxin by MBA which contributed to the rapid developments in lipophilic shellfish toxins research in 1980s. In USA, a method based on acid digestion and ether extraction was developed for NSP toxins (brevetoxins) in shellfish (APHA, 1985).

MBA can provide a measurement of toxic potency of purified toxins or shellfish extracts using i.p. injection. Several characteristic symptoms exhibited within minutes to several hours after injection were observed and recorded to identify the types of known shellfish toxins (Table 2-3) or to guide isolation of a potential new toxin. In Europe, a rat bioassay using oral feeding is also used to mimic human intoxication via the oral route. However, these tests are

time-consuming and easily affected by uncontrolled factors (Cembella *et al.*, 1995). For toxicological evaluation of a marine toxin by MBA, the dose-response curve and dose-death-time relationships are established based on multiple tests at increasing doses (OECD, 2001). Mouse units (MU) and LD<sub>50</sub> are the usual parameters used to express toxicity. One MU is commonly defined as the amount of toxin required to kill a 20g mouse within a specific time depending on the type of toxin (e.g. 15 min for PSP, 24 hr for DSP) (Cembella *et al.*, 1995; Prassopoulou *et al.*, 2009). LD<sub>50</sub> is the dose required to kill 50% of test animals within a specified observation time (generally 24 hr).

**Table 2-3.** Symptoms in mice after i.p. injection of marine algal toxins (Riobó *et al.*, 2008).

Toxins	Symptoms after i.p. injection
PSP <sup>a</sup>	Jumping in the early stages, ataxia, ophthalmia, paralysis, gasping and death (usually < 15 min) by respiratory arrest
Domoic acid	Spasms, Scratching ears
OA <sup>b</sup> , DTX1 <sup>c</sup> , DTX2 <sup>c</sup>	Deep depression, weakness of limbs, convulsion (40 min -24h)
DTX3 <sup>c</sup>	Deep depression, weakness of limbs, convulsion (1h-24h)
Pectenotoxins	Similar to PSP, survival time > 20 min (3 min-24h)
Yessotoxins	Similar to PSP, survival time > 20 min (40 min-5h)
Brevetoxins	Similar to PSP, survival time > 20 min (40 min-48h)
Azaspiracid	Similar to PSP, survival time > 20 min (40 min-36h) (with low doses, creeping paralysis)
Gymnodimine	Similar to PSP
Spirolides	Similar to PSP
Ciguatoxins	Diarrhea, dysnoea, paralysis, convulsion
Palytoxins	Creeping paralysis, cyanosis, deep depression

<sup>a</sup>PSP, paralytic shellfish poisoning); <sup>b</sup>OA, Okadaic acid; <sup>c</sup>DTX, Dinophysitoxins.

Before 1980s, most toxicologists focused on the potential risks of MATs to human health and other mammals (Landsberg, 2002). However, some harmful algae do not pose a high risk to mammals but may cause adverse effects on aquatic organisms in a natural HAB event (Hallegraeff, 1995). Many *in vivo* models based on aquatic organisms e.g. finfish, molluscs, brine shrimp and other marine or freshwater invertebrates have been developed for investigation of MATs and harmful algae (Landsberg, 2002). These models have contributed to better understanding of the potential influences of harmful algae and their toxins on aquatic organisms and ecosystems. However, there is no single internationally recognized model

organism and particular growth stage (embryo, larvae, or juvenile) for MATs investigation, such as Swiss mice for MBA. Therefore toxicological data obtained from different laboratories is often difficult to compare, and can result in misevaluation of the toxic potency of particular MATs or harmful algae species. Similar to other *in vivo* bioassays, large scale testing of live fish can be problematic due to animal ethics considerations. A novel bioassay based on salmon fish gill cells was developed to mimic exposure under laboratory conditions between fish gill and toxic algae in a HAB event and is a potential *in vitro* cell bioassay to replace many fish bioassays in the future (Dorantes-Aranda *et al.*, 2011).

### **2.2.3 *In vitro* cell assays for investigations of cytotoxicity and mode of action**

#### **2.2.3.1 Overview - *in vitro* cell assays**

*In vitro* cell assays were initially designed in the early 20<sup>th</sup> century for pathology and pharmacology and rapidly developed after 1946 with the beginning of cancer chemotherapy (Waud, 2004), as alternative and supplementary methods to animal assays. *In vitro* assay has been recommended as an alternative to live animal assays for routine monitoring and investigation of MAT (EFSA, 2009). Compared with traditional MBA, the advantages of *in vitro* assay include:

- higher sensitivity
- higher selectivity/specificity
- lower cost for single sample
- quantitative measurement of toxicity
- higher throughput and shorter testing time for multiple samples
- contributes to understanding the mechanism of action of unknown toxins
- higher reproducibility
- no ethical concerns

Figure 2-4 summarises potential assay methods for unknown MATs. Three types are recognised: (1) model system (*in vivo* or *in vitro*), (2) recognition element (receptor or antibody recognition), and (3) assay system (purified enzyme, tissue homogenates, living cells) (Fairey & Ramsdell, 1999).

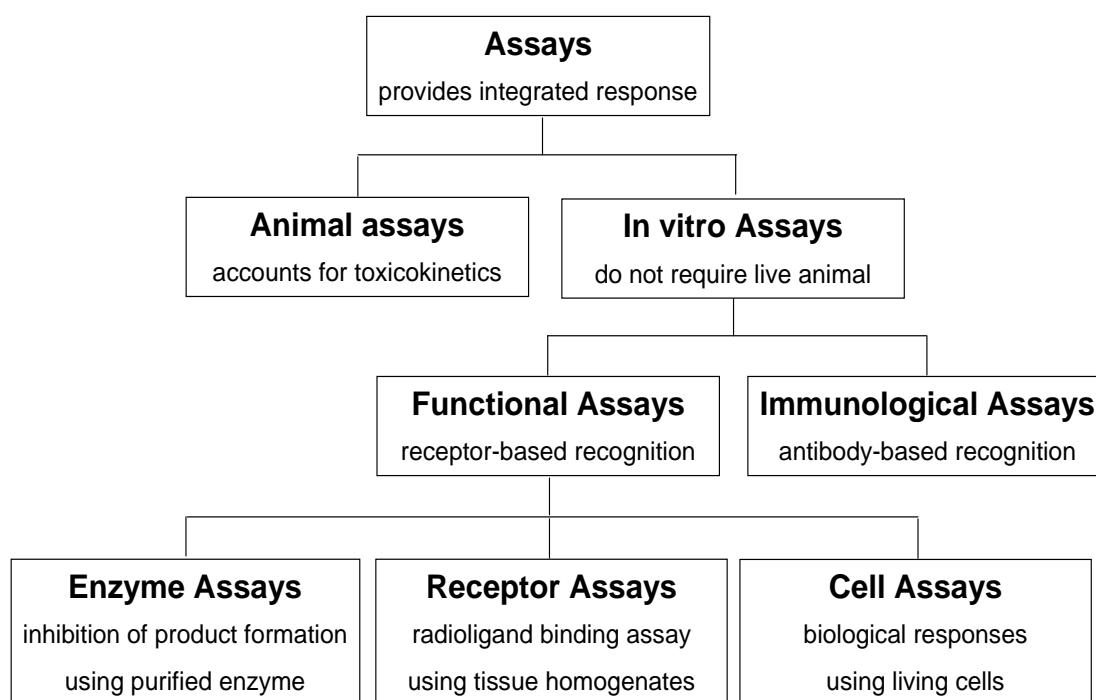


**Figure 2-4.** Flow diagram of potential bioassay methods for marine algal toxins research. Each box contains a distinguishing feature for the assay type (Faurey & Ramsdell, 1999).

*In vitro* cell-based assays are a subtype of the *in vitro* functional assays, which are based on the biological response of living cells. Features of this assay type are (Briggs, 2008; Faurey *et al.*, 1999):

- 1) They do not require prior knowledge of the initial cellular target for the toxin;
- 2) The sensitivity is dependent on cell line response, cell number, toxin concentration and length of time for cell exposure to toxin;
- 3) The selectivity of response depends on the particular combination of receptors, ion channels, enzymes, gene response elements and other signal-generating molecules unique to each cell type;
- 4) Usually chosen as an initial method to screen for possible toxin activity
- 5) Can identify the mode of action of unknown toxins based on the use of a diverse group of cell types;
- 6) They are possible to be further developed to receptor-based assay by changing the end point.



### **2.2.3.2 Mammalian cell lines**

Isolation and establishment of a primary cell culture is far more demanding and troublesome compared to establishing a culture of cells obtained from a collection such as American Type Culture Collection (ATCC) and European Collection of Cell Cultures (ECACC) (Bulter, 2004). Over 3000 cell lines are stored in collections and are well characterized in terms of growth, origin and genetic traits. The cells can be simply categorised into adherent (anchorage dependent), semi-adherent, and suspension cells dependent on its growth characteristics. Most cells from the bloodstream are typical suspension cells which can be grown without being attached to a surface. The anchorage dependent cells e.g. Vero and Neuro2a cell, require a solid substrate (e.g. plastic surface or micro-carriers) to attach and grow (Nor *et al.*, 2010). A combination of electrostatic attraction and van der Waal's forces contribute to the attachment of cells onto the growth surface, usually involving divalent cations ( $\text{Ca}^{2+}$ ), and basic proteins derived from supplemental serum or secreted from the cells (Bulter, 2004). There are some cell lines (semi-adherent cells) that can form both suspension and adherent cultures. Cell lines that have been used to evaluate cytotoxicity of marine algal toxins include Neuro2a mouse neuroblastoma cell line, P388 mouse leukemia cell line, and Vero monkey kidney epithelial cells (Briggs, 2008). Response comparisons using more than one cell line can contribute to better cytotoxicity evaluation and understanding of a new toxin based on different sensitivity, selectivity and specificity of each cell line. Three cell lines which will be introduced in this section have commonly been used as cytotoxicological models for algal toxin investigation (Table 2-4). They may also be developed at Cawthron Institute in the future for routine use in biotoxin monitoring and investigation of novel algal toxins.

Mouse neuroblastoma cell line (Neuro2a) was the first cell line used for marine algal toxin investigation (Neuro2a assay) and is suitable for almost all VGSC-dependent marine algal toxins including STX, brevetoxins and CTX but with varying sensitivities (Table 2-4) (Dechraoui *et al.*, 2005; Fairey *et al.*, 2001; Manger *et al.*, 2003; Truman *et al.*, 2002). Two reagents are usually added to sensitize the Neuro2a cells: veratridine, a sodium channel activator acting on site 2 of VGSC (see Section 2.3.2), and ouabain, an inhibitor of  $\text{Na}^+/\text{K}^+$  ATPase (Shimojo & Iwaoka, 2000). Each VGSC-dependent toxin should have a unique dose-response curve ("signature") to sensitised and non-sensitised Neuro2a cells based on its cytotoxicity. Neuro2a assay is extremely sensitive to VGSC toxin detection (e.g. < 100 pg STX/well), is relatively unaffected by matrices and is suitable for measurement of toxicity of

crude extracts. Compared with other neuroblastoma cell lines such as SK-N-SH, Neuro2a cells are highly sensitive to a large number of toxins (Xia *et al.*, 2008).

Vero cell line was isolated from the kidney of a normal, adult, African green monkey in 1962 in Japan and has been extensively used in viral vaccine production and virus studies (Nor *et al.*, 2010; Sheets, 2000). Few applications of the Vero cell line to study of marine algal toxins, such as biotoxins produced by cyanobacteria (Rao *et al.*, 2002) and some species of the dinoflagellates *Heterocapsa* and *Alexandrium* (Katsuo *et al.*, 2007), have been reported (Table 2-4). Unlike Neuro2a cell lines, Vero cells are not specifically sensitive to VGSC toxins, and the monkey kidney cell line may be useful to cover hepatic and nephrotic toxins. Vero cells have been developed as a new simple screening method to detect algal toxins in samples of seawater and cell extracts (Katsuo *et al.*, 2007). In this study, the Vero cells were exposed to sterilized Erd-Schreiber modified (ESM) medium (a medium for dinoflagellates) and showed high resistance to sea water and ESM medium for 3 hrs. However, the cytotoxicity against Vero cells was poorly correlated to the ichthyotoxicity to fish and toxic potency to marine invertebrates.

P388 murine leukemia cell line was developed in 1955 as an important *in vitro* model for screening and detailed evaluations of candidate anticancer agents (Waud, 2004). The P388 cell line exhibits higher sensitivity to most clinical agents than other leukemia cells such as L1210 (mouse). The model has been shown to be rapid, reproducible and relatively inexpensive in pharmacological investigations over the past fifty years. The development of P388 leukemia cells for algal toxin research started in 1981 with okadaic acid (Tachibana *et al.*, 1981), and this model has subsequently been widely used to investigate novel algal toxins. Cytotoxicities of typical algal toxins against P388 cells are summarised in Table 2-4. For *K. brevisulcata* research, P388 cytotoxicity assay has proved a good model to guide isolation of KBTs from the lipophilic extract (Oshima, 2007). The development of P388 leukemias may be necessary and feasible for shellfish toxin monitoring and for toxin isolation at Cawthron Institute.

**Table 2-4.** Cytotoxicities of marine algal toxins against three American Type Cell collection (ATCC) cell lines (Neuro2a, Vero and P388).

Cell line	Biotoxins <sup>a</sup> tested	Sensitivity <sup>b</sup>	Mode of action	References
Neuro2a mouse neuroblastoma	STX	24 h incubation experiment, <b>LOD</b> 100 pg/well <b>EC<sub>50</sub></b> 1.5 nM <b>EDR</b> 0.1-10 ng/well	Sodium channel blocker	(Katsuo <i>et al.</i> , 2007; Manger <i>et al.</i> , 2003; Perreault <i>et al.</i> , 2011)
	BTX-1, CTX-1 STX	<b>EC<sub>50</sub></b> 5.3 nM BTX-1 (12h) <b>EC<sub>50</sub></b> 2.7 nM CTX-1(12 h) <b>EC<sub>50</sub></b> 11.7 nM STX-1 (12 h)	BTX-1 & CTX-1 are sodium channel agonists; STX is a sodium channel antagonist. The EC <sub>50</sub> of STX is based on measurement of inhibition of BTX-1 toxicity	(Fairey & Ramsdell, 1999)
	BTX-2	<b>EC<sub>50</sub></b> : 5.8 nM	BTX-2/ -3: Sodium channel opener Ring-opened BTX lose toxicity	(Roth <i>et al.</i> , 2007)
	BTX-3	<b>EC<sub>50</sub></b> : 2.7 nM		
	Ring-opened BTX-2	<b>EC<sub>50</sub></b> : 447.9 nM		
	Ring-opened BTX-3	<b>EC<sub>50</sub></b> : 381.7 nM		
	BTX-1 BTX-3	<b>LOD</b> : 20 pg/well BTX-1 50 pg/well BTX-3	BTX: sodium channel opener	(Truman <i>et al.</i> , 2005; Truman <i>et al.</i> , 2002)
	GYM and the analogues; OA (to GYM sensitised Neuro2a cells 24h)	Not mentioned	GYM: neurotoxins acting at the nicotinic ACh receptor.	(Dragunow <i>et al.</i> , 2005; Kharrat <i>et al.</i> , 2008)
	Azaspiracid-1	<b>EC<sub>50</sub></b> : 2.3 nM AZA-1(48 h/72 h)	Via cytosolic Ca <sup>2+</sup>	(Twiner <i>et al.</i> , 2005)
Vero African green monkey kidney	Algal extracts: <i>Heterocapsa</i> (H.) <i>circuisquama</i> and <i>Alexandrium</i> spp Fresh culture: <i>Alexandrium</i> spp. and <i>H.circuisquama</i>	Not mentioned	The presence of cytotoxic substances in the extract of <i>A. tamarense</i> extracts in addition to PSP toxins	(Katsuo <i>et al.</i> , 2007)

	Anatoxin-containing cell-free extracts (ACE) from <i>Anabena flosaquae</i> and purified anatoxin- $\alpha$	<b>IC<sub>50</sub></b> 24.4 nM anatoxin- $\alpha$ (6 h); 30 ng mL <sup>-1</sup> ACE (6 hr)	ACE and anatoxin- $\alpha$ showed caspase-3 activation, and pretreatment with the caspase-3-specific inhibitor, Ac-DEVD-CHO abolished the DNA fragmentation and reduced the incidence of apoptotic cells.	(Rao <i>et al.</i> , 2002)
<b>P388 mouse leukemia</b>	OA	<b>ED<sub>50</sub></b> : 2.1 nM	Inhibition of protein phosphatase 2A	(Tachibana <i>et al.</i> , 1981)
	Yessotoxin	Cytotoxicity of yessotoxin against P388 (over 8 $\mu$ M), > 80 times less than OA (0.01 $\mu$ M)	An apoptotic inducer through activation of multiple signalling pathways	(Suárez Korsnes & Espenes, 2011; Tubaro <i>et al.</i> , 2010; Yasumoto & Satake, 1998)
	Pinnatoxin D	<b>IC<sub>50</sub></b> : 3.2 $\mu$ M pinnatoxin D	Agonist of nicotinic ACh receptor	(Kita & Uemura, 2005)
	Gymnocins	<b>IC<sub>50</sub></b> : 1.3 $\mu$ M gymnocin-A 1.5 $\mu$ M gymnocin-B	Mode of action not known	(Satake <i>et al.</i> , 2002; Satake <i>et al.</i> , 2005)

<sup>a</sup>STX, saxitoxin; BTX, brevetoxin; CTX-1, ciguatoxin-1; GMY, gymnodimine; OA: okadaic acid; KBTs, brevisulcenals

<sup>b</sup>LOD, limit of detection; EC<sub>50</sub>, the half maximal effective concentration; EDR, effective detection range; IC<sub>50</sub>, the half maximal inhibitory concentration; ED<sub>50</sub>, the half maximal effective dose.

### 2.2.3.3 Cytotoxicity measurements and mode-of-action investigations

The term “cytotoxicity” was defined as “the cumulative effect of a compound over a given period of time on cell number, whether due to apoptosis, necrosis, or a reduction in the rate of cell proliferation” (Xia *et al.*, 2008, p. 284). *In vitro* cell-based cytotoxicity assays can be separated into three types according to the endpoint measured (Promega, 2009):

1. Measurements of the number of dead cells, e.g. protease measurement assay and lactate dehydrogenase (LDH) release assay
2. Assays for the number of live cells, e.g. ATPase assay and tetrazolium-based assays (MTT or MTS)
3. Assays for the mechanism of cell death (e.g. apoptosis).

#### Cell viability assay

Measurement of viable cells using a tetrazolium-based assays (MTT or MTS) has been the most popular end-point for *in vitro* cell based studies of marine algal toxins including AZA-1, brevetoxins, CTX, DA, KBT, maitotoxin (MTX), microcystin-LR, OA and STX (Carvalho *et al.*, 2006; Chong *et al.*, 2000; Dragunow *et al.*, 2005; Larm *et al.*, 1997; Manger *et al.*, 2003; Manger *et al.*, 1993; Obara *et al.*, 1999; Truman, 2007; Truman *et al.*, 2005; Truman *et al.*, 2002; Tubaro *et al.*, 1996; Twiner *et al.*, 2007; Twiner *et al.*, 2005). Yellow MTT [3-(4,5-Dimethyl-2-thiazolyl)-2,5-diphenyl-2H-tetrazolium bromide] is reduced to a purple formazan compound via dehydrogenase(s) produced by viable cells' mitochondria. Therefore, this colorimetric assay is widely used to determine cell viability, the results of which also reflect the activity of electron transport (metabolic activity or functional activity of mitochondria) (Arbab *et al.*, 2003; Cardoso *et al.*, 2001; Issa *et al.*, 2004). The purple formazan compound is not soluble in water, so the solubilisation is an issue in MTT assay. The solubilisation solution usually includes either dimethyl sulfoxide (DMSO), an acidified ethanol solution, or the detergent sodium dodecyl sulphate (SDS) in dilute hydrochloric acid. The coloured solution can be quantified by measuring absorbance at a certain wavelength (at 570-630 nm for MTT). However, the absorbance is not stable, so measurements must be carried out as soon as possible after MTT reduction. The mechanism of MTS [3-(4,5-dimethylthiazol-2-yl)-5-(3-carboxymethoxyphenyl)-2-(4-sulfophenyl)-2H-tetrazolium]] reduction is similar to that of MTT, but the formazan product (Figure 2-5) is more water soluble and can be directly quantified in a spectrophotometer at 460 nm. This method is

simpler to use. Reducing substances in the cell culture medium produce a background absorbance typically 0.2-0.3 absorbance units after 4 hr incubation with MTS. Absorbance values from control wells containing medium without cells at various concentrations of test compound are used to eliminate this medium specific interference.

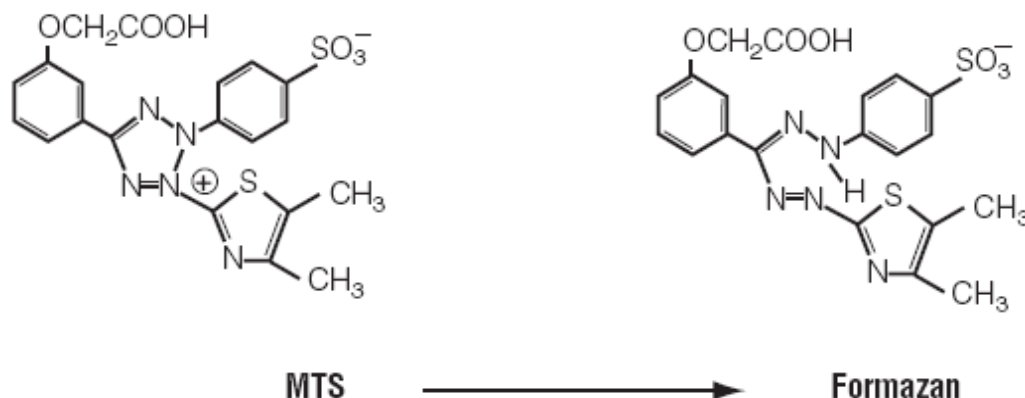


**Figure 2-5.** Structures of MTS and Formazan (Promega, 2009).

### Cytotoxicity and membrane integrity bioassay

Cell death and viability are most often defined based on the integrity of the cell membrane. Measurement of leakage of components from the cytoplasm into surrounding culture medium has been widely accepted as a valid method to estimate the number of non-viable cells (cytotoxicity). Several biomarkers have been described and employed to measure membrane integrity and cytotoxicity including LDH, 6-phosphate dehydrogenase (G6PD) and dead cell protease. LDH is located in the cytoplasm and catalyses the inter-conversion of pyruvate and lactate with concomitant inter-conversion of NADH and NAD<sup>+</sup>. A simple method has been developed based on the decrease of the peak absorbance of NADH at 340 nm in the presence of NADH and pyruvate and was used in cytotoxicity studies of microcystin-LR and palytoxin (Aune & Berg, 1986; Bellocchi *et al.*, 2008; Chong *et al.*, 2000). In addition, commercial cytotoxicity kits are available to provide homogeneous methods of LDH release by colorimetric reaction, or fluorescent signal generation (Figure 2-6). These kits have been widely used due to i) simpler operation, ii) higher sensitivity, iii) less requirements for samples and cells and iv) possible multiple kinetic readings of the same plate. Animal serum used to supplement cell culture media contains significant amount of LDH that can lead to high background absorbance or fluorescence. Reduction in serum supplement is usually recommended to eliminate the background signal in LDH release bioassay. LDH has a half-life of approximately 9 h after release from cells. Riss *et al.* (2004) showed the maximum

LDH activity in culture medium from HepG2 cells treated with tamoxifen (> 30 nM) for 1-6 hr was much higher than that at 24 hr.

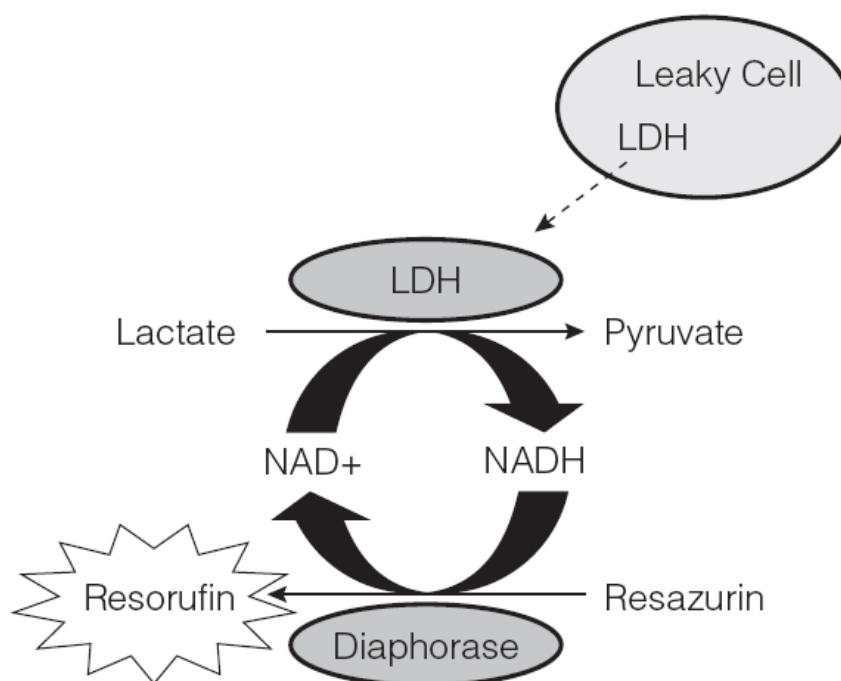


**Figure 2-6.** The principle of the fluorescence bioassay for LDH. Release of LDH from damaged cells is measured by supplying lactate,  $\text{NAD}^+$ , and resazurin as substrates in the presence of diaphorase. Generation of the fluorescent resorufin product is proportional to the amount of LDH (Promega Technical Bulletins TB306).

### Identification of cell death mechanism

Mechanisms of cell death can be simply separated into necrosis or apoptosis. Necrosis is a passive, energy-independent cell death and is characterised by cell swelling, chromatin flocculation, loss of membrane integrity, cell lysis and generation of a local inflammatory reaction. Apoptosis is programmed cell death and can be characterised by morphological features including membrane blebbing, nuclear and cytoplasmic shrinkage, and chromatin condensation. The apoptotic cells eventually form apoptotic bodies which can be quickly phagocytised by adjacent cells or macrophages without generating an inflammatory response *in vivo*. “Secondary necrosis” occurs at the terminal phase of *in vitro* cell apoptosis, in which the apoptotic bodies as well as the remaining cell fragments ultimately swell and finally lyse.

Further studies found that apoptosis can trigger an energy-dependent mechanism by activation of related genes and signalling, and result in DNA fragmentation and cell death (Elmore, 2007). Several biochemical features have been identified including phagocytic recognition, protein cleavage and signalling activation, expression of specific genes and DNA

fragmentation and were developed for apoptosis studies. There are currently six groups of apoptosis assays classified based on detection/measurement of morphological changes or biochemical biomarkers (Elmore, 2007):

- (1) cytomorphological alterations, e.g. transmission electron microscopic observations of certain ultrastructural morphological characteristics;
- (2) DNA fragmentation e.g. DNA ladder electrophoresis and TUNEL (Terminal dUTP Nick End-Labeling) assay;
- (3) detection of caspases, cleaved substrates, regulators and inhibitors, e.g. caspase-3/7 colorimetric assay and apoptosis PRC microarray;
- (4) membrane alterations, e.g. Annexin V FITC/EG staining assay to detection phosphatidylserine externalization (van Engeland *et al.*, 1998);
- (5) detection of apoptosis in whole mounts (Zucker *et al.*, 2000),
- (6) mitochondrial assays (Christensen *et al.*, 2008; Galluzzi *et al.*, 2007).

However, apoptosis cannot be confirmed by a single assay because many features of apoptosis and necrosis can overlap (Elmore, 2007). For example, mitochondrial permeability transition has been identified as a common pathway in necrosis and apoptosis (Kim *et al.*, 2003). The mitochondrial parameters monitored e.g. depolarization of the inner mitochondrial membrane,  $\text{Ca}^{2+}$  fluxes, mitochondrial redox status and reactive oxygen species (ROS) can also occur in necrosis and gave a false positive result for apoptosis. Inappropriate timing of assays may also result in false negative results. For example, DNA fragmentation occurs late in apoptosis, so DNA ladder assays are not able to detect apoptotic cells at early stages (Elmore, 2007) (Collins *et al.*, 1997; Huerta *et al.*, 2007). Therefore, identification of apoptosis usually employs two or more distinct assays. Multiple kinetic measurements using a single sample are also recommended. Many commercial kits are available to provide simple, fast, flexible and sensitive bioassays such as Promega ApoTox-Glo<sup>TM</sup> Triplex Assay. This kit measures three end-points: cell viability, cytotoxicity and caspase 3/7 activity. Caspase-3 is critical in caspase-dependent apoptosis and cleavage of caspase-3 activates downstream targets and irreversibly commits the cell to apoptosis (D'Amelio *et al.*, 2010; Slee *et al.*, 2001; Walsh *et al.*, 2008). Riss and Moravec (2004) suggested a mixed method by measurement of LDH release and caspase-3/7 activity or cell viability. Induced cell apoptosis resulted in a dose-dependent decrease in cell viability, and a corresponding increase in caspase-3/7



activity. However, cell necrosis decreases cell viability in a dose-dependent manner and increases in LDH release with no caspase-3/7 activation. This mixed method appears to offer advantages in simplicity of operation which may lead to more reproducible results, and savings in both time and costs. However, there appears to be few uses of this assay in the literature. The information supplied by Promega data sheet and Riss and Moravec (2004) were relied on for development of the assay.

## **2.2.4 Physico-chemical methods**

The main physico-chemical methods used in toxin analysis are chromatographic methods with optical (UVD and FLD) or mass spectrometric detectors (Quilliam, 2003b). Most natural toxins are too polar and high m.w. to be amenable to gas chromatography (GC). Therefore LC is the preferred technique for separation of toxins. LC-MS is being adopted by many countries as an alternative method to MBA for shellfish toxicity testing due to its greater selectivity, sensitivity, reliability, shorter analysis time and the quantitative results obtained (Christian & Luckas, 2008; Draisci *et al.*, 1999; EFSA, 2009; Fux *et al.*, 2007; Hess *et al.*, 2002; Holland *et al.*, 2002; McNabb *et al.*, 2005; Suzuki *et al.*, 2005; Turrell & Stobo, 2007). In addition, LC-MS is suitable for detection of multiple marine toxins, including yessotoxins, OA, DTXs, brevetoxins, pectenotoxins, STXs and AZAs (Aasen *et al.*, 2002; Draisci *et al.*, 1999; Turrell & Stobo, 2007). A validation study conducted at Cawthron Institute with collaborating laboratories showed that LC-MS provided acceptable single laboratory validation and inter-laboratory reproducibility for several toxin groups (McNabb *et al.*, 2005). Two method comparison studies have also demonstrated a high degree of agreement between MBA and LC-MS for shellfish toxins (Hess *et al.*, 2002; Suzuki *et al.*, 2005).

### **2.2.4.1 LC-MS**

LC-MS techniques developed rapidly throughout the 1980s (Quilliam, 2003b). A typical LC-MS system comprises a HPLC for analyte separation, an atmospheric pressure ionisation interface to produce ionised molecules and a MS in which ions are separated and detected in a high vacuum environment. Analyte separation by HPLC requires a suitable column and mobile phase. The reversed phase HPLC columns used in shellfish toxins testing are packed with silica particles (5 µm size) with alkyl chains (C8 or C18) bound to the surface. Recently, Ultra-Performance Liquid chromatography (uPLC) technology was developed (Waters, 2009). uPLC has dramatically increased the resolution, speed and sensitivity, through use of columns

with smaller particles (1.7 -1.8  $\mu\text{m}$  size) that require a mobile phase delivery at pressures up to 15,000 psi. The separation of 15 marine toxins was reduced from 30 minutes to less than 6 minutes by changing from regular HPLC to uPLC (Fux *et al.*, 2007). Mobile phase composition is determined by the column and the analyte properties. Percentage of organic solvent, type of buffer pH and ionic strength are important in preparing the mobile phase for reversed phase HPLC. The main mobile phases for LC-MS include either methanol/water or acetonitrile/water mixtures plus a volatile buffer composed of formic acid (FA), acetic acid, trifluoroacetic acid (TFA), the ammonium salts of these acids, or ammonium hydroxide. A gradient from low to high solvent strength is generally used to elute compounds of widely varying polarity.

Figure 2-7 shows the internal-structure of a triple stage quadrupole (TSQ) mass spectrometer. Atmospheric pressure ionisation is the key step for detection of toxins by MS. There are several types including electrospray ionisation (ESI), atmospheric pressure chemical ionisation (APCI), atmospheric pressure photo-ionization (APPI), fast atom bombardment (FAB) and matrix-assisted laser desorption ionisation (MALDI). ESI is commonly used for marine toxins because of its simplicity and robustness, sensitivity, and suitability for compounds with widely ranging polarities and molecular weight (Núñez *et al.*, 2005; Quilliam, 2003b). ESI generally produces protonated molecular ions  $[\text{M}+\text{H}]^+$  in positive mode and proton abstracted molecular ions  $[\text{M}-\text{H}]^-$  in negative mode. Acidic and macrolide toxins such as OA and pectenotoxin also readily produce ammonia or sodium adduct molecular ions ( $[\text{M}+\text{NH}_4]^+$  or  $[\text{M}+\text{Na}]^+$ ) in ESI positive mode (Quilliam, 2003b). Acidic toxins with sulphate or free carboxyl functions can be detected in both positive and negative ion mode in the form of  $[\text{M}+\text{H}]^+$  and  $[\text{M}-\text{H}]^-$ , respectively (Quilliam, 2003b). Multiple ionised states can result where molecules contain two or more highly ionisable groups such as  $-\text{NH}_2$  or  $-\text{COOH}$ .

In a single mass analyser (MS1 in Figure 2-7 with collision cell and MS2 set to transfer all ions) there are two operating modes: MS scan (scan over a set mass range) and selected ion recording (SIR with monitoring of several specified masses). With multi-analyser instruments such as the TSQ, there are also several MS/MS operating modes including daughter ion spectrum, parent (product) ion spectrum, neutral loss scan and multiple reaction monitoring (MRM). In these experiments, specified masses are selected or scanned in MS1, the ions are fragmented in the collision cell using a gas (argon) plus electrostatic energy and the fragment ions are selected or scanned in MS2. The most sensitive mode is MRM where specific ion parent masses are selected in MS1, fragmented in the collision cell and specific

fragment ions are selected in MS2 for detection. Typical LODs in this mode are 5-50 pg of toxin.

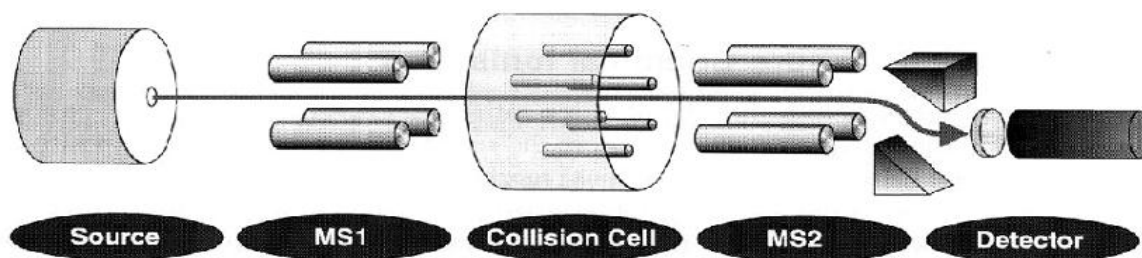


**Figure 2-7.** Internal structure of triple quadrupole (TSQ) mass spectrometer for MS/MS (Waters, 2005).

Validated LC-MS methods now provide an appropriate alternative to MBA. However, LC-MS and other instrumental methods must be calibrated daily using reference solutions containing each toxin at known concentrations. Primary standards for LC-MS include certified reference material, purified reference material and laboratory materials (Holland, 2008). Production of a certified reference material (CRM) requires large amounts (> 10 mg) of generally rare toxin and multiple tests for reference purity and concentration. Commercial CRMs are now available for many of the key marine biotoxins required for shellfish testing, particularly from the Institute for Marine Biosciences, National Research Council Canada (NRCC), Halifax, Canada.

#### **2.2.4.2 Nuclear magnetic resonance (NMR)**

NMR is the key technique for the full elucidation of the chemical structures of novel biotoxins. Proton ( $^1\text{H}$ ) NMR enables determination of the proton environment (number and configuration of neighbouring protons). Carbon-13 ( $^{13}\text{C}$ ) NMR similarly enables the identification of the number and type of carbon atoms in an organic molecule. The combination of  $^{13}\text{C}$  and  $^1\text{H}$  NMR in 2D experiments allows the elucidation of the carbon connectivity and 3-dimensional chemical structure of complex organic molecules. Compared with  $^1\text{H}$  NMR,  $^{13}\text{C}$  NMR is less sensitive because  $^{13}\text{C}$  has only about 1.1% natural abundance. The main carbon isotope,  $^{12}\text{C}$ , cannot be detected by NMR due to its spin quantum number of zero (no net spin) (Hunt, 2006; Rzepa, 1995; Shanks, 2001). Compounds produced by microorganisms can be enriched with  $^{13}\text{C}$  by growing in media containing labeled substrate such as  $\text{NaH}^{13}\text{CO}_3$ . Such enrichment was used to assist the structural elucidation of MTX from the tropical dinoflagellate *Gambierdiscus toxicus* (Satake *et al.*, 1995).

## 2.3 *Karenia* dinoflagellate and their biotoxins

### 2.3.1 *Karenia* species in New Zealand

The *Karenia* genus of unarmoured (non-thecate or naked) dinoflagellates contains a number of species that have caused widespread damage to aquaculture and marine ecosystems from major blooms during the past 60 years in Europe, Japan, New Zealand and United States. The first identified *Karenia* species was *K. brevis* which was isolated from red tides in the Gulf of Mexico, USA during 1947-1948 (Davis, 1948). During the past six decades, the name of this genus has changed several times, which gives rise to some confusion in the literature over exactly which species is being discussed. Furthermore, the names of marine algal toxins are often related to the origin, and the change in algal name also results in problems in the toxin naming. For example, *Karenia brevis* was firstly named *Gymnodinium brevis* sp. nov, then *Gymnodinium breve*, and then *Ptychodiscus brevis*. The NSP toxins produced by *K. brevis*, now named as brevetoxins, were previously named as *Ptychodiscus brevis* toxins (PbTx). At the end of 1990s, a new genetic method was developed for identification and classification of different naked dinoflagellates based on ultrastructural and partial large subunit (LSU) ribosomal RNA (rRNA) sequence data. The old *Gymnodinium* group was then subdivided into at least four new genera: *Karenia*, *Karlodinium*, *Akashiwo* and *Takayama* (Daugbjerg *et al.*, 2000; De Salas *et al.*, 2003; MacKenzie, 2008). At least six *Karenia* species have been identified from previous HAB events in New Zealand's waters: *K. cf. brevis*, *K. mikimotoi*, *K. brevisulcata*, *K. selliformis*, *K. longicanalis*, *K. umbella* and *K. bidigitata* (Figure 2-8). Four species of these caused widespread damage to New Zealand's aquaculture and marine ecosystems from severe HABs during 1992/93, 1994, 1998, 2002 and 2007 (MacKenzie, 2008).

*K. cf. brevis* was identified in the 1992-3 HAB event in Hauraki Gulf, New Zealand. It is similar to *K. mikimotoi* and *K. brevis* in morphology and produced 'brevetoxin-like' lipid soluble toxins (MacKenzie *et al.*, 1995). This HAB caused wide spread human illness (over 100 cases) and was the first report of NSP outside of the eastern American coast (Chang, 1995; Chang *et al.*, 1995; MacKenzie, 2008; MacKenzie *et al.*, 1995). Unfortunately, *K. cf. brevis* was not successfully isolated from contaminated seawater samples at that time and there has been no progress in the investigation of this dinoflagellate since 1993. More recently, a *Karenia* species was isolated from the Hauraki Gulf during a HAB event in 2002 and was tentatively linked to the 1992/3 event. This species was named *K. concordia* (Chang & Ryan, 2004; Chang *et al.*, 2008). Contaminated shellfish from the 1992-93 event were used by Japanese researchers to isolate and characterise several novel toxic metabolites of

brevetoxins (Ishida *et al.*, 2004a; Ishida *et al.*, 2004b; Ishida *et al.*, 2004c; Ishida *et al.*, 1995; Morohashi *et al.*, 1995; Morohashi *et al.*, 1999; Murata *et al.*, 1998; Nozawa *et al.*, 2003).

*K. mikimotoi* is a widely distributed and well known fish-killing dinoflagellate that has caused economic losses in many countries. It produces complex toxic metabolites (Garthwaite, 2000; Haywood *et al.*, 2004; Munday *et al.*, 2004; Satake *et al.*, 2002; Satake *et al.*, 2005) but the fish-killing mechanisms have not been recognized. In New Zealand, almost annual blooms of *K. mikimotoi* have occurred in Hauraki Gulf in the past two decades. In 2007, another fish-killing HAB caused by *K. mikimotoi* occurred in the Te Puna Inlet, Northland, New Zealand, accompanied by red water discolouration in which the cell concentration reached more than  $2 \times 10^6$  cells L<sup>-1</sup> (Smith *et al.*, 2007).

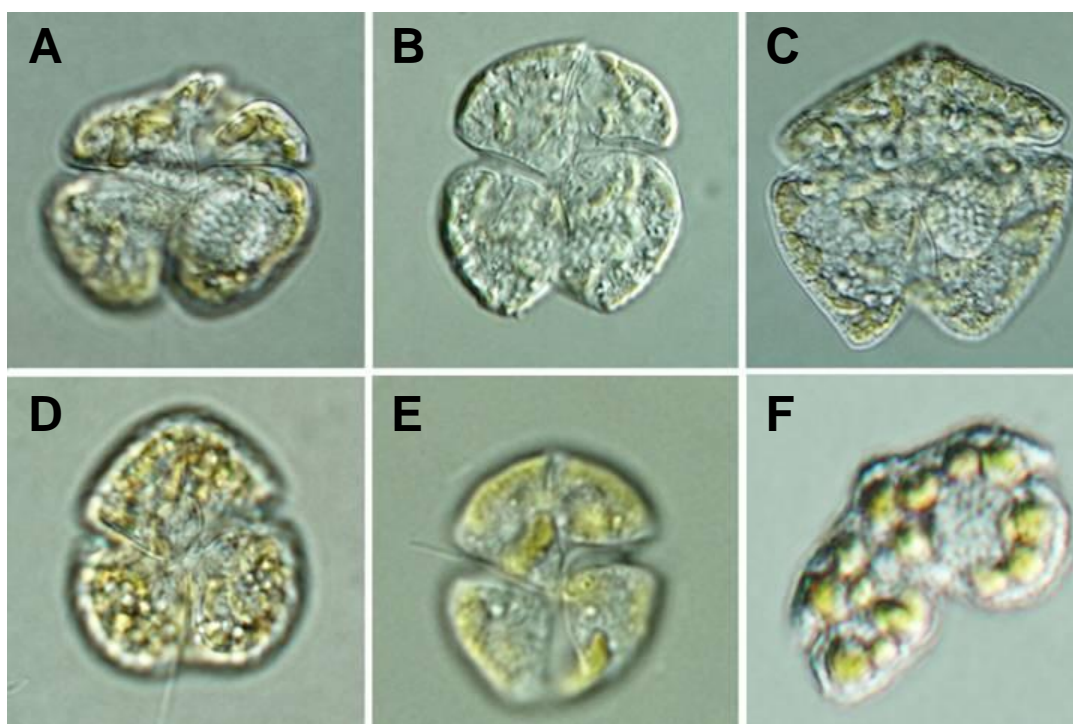


**Figure 2-8.** Photomicrographs of six *Karenia* species held at Cawthron Institute, Nelson, New Zealand (courtesy Lincoln MacKenzie): (A) *K. brevis* (Florida, USA); (B) *K. selliformis* (NZ); (C) *K. bidigitata* (NZ); (D) *K. mikimotoi* (NZ); (E) *K. brevisulcata* (NZ); and (F) *K. papilionacea* (NZ). *K. umbella* is not shown in this picture. Cell sizes of *Karenia* species vary between 13 and 50  $\mu$ m.

A fast-acting lipophilic toxin, gymnodimine, was identified and isolated from dredge oysters (*Tiostrea chilensis*) collected from Foveaux Strait, New Zealand during a 1994 bloom of *K. selliformis* (Daranas *et al.*, 2001; MacKenzie *et al.*, 1995; Mountfort *et al.*, 2006; Seki *et al.*, 1995). Although there were no reports of human intoxication, this species has been threatening New Zealand's rapidly developing aquaculture industry due to its ability to kill

shellfish (da Silva *et al.*, 2008; MacKenzie *et al.*, 1996). *K. selliformis* was also responsible for mass mortalities of fauna in the Gulf of Gabes and Tunisia in 1994, and probably in Kuwait Bay, Arabian Sea (da Silva *et al.*, 2008).

Wellington Harbour experienced a severe HAB in late summer 1998 (Chang, 1999b). A new species of *Karenia* genus was isolated and named *K. brevisulcata* (etymology: Latin brevis = short, sulcatum = groove) (Chang, 1999a). *K. brevisulcata* resembles *K. brevis* and *K. mikimotoi* in morphology but has a smaller cell size (13-25 µm long). Two distinct features were used to distinguish *K. brevisulcata* from other *Karenia* species: i) a very short apical groove on the ventral surface of the epicone (Figure 1-1); and ii) the position and shape of the nucleus. The spherical nucleus is located in the left lobe of the epicone or sometimes horizontally elongated (wider than long), extending from left to right in the hypocone during the division phase (Chang, 1999a). The identification of this as a new species of *Karenia* was confirmed by morphological differences and confirmatory phylogenetic analysis of LSU rRNA sequences (Chang, 1999a; Haywood *et al.*, 2007; Haywood *et al.*, 2004).

The 1998 bloom reached a maximum cell concentration of  $33.3 \times 10^6$  cells L<sup>-1</sup> in seawater and extended around the central and south-eastern coast of North Island, New Zealand from January to April, 1998 (Chang, 1999b; Chang *et al.*, 2001). Mass mortalities of marine biota were reported in the Wellington Harbour area from late February, 1998 (Chang, 1999b). The first deaths noticed were eels and flounder, which then spread across to other pelagic fish (e.g. yellow-eyed mullet, barracouta, mackerel, leather jacket, stargazers and kahawai) and marine invertebrates (e.g. sea slug, starfish, sea urchin and abalone). *K. brevisulcata* also threatened micro- and macroalgae. The organism can kill diatoms, and both naked and thecate dinoflagellates (naked: e.g. *K. mikimotoi*; thecate: e.g. *Alexandrium minutum* and *Prorocentrum lima*). Seaweeds, especially *Macrocystis pyrifera* were also killed by exposure to *K. brevisulcata*. Long term effects of the 1998 bloom on the local ecosystem of Wellington Harbour have been investigated (Gardner & Wear, 2006; Kröger *et al.*, 2006; Wear & Gardner, 2001). A recent study indicated that the subtidal benthic communities, particularly macro-invertebrate, require a longer period (> 4-5 years) to completely recover than the previous model predictions of approximately two years (Kröger, 2008).

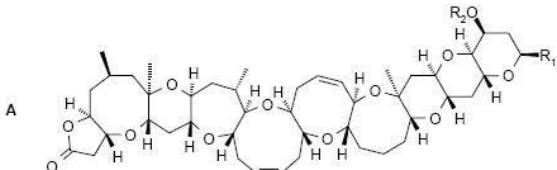
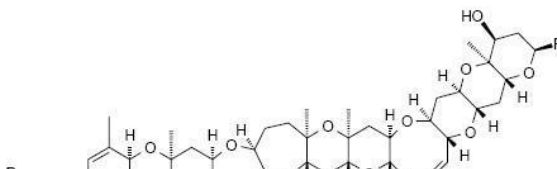
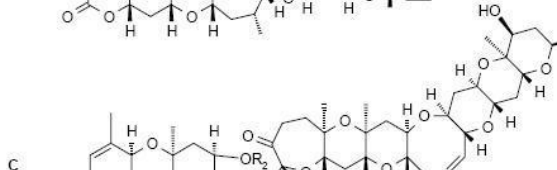
Respiratory and cutaneous illnesses were the major human symptoms reported, probably caused by direct exposure to seawater aerosols containing *K. brevisulcata* cells. Beach-goers, swimmers, and wind-surfers complained of a dry cough, a severe sore throat (like swallowing razor blades), runny nose, and skin and eye irritation. Cases of respiratory illness were first

reported along the Wairarapa Coast between late January and early February (over 250 people). By mid-February, the respiratory episode had spread north as far as Hawke Bay (over 100 cases), and from late February to the early March, over 150 people suffered from respiratory distress in the Wellington region with 87 cases in the Wellington Harbour (Chang, 1999b; Chang *et al.*, 2001). Furthermore, hatchery workers and divers working for the National Institute of Water and Atmospheric (NIWA) reported other symptoms including severe headaches, and a facial sun-burn sensation (Chang, 1999b).

### **2.3.2 *K. brevis* and NSP toxins**

NSP has been reported annually in the Gulf of Mexico, United States due to consumption of shellfish exposed to harmful algal blooms. The ciguatera-like symptoms include nausea, diarrhoea, abdominal pain and neurological symptoms. More recently respiratory distress and eye or nasal membrane irritation have been recognized following exposure to toxic aerosols or to contaminated seawater (Aune, 2008; Ciminiello & Fattorusso, 2006). NSP is not lethal and the patients generally recover in a few days. Davis (1948) first isolated the dinoflagellate *Karenia brevis*. However, the relationship between NSP and *K. brevis* was only confirmed nearly 20 years later in the 1960s (McFarren *et al.*, 1965).

Brevetoxins were isolated from *K. brevis* cultures using HPLC and the chemical structures of these compounds were elucidated by X-ray crystallography and nuclear magnetic resonance (NMR) in the 1980s (Lin *et al.*, 1981; Shimizu *et al.*, 1986). Brevetoxins are large, heat-stable polycyclic ether compounds which can be divided into three types (A, B, and C) according to their backbone structures (Figure 2-9). Backbones A and B are mainly ether ring structures for brevetoxins. The previous abbreviations for brevetoxin-A, brevetoxin-B and dihydrobrevetoxin-B are now brevetoxin-1, -2 and -3 respectively due to increased number of their analogues (Ishida *et al.*, 2004a; Ishida *et al.*, 1995; Lin *et al.*, 1981; McNabb *et al.*, 2006; Morohashi *et al.*, 1995; Morohashi *et al.*, 1999; Murata *et al.*, 1998; Ramsdell, 2008; Roth *et al.*, 2007; Shimizu *et al.*, 1986). The backbone C is only observed for brevetoxin-B3 (Morohashi *et al.*, 1995), and is partially similar to the backbone B in ether ring structure (Figure 2-9).

							
							
							
Backbone	R1	R2	[M+H] <sup>+</sup> , [M+NH <sub>4</sub> ] <sup>+</sup>	Backbone	R1	R2	[M+H] <sup>+</sup> , [M+NH <sub>4</sub> ] <sup>+</sup> , [M-H] <sup>-</sup>
BTX1	A	H	867.5, 884.5	BTX-B1	B	–	1018.5, 1035.5 1016.5
BTX7	A	H	869.5, 886.5	BTX-B2	B	–	1034.5, 1051.5 1032.5
BTX10	A	H	871.5, 888.5	BTX-B4	B	–	n = 12 1244.7, 1261.7 1242.7 n = 14 1272.7, 1289.7 1270.7
BTX2	B	H	895.5, 912.5	BTX-B3	C	–CO(CH <sub>2</sub> ) <sub>n</sub> CH <sub>3</sub>	n = 12 1137.7, 1154.7 1135.7 n = 14 1165.7, 1182.7 1163.7
BTX3	B	H	897.5, 914.5	BTX-B5	B	–	911.5, 928.5 909.5
BTX9	B	H	899.5, 916.5				
BTX8	B	H	917.5, 934.5				
BTX6	B	H	911.5, 928.5				
BTX5	B	–COCH <sub>3</sub>	937.5, 944.5				

**Figure 2-9.** Structures and molecular masses of brevetoxins (Quilliam, 2003a).

Brevetoxins can also be categorised into the primary toxins isolated from *K. brevis* culture (e.g. brevetoxin-1, brevetoxin-3) and the metabolites produced in shellfish (brevetoxin-B1 to brevetoxin-B4) (Ishida *et al.*, 2004b; Ishida *et al.*, 2004c). Brevetoxin-B5 is found in both algal and shellfish samples (Ishida *et al.*, 2004a; Ishida *et al.*, 2004b).

Figure 2-10 shows the metabolic routes of brevetoxin-2/-3 to shellfish metabolites brevetoxin-B1 to -B5. Brevetoxin-B5 is oxidative analogue of brevetoxin-2 through oxidation of the terminal aldehyde in brevetoxin-2 to a carboxylic acid (Ishida *et al.*, 2004a).





Brevetoxin-2 is the predominant brevetoxin isolated from *K. brevis* culture. Mouse bioassays showed the oral and i.p. LD<sub>50</sub> of brevetoxin-2 to be 6600 and 200 µg kg<sup>-1</sup> bw respectively (Baden & Mende, 1982). Brevetoxin-3 is more potent than brevetoxin-2 with oral and i.p. LD<sub>50</sub> of 520 and 170 µg kg<sup>-1</sup> bw, respectively (Baden & Mende, 1982). There is no accurate data for the acute mammalian toxicity of brevetoxin-1, but cytotoxicity experiments suggested Type A brevetoxins such as brevetoxin-1 were more potent than Type B brevetoxins (e.g. brevetoxin-2 or brevetoxin-3) in Neuro2a cells (Dechraoui *et al.*, 1999). The acute toxicity of brevetoxins to finfish has been tested using several species of small fish including zebrafish (*Danio rerio*), mosquito fish (*Gambusia affinis*), and minnow (*Cryptinodon variegates*). The potency of brevetoxins for ichthyotoxicity in the fish bioassays parallels their cytotoxicity (Landsberg, 2002; Ramsdell, 2008). Lethal concentration for 50% of fish (LC<sub>50</sub>) exposed for 24 h were 3-4 nM for brevetoxin-1, 16-25 nM for brevetoxin-2 and 10-37 nM for brevetoxin-3 (Baden, 1989). Opening the A ring (hydrolysis of the lactone) contributes to significant loss of binding affinity and elimination of cytotoxicity (Gawley *et al.*, 1995; Roth *et al.*, 2007). Both ring-closed and ring-opened brevetoxins were detected in eastern oyster (*Crassostrea virginica*) and *K. brevis* cultures using LC-MS (Plakas *et al.*, 2004; Wang *et al.*, 2004). Abraham *et al.* (2006) proposed that ring-closed brevetoxins produced by *K. brevis* cells are easy to hydrolyse to ring-opened analogues when released to seawater.

Brevetoxins are neurotoxins and acting on VGSC which is a single trans-membrane protein complex which consists of a large primary (alpha) subunit of approximately 220-260 kDa, and auxiliary beta subunits of 33-36 kDa (Catterall, 1984, 2000; Catterall *et al.*, 2007). The beta subunits have only been identified in vertebrates and the four members (β1 to β4) can indirectly alter the physiological properties of VGSC and subcellular localization through interacting with different alpha subunits (Catterall *et al.*, 2007). The alpha subunit is a large polypeptide consisting of four homologous domains (DI-DIV) each with six trans-membrane segments (S1-S6) (Catterall *et al.*, 2007; Marban *et al.*, 1998; Ramsdell, 2008). The central pore consists of four domains is highly selective and controlled by a voltage sensor (S4 segment of each domain) which responds to the level of the membrane potential (Marban *et al.*, 1998). To date, six neurotoxin receptor sites have been identified on VGSC (Catterall *et al.*, 2007) and five sites are shown in Figure 2-11. The preliminary studies found brevetoxins did not interact with the receptor sites 1 to 4 but enhance Na<sup>+</sup> uptake through a veratridine-enhanced pathway (Catterall & Risk, 1981; Poli *et al.*, 1986). Later studies found that brevetoxins and CTXs can bind to the same segments IS5 and IVS6, resulting in VGSC to remain open and uncontrolled Na<sup>+</sup> influx into the cells (Bidard *et al.*, 1984; Dechraoui *et al.*,

1999; Lombet *et al.*, 1987; Rein *et al.*, 1994). These two trans-membrane segments have been named Site 5 for VGSC (Catterall & Risk, 1981). In contrast STX and tetrodotoxins (TTX) are VGSC antagonists (blockers) acting at Site 1 and Veratridine is a neurotoxin that acts at the receptor site 2 (IS6) and persistently activates VGSC through an allosteric mechanism (Catterall *et al.*, 2007).

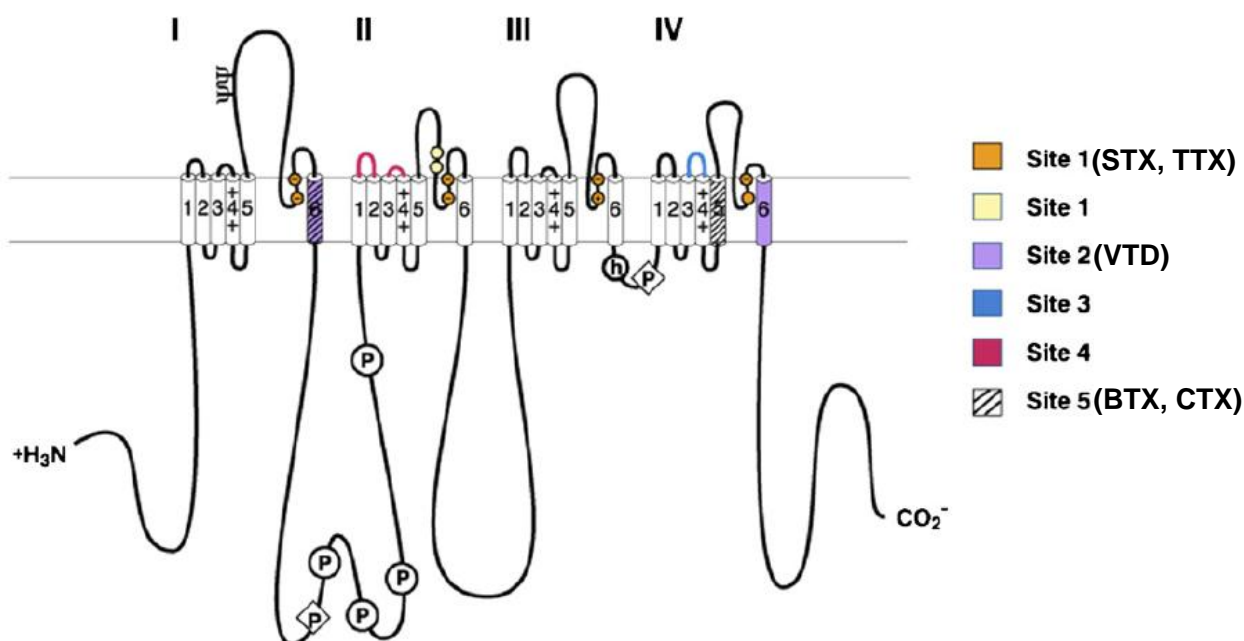


**Figure 2-11.** Neurotoxin receptor sites on voltage-gated sodium channel (VGSC) (modified from Catterall *et al.*, 2007). Locations of the neurotoxin receptor sites on mammalian sodium channels are illustrated by colours. Saxitoxin (STX) and tetrodotoxin (TTX) bind to Site 1 and act as pore blockers. Veratridine (VTD) binds to Site 2 and persistently activates VGSC through an allosteric mechanism. Brevetoxins (BTX) and ciguatoxins (CTX) binds to Site 5 and act as pore openers, causing enhanced activation of VGSC.

### 2.3.3 *K. mikimotoi* and its complex toxins

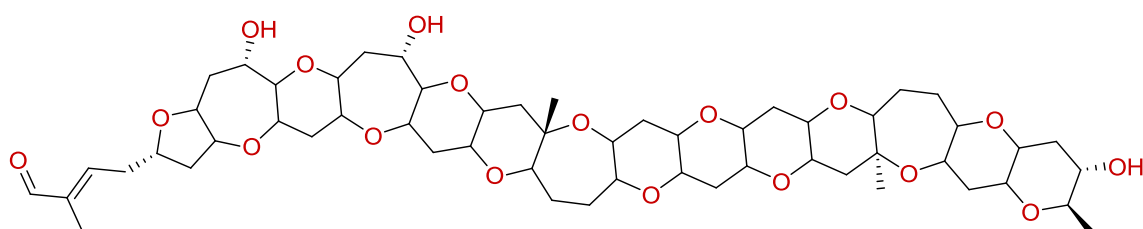
*K. mikimotoi* was responsible for widespread HABs around the world and mass mortalities of marine biota. Although the related studies on this species have been carried out for decades, the fish kill mechanisms of *K. mikimotoi* are complicated and have not been solved. *K. mikimotoi* produces an array of potentially toxic compounds including gymnocins, haemolysins (glycolipids and polyunsaturated fatty acids) and ROS (Haywood *et al.*, 2004; Satake *et al.*, 2002; Satake *et al.*, 2005; Yamasaki *et al.*, 2004; Yasumoto *et al.*, 1990). Fish gill damage by haemolysins was proposed as the primary fish kill mechanism of *K. mikimotoi* (Hallegraeff, 1995). However, more work based on laboratory bioassays suggested environmental stressors resulting from high cell densities may also contribute to fish mortality in *K. mikimotoi* HABs (Landsberg, 2002; Silke *et al.*, 2005; Yamasaki *et al.*, 2004).

Gymnocins have typical ladder-like polycyclic ether structures analogous with brevetoxins, yessotoxin, CTX and MTX. There have been three derivatives identified and purified from *K. mikimotoi* cultures (Figure 2-12). Gymnocin-A and -B have the same 2-methyl-2-butenal side-chain, but their ether ring structures are different (Hashimoto *et al.*, 1981; Satake *et al.*, 2002; Satake *et al.*, 2005). The number of contiguous ether rings (CERs) for gymnocin-B is 15, the largest among the polyether toxins prior to the structural elucidation of KBT-F (Hamamoto *et al.*, 2012; Satake *et al.*, 2005). Gymnocin-C (m.w. 1143) is a new analogue produced by a Japanese strain of *K. mikimotoi* and is characterized by 15 CERs and a propenal side chain (Y. Oshima, pers. comm.).

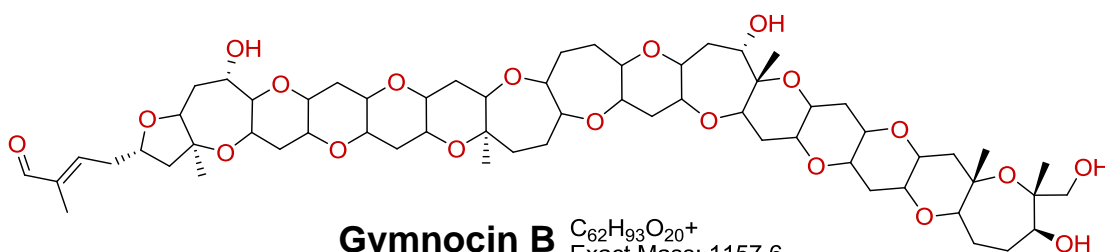
The IC<sub>50</sub>'s against mouse leukemia cells were 1.3  $\mu$ M for gymnocin-A and 1.5  $\mu$ M for gymnocin-B (Satake *et al.*, 2002; Satake *et al.*, 2005). The fish bioassay against minnow (*Tanichthys albonubes*) revealed gymnocins are weakly toxic to fish (Satake *et al.*, 2002; Satake *et al.*, 2005). Enhanced toxicity of *K. mikimotoi* through direct cell to cell contact (Zou *et al.*, 2010) supported the hypothesis by that the toxic agents produced by this species are short-lived and act short-range ( $< 175 \mu$ m) (Gentien *et al.*, 2007). The extremely low solubilities of these toxins in water may explain the discrepancy between mass mortalities of fish in the field and the weak toxicity assessed in laboratory fish bioassays. The mammalian toxicity of these toxins remains unknown. A larger compound (gymnocin F, m.w. 2079) was isolated and purified by Japanese researchers (Oshima, 2007). This toxin shows extremely highly cytotoxicity against P388 and is likely to be the main toxic agent produced by *K. mikimotoi* to fish in red tide events (M. Satake, pers. comm.).

Haemolysins derived from *K. mikimotoi* have been reported including digalactosyl monoacylglycerol (MGDG), digalactosyl diacylglycerol (DGDG) and polyunsaturated fatty acids (PUFAs) (Landsberg, 2002). Parrish *et al.* (1998) evaluated lipid compositions of *K. mikimotoi* (7.6% MGDG & 8.9% DGDG) and another *Gymnodinium* spp (14.2% MGDG & 20.8% DGDG). Although the fatty acid compositions were different in each species, the dominant fatty acid was C18:5n3 (up to 25.1% in *K. mikimotoi*). The toxic effects of these PUFAs (C18:5n3, C20:5n3, C20:4n6, and C22:6n3) produced by *K. mikimotoi* (as *Gyrodinium aureolum* or *Gymnodinium* cf. *nagasakiense*) were reported including haemolysis of red blood cells, growth inhibition of the diatom *Chaetoceros gracile*, and reduction of bioluminescence in *Photobacterium phosphoreum* (Arzul *et al.*, 1995; Landsberg, 2002; Yasumoto *et al.*, 1990). ROS such as superoxide anion (O<sub>2</sub><sup>-</sup>) and hydrogen peroxide (H<sub>2</sub>O<sub>2</sub>), are main toxic agents involved in fish kills caused by raphidophyceae flagellates e.g. *Chattonella marina* and *Heterosigma akashiwo* (Marshall *et al.*, 2003). *K. mikimotoi* was also

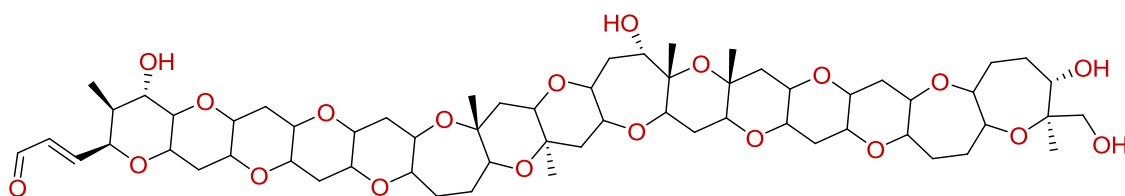
reported to produce ROS (Yamasaki *et al.*, 2004), but ROS production depends on the strains (Zou *et al.*, 2010). Yamasaki *et al.* (2004) suggested that  $O_2^-$  and  $H_2O_2$  were generated via separate pathways in *K. mikimotoi* cells. High intracellular concentrations of  $H_2O_2$  indicate that such polyunsaturated molecules are prone to peroxidation (Mooney *et al.*, 2007). In addition, PUFAs can pose biological effects on fish gill or liver through inhibition of Na-, K-, Mg- and vacuolar ATPases (Fossat *et al.*, 1999; Sola *et al.*, 1999), but ROS from PUFA degradation are unlikely to be directly involved in lethal effects of *K. mikimotoi* on marine life (Fossat *et al.*, 1999; Zou *et al.*, 2010). The relationship of PUFAs, ROS and associated toxicity are still unclear. The synergistic effects of ROS and fatty acids are more likely to contribute to the ichthyotoxicity (Marshall *et al.*, 2003; Mooney *et al.*, 2007). It is also possible that more toxic aldehydes are formed by ROS catalysed peroxidation of PUFAs.



**Gymnocin A**  $C_{55}H_{81}O_{18}^+$   
Exact Mass: 1029.5



**Gymnocin B**  $C_{62}H_{93}O_{20}^+$   
Exact Mass: 1157.6



**Gymnocin C**  $C_{61}H_{91}O_{20}^+$   
Exact Mass: 1143.6

**Figure 2-12.** Structures of gymnocin-A, -B and -C.

### 2.3.4 *K. selliformis* and gymnodimines

Gymnodimine was first identified in 1994 when oysters (*Tiostrea chilensis*) from Foveaux Strait, New Zealand were found to be toxic at high levels to mice (MacKenzie *et al.*, 1995). *K. selliformis* was finally confirmed as the gymnodimine producer and was implicated in the widespread damage to wild shellfish during the 1994 bloom event in the South Island. Furthermore, gymnodimine was isolated and its structure was elucidated by UV, LC-MS and NMR (Seki *et al.*, 1995, 1996; Stirling, 2001). It is a complex pentacyclic compound (C<sub>32</sub>H<sub>45</sub>NO<sub>4</sub>) incorporating a 16-membered carbocyclic ring, a cyclic imine and a butenolide ring (Figure 2-13).

Gymnodimine did not show haemolytic activity or cytotoxicity (Seki *et al.*, 1996), but this compound is a neurotoxin acting on the nicotinic ACh receptor without potency to activate VGSC (Kharrat *et al.*, 2008; Seki *et al.*, 1996). It is highly toxic to mammal by i.p. administration and can cause similar poisoning symptoms to 13-desmethyl-C-spirolide in mice (Munday *et al.*, 2004). The LD<sub>50</sub> was 96 µg kg<sup>-1</sup> bw following i.p. administration and 755 µg kg<sup>-1</sup> bw after oral administration by gavage (Munday *et al.*, 2004). No toxicity was observed in mice after administration with food containing gymnodimine up to a dose of 7500 µg kg<sup>-1</sup> bw suggesting that gymnodimine was a low risk to humans through contaminated seafood (Munday *et al.*, 2004). Gymnodimine is toxic to shellfish (MacKenzie *et al.*, 1996) and potential ichthyotoxic (Seki *et al.*, 1996). The lethality to freshwater fish, *Tanichthys albonubes*, was 0.10 ppm (20 nM) (Seki *et al.*, 1996). When *T. albonubes* were exposed to 0.2 mM gymnodimine, both damages of gill lamellar epithelial cells and the chloride cells were observed (Terao *et al.*, 1996).

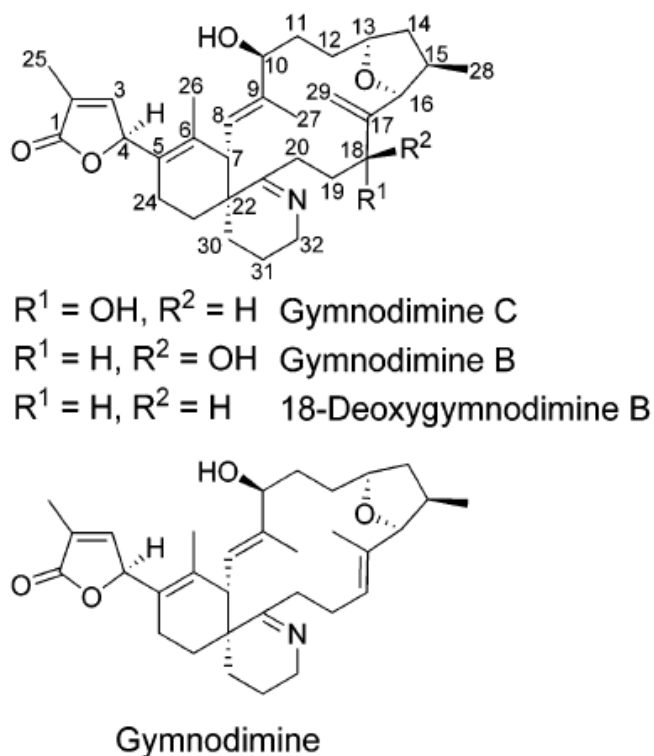


**Figure 2-13.** Structures of gymnodimines (Miles *et al.*, 2003).

Two analogues (gymnodimine-B and -C) were also identified and isolated from *K. selliformis*, the NZ strain (Miles *et al.*, 2000, 2003). Both are oxidised analogues of gymnodimine and contain an exocyclic methylene at C-17 and an allylic hydroxyl group at C-18 (Figure 2-13). Gymnodimine-B is isomeric with gymnodimine-C at C18. It was proposed that both analogues originated from a precursor such as 18-deoxygymnodimine B (an isomer of gymnodimine, Figure 2-13) via oxidation. Although the toxicities of gymnodimine-B and -C remains unknown, they are expected to be highly toxic because the spiro-imine moiety appears to be crucial to the biological activity of these compounds including gymnodimines, spirolides and pinnatoxins (Miles *et al.*, 2000, 2003).

### 2.3.5 *K. brevisulcata* and its biotoxins

The toxin complex produced by *K. brevisulcata* was initially characterized using a crude extract of cultures and was designated Wellington Harbour toxin (WHT). The toxic effects of WHT appear to be mediated by a range of toxins. Initial research on biological, chemical and toxicological aspects of WHT were carried out by New Zealand researchers (Chang, 1999a, b; Haywood *et al.*, 2004; Keyzers, pers, comm.; Truman, 2007; Truman *et al.*, 2005). WHT was stable in neutral and acidic conditions but was less stable in the presence of base. WHT

contained an acidic group such as carboxylic or sulfamic acid, but no basic group (Keyzers, pers, comm.). Thermal- and oxidative stabilities were tested by Chang (1999b). Boiling cultures for half an hour did not completely eliminate toxicity. Ozonation treatment was the most effective and efficient way to eliminate toxicity. During the 1998 outbreak in the Wellington Harbour, ozone was used to protect the NIWA hatchery facilities (Chang, 1999b).

Toxicological tests by MBA (i.p injection) conducted at two independent labs revealed WHT contained nephrotoxins and gymnodimine-like fast acting toxins (Chang, 1999b; Keyzers, pers, comm.). Chang (1999b) reported that WHT is less likely to cause human intoxication via ingestion, but this toxin has strongly haemolytic activity (L. Briggs, per. comm.). Neuro2a assay indicated that WHT had a unique, distinctive and reproducible “signature” that is different from the known VGSC-dependent algal toxins such as brevetoxins, STX and CTX (Keyzers, pers, comm.; Truman *et al.*, 2005). Truman (2007) suggested some of the activity of WHT was attributed to activation of sodium channels (Figure 2-14). However, WHT might also exert effects on calcium channels (Y. Oshima, pers. comm.). The final isolation of WHT was incomplete, although the Neuro2a assay did assist in isolation of some chemical fractions containing WHT activity (Keyzers, pers, comm.).

Researchers at Tohoku University, led by Yasukatsu Oshima, partially identified 6-8 bioactive polyether compounds with m.w. 1900 to 2200 from the lipophilic extract of *K. brevisulcata* cultures produced at Cawthron Institute (Oshima, 2007). The multistep chromatographic separations were guided by cytotoxicity assays (P388 mouse leukemia cell line). These lipophilic toxins were named KBTs which are components of the toxin complex formerly named WHT. NMR data suggested some structural similarities to gymnocins including many fused polycyclic ether rings and a  $\beta$ -unsaturated aldehyde. Their molecular size is approximately double that of gymnocin-A. The complete structures of all the KBTs remain to be determined and are the subject of continuing collaboration between Cawthron Institute and the University of Tokyo (with Masayuki Satake).



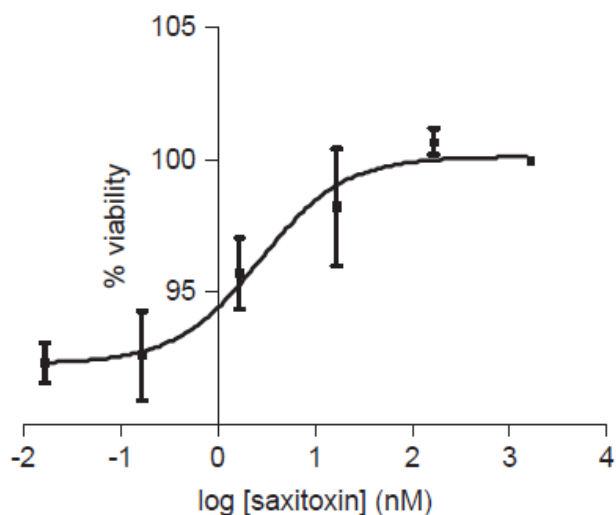


**Figure 2-14.** The effect of saxitoxin (STX) in antagonising Wellington Harbour toxin (WHT) in the Neuro2a assay (Truman, 2007). Values are means  $\pm$  SEM of three independent dose-response experiments where cells were exposed to the same concentration of WHT and increased concentration of STX.

In addition to the large lipid soluble KBTs, preliminary research using LC-MS at Cawthron Institute has shown that *K. brevisulcata* cultures produce two more water-soluble compounds: BSX-1 ( $[M+H]^+$  917  $m/z$ ) and BSX-2 ( $[M+H]^+$  873  $m/z$ ). Both compounds are less toxic than the KBTs in MBA and *in vitro* cell assays (R. Munday & P. Truman, pers. comm.). Studies on both KBTs and BSXs are at an early stage due to the lack of purified toxins. This thesis details the chemical and toxicological investigations of these novel toxins.

## Chapter 3

### Laboratory culturing of *Karenia brevisulcata*

#### 3.1 Introduction

Some bioactive secondary metabolites produced by microalgae are potentially toxic to mammal and aquatic organisms (Shimizu, 1993). However, it has only recently emerged that these toxins possess structures that might interest pharmacologists (López *et al.*, 2011; Waters *et al.*, 2010). Investigations of the activities of toxins using either *in vivo* or *in vitro* models have often been constrained by lack of sufficient amounts of materials for detailed studies of their mode-of-action and pharmacology. Commercial analytical standards are expensive and also limited in amounts and the range of toxins. For a new toxin, the minimum amount of pure compound usually required to start preparation of a certified standard is 10 mg. Chemical syntheses of marine biotoxins are generally complex and inefficient due to their molecular complexity (Johannes *et al.*, 2005; Stivala & Zakarian, 2009; Tsujimoto *et al.*, 2002).

Biosynthesis of these phytotoxins by marine algae is still the major access route to obtain sufficient compounds for research. Dinoflagellates and cyanobacteria are major producers of novel bioactive compounds, although some toxins are produced by diatoms, green algae, brown algae and red algae (Faulkner, 1996; Shimizu, 2003). While culturing non-dinoflagellate microalgae in up-scaled cultures has been possible (Grima *et al.*, 2000; Grima *et al.*, 2001; Grima *et al.*, 2003), dinoflagellate cultures are often difficult to mass culture. These microalgae have fastidious growth requirements and have low growth rates compared with other genera of marine micro-algae (Camacho *et al.*, 2007; Hallegraeff & Gollasch, 2006; John *et al.*, 2000). Studies concerning this issue have been carried out for decades (Tang, 1996). Slower photosynthetic rates are believed to be the major reason for lower growth rates of dinoflagellate in comparison to diatoms (Chan, 1980). The yields of biomass for dinoflagellates are usually low ( $10^6$  to  $10^7$  cells L<sup>-1</sup>) and typical toxin quotients are in the range 0.1 – 10 pg cell<sup>-1</sup>. As a result the yields of biotoxins in the culture medium are also low, typically 10 – 100 µg L<sup>-1</sup> (Hu *et al.*, 2006; Reguera & Pizarro, 2008). Large scale production of biotoxins at Cawthron has employed 15 L or 200 L plastic carboys to bulk culture microalgae (Dragunow *et al.*, 2005; Loader *et al.*, 2007; Miles *et al.*, 2003; Munday *et al.*, 2004). This approach however has limitations because: i) the series cultures have a large footprint; ii) the cultures are not growth optimised; and iii) with the exception of the lighting

regime and ambient temperature, there are limited mechanisms for control of culture conditions.

*K. brevisulcata* is a toxic dinoflagellate which caused a severe harmful algae bloom event in Wellington Harbour, NZ in 1998 (Chang, 1999a, b). This dinoflagellate can produce at least two BSXs and 6-8 KBTs. However, the studies of *K. brevisulcata* and its novel toxins are at early stage due to lack of pure compounds. Knowledge of *K. brevisulcata* growth, toxin production, and fate under laboratory conditions is still limited. In this study several culturing systems were investigated for *K. brevisulcata* to optimise cell growth and toxin production. LC-MS/MS techniques were used to detect, identify and monitor novel toxins in both batch and continuous cultures. These studies will contribute to a better understanding of *K. brevisulcata* dinoflagellate growth and toxin production mechanisms. The crude toxins produced by large scale cultures of *K. brevisulcata* in this study were eventually isolated and purified using multi-step column chromatography for characterisation and further application in analytical, chemical, biochemical and pharmacological research.

## **3.2 Materials and methods**

### **3.2.1 Microalgae and batch cultures**

The toxic dinoflagellate *K. brevisulcata* (CAWD 82) was collected from the Wellington Harbour in 1998 and is held in Cawthron Institute culture collection of microalgae (CICCM), Nelson (Haywood *et al.*, 2004). Cultures of *K. brevisulcata* were grown in batch cultures (15L or 70 L plastic carboys) in 100% GP artificial seawater medium enriched with selenium (100% GP+Se medium) (Loeblich & Smith, 1968) at  $18 \pm 1^\circ\text{C}$  under a 12/12 light/dark cycle at  $60 \mu\text{Ein.m}^{-2}\text{s}^{-1}$ . Growth culture stock grown in glass flasks (2 L) were initiated by inoculation of 10 to 20 % by volume of culture stock (maintained by monthly transfer). Toxin yields and cell growth were monitored by subsampling ( $n \geq 2$ ) at intervals of 2-3 days. LC-MS was conducted to analyse toxin production using SPE of 50 mL aliquots of culture (Sections 3.2.3 & 3.2.4). For cell counting, 25  $\mu\text{L}$  aliquots of culture were diluted to 1 mL with seawater medium in 12 well plates (Becton, Dickinson, UJ, USA) and treated with Lugol's iodine preservative (20  $\mu\text{L}$ /well). Lugol's kills, stains and preserves normal shape of microalgal cells over 1-2 weeks storage. Following incubation for 2 hr, cell densities were determined using inverted microscopy (Olympus TMT-2).

For  $^{13}\text{C}$  culturing,  $^{13}\text{C}$ -labelled sodium bicarbonate (99%  $\text{NaH}^{13}\text{CO}_3$ ) was purchased from Masstrace, Inc. (MA, USA), or Cambridge Isotope Laboratories, Inc. (MA, USA). *K. brevisulcata* was grown in 15 L carboys and 250 mg  $\text{NaH}^{13}\text{CO}_3$  were added at Day 0 and Day 7 (total 500 mg/carboy). Cell growth was monitored as above. The cultures were maintained for 12-20 days, and harvested at nearly maximal cell density.

### 3.2.2 Photobioreactor system cultures

A prototype automated bioreactor system was designed to optimise dinoflagellate growth and biotoxin yields under laboratory conditions and applied to the growth of *K. brevisulcata* (Beuzenberg *et al.*, 2012; Mountfort *et al.*, 2006). The preliminary experiments used a large acrylic plastic cylinder (52 L) with diameter of 20 cm to culture dinoflagellates. This reactor vessel was substituted with a 5.4 L glass cylinder with diameter of 9 cm for later experiments (Figure 3-1). The glass vessel was manufactured for optimal light access to reduce any effects of photo-inhibition on cell growth. Culture growth and condition were monitored and controlled using an Omron Corporation CJM series programmable logical control unit (PLCU) coupled with a pH probe (AlphaTech Systems Ltd) and a through-beam optical sensor (E3X series, Omron Corporation), using turbidity as a measure of cell density. pH was automatically controlled by PLCU by  $\text{CO}_2$  injections while turbidity (or cell density) was controlled in continuous mode to a set value equivalent to a maximum cell density by pumping fresh media into the bioreactor. Data logging of values from both sensors and process parameters e.g. output actions, out-of-limit alarms, mains power on/off, lighting on/off, occurred at intervals of at least every 15 minutes.

Batch photobioreactor culture was initiated by addition of 15 to 20 % by volume of inoculum (*K. brevisulcata* culture stock in 1 L glass flasks) in the late log phase of growth to medium (52 L for the large bioreactor and 5.4 L for the glass bioreactor). A magnetic stirrer was used to gently mix medium. The photobioreactor was aerated with sterile air through a syringe filter (0.22  $\mu\text{m}$ , Millipore, France) using an aquarium pump at low flow. The culturing conditions were similar to those for batch barrel and carboy cultures except the lighting strength was 38  $\mu\text{Ein.m}^{-2}\text{s}^{-1}$  and  $\text{CO}_2$  was introduced to maintain the pH at 8.3. After subsampling for initial cell density, the photobioreactor was operated under batch mode until optimal growth was achieved. Turbidity and pH were continuously monitored throughout and subsamples ( $n \geq 2$ ) were taken twice per week for cell counts and toxin monitoring. Because the turbidity units decreased with increased growth, units were plotted highest to lowest

against time of batch culturing. Correlations between growth determined by turbidometry and cell counts were good ( $R^2 = 0.88-0.92$ ) for mid-log growth (Beuzenberg *et al.*, 2012). In batch mode without pH control, the pH shift over the 24 hr because of algal cell “breath” was 0.15 to 0.2 pH units in early to mid log phase of growth but near full growth the shift could be as much as 0.6 pH units (Beuzenberg *et al.*, 2012). Variation in pH in consecutive readings for 15 seconds was  $< 0.05$  units. An initial pH of 8.3 provided the maximum biomass yields of *K. selliformis* in our preliminary bioreactor experiments (Beuzenberg *et al.*, 2012), and was applied as the pre-set control pH in this *K. brevisulcata* experiment.

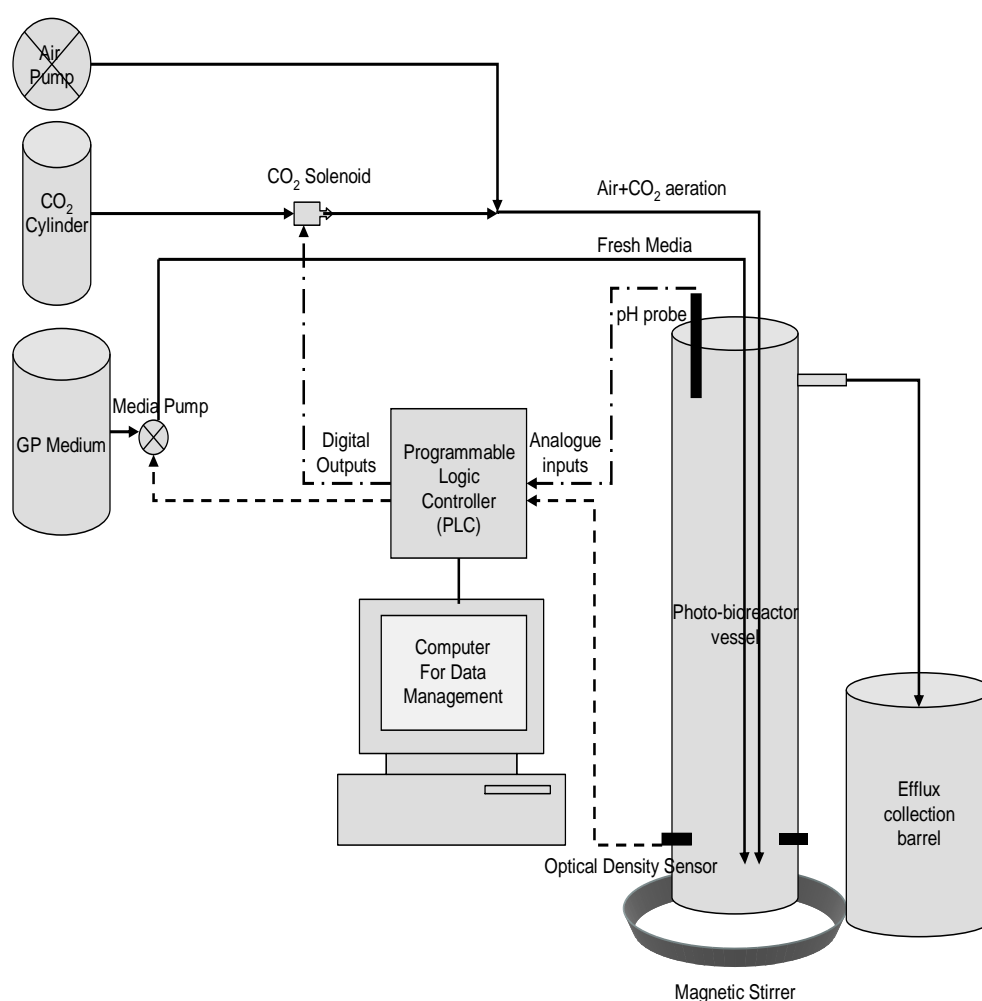


**Figure 3-1.** Schematic diagram showing automated photobioreactor system with electronic process control for pH ( — · — · — ) and optical density ( - - - - - ) [modified from (Beuzenberg *et al.*, 2012)].

During bioreactor batch culturing, the turbidity and cell density were well correlated and the growth was allowed to proceed to near 50% maximal growth. The bioreactor was then

operated in continuous mode during which a pre-set turbidity was maintained by pumping of fresh media into the bioreactor controlled by the PLCU using feedback from the turbidity sensor. Cell densities were also confirmed through cell counts twice per week ( $n \geq 2$ ) when subsamples were collected for toxin monitoring. Dilution rate was determined from the displacement volume. The outflow culture was stored in a covered container at  $-20\text{ }^{\circ}\text{C}$  and eventually combined for harvesting.

### **3.2.3 Extraction of toxins from *K. brevisulcata* culture for LC-MS monitoring**

For monitoring of toxins production in both carboy and photobioreactor cultures, subsamples (50 mL) were extracted using Strata-X Solid Phase Extraction (SPE) cartridges (60 mg per 3 mL, Phenomenex Inc, USA) preconditioned with methanol (3 mL) and Milli-Q water (MQ, 3 mL). After loading the culture, the cartridges were washed with MQ (3 mL) and 20% methanol (3 mL). The toxins were then eluted with methanol (3 mL) followed by acetone (3 mL). A portion of the acetone eluant (0.6 mL) was dried under a gentle steam of oxygen-free nitrogen and redissolved in 0.6 mL of methanol eluant and 0.15 mL of MQ for LC-MS (total 0.75 mL in 80% methanol per sample; concentration factor 13.3x).

### **3.2.4 LC-MS analysis of toxins**

LC-MS analysis of BSX toxins was conducted using a Waters Acquity uPLC system (Waters, Milford, MA) coupled with a Waters-Micromass Quattro Premier XE MS (Manchester, UK). MassLynx Ver.4.1 software (Waters, Milford, MA) was used for instrument control, data acquisition and data processing. Separation of BSXs was achieved based on the same column and gradient as described in Section 4.2.3.1. The electrospray ionisation source was operated in positive-ion mode ( $\text{ESI}^+$ ) at  $100\text{ }^{\circ}\text{C}$ , capillary 2.5 kV, cone 45 V, nitrogen gas desolvation  $800\text{ L hr}^{-1}$  ( $400\text{ }^{\circ}\text{C}$ ). Toxins were quantitatively analysed using a seven channels SIR method (Method 1, Section 4.2.3.1) (see Table 4-2). For initial large photobioreactor cultures, only BSX-1 and BSX-2 were monitored. The concentrations of BSXs were calculated using the linear calibration for the response of brevetoxin-2. A research standard material (RSM) for brevetoxin-2 was purchased from University of North Carolina, Wilmington (UNCW), USA and calibration solutions prepared (50 – 1000 ng/mL in 80% methanol). Note: an RSM is not as thoroughly characterised as a CRM where a variety of techniques and comparisons are carried out to provide a certified value, usually for a solution

concentration e.g. the CRMS for some marine biotoxins available from NRCC, Halifax.

### 3.2.5 Harvesting of bulk cultures

The harvesting method for *K. brevisulcata* cultures was modified from that used in a previous study for yessotoxin (Loader *et al.*, 2007). The toxins were extracted from mature cultures of *K. brevisulcata* using Diaion HP20 resin (250-850  $\mu\text{m}$ , Sigma-Aldrich, Castle Hill, NSW). Pre-washed resin was packed in a polypropylene column (40 x 8 cm i.d.). *K. brevisulcata* cultures were transferred to a 200 L barrel and cells lysed by addition of acetone to 7% v/v. The cultures were settled for 1 hour and diluted with reversed osmosis purified water (RO water) to 5% v/v acetone before pumping at 0.3 L/min through a filter system (10  $\mu\text{m}$  glass fibre string filter plus a 125 mm GS25 flat filter) followed by the HP20 resin column. The column was then washed with RO water and the HP20 resin was transferred to a 2 L flask. Toxins were recovered by soaking the resin with AR acetone (1L) and decanting (3x). The combined acetone extract was rotary evaporated to produce a dried crude extract.

## 3.3 Results and discussion

### 3.3.1 Batch culturing of *K. brevisulcata* in different culturing systems

Three culturing systems (barrels, carboys and photobioreactor) were investigated for *K. brevisulcata* to optimise cell growth and toxin production. A total of 1428 litres of mass cultures were produced under laboratory conditions being 368 litres of batch barrel cultures, 794 litres of batch carboy culture, and 266 litres of bioreactor culture (batch and continuous).

Cell growth and toxin production in different vessels are shown in Figure 3-2. The batch *K. brevisulcata* cultures in carboys, barrels, and bioreactor reached the maximum growth ( $G_{\text{max}}$ ) at day 14, 24, and 26 respectively (Table 3-1). The  $G_{\text{max}}$  in batch carboy cultures ( $31 \times 10^6$  cells  $\text{L}^{-1}$ ) is very similar to the reported highest cell population ( $33.3 \times 10^6$  cells  $\text{L}^{-1}$ ) in Wellington Harbour Bloom, 1998 (Chang, 1999a, b). The bioreactor system (5.4 L glass cylinder) was designed to maximize light access to cultures and culture pH was controlled by PLCU through automated injection of  $\text{CO}_2$  to optimise microalgae growth and toxin production (Mountfort *et al.*, 2006). The bioreactor operated in batch mode produced 4-fold higher  $G_{\text{max}}$  ( $119 \times 10^6$  cells  $\text{L}^{-1}$ ) than batch carboy culture ( $31 \times 10^6$  cells  $\text{L}^{-1}$ ) and 5-fold higher  $G_{\text{max}}$  than batch barrel cultures ( $24 \times 10^6$  cells  $\text{L}^{-1}$ ) (Table 3-1, Figure 3-2), confirming that a

photobioreactor can provide enhanced growth of *K. brevisulcata* over barrels or carboys where lighting and pH may be sub-optimal. However, growth of *K. brevisulcata* was the most efficient in carboys in terms of growth rate ( $\mu = 0.086 \text{ days}^{-1}$ ), compared with barrels and bioreactor ( $\mu = 0.05 - 0.057 \text{ days}^{-1}$ ) (Table 3-1).

Most of the *K. brevisulcata* cultures used for toxin production were grown in carboys. Cultures in these vessels followed a reproducible pattern of growth. Cell numbers peaked at  $20\text{-}40 \times 10^6 \text{ cells L}^{-1}$  at 12-18 days following inoculation and declined rapidly to less than  $5 \times 10^6 \text{ cells L}^{-1}$  at day 30 (Figure 3-2B). The culture was essentially dead after 40 days. These changes in cell growth were probably mainly due to changes in media pH (starting 8.3, rising to over 9 at day 40) and nutrient levels because the bioreactor with pH control and media replacement gave a time-dependent increase in *K. brevisulcata* cell growth (Figure 3-2C). A similar cell growth trend was also observed for batch barrel cultures in Figure 3-2A. Because there was no validated method to monitor KBTs production at the time that *K. brevisulcata* was cultured, the barrel cultures were harvested and the bioreactor was switched to continuous mode at day  $25 \pm 1$  to minimise losses of KBTs by degradation.

During the culturing of *K. brevisulcata*, LC-MS SIR was used to quantitatively analyse six BSXs in *K. brevisulcata* cultures using brevetoxin-2 as the calibrant. BSX-1 was predominant and accounted for 67%, 44%, and 60% of total BSXs produced at  $G_{\max}$  in bioreactor, carboys, and barrels, respectively (Table 3-1). BSX-2 was the second most dominant BSX toxin in barrels and bioreactor. However, in carboys, BSX-3 plus its ring-closed analogue (BSX-6) accounted for 48% of total BSXs, which was the same as that for BSX-1 plus BSX-4 (ring-closed BSX-1).

The concentration of total BSX toxins ( $33 \mu\text{g L}^{-1}$ ) in bioreactor batch culture was 1.3-fold higher than in batch carboy culture ( $25 \mu\text{g L}^{-1}$ ) and 3.6-fold higher than in batch barrel culture ( $9.1 \mu\text{g L}^{-1}$ ) at  $G_{\max}$  (Table 3-1). The production of ring-opened BSXs (BSX-1 to -3;  $8.6$  to  $30.2 \mu\text{g L}^{-1}$ ) was higher than that of ring-closed BSXs (BSX-4 to -6;  $0.5$  to  $6 \mu\text{g L}^{-1}$ ) in all batch cultures. The concentrations of ring-opened BSXs increased consistently over time in all batch cultures (Figure 3-2), even after the batch carboy culture collapsed (no swimming algal cells observed). This suggested that the ring-opened products except BSX-3 were very stable in seawater. BSX-3 was degraded later in culturing stage when the pH exceeded 9. The production of ring-closed BSXs appeared to be cell concentration-dependent (Figure 3-2B, C) except in barrels where the highest concentration of ring-closed BSXs reached at day 18 (Figure 3-2A). The observation from barrel cultures supported the previous finding that



changes in media pH and nutrient levels at later culturing stage significantly affected dinoflagellate growth as well as toxin production. Recent studies on *K. brevis* confirmed that brevetoxins can be hydrolysed in the A ring when released from algal cells into seawater (Abraham *et al.*, 2006; Hua & Cole, 1999; Roth *et al.*, 2007). We also hypothesize that ring-closed BSXs are biosynthesised prior to production of ring-opened metabolites. These latter hydrolysed products may be mainly released to or formed in seawater culture medium which BSX-3 is less stable than the other two ring-opened BSXs.

The highest cell yields for ring-opened and ring-closed BSXs were both produced in carboys (0.58 and 0.19 pg cell<sup>-1</sup> respectively) where *K. brevisulcata* growth was the most efficient. The mean cell yields for total BSX at  $G_{\max}$  was ordered: carboys (0.77 pg cell<sup>-1</sup>) > barrels (0.38 pg cell<sup>-1</sup>) > the bioreactor (0.30 pg cell<sup>-1</sup>) (Table 3-1). It is strange that bioreactor gave the lowest cell yields for total BSXs, but the highest  $G_{\max}$  (Table 3-1). The results showed that conditions favouring *K. brevisulcata* growth do not necessarily enhance BSXs production and that the pathways for cell growth and for BSXs metabolism may respond differentially to different culture conditions (Beuzenberg *et al.*, 2012). The fate of KBTs production under laboratory conditions is still unclear. KBT production is probably more associated with *K. brevisulcata* cell proliferation.

### 3.3.2 Bioreactor culturing of *K. brevisulcata* under continuous mode

Continuous culture of *K. brevisulcata* was obtained by switching from the batch mode with introduction of fresh media to maintain the cell concentration at between one half and two thirds that for maximal growth in batch culture. The concentrations of cells and total BSXs in continuous culture mode generally reflected this operation at around 70% of maximal growth (Tables 3-1; 3-2), and the cell yield for total BSXs under continuous mode was similar to that at  $G_{\max}$  (day 26) under batch mode (0.28 versus 0.295 pg cell<sup>-1</sup>) (Tables 3-1; 3-2). After the bioreactor was run continuously for 19 days, the volume of effluent culture collected was 11.8 L and the total production of BSXs was almost 0.27 mg. *K. brevisulcata* grew better in continuous culture than their batch culture counterparts (barrels, carboys, and photobioreactor) assuming the dilution rate in continuous culture is equivalent to growth rate in batch cultures ( $0.11 > 0.05-0.086 \text{ day}^{-1}$ ) (Tables 3-1; 3-2).

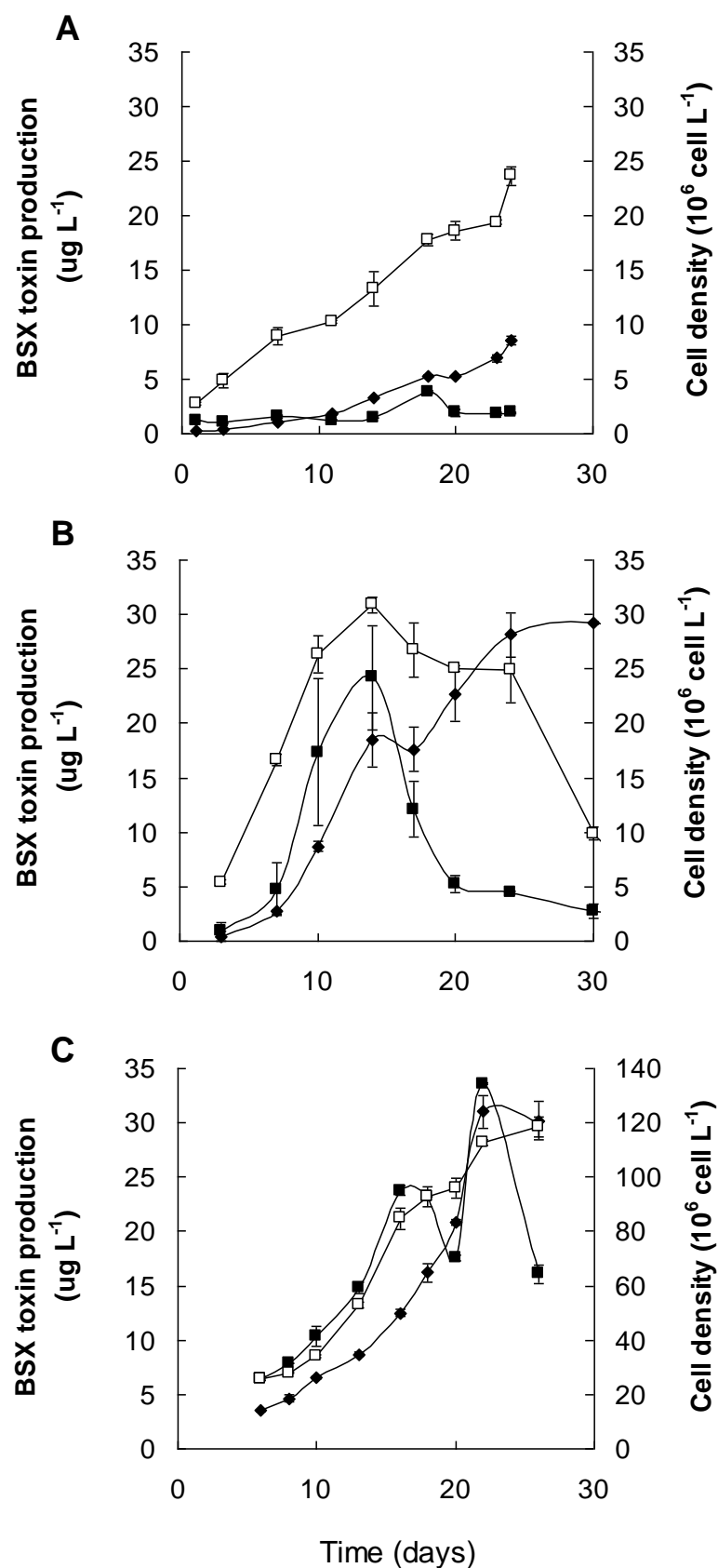


**Figure 3-2.** *K. brevisulcata* growth vs. time and BSX production vs. time in three culture systems operated in batch mode: (A) barrel, (B) carboy and (C) photobioreactor:  $\square$  cell density;  $\blacklozenge$  ring-opened BSX-1, BSX-2 and BSX-3;  $\blacksquare$  ring-closed BSX-4, BSX-5 and BSX-6 (x 4). BSX concentrations in brevetoxin-2 response equivalents. The points/bars depict the Mean  $\pm$  SEM ( $n \geq 2$ ). Note different scales on Y-axis.

**Table 3-1.** Comparison of *K. brevisulcata* growth and toxin production in three culture systems operated in batch mode.

Culture type	Initial pH	Culture volume (L)	Growth rate $\mu$ (day <sup>-1</sup> ) <sup>a</sup>	Maximum growth G <sub>max</sub> (x 10 <sup>6</sup> cells L <sup>-1</sup> ) <sup>b</sup>	Time to maximum growth (days)	Product	Yield of Product ( $\mu$ g L <sup>-1</sup> ) <sup>b</sup>	Yield per cell (pg toxin cell <sup>-1</sup> ) <sup>b</sup>
Carboys	8.0	15	0.086	30.9 $\pm$ 0.7	14	BSX-1	11 $\pm$ 1.9	0.35
						BSX-2	1.0 $\pm$ 0.1	0.03
						BSX-3	6.9 $\pm$ 0.5	0.2
						BSX-4	1.0 $\pm$ 0.3	0.03
						BSX-5	0.04	0.001
						BSX-6	5.0 $\pm$ 0.2	0.16
Plastic barrel	8.0	80	0.05	23.6 $\pm$ 0.8	24	BSX-1	5.5 $\pm$ 0.8	0.23
						BSX-2	2.3 $\pm$ 0.2	0.1
						BSX-3	0.8 $\pm$ 0.1	0.03
						BSX-4	0.15 $\pm$ 0.01	0.006
						BSX-5	0.03 $\pm$ 0.005	0.001
						BSX-6	0.3 $\pm$ 0.01	0.01
Bioreactor <sup>c</sup>	8.3	5.4	0.057	119 $\pm$ 3	26	BSX-1	22 $\pm$ 1.5	0.19
						BSX-2	8.0 $\pm$ 0.3	0.07
						BSX-3	0.2 $\pm$ 0.02	0.002
						BSX-4	1.2 $\pm$ 0.1	0.01
						BSX-5	1.5 $\pm$ 0.2	0.013
						BSX-6	1.3 $\pm$ 0.1	0.01

<sup>a</sup> Determined from the slope of log<sub>10</sub> counts versus incubation time

<sup>b</sup> As determined at maximum growth. Values are means of at least duplicate samples  $\pm$  SEM

<sup>c</sup> Bioreactor cultures were pH controlled throughout the duration of the experiment

**Table 3-2.** Cell growth and toxin production of *K. brevisulcata* in a photobioreactor (5.4 L) operated in continuous mode.

Continuous culturing	Culture volume (L)	Dilution rate (days <sup>-1</sup> )	Cell number (x 10 <sup>6</sup> cells L <sup>-1</sup> ) <sup>a</sup>	Product	Toxin concentration (µg L <sup>-1</sup> ) <sup>b</sup>	Yield (pg toxin cell <sup>-1</sup> )	Displacement volume (L day <sup>-1</sup> )	Toxin production (µg day <sup>-1</sup> )	Duration (days)	Total toxin produced (mg) <sup>c</sup>
<i>K. brevisulcata</i>	5.4	0.11	80.8 ± 4.2	BSX-1	13.6 ± 1.9	0.28 <sup>d</sup>	0.62	14.2 <sup>d</sup>	19	0.27 <sup>d</sup>
				BSX-2	5.1 ± 0.7					
				BSX-3	0.2 ± 0.02					
				BSX-4	1.6 ± 0.3					
				BSX-5	1.4 ± 0.2					
				BSX-6	1.0 ± 0.4					

<sup>a</sup> Values are means of at least triplicate counts (each a mean of two determinations per time point) taken over the time-course of the continuous culture run ± SEM

<sup>b</sup> Values are means of at least triplicate determinations (each a mean of two determinations per time point) taken over the time course of continuous culture in a single experiment ± SEM

<sup>c</sup> Product of toxin concentration, displacement volume and duration.

<sup>d</sup> Sum of six brevisulcatic acids

### 3.3.3 Performance of large bioreactor for *K. brevisulcata* culturing

In the preliminary experiment, the batch photobioreactor culture (52 L) reached  $23.7 \times 10^6$  cells L<sup>-1</sup> at day 10, which is lower than the cell density ( $34.3 \times 10^6$  cells L<sup>-1</sup>) observed in the 5.4 L bioreactor at the same day (Figure 3-2C). Then the 52 L photobioreactor was switched to continuous mode through draw-off of approximately 9 L culture per day and replacement with fresh medium. Over a 28 day period, the cell density increased from  $23.7 \times 10^6$  to  $57 \times 10^6$  cells L<sup>-1</sup> (optical density feedback deactivated). LC-MS was used to monitor BSXs production, but only BSX-1 and BSX-2 were quantified using brevetoxin-2 calibration (other four BSXs had not been identified). During continuous operation, 251 L of culture was collected containing 1.8 mg total BSX-1 plus BSX-2. The mean cell yield for the two BSXs was 0.16 pg cell<sup>-1</sup>, slightly lower than that (0.23 pg cell<sup>-1</sup>) subsequently formed in the 5.4 L glass bioreactor under the continuous mode. It was predicted that scaling up of the photobioreactor to approximately 10 times the size of the reactor vessel should result in proportionally the same growth yields and cell toxin yields on a volumetric basis. However both lower growth yields (cells L<sup>-1</sup>) and cell yields for total BSXs (pg cell<sup>-1</sup>) in the 52 L photobioreactor under continuous operation suggested that additional factors need to be considered in scale-up to maintain culturing efficiency. Light penetration is the most obvious factor. The larger acrylic reactor vessel was 20 cm diameter while the smaller glass reactor vessel was 9 cm. Under the same light strength ( $38 \mu\text{Ein.m}^{-2}\text{s}^{-1}$ ), it is possible that lower light penetration due to the vessel material and larger cross-section lead to reductions in both toxin and cell production in the larger bioreactor.

### 3.3.4 Production of <sup>13</sup>C-labelled compounds for <sup>13</sup>C-NMR research

<sup>13</sup>C-NMR and related 2D techniques are very powerful but relatively insensitive because the natural abundance of <sup>13</sup>C is only 1.1%. By producing toxin labelled with <sup>13</sup>C, structure elucidation by <sup>13</sup>C-NMR is facilitated (Satake *et al.*, 1995). 492 litres of *K. brevisulcata* cultures were grown in media containing NaH<sup>13</sup>CO<sub>3</sub> to produce <sup>13</sup>C-enriched toxins. The toxins measured by LC-MS scanning of SPE extracts gave complex mass spectra due to the successful incorporation of <sup>13</sup>C. However, the spread of ionisation over many mass species indicated that LC-MS SIR or MRM were not suitable for quantitative analysis of <sup>13</sup>C-labelled BSXs. Figure 3-3 shows the MS mass spectra of both labelled and unlabelled BSX-1 at *m/z* 500-1100. The [M+H]<sup>+</sup> peak for the unlabeled sample shows an isotope pattern due to natural <sup>13</sup>C abundance (1.1%). The isotope pattern for the labelled sample shows a shift due to the

incorporation of 2 – 14  $^{13}\text{C}$  atoms per molecule – median incorporation of 7-9 atoms. Labelled BSX toxins were isolated and purified for  $^{13}\text{C}$ -NMR studies at Massey University (Sections 5.3.2.4 & 5.3.3.5). Labelled KBTs were also separated from BSXs for isolation and purification at the University of Tokyo (Section 5.3.4.1).

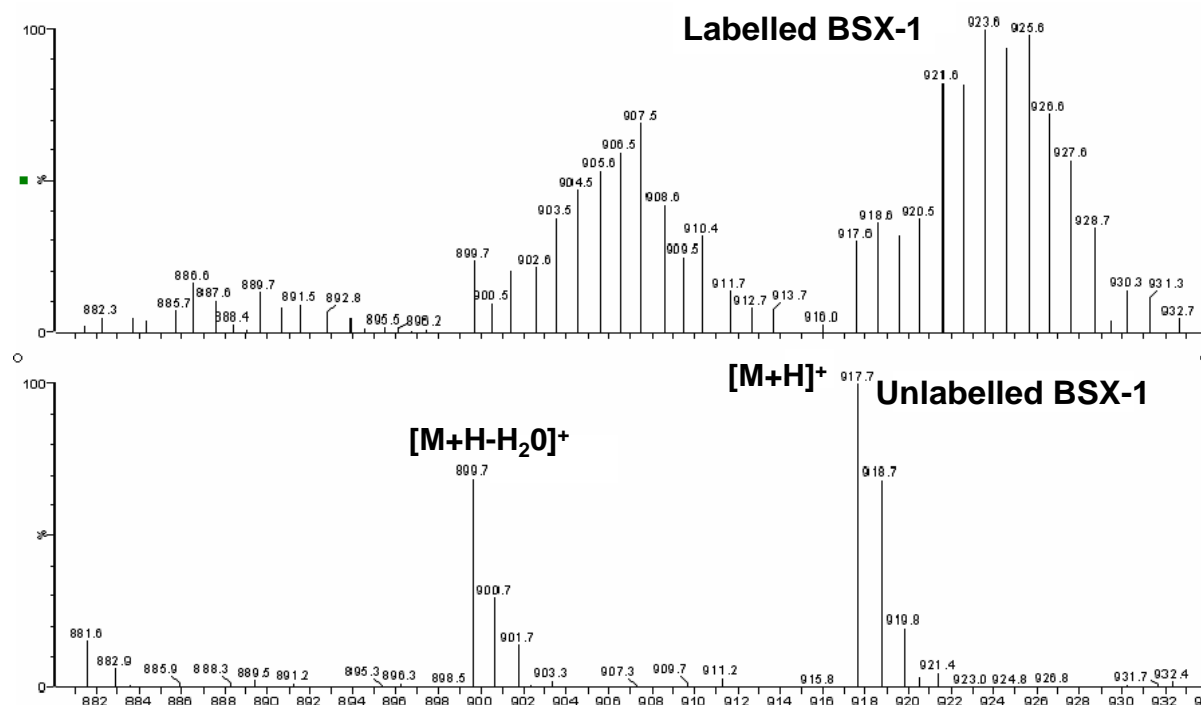


**Figure 3-3.** Mass spectra (ESI<sup>+</sup>) of  $^{13}\text{C}$ -labelled BSX-1 (top) and unlabelled BSX-1 (bottom).

### 3.3.5 Culture harvesting

Total 936 litres unlabeled and 492 litres  $^{13}\text{C}$ -labelled *K. brevisulcata* cultures were grown under laboratory conditions during 2009 and 2011 (Table 3-3). Approximately 70 litres of mass cultures were used to investigate cell growth and toxin production in cultures or were stored at  $-20\text{ }^{\circ}\text{C}$  for future study. A total of 1356 litres mass cultures were harvested between day 16-24 (Table 3-3). Addition of acetone to 7% v/v and filtering was adequate to lyse the cells. Less than 5% of total toxicity was detected by mouse bioassay in ethanol extracts of the filters. Adsorption of toxins to the HP20 resin from the filtered 5% acetone media was also efficient with the eluant containing <5% of the more polar toxins based on analysis by SPE and LC-MS. After harvesting, the HP20 column was washed with RO water for 20 min to desalt. Toxins were recovered from HP20 resin using acetone extraction (3x). The crude extracts were evaporated by rotary evaporation and nitrogen blow down. The weights of dry extracts obtained are recorded in Table 3-3 as well as the estimated amounts of the BSX toxins.

**Table 3-3.** Yields of each batch culture after harvesting.

Batch	Volume (L)	Harvest Date	Crude weight of HP20 extract (g dw <sup>a</sup> )	BSX-1 <sup>b</sup> (mg)	BSX-2 <sup>b</sup> (mg)	BSX-4 <sup>b</sup> (mg)	BSX-5 <sup>b</sup> (mg)
WHT 8-1 <sup>c</sup>	251	15/02/08	NT <sup>d</sup>	1.16	0.64	NT	NT
WHT 9-1	140	24/03/09	1.73	0.67	0.29	0.25	0.03
WHT 9-2	75	14/06/09	1.15	0.53	0.27	0.19	0.03
WHT 9-3	153	29/06/09	2.43	1.32	0.39	0.10	0.02
WHT 9-4	170	10/07/09	2.49	2.20	0.48	0.15	0.03
WHT 9-5 <sup>e</sup>	13	29/07/09	0.09	NT	NT	NT	NT
WHT 9-6	75	30/11/09	1.47	0.68	0.31	0.21	0.02
WHT 10-1 <sup>f</sup>	30	Not harvested	NT	NT	NT	NT	NT
WHT 10-2 <sup>e</sup>	245	11/05/10	NT	NT	NT	NT	NT
WHT 11-1 <sup>g</sup>	42	Not harvested	NT	NT	NT	NT	NT
WHT 11-2 <sup>e</sup>	234	29/06/11	1.26	NT	NT	NT	NT

<sup>a</sup> dw, dry weight after evaporation.

<sup>b</sup> Data from LC-MS SIR calibrated with 1 µg mL<sup>-1</sup> brevetoxin-2 standard solution.

<sup>c</sup> WHT 8-1 was continuously cultured in the 52L bioreactor and harvested by V. Beuzenberg. The extracts were stored at -20 °C freezer and the biotoxins were isolated and purified in 2010.

<sup>d</sup> Not tested.

<sup>e</sup> *K. brevisulcata* was grown in the medium containing NaH<sup>13</sup>CO<sub>3</sub> to produced <sup>13</sup>C-enriched toxins that are not suitable for monitoring by LC-MS (Method 1, SIR).

<sup>f</sup> WHT 10-1 was used to compare toxin productions in 15L carboys and 5.4 L bioreactor. The bioreactor cultures were collected and stored in -20 °C freezer. The carboy cultures were disposed following Cawthron Institute biological safety protocol at day 81 (cultures free of living cells for 6 weeks).

<sup>g</sup> WHT 11-1 was grown in 15 carboys to investigate the profiling of cell growth and toxin productions using LC-MS MRM methods. The culture was eventually disposed following Cawthron Institute biological safety protocol at day 42.

### 3.4 Summary

*K. brevisulcata* was successfully bulk cultured under laboratory conditions to produce crude BSXs and KBTs. The efficiencies of cell growth and BSXs production in three culturing systems were investigated. Carboys are more efficient to grow *K. brevisulcata* and produce BSXs because of its highest growth rate and cell toxin yields. More than half of mass cultures were grown in carboys. Carboy cultures only required 12-18 days to reach G<sub>max</sub>

compared to batch barrel and bioreactor cultures with  $G_{\max}$  at day 24 and 26 respectively. High  $G_{\max}$  and BSXs production were both observed in batch and continuous bioreactor cultures, suggesting that a large volume automated photobioreactor could be developed to produce sufficient levels of toxins from dinoflagellate cultures for structural characterisation, analytical standard production, investigation of mode-of-action and pharmaceutical appraisals in the future. A total of 936 litres unlabelled and 492 litres  $^{13}\text{C}$ -labelled mass cultures were grown during 2009 and 2011. The crude BSXs and KBTs had been extracted from mass cultures following the method modified from that for yessotoxin (Loader *et al.*, 2007), and were then isolated and purified for chemical and toxicological investigations.



## Chapter 4

### LC-MS analysis of toxins produced by *Karenia* species

#### 4.1 Introduction

Identification of new algal toxins and assessment of their production by microalgae present significant challenges to marine chemists and biologists due to their complex structures. Methods for determination of these toxins may be divided into bioassay-directed and physico-chemical methods (Holland, 2008; Quilliam, 2003b). Bioassays are based on the biological responses of tested organisms (animals, cultured cells or tissues) and are most useful for assessment of overall toxicity and mode-of-action. However, they are not generally applicable to characterise individual toxins in terms of chemical structure, especially in mixtures. Physico-chemical methods based on chromatographic and spectroscopic techniques have the potential to provide both quantitative analysis of known algal toxins, and identification of new compounds (Quilliam, 2003b). Methods that are widely used include GC, thin-layer chromatography (TLC), HPLC-UV/FLD, LC-MS, and capillary electrophoresis (CE). LC-MS is the most suited for both algal toxin research and routine monitoring because of its universal detection capability, high sensitivity, high selectivity and specificity. LC-MS systems are capable of automation and high throughput, separation of complex mixtures of toxins. LC-MS provides precise and accurate quantitation, gives information about compound structure, and has the ability to identify novel compounds (McNabb *et al.*, 2005; Quilliam, 2003b).

A basic LC-MS system comprises a HPLC system for analyte separation, an ionisation interface to remove volatile solvent and produce ionised molecules, and a MS in which the ions are separated according to their mass-to-charge ratio ( $m/z$ ) and detected in a high vacuum environment (McMaster, 2005). Analyte ionisation is the key step for detection by MS. There are five types of ionisation interfaces used with modern MS systems: ESI, APCI, APPI, FAB and MALDI. Some ionisation interfaces such as FAB and MALDI are difficult to interface for routine use with LC (Cai *et al.*, 2005; Quilliam, 2003b). ESI is the most common ionisation interface for LC-MS, because it is well suited for compounds of widely ranging polarities and is easily interfaced with LC (Quilliam, 2003b). In addition, ESI produces both positive and negative ions and therefore LC-MS using ESI can be used to acquire positive and negative ion spectra (McNabb *et al.*, 2005).

The heart of MS is the mass analyser which is designed to separate ions based on  $m/z$ . As well as scans over a range to produce mass spectra, the analyser can be set to select specific ion masses for quantitative analysis. There are currently three important types of MS in term of their mass analyser: quadrupole, ion trap (IT), and time of flight (TOF).

ITMS technique was initially used by physicists for isolated ion investigation (March, 1997). The relatively low dynamic range due to ion accumulation limit ITMS uses for quantitation (Aebersold & Mann, 2003; March, 1997). The mass range for TOF MS is higher than that for quadrupole MS or ITMS. Thus MALDI-TOF-MS has been widely used for analysis of large biological molecules in proteomic laboratories (Cai *et al.*, 2005; McMaster, 2005; Moyer *et al.*, 2002; Reyzer & Caprioli, 2007). TOF-MS can also obtain high mass resolutions to enable accurate mass measurements and provide the chemical formulae of novel toxins (Moyer *et al.*, 2002). However, MALDI cannot be combined with LC and provides relatively poor quantitative reproducibility (Cai *et al.*, 2005). Triple stage quadrupole (TSQ) MS/MS comprises MS1, collision cell and MS2 (Figure 2-7). ESI-TSQ-MS/MS is the most common MS setup for algal toxin research which, equipped with LC, not only provides molecular mass and structural information by operation in full scan and/or daughter ion scan mode, but also acts as highly sensitive and selective detector for quantitative analysis of complex mixtures by operation in SIR or MRM mode.

*K. brevisulcata* produces multiple classes of biotoxins which are difficult to monitor by bioassays (Keyzers, pers, comm.). In this study, LC-ESI-TSQ-MS methods were used to compare novel compounds produced by *K. brevisulcata* and two other *Karenia* species. Validated methods were also developed to monitor BSXs and KBTs in the SPE extracts of *K. brevisulcata* cultures.

## **4.2 Materials and methods**

### **4.2.1 Microalgae investigated and standard materials**

Nine unialgal isolates of three *Karenia* species were investigated in this study. Eight strains were held in the Cawthron Institute Culture Collection of Micro-algae (CICCM), and a strain of *K. mikimotoi* was isolated from the South China Sea, and held in the First Institute of Oceanography, State Oceanic Administration (SOA), China (Table 4-1). *K. brevis* was grown in modified L1 medium (Guillard & Hargraves, 1993) at  $25 \pm 1$  °C. *K. brevisulcata*, CICCM strains of *K. mikimotoi*, and the China strain of *K. mikimotoi* were grown at  $19 \pm 1$  °C in 100%

GP+Se medium, 50% GP medium, and modified L1 medium, respectively (Beuzenberg *et al.*, 2012; Loeblich, 1975; Loeblich & Smith, 1968). Mass cultures were grown in glass flasks (500 mL) with 90  $\mu\text{Ein.m}^{-2}\text{s}^{-1}$  (12:12 hr L:D). All isolates were grown for 12-20 days and harvested at late log phase for LC-MS analysis. The number of cells per litre of each mass culture (cell density) was calculated using the method described in the Section 3.2.1.

BSXs (-1, -2, -4 & -5) and KBTs (-F, -G, -H & -I) were isolated and purified from *K. brevisulcata* cultures by New Zealand researchers at Cawthron Institute and Japanese researchers at the University of Tokyo respectively (Sections 5.3.2 & 5.3.4.1). Gymnocin-A was kindly provided by Prof. Satake, the University of Tokyo. Brevetoxin-1, -2, -3 and -B5 were purchased from UNCW, USA.

**Table 4-1.** *Karenia* species tested by LC-MS.

Species	Culture collection number or strain	Site of Isolate and/ or source	Year of collection or isolation	Culture media	Culture collection <sup>a</sup>
<i>K. brevisulcata</i>	CAWD 82	Wellington Harbour, New Zealand (NZ)	1998	100% GP+Se	CICCM
<i>K. brevis</i>	CAWD 122	Pensacola Beach, Florida, USA	1999	L1	CICCM
<i>K. mikimotoi</i>	CAWD 05	Kushimoto, Japan	1970	50% GP	CICCM
	CAWD 63	Waimangu, Hauraki Gulf, NZ	1993	50% GP	CICCM
	CAWD 117	East Bay, Marlborough Sounds, NZ	2001	50% GP	CICCM
	CAWD 133	Kennedy Bay, NZ	2002	50% GP	CICCM
	CAWD 134	Whangaporoa, NZ	2002	50% GP	CICCM
	Ruakaka spp 1	Ruakaka Bay, Marlborough Sounds, NZ	2010	50% GP	CICCM
	China Strain	South China Sea, China	2010	L1	The First Institute of Oceanography, SOA, Qingdao, PRC

<sup>a</sup>CICCM, Cawthron Institute Culture Collection of Micro-algae; SOA, State Oceanic Administration, China.

#### **4.2.2 Extraction of toxins from *Karenia* culture for LC-MS monitoring**

A *K. brevisulcata* culture stock at late log phase (500 mL in glass flask) was extracted using a Strata-X SPE cartridge (1g/20 mL, Phenomenex Inc, USA) preconditioned with methanol (50 mL) and MQ (50 mL). After loading the culture, the cartridge was washed with MQ (50 mL) and 20% methanol (50 mL), and the toxins were eluted with 50 mL methanol. The methanol eluant (50 mL) was removed by a gentle flow of oxygen free nitrogen at 40 °C and the extract was reconstituted in 1 mL of 80% methanol (concentration factor 500x) for LC-MS MS scan (Method 3).

*K. brevis* culture (50 mL) at late log phase was extracted using a Strata-X SPE cartridge (60 mg per 3 mL) and following the procedure described in Section 3.2.3 for routine monitoring of BSXs except the second elution with acetone was not used. The methanol eluant (3 mL) was removed by a gentle flow of oxygen free nitrogen at 40 °C and the extract was reconstituted in 1 mL of 80% methanol (concentration factor 50x) for LC-MS MS scan (Method 3).

For *K. mikimotoi*, samples (50 mL) at late log phase of each cultured isolate were centrifuged at 1000g for 10 min. The cell-free supernatants were gently decant and the cell pellets were re-suspended in isopropanol (IPA, 1 mL), sonicated for 1 min, and centrifuged at 17000g for 10 min. The IPA supernatants (1 mL) was removed by a gentle flow of oxygen free nitrogen at 40 °C and the dry cell pellets were stored at -20 °C. Prior to LC-MS analysis, the cell pellets was reconstituted in 1 mL of 80% methanol (concentration factor 50x) for LC-MS MS scan (Method 3).

#### **4.2.3 LC-MS analysis**

LC-MS analysis of the extracts of *Karenia* cultures were conducted using either a HPLC-Waters Quattro Ultima or an uPLC-Waters Premier XE instruments (Waters-Micromass, Manchester, UK). MassLynx Ver.4.1 software (Waters, Milford, MA) was used for instrument control, data acquisition and data processing in both methods followed.

#### 4.2.3.1 uPLC-Premier MS

A Waters Acquity uPLC system (Waters, Milford, MA) coupled with a Waters-Micromass Quattro Premier XE TSQ MS (Manchester, UK) with ESI was used to i) detect BSXs and KBTs produced by *K. brevisulcata*, and ii) quantitatively analyse BSXs in a *K. brevisulcata* culture. Two mobile phase solutions were prepared: (A) 5% acetonitrile plus 10% buffer (500 mM FA & 20 mM ammonia solution); and (B) 95% acetonitrile plus 10% buffer. Separation of BSXs was achieved using a Waters Acquity uPLC C8 BEH 1.7  $\mu\text{m}$  50  $\times$  1.0 mm column plus 0.2  $\mu\text{m}$  prefilter at 30°C, eluted at 0.3 mL min<sup>-1</sup> with linear gradient of 90% A to 100% B over 4 min, 100% B was held for 0.5 min, changing to 10% of B over 0.5 min, before returning to initial conditions. Separation of KBTs was achieved using a Waters Acquity uPLC C18 BEH 1.7  $\mu\text{m}$  50  $\times$  1.0 mm column plus 0.2  $\mu\text{m}$  prefilter at 30°C, eluted using the same gradient but with 0.1% FA rather than buffer in the mobile phases. The electrospray ionisation source was operated in positive-ion mode (ESI<sup>+</sup>) at 100 °C, nitrogen gas desolvation 800 L h<sup>-1</sup>(400 °C), capillary 2.5 kV for SIR quantitation (Method 1, SIR) and 4.0 kV for MS scan (Method 2), cone 45 V for SIR quantitation (Method 1, SIR) and 50-250 V for MS scan (Method 2).

**Method 1 SIR quantitation:** BSXs were monitored using SIR operating mode. There were seven channels in total, six for BSXs using the respective [M+H]<sup>+</sup> and [M+H-H<sub>2</sub>O]<sup>+</sup> ions and one for brevetoxin-2 (calibrant) (Table 4-2). BSX-3 and BSX-6 were not monitored in preliminary studies (Chapter 7). The area responses for the BSXs were quantified using a linear calibration prepared with solutions of a brevetoxin-2 RSM purchased from UNCW.

**Table 4-2.** Analytes, retention times, mass ions monitored and quantitative standards for SIR quantitation of BSXs using LC-MS Method 1.

Toxin channels <sup>1</sup>	Retention time (min)	[M+H] <sup>+</sup> ( <i>m/z</i> )	[M+H-H <sub>2</sub> O] <sup>+</sup> ( <i>m/z</i> )	Quantitative Standards <sup>a</sup>
BSX-1	1.55	917.5	899.5	BTX-2
BSX-2	1.64	873.5	855.5	BTX-2
BSX-3	1.75	857.5	839.5	BTX-2
BSX-4	1.94	899.5		BTX-2
BSX-5	2.06	855.5		BTX-2
BSX-6	2.21	839.5		BTX-2
BTX-2	2.30	895.5		Calibrant

<sup>a</sup>Toxin channels: BSX, brevisulcatic acid; BTX-2, brevetoxin-2

**Method 2 MS scan:** the MS was operated under ESI<sup>+</sup> at unit mass resolution at two full scan mass ranges  $m/z$  700-1100 for detection of BSXs and other algal metabolites, and  $m/z$  1900-2200 for detection of KBTs. Scan data was acquired between 1 and 4.2 min.

#### 4.2.3.2 HPLC-Ultima MS

A Waters 2695 HPLC system (Waters, Milford, MA) coupled with a Waters-Micromass Quattro Ultimate TSQ MS (Manchester, UK) with Z-spray electrospray ionization (ESI) was used to i) detect toxins produced by *Karenia species* using scanning mode, and ii) quantitatively analyse BSXs and KBTs in *K. brevisulcata* cultures using MRM operation mode. The column was a Thermo BDS Hypersil C8 2.1×50 mm column at 30 °C, and the injection volume was 10 µL. Three mobile phase solutions were prepared: (A) 10% acetonitrile; (B) 90% acetonitrile; and (C) 1% FA in MQ. The linear gradient was run with a flow rate of 0.2 mL/min at constant 10% of C from 70% of A plus 20% of B to 90% of B over 10 min, held for 3.9 min, and returning to the initial gradients over 0.1 min. A 1 min post inlet method was run to speed up re-equilibration to initial conditions. The electrospray source was operated in positive ion mode (ESI<sup>+</sup>) with nitrogen gas for nebulisation and optimized conditions of capillary 4.0 kV. The desolvation gas flow was 460 Lhr<sup>-1</sup> (400 °C), cone gas 58 Lhr<sup>-1</sup> and cone 100 V.

**Method 3 MS scan:** the MS was operated at unit mass resolution at two full scan mass ranges of  $m/z$  500-1000 and  $m/z$  1000-2300 for MS scan. Scan data was acquired between 3 and 14 min.

**Method 4 MRM quantitation:** The TSQ MS/MS was operated in MRM mode with collision cell gas pressure (argon) set at  $1 \times 10^{-4}$  T. The retention times (Rt), parent [M+H]<sup>+</sup> mass ions, MRM transitions, and collision energies for each toxin are given in Table 4-3. The various toxins were quantified by comparison with a set of five dilutions of a mixture of BSXs and KBTs (5 – 200 ng mL<sup>-1</sup> in 80% methanol, Table 4-2; Sections 5.3.2 & 5.3.4.1). The assumption was made that closely related analogues (BSX-3 and BSX-6) gave similar responses to BSX-1 and BSX-4 and the calibration curves for solutions of these RSMs were therefore applied to estimate concentrations of the respective related compounds (Table 4-3).

**Table 4-3.** Analytes, retention times, parent mass ions, MRM transitions, collision energies and quantitative standards for MRM quantitation of BSXs and KBTs using LC-MS Method 4.

Toxins <sup>a</sup>	Retention time (min)	[M+H] <sup>+</sup> <sup>b</sup>	MRM transition	Collision energy (eV)	Quantitative Standards
<b>BSX-1</b>	7.8	917.5	917.5>899.5 917.5>381.3	10 25	BSX-1
<b>BSX-2</b>	8.2	873.5	873.5>855.5 873.5>337.3	10 25	BSX-2
<b>BSX-3</b>	8.4	857.5	857.5>839.5 857.5>321.3	10 25	BSX-1
<b>BSX-4</b>	9.6	899.5	899.5>881.5 899.5>381.3	15 25	BSX-4
<b>BSX-5</b>	10.2	855.5	855.5>837.5 855.5>337.3	15 25	BSX-5
<b>BSX-6</b>	10.6	839.5	839.5>821.4 839.5>321.3	15 25	BSX-4
<b>KBT-F</b>	9.4	2055.1	2055.1>1971.0	45	KBG-F
<b>KBT-G</b>	9.4	2085.1	2085.1>2001.0	45	KBT-G
<b>KBT-H</b>	8.2	2071.1	2071.1>1971.0	45	KBT-H
<b>KBT-I</b>	8.2	2101.1	2101.1>2001.0	45	KBT-I

<sup>a</sup> BSX, brevisulcatic acid; KBT, brevisulcenal.

<sup>b</sup> Most abundant peak of molecular cluster (second isotope peak for KBTs).

## 4.3 Results and Discussion

### 4.3.1 Novel toxins produced by *K. brevisulcata*

A mature *K. brevisulcata* culture (500 mL;  $> 25 \times 10^3$  cells mL<sup>-1</sup>) was extracted using 1g/20mL Strata-X SPE cartridge followed by elution with methanol. The extract in 80% methanol was analysed by LC-MS (Method 3, scanning). Total ion chromatograms (TIC) from 7 to 11 min of *K. brevisulcata* extract at  $m/z$  500-1000 and  $m/z$  1000-2300 are shown in Figure 4-1.

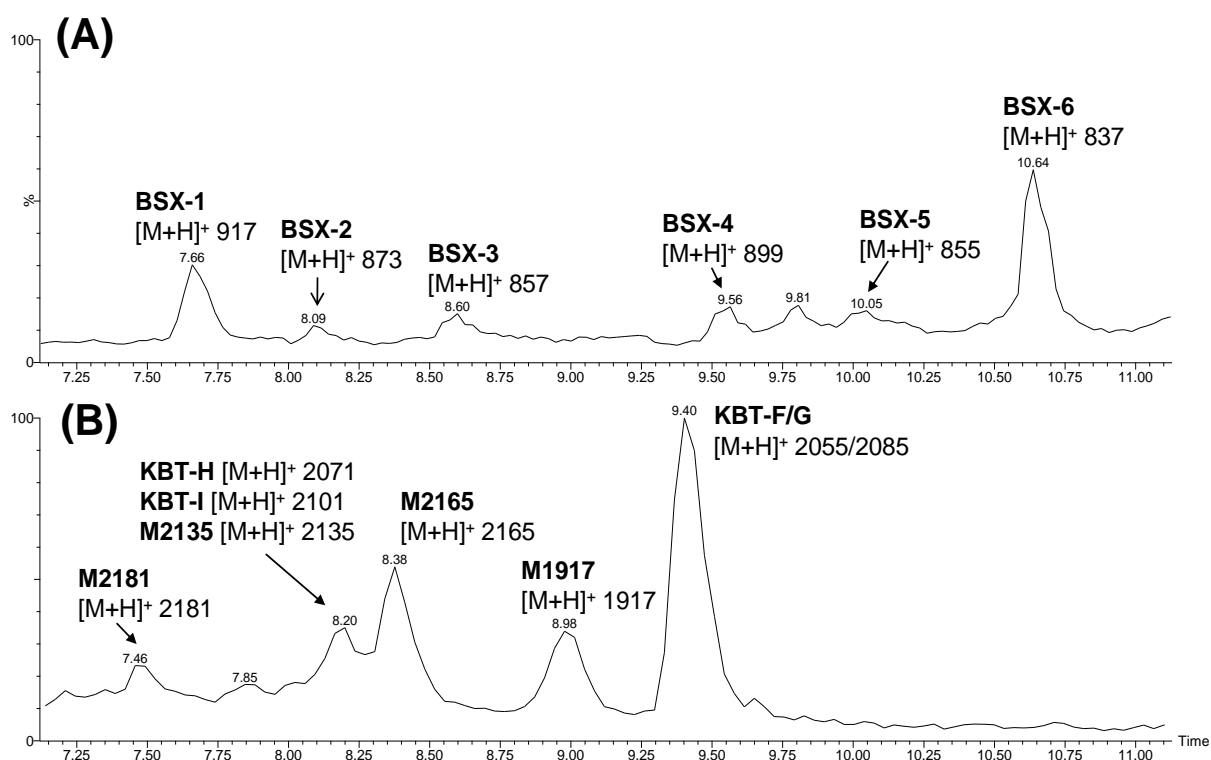


**Figure 4-1.** TIC from 7 to 11 min (Method 3, scanning) of an SPE extract of *K. brevisulcata* culture: (A) at  $m/z$  500-1100; (B) at  $m/z$  1100-2300.

#### 4.3.1.1 BSXs identification

At scanning range of  $m/z$  500-1000 (Figure 4-1A), the most polar component (peak at 7.66 min), corresponding to BSX-1, gave a mass spectrum with an  $[M+H]^+$  of  $m/z$  917 and a prominent fragment ion at  $m/z$  899 ( $[M+H-H_2O]^+$ ). The ion at  $m/z$  939 ( $[M+Na]^+$ ) supported the assignment of 916 Da as the molecular mass of BSX-1 (Section 5.3.3.1, Figure 5-10A). Following BSX-1, the small peak at 8.09 min with  $[M+H]^+$  at  $m/z$  873 and  $[M+H-H_2O]^+$  at  $m/z$  855 was identified as BSX-2 (Section 5.3.3.1, Figure 5-10B). Following BSX-2, a more prominent peak at 8.6 min gave a spectrum with  $[M+H]^+$  of  $m/z$  857,  $[M+Na]^+$  of  $m/z$  879 and



$[M+H-H_2O]^+$  of  $m/z$  839 (Figures 4-2B). This natural compound had not been observed in earlier studies on older *K. brevisulcata* cultures and was named BSX-3 (Section 4.3.1.2). A significant peak at 9.56 min had  $[M+H]^+$  at  $m/z$  899 and was confirmed as BSX-4, which is the lactone derivative of BSX-1. Similarly, BSX-5 (BSX-2 lactone derivative,  $[M+H]^+$  at  $m/z$  855, Rt 10.02 min) was also detected at low levels in culture extracts using LC-MS. At 10.64 min, the strongest peak was observed, giving a spectrum with  $[M+H]^+$  at  $m/z$  839 (Figure 4-2D). This compound was proposed as the lactone derivative of BSX-3, and assigned as BSX-6 (Section 4.3.1.2).

#### **4.3.1.2 Identification of new BSX toxins (BSX-3 and BSX-6)**

In my initial studies on culture of *K. brevisulcata*, the novel toxins BSX-1, BSX-2, BSX-4 and BSX-5 were identified by LC-MS and isolated from bulk cultures for structural elucidation (Chapter 5) and toxicological investigations (Chapters 6 & 7). Although bulk culturing of *K. brevisulcata* in  $NaH^{13}CO_3$  labelled media was mainly for production of labelled toxins for  $^{13}C$ -NMR experiments, the extracts also contributed to the discovery of several novel compounds produced by *K. brevisulcata*. Two significant peaks at Rt 8.6 and 10.6 min respectively were firstly highlighted in the LC-MS TIC of  $^{13}C$  labelled SPE extract (data not shown, similar to Figure 4-1A). The mass spectra revealed these two compounds were potential metabolites of *K. brevisulcata* due to the high incorporation of  $^{13}C$  isotope (Figures 4-2, 5-10). Comparison of LC-MS data suggested these belong to the BSX toxin class and were named BSX-3 ( $[M+H]^+$   $m/z$  857) and BSX-6 (BSX-3 lactone derivative,  $[M+H]^+$   $m/z$  839) according to the polarity of each BSX (Figure 4-1A). It seems that BSX-3 contains a carboxyl and a labile hydroxyl in a configuration that readily allows formation of a lactone by loss of water similar to BSX-1 and -2. The mass difference to BSX-1 is 60 Da (Figures 4-2A, 5-10A) which indicates that the second carbonyl may be missing in BSX-3 (less elements of acetic acid, with introduction of a double bond or another ring). This was confirmed by the negative ion ESI spectra which were weak for BSX-6 and the doubly charged anion for BSX-3 was not absent. BSX-3 and BSX-6 were not further studied or isolated in my PhD project. They are lipophilic and partially transferred to the neutral chloroform phase after solvent partitioning, along with KBTs. The bulk of these fractions were sent to Japanese co-workers for KBTs study. Therefore, insufficient toxins were available for further chemical and toxicological studies at Cawthron Institute.

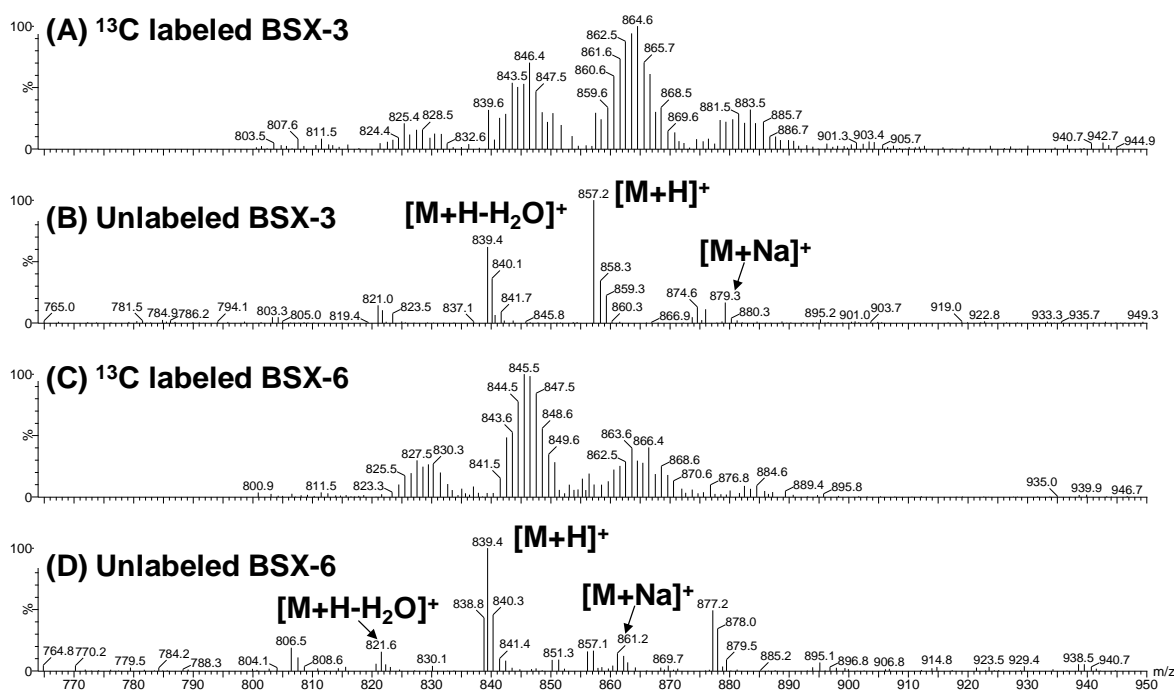


**Figure 4-2.** Mass spectra (ESI<sup>+</sup>) of (A) <sup>13</sup>C-labelled BSX-3, (B) unlabelled BSX-3, (C) <sup>13</sup>C-labelled BSX-6, and (D) unlabelled BSX-6.

#### 4.3.1.3 Identification of KBTs in *K. brevisulcata*

The preliminary studies on KBTs used uPLC-Premier MS (Method 2, scanning) with standards of KBT-F and -G supplied to Cawthron Institute by Prof. Satake (Section 5.3.4.1). The unusually high m.w. required special tuning of the ion source and detection conditions. KBT-F and -G coeluted under the C18 reversed phase conditions. For ESI<sup>+</sup> with FA at low cone voltage (50 V), [M+H]<sup>+</sup> predominated but sensitivity was higher at high cone voltage (250 V) where [M+Na]<sup>+</sup> predominated. Some less intense peaks from successive losses of water were also present. Mac<sup>-</sup> (acetate adduct) predominated using ESI<sup>-</sup> and neutral buffer. The abundance of the first peak in the molecular cation isotope cluster (all <sup>12</sup>C) is exceeded by the second peak (1x <sup>13</sup>C) for compounds with more than ca. 90 carbons (molecular weights typically >1900). The mass of the largest peak in the cluster is reported by the MS data system and this mass was used for the KBTs and related compounds reported here. Thus, for example, the conventional mono-isotopic [M+H]<sup>+</sup> for KBT-F of 2054 is actually reported one mass higher at 2055. LC-MS analysis of SPE extracts of *K. brevisulcata* cultures revealed a rich suite of high m.w. toxins (Figure 4-3, Table 4-4). KBT-F and -G were the principal components in the 1900 – 2200 Da mass region. There were at least five other related compounds in this retention and mass region. There was a high degree of correspondence of the UVD (230 nm) and TIC chromatograms (Figure 4-3), allowing for dead volume of the

connecting tubing. Apparently the compounds share a common UV absorbing moiety, except for the compound M1917. The retention times for KBT-F and -G and the compounds M2071 (possibly KBT-H, no standard at that time), and M1917 using mobile phase with neutral buffer remained the same as for acidic conditions confirming their neutral character (Table 4-4). However, the compounds M2181, M2135 and M2165 moved to shorter retention times (Table 4-4), indicating some acidic character. The latter compounds also showed a peak in their ESI<sup>+</sup> spectra corresponding to loss of 80 Da from [M+H]<sup>+</sup> and thus they are probably sulphated KBT analogues.

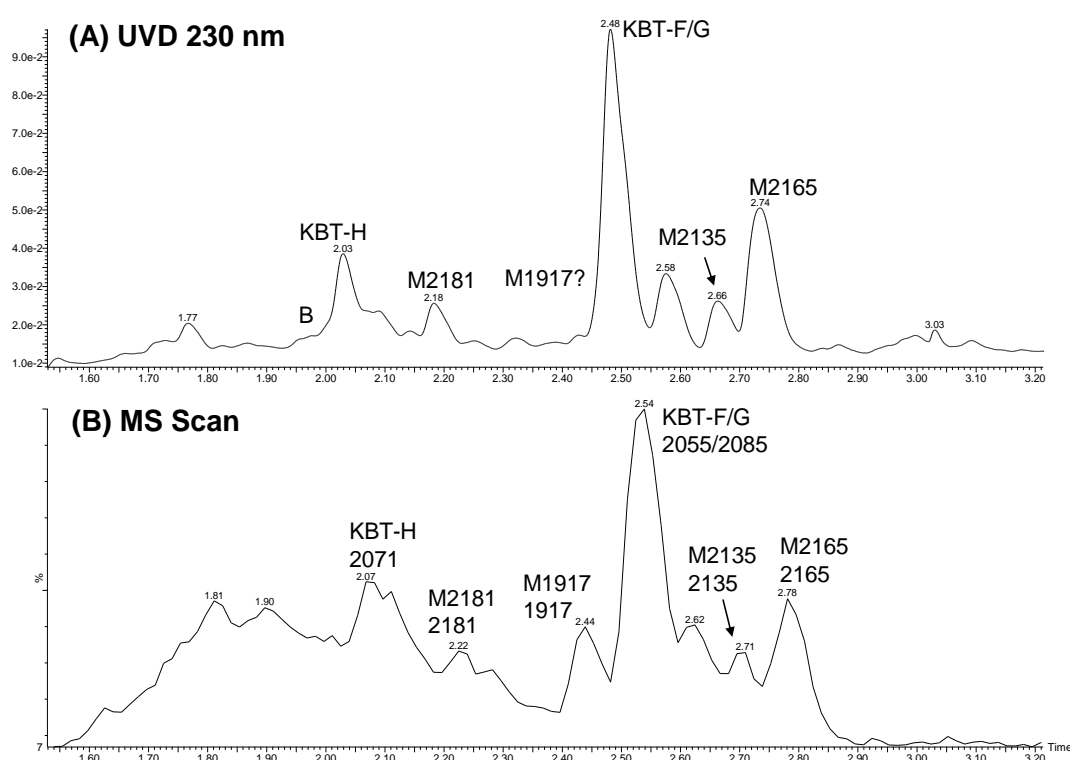


**Figure 4-3.** A) LC-UV (230 nm) and B) LC-MS (Method 2, scanning  $m/z$  1800-2200) chromatograms for the crude HP20 extract of a bulk culture of *K. brevisulcata*. See text for uPLC reversed phase column and gradient conditions. Retention time off-set (ca 0.05 min) due to connecting tubing. Peaks in MS TIC are annotated with m.w. (mono-isotopic) of components calculated from the observed molecular cations ([M+H]<sup>+</sup> and [M+Na]<sup>+</sup>).

**Table 4-4.** Novel compounds identified in SPE extracts of unlabelled *K. brevisulcata* cultures by LC-MS (Method 2) scanning at  $m/z$  1900-2200.

Compound	Rt (min) Acidic eluant (formic acid)	Rt (min) Neutral eluant (amm. acetate)	[M+H] <sup>+</sup> ( $m/z$ )	[M+Na] <sup>+</sup> ( $m/z$ )	[M+H-SO <sub>3</sub> ] <sup>+</sup> ( $m/z$ )
KBT-H	2.07	2.07	2071	2093	
M2181	2.22	2.01	2181	2203	2201
M1917	2.44	2.44	1917	1939	
KBT-F	2.54	2.54	2055	2077	
KBT-G	2.54	2.54	2085	2107	
M2135	2.71	2.32	2135	2157	2055
M2165	2.78	2.45	2165	2187	2085

Further LC-MS analysis was carried out using HPLC-Ultima MS (Method 3, scanning). The system was optimised using standards for KBT-F and -G. The mass spectra showed [M+H]<sup>+</sup> predominating and low [M+Na]<sup>+</sup> as well as some doubly charged species (Figure 4-4). KBT-G appears to be ionised less efficiently than KBT-F by ESI and these toxins are not separated under either C8 or C18 reverse phase conditions (Figure 4-4). In addition, Japanese researchers have isolated and purified another two KBTs from the *K. brevisulcata* extracts produced at Cawthron and named them KBT-H and KBT-I. MALDI-TOF MS analysis gave [M+Na]<sup>+</sup> for KBT-H and KBT-I at  $m/z$  2092 and 2122 respectively (mono-isotopic masses) and it is suggested that these are analogues of KBT-F and KBT-G respectively where the methyl-2-butenal side chain has been oxidised (16 Da increase in m.w.) (M. Satake, pers. comm.). The mass spectrum of KBT-H gave an [M+H]<sup>+</sup> of  $m/z$  2071 (Figure 4-5A) and [M+2H]<sup>2+</sup> at  $m/z$  1036, indicating that KBT-H is similar to KBT-F, with at least two protonating sites. KBT-H and -I coeluted (Table 4-5) and also gave disparate ionisation efficiencies, similar to KBT-F and -G.

SPE extracts of labelled and unlabelled *K. brevisulcata* cultures were analysed with this system (Figure 4-1B) and eight high m.w. compounds were detected (Table 4-5). The most abundant components were KBT-F and -G (Table 4-5). Our LC-MS scanning experiments on both <sup>13</sup>C-labelled and unlabelled extracts also revealed a component at 8.23 min corresponding to KBT-H (Figure 4-5). A median shift of 9-10 Da in the isotope pattern of [M+H]<sup>+</sup> for the <sup>13</sup>C-labelled sample was observed and was supported by an average shift of 5 in that of [M+2H]<sup>2+</sup> (Figure 4-5B). KBT-I could not be directly detected in SPE extracts by LC-MS due to its poor ionisation efficiency. Three other interesting compounds with m.w. >2100 Da were observed by both LC-MS systems (Figures 4-1B, 4-3B; Tables 4-4, 4-5). These compounds (M2135, M2165 and M2181) differ in mass by 80 Da from KBT-F, -G, and

-I respectively (Table 4-5), indicating they may be the sulphated analogues. The  $[M+H-80]^+$  ( $[M+H-SO_3]^+$ , sulphate abstracted protonated molecular ion) mass ions were observed in ESI<sup>+</sup> mass spectra for all three compounds (Tables 4-4, 4-5; Figure 4-6), indicating the presence of a  $SO_3$  group that can be easily cleaved from  $[M+H]^+$ . The further isolation and purification of these sulphated analogues will be interesting and helpful to understanding their chemical structures, the complex metabolism of KBTs, and their biological activities.

M1917 produced the second largest peak at 8.95 min in Figure 4-1B. The mass spectrum matched the observation in the preliminary study using uPLC-Premier MS and confirmed that M1917 can be also highly incorporated with  $^{13}C$  atoms by adding  $NaH^{13}CO_3$  into *K. brevisulcata* cultures. This compound cannot be detected by UVD at 230 nm, indicating that M1917 does not have UV absorbing moiety of  $\beta$ -unsaturated carbonyl. Therefore, it is either a KBT with modified side chain or another polyether not directly related to KBTs.

**Table 4-5.** Novel compounds identified in SPE extracts of both unlabelled and  $^{13}C$ -labelled *K. brevisulcata* cultures by LC-MS (Method 3) scanning at  $m/z$  1000-2300.

Compound	Rt (min) Acidic eluant (formic acid)	$[M+H]^+$ ( $m/z$ )	$[M+Na]^+$ ( $m/z$ )	$[M+H-SO_3]^+$ ( $m/z$ )
M2135	8.23	2135	2157	2055
M2181	7.49	2181	2203	2101
KBT-H	8.23	2071	2093	ND
KBT-I	8.20	2101	2103	ND
M2165	8.38	2165	2187	2085
M1917	8.98	1917	1939	ND
KBT-F	9.40	2055	2077	ND
KBT-G	9.40	2085	2085	ND

ND, not detected

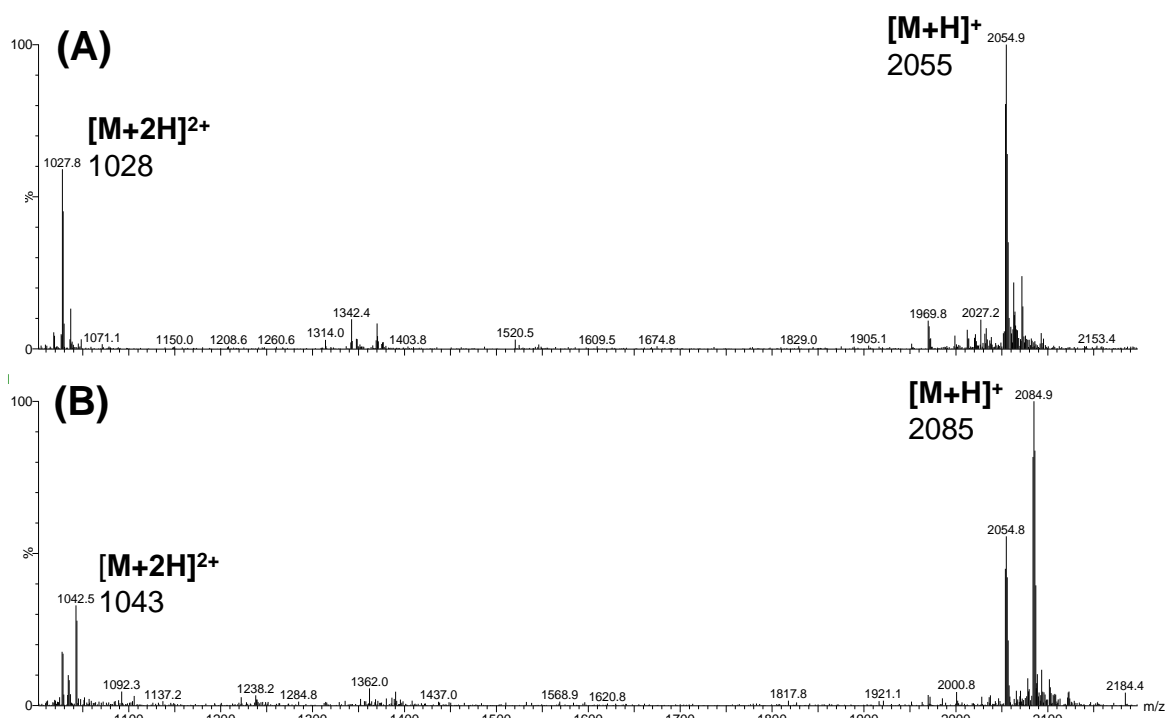


**Figure 4-4.** Mass spectra (ESI<sup>+</sup>) of (A) KBT-F,  $[M+H]^+$   $m/z$  2055; (B) KBT-G,  $[M+H]^+$   $m/z$  2085.

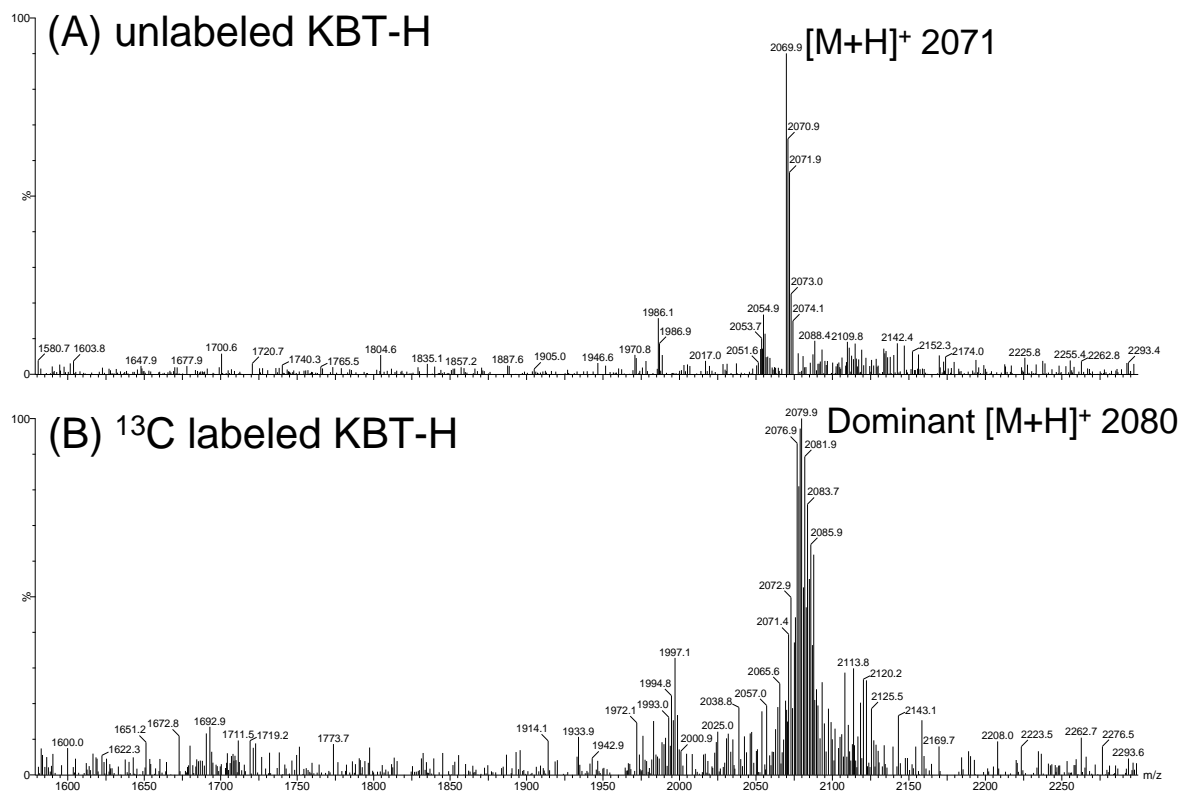


**Figure 4-5.** Mass spectra (ESI<sup>+</sup>) of (A) unlabelled and (B) <sup>13</sup>C-labelled KBT-H.

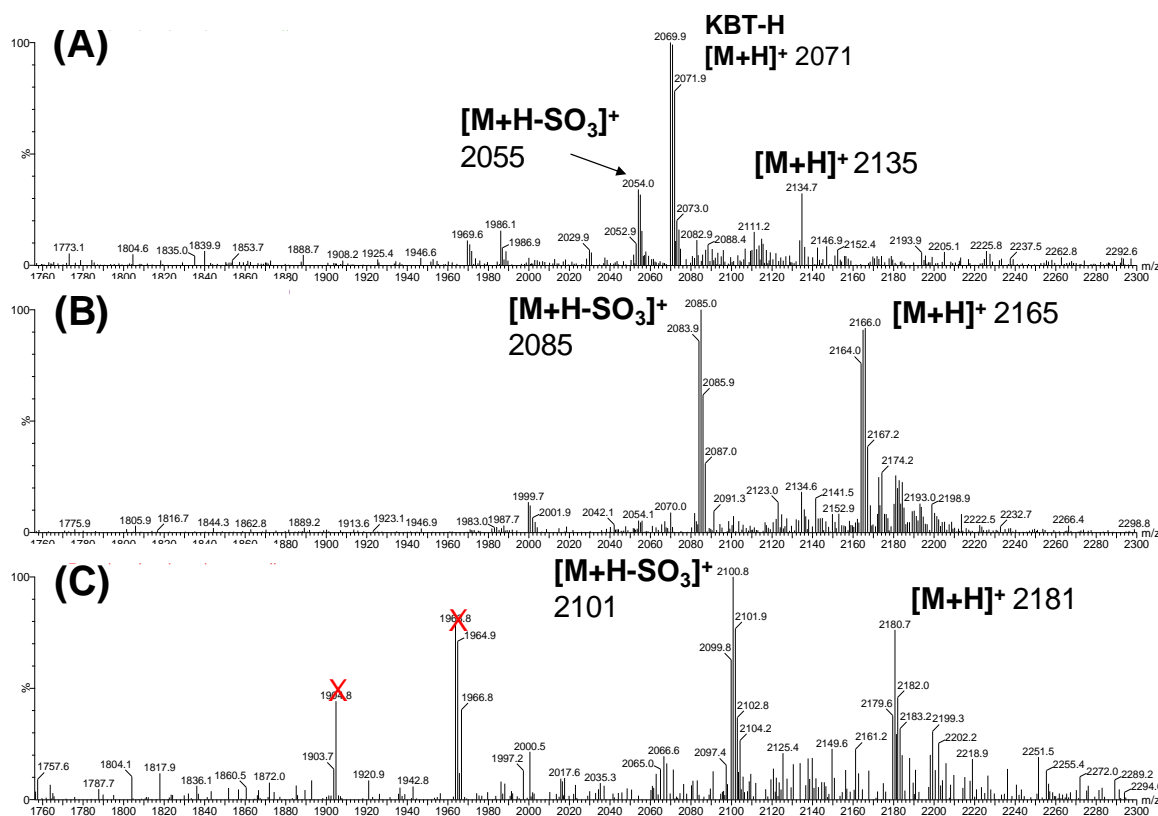


**Figure 4-6.** Mass spectra (ESI<sup>+</sup>) of (A) M2135, (B) M2165 and (C) M2181. Note: [M+H-SO<sub>3</sub>]<sup>+</sup> represents proposed sulphate abstracted protonated molecular ions (-80 Da). Red X: background peaks.

### 4.3.2 LC-MS method development for *K. brevisulcata* studies

#### 4.3.2.1 LC-MS (SIR) method for BSX toxins (Method 1)

Prior to toxins isolation, LC-MS SIR quantitation (Method 1) was established to determine levels of BSXs in cultures. The dominant ions identified for the BSXs in the scanning experiments on SPE extracts of cultures were used to set up mass channels for SIR. The uPLC-Premier MS was used in this study because of the faster separation times achievable with uPLC technology. SIR enables a sensitive and reproducible analysis for the selected components by measuring the response at selected mass channels (generally [M+H]<sup>+</sup>). The method was used for quantitative determination of toxin levels as calibrated against the response for brevetoxin-2 (*m/z* 895, [M+H]<sup>+</sup>). Three SIR channels for BSX-1, BSX-2 and brevetoxin-2 (RSM calibrant) were initially set up but this method was eventually increased to seven channels as more BSX analogues were discovered (Table 4-2). The sum of the peak area responses at [M+H]<sup>+</sup> and [M+H-H<sub>2</sub>O]<sup>+</sup> were used for quantitation of the six BSXs using the TargetLynx peak integration and quantitation software package (Waters, USA).

To determine the linearity of the LC-MS (SIR) responses and their relative response factors, solutions of pure BSX-1 and BSX-2 (Section 5.3.2) were prepared at concentrations of 500, 1000, 1500, 2000 and 10,000 ng mL<sup>-1</sup> and analysed by LC-MS (Method 1). Figure 4-7 shows the linearity plots, including equations and correlation coefficients. The R<sup>2</sup> for both compounds were >0.9996, which proved the high linearity of the LC-MS responses and this was maintained if only the four lower concentrations were plotted i.e. the high concentration point was not biasing the regression. The slopes of the plots indicating the relative sensitivities of the compounds were 103.9 for BSX-1 and 58.6 for BSX-2. The corresponding slope for brevetoxin-2 standards was 85.0. Thus BSX-1 showed higher sensitivity than brevetoxin-2, while BSX-2 was less sensitive than brevetoxin-2. Repeatability relative standard deviations (RSD), dominates the precision for this LC-MS SIR method, and were estimated using replicate SPE extracts of batch carboy cultures (Figure 3-2B) obtained at different time points. The measurements for ring-opened BSXs were highly repeatable with <15% RSD. However, the repeatabilities were relatively poor for ring-closed BSXs (>20% RSD) which were generally only present at low concentrations. The LC-MS limits of quantitation (LOQs) as determined from the signal to noise ratios (5:1) of toxin peaks were similar for brevetoxins and BSXs at ca. 5 ng mL<sup>-1</sup> solution for each toxin as injected into the LC-MS. These LOQs correspond to 0.4 µg L<sup>-1</sup> algal culture (50 mL of cultures extracted and concentrated by SPE to 5 x 0.75 mL, Section 3.2.3). The sensitivities for BSX-4 and BSX-5 were expected to be similar to those of their ring-opened derivatives. Following purification of these ring-closed BSXs, a more sensitive MRM method was developing to monitor both BSXs and KBTs (Section 4.3.2.2).

Quantitative analysis of KBTs was attempted using the uPLC-Premier MS system. These large molecules with m.w. > 1800 Da were predominantly ionised to [M+Na]<sup>+</sup> which showed poor repeatability and high variability (Section 4.3.1.3). 5-35 fold changes in sensitivity were observed using the same sample at different running times. Thus it was difficult to use the uPLC-Premier MS to establish a method of adequate sensitivity and reproducibility for quantitative measurements. The quantitative analysis of KBTs was further developed using HPLC-Ultima MS under MRM operation mode (Method 4), which is described in the next section.



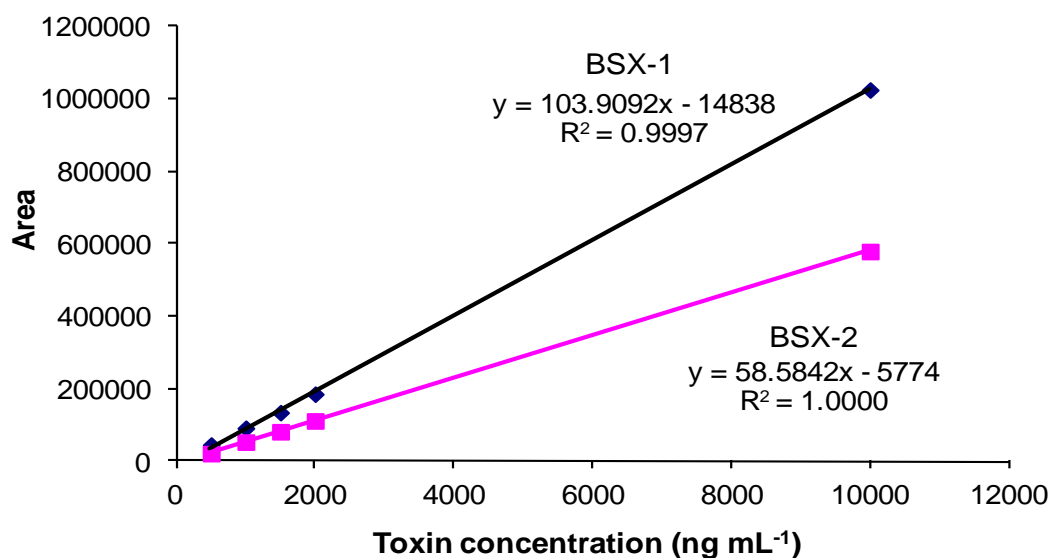


**Figure 4-7.** Linearity of LC-MS (SIR) response for determination of BSX-1 and BSX-2.

#### **4.3.2.2 Establishment of a MRM method (Method 4) for quantitation of BSXs and KBTs**

LC-MS/MS MRM methods are more sensitive, selective and specific for detection and quantitative analysis of novel compounds than LC-MS SIR methods. A MRM method was developed and validated for determining four six BSX toxins and KBT toxins using HPLC-Ultima MS (Method 4, Table 4-3). The mass transitions were chosen based on prominent ions observed in the daughter ion spectrum for each toxin.

#### **Mobile phase optimisation**

Preliminary study using this LC-MS system showed the best separation of BSXs and KBTs was achieved using an acidic mobile phase rather than a neutral mobile phase. The Waters 2695 HPLC is a low pressure HPLC using a single pump to drive three mixed mobile phase solutions. Solution C mixed at a constant 10% was selected to modify the pH of the neutral mobile phases A and B. Three acidic mobile phase modifiers were tested: (C-1) 10% FA in MQ; (C-2) 1% FA in MQ; and (C-3) 50 mM ammonium formate plus 0.02% (v/v) FA in MQ. The modifier C-3 gave enhanced  $[M+NH_4]^+$  ionisation for both KBTs and BSXs. The the mobile phase modifier C-2 was selected for the method because it provided i) 2x more efficient ionisation of BSXs and KBTs than C-1; ii) dominant  $[M+H]^+$  ionisation.

## MRM transitions and optimisation of collision energy

The second stage of mass analysis (MS2) detects daughter ions formed in the collision cell from ions selected in the first stage of mass analysis (MS1). This excludes ions from most related compounds, contaminants and mobile phase. This higher specificity of detection enables lower detection limits for the selected analytes. Water-lost fragments  $[M+H-(H_2O)_n]^+$  are abundant in daughter ion spectra of BSXs at low collision energies. Therefore significant  $[M+H-H_2O]^+$  were observed in the daughter ion spectra of  $[M+H]^+$  of all BSXs and were selected as daughter ions for MRM quantitation (Table 4-3). The collision energy was optimised for maximum sensitivity in the range from 10 to 40 eV. The optimal collision energy was 10 eV for ring-opened BSXs quantitation (-1 to -3) and 15 eV for ring-closed BSXs (-4 to -6) quantitation respectively. Several unique fragments at 300-800 Da were observed in the daughter ion spectra of the  $[M+H]^+$  ions of BSXs (Table 5-4) at high collision energies (> 25 eV). However, although these fragment ions were found to be very specific, they were relatively insensitive for monitoring by MS-MS. The F3 fragment ions ( $m/z$  321, 337, and 381) were selected to establish MRM transitions for BSXs confirmation (Table 4-3). For these MRM confirmation ions, 25 eV was selected as the optimum collision energy for all BSXs.

MRM monitoring of KBT-F (2055.1>1971.0) and KBT-G (2085.1>2001.0) used the  $[M+H-84]^+$  daughter ions produced by cleavage of the 2-methyl-2-butenal side chain (Section 5.3.4.2). The daughter ion spectra for  $[M+H]^+$  of KBT-H and KBT-I showed significant fragment ions ( $[M+H-100]^+$ ) of 1970 and 2101 Da respectively at high collision energy (data not shown). The cleaved fragment with 100 Da for KBT-H is 16 Da higher than that for KBT-F (84 Da), supporting Satake's hypothesis that KBT-H and KBT-I are oxidised analogues of KBT-F and KBT-G respectively and the oxidation might occur on the aldehyde terminus. MRM monitoring of KBT-H (2071.1>1971.0) and KBT-I (2101.1>2001.0) used the  $[M+H-100]^+$  ions as daughter ions. The collision energy was optimised from 25 to 50 eV, and 45 eV was selected for all KBT MRM transitions.

## LC Separation and Specificity

The LC-reversed phase gradient used with the MRM method was optimised for a total cycle time of 14 min. Figure 4-8 shows the MRM chromatographs for an extract of a batch carboy *K. brevisulcata* culture at day 14 when the maximal cell concentration was achieved. The peak responses and integrations were satisfactory for quantitation and confirmation of all

toxins. The retention times for BSXs and KBTs were reproducible to 0.03 min over a 12 hr run of batches of samples and standards. BSXs were well separated by C8 column (Figure 4-1A). However, KBT-G and its oxidative analogue KBT-I were coeluted with KBT-F and KBT-H respectively (Figure 4-1B). Thus MRM channels were established for KBT-H plus KBT-I and KBT-F plus KBT-G (Figure 4-8).

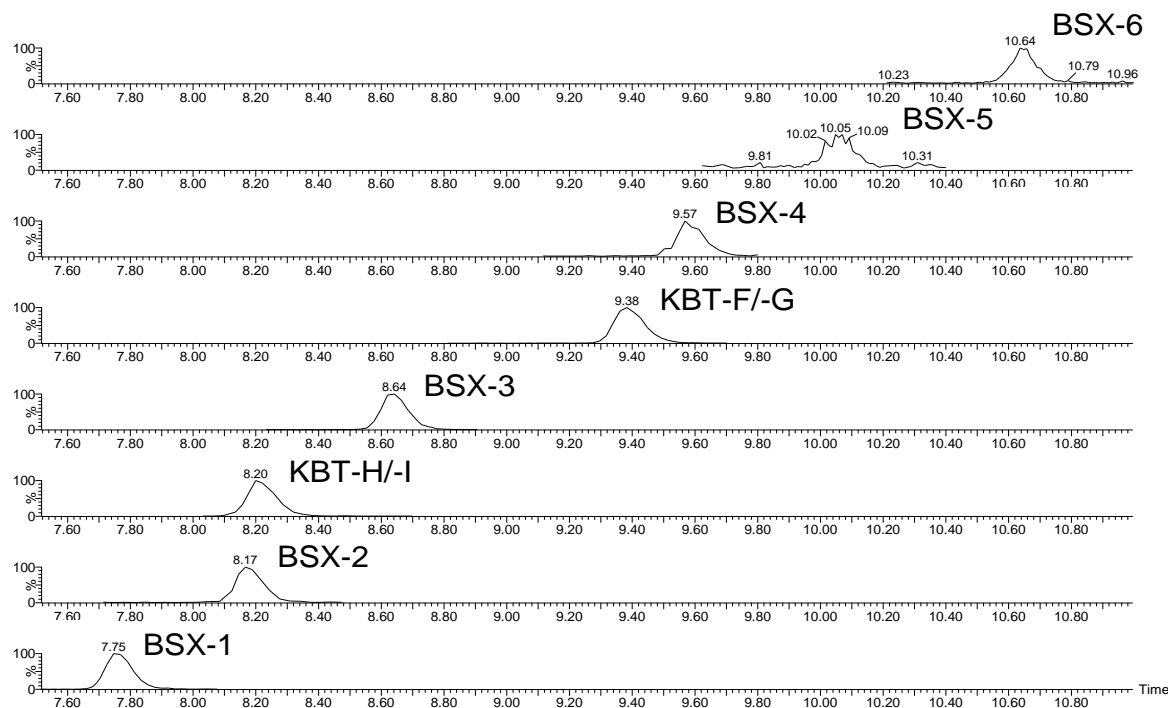


**Figure 4-8.** LC-MS/MS MRM chromatographs for a SPE extract of a batch carboy *Karenia brevisulcata* culture. Six BSXs and four KBTs were quantitatively analysed. See Table 4-3 for MRM parameters.

## ESI optimisation

The initial conditions tested for ESI source operation were capillary voltage of 2.5 kV, cone energy of 50 V, source temperature 80°C and desolvation temperature 350°C. After a series of experiments to optimise source parameters, the following ESI conditions were selected for the method: 4 kV for capillary voltage, 100 V for cone energy, 100°C for source temperature and 400°C for desolvation temperature with increased responses over initial conditions by 96-120% for four BSXs and four KBTs.

## Calibration

The MRM method used 7-point calibrations of the LC-MS responses obtained for solutions of four BSXs (BSX-1, -2, -4 & -5) and four KBTs (-F, -G, -H & -I). RSMs for these BSXs and KBTs were isolated and purified at Cawthron Institute, New Zealand and the

University of Tokyo, Japan respectively. Calibrations were linear for all toxins tested with  $R^2$  values consistently  $> 0.98$  over the concentration range of  $0.5\text{--}200\text{ ng mL}^{-1}$ . However, the standard concentrations of  $<2\text{ ng mL}^{-1}$  gave poor precision (RSDs  $>30\%$ ). Therefore, the MRM quantitation mainly used 5-points standard solutions ( $5\text{--}200\text{ ng mL}^{-1}$ ) to calibrate concentrations of BSXs and KBTs in *K. brevisulcata* cultures. Over this concentration range, the calibration showed higher linear correlation with  $R^2 > 0.99$ .

BSX-3 and BSX-6 have not been isolated and purified, and these two compounds are probably analogues of BSX-1 and BSX-4 respectively (Section 4.3.1.2). The MRM quantitation of BSX-3 and BSX-6 were achieved by i) calibrations with BSX-1 and BSX-4 respectively and ii) using relative response factors of 1.0 for both BSX-3 and BSX-6.

### **Recovery of toxins from RSMs (method accuracy)**

Toxin recovery experiments were conducted using culture media fortified with pure BSXs and KBTs at two concentration levels and with an algal extract (Figure 4-9). The latter was prepared from SPE of a  $200\text{ mL}$  *K. brevisulcata* carboy culture collected at late log phase and contained all toxins. For the recovery experiment at low concentration,  $7.5\text{ ng}$  of each pure BSX and KBT were dissolved in  $1\text{ mL}$  methanol and diluted with culture medium to  $50\text{ mL}$  ( $n=3$ ), corresponding to  $0.15\text{ }\mu\text{g L}^{-1}$  in culture media. These recovery samples were prepared following the SPE procedure as described in Section 3.2.3, and the expected final concentration of each toxin in  $80\%$  methanol ( $0.75\text{ mL}$ ) for LC-MS corresponded to  $2\text{ ng mL}^{-1}$  for a recovery of  $100\%$ . For the recovery experiment at high concentration, lack of pure materials necessitated use of only a single toxin fortified sample ( $50\text{ mL}$  culture medium containing  $375\text{ ng}$  of each KBT and BSX), corresponding to  $7.5\text{ }\mu\text{g L}^{-1}$  in culture media ( $n=1$ ). The recovery samples ( $0.75\text{ mL}$  in  $80\%$  methanol,  $n=3$ ) were prepared from the SPE eluant of this single fortified sample. The expected toxin concentration in the recovery samples was  $100\text{ ng mL}^{-1}$  for a recovery of  $100\%$ .

For the recovery experiment using an algal extract, the dried extract was dissolved in  $4\text{ mL}$   $80\%$  methanol, sonicated for  $5\text{ min}$  and  $1\text{ mL}$  aliquots were diluted to  $50\text{ mL}$  with culture medium ( $n=3$ ; corresponding to  $50\text{ mL}$  *K. brevisulcata* culture). The eluants following SPE were prepared for LC-MS by the same procedure as described in Section 3.2.3 ( $0.75\text{ mL}$  in  $80\%$  methanol, concentration factor  $13.3\times$ ). Aliquots ( $0.2\text{ mL}$ ) of the algal extract corresponding to  $10\text{ mL}$  *K. brevisulcata* culture also were diluted to  $0.75\text{ mL}$  with  $80\%$  methanol to prepare controls ( $n=3$ , concentration factor  $13.3\times$ ) for direct comparison to the SPE recovery samples.

The concentrations of individual toxins in the recovery samples were expected to equal that in the control samples for 100% recovery.

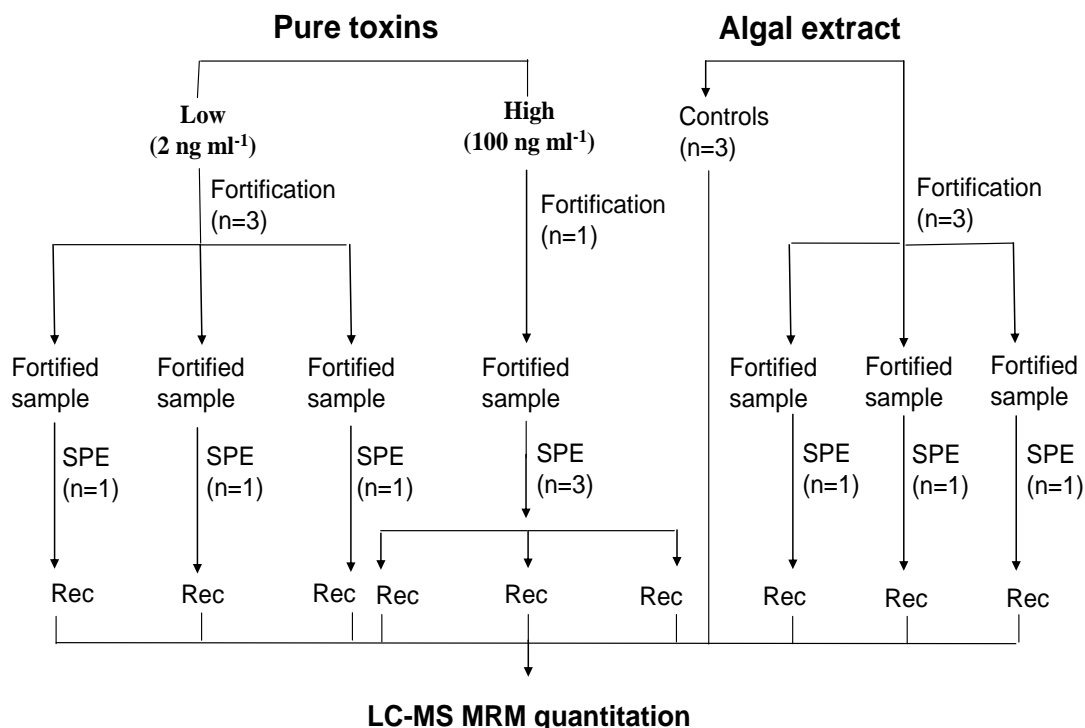


**Figure 4-9.** Flow diagram for toxin recovery experiments. Rec represents recovery samples (SPE eluant) diluted in 80% methanol as described.

All recovery samples were tested by LC-MS with MRM quantitation (Method 4) to calculate the recovery of each individual toxin. The recovery data are shown in Table 4-6. The total pure toxin recoveries based on two concentration experiments were 46-83% for BSXs and 61-90% for KBTs. At 2 ng mL<sup>-1</sup>, most of the toxins tested showed good accuracy (> 70% recovery) except BSX-1, BSX-5 and KBT-F. At 100 ng mL<sup>-1</sup>, recoveries were 58-90%. The precision was generally excellent (RSDs < 10%) except for a few of the toxins at the low concentration.

The recoveries from SPE fortified samples were higher for BSXs (73-102%) but lower for KBTs (50-61%) than those from pure toxin fortification (Table 4-6). However, all SPE recovery samples gave excellent repeatabilities for BSXs and KBTs (RSDs < 15%). The SPE solutions (Section 3.2.3) including load (SPE extract fortified medium), wash (MQ and 20% methanol) and eluants (methanol and acetone) were collected and tested by LC-MS (Method 4, MRM). No significant toxin losses (< 10%) occurred in load or wash stages. To check whether toxins still retained in SPE cartridge, an extra elution with 3 mL acetone was carried out. This extra acetone fraction contained < 1% BSXs and some KBTs but only ca. 5%.

Therefore loss of toxins through irreversible absorption to the SPE cartridge was not significant. Recoveries of <70% are not acceptable for a fully validated method. The apparent losses, particularly of KBTs, observed in these preliminary experiments may have arisen from i) shifts in MS sensitivity; ii) suppression/enhancement of ionisation in the ESI source due to co-extractives; iii) losses of toxins due to degradation or reduction during SPE (the aldehyde group in KBTs may be reactive). Further more detailed experiments are required to investigate these factors and further develop and validate the method for use in regulatory testing.

**Table 4-6.** Recovery of BSXs and KBTs from the culture media fortified with pure toxin or algal extract containing all toxins. Fortified samples were extracted using SPE (Strata-X) to prepare recovery samples for LC-MS (Method 4, MRM).

Toxins <sup>a</sup>	<b><u>BSX-1</u></b>			<b><u>BSX-2</u></b>			<b><u>BSX-4</u></b>			<b><u>BSX-5</u></b>		
	Pure toxin <sup>b</sup>		AE <sup>c</sup>	Pure toxin		AE	Pure toxin		AE	Pure toxin		AE
	2	100	283.1	2	100	36.9	2	100	21.9	2	100	3.0
Rep 1	0.89	57.33	235.8	1.61	58.27	32	1.53	72.43	24.4	1.37	74.5	3.3
Rep 2	0.93	59.07	192.6	1.57	60.25	30.5	1.73	72.55	19.1	0.93	73.04	2.7
Rep 3	0.91	56.3	194.0	1.12	62.42	33.3	1.73	73.3	18.9	1.17	72.59	3.2
<b>Mean</b>	0.9	57.6	207.5	1.4	60.3	31.9	1.7	72.8	20.8	1.2	73.4	3.1
SD <sup>e</sup>	0.020	1.40	24.5	0.272	2.08	1.401	0.115	0.471	3.104	0.220	0.999	0.325
%RSD <sup>e</sup>	2.2	2.4	11.8	19.0	3.4	4.4	6.9	0.6	14.9	19.0	1.4	10.6
<b>Recovery%</b>	45.5	57.6	73.3	71.7	60.3	86.6	83.2	72.8	94.8	57.8	73.4	101.8

**Table 4-6.** (continued)

Toxins	<b><u>KBT-F</u></b>			<b><u>KBT-G</u></b>			<b><u>KBT-H</u></b>			<b><u>KBT-I</u></b>		
	Pure toxin		AE	Pure toxin		AE	Pure toxin		AE	Pure toxin		AE
	2	100	67.8	2	100	28.6	2	100	95.5	2	100	34.6
Rep 1	1.37	62.13	43.8	1.70	56.9	16.7	1.55	64.7	66.8	1.71	91.51	16.0
Rep 2	1.27	59.68	37.7	1.13	66.18	13.2	1.82	67.54	63.9	1.08	85.46	20.3
Rep 3	1.14	61.95	42.1	1.43	65.38	12.8	1.73	69.3	60.9	1.70	91.4	18.9
<b>Mean</b>	1.3	61.3	41.2	1.4	62.8	14.2	1.7	67.2	63.8	1.5	89.5	18.4
SD	0.115	1.37	3.13	0.285	5.14	2.15	0.137	2.32	2.95	0.361	3.46	2.15
%RSD	9.2	2.2	7.6	20.1	8.2	15.1	8.1	3.5	4.6	24.1	3.9	11.7
<b>Recovery%</b>	63.0	61.3	60.8	71.0	62.8	49.7	85.0	67.2	66.8	74.8	89.5	53.2

<sup>a</sup> BSX, brevisulcatic acid; KBT, brevisulcinal; <sup>b</sup> Fortification with four pure BSXs (-1, -2, -4, and -5) and four pure KBTs (-F, -G, -H & -I) at two concentrations;

<sup>c</sup> Fortification with an algal extract of a *K. brevisulcata* carboy culture at late log phase; <sup>d</sup> Pure toxin: the expected concentrations of 2 and 100 ng mL<sup>-1</sup> in recovery samples correspond to toxin concentrations in culture media of 0.15 and 7.5 µg L<sup>-1</sup> respectively (concentration fraction from culture 13.3x); AE: algal extract, the concentration of each individual toxin in controls (concentration fraction from culture 13.3x) determined by LC-MS; <sup>e</sup> SD, standard deviation; RSD, relative standard deviation.

## LOQ determination

The LOQ for each toxin was determined using the ‘Bioanalytical Method Validation’ criteria as detailed by the Food and Drug Administration, USA (FDA, 2001): i) the signal to noise ratios  $\geq 5:1$ , ii) the accuracy of 80-120%, and iii) the precision of  $\leq 20\%$  RSD. On this basis LOQs in 80% methanol solution directly applicable for LC-MS were ca. 2 ng mL<sup>-1</sup> for all BSXs and KBTs tested. These LOQs correspond to 0.15 µg L<sup>-1</sup> algal culture (50 mL of cultures extracted and concentrated by SPE to 5x0.75 mL, Section 3.2.3). For BSXs, the LOQs in MRM method are 2.5 fold lower than those in SIR quantitation (Section 4.3.2.1), supporting MRM quantitation as providing lower detection limits than SIR.

## Method Precision

The precision of LC-MS MRM quantitation (Method 4) was estimated using SPE extracts of *K. brevisulcata* cultures collected at different ages. Culture samples (50 mL each, n=1) were collected at day 3 (the early stage with the lowest cell concentration), day 14 (the late log phase with the highest cell concentration) and day 28 (the late stage where the culture collapsed respectively). SPE extract samples were prepared following the same procedure as described in Section 3.2 and were applied to MRM quantitation with replicated injections (n=5). Toxin concentrations were calibrated from 5-points standard solutions (5-200 ng mL<sup>-1</sup>; four BSXs and four KBTs).

Table 4-7 summarizes the estimates for MRM method precision. The results showed high repeatability with  $\leq$  RSD 2-15% for all samples where the concentrations of toxins tested were higher than 10 ng mL<sup>-1</sup>. Relatively poor repeatability was observed for BSX-6 at day 28 where the concentration was  $< 2$  ng mL<sup>-1</sup>. BSX-3 and -6 are calibrated with BSX-1 and -4 respectively. The results obtained from the precision study supported that BSX-6 has similar LC-MS characteristics to BSX-4, and suggested that the MRM LOQ for BSX-6 should be similar to that for BSX-4 at ca. 2 ng mL<sup>-1</sup> level.



**Table 4-7.** Precision of LC-MS MRM quantitation (Method 4, MRM) using samples from a *K. brevisulcata* batch carboy culture (1 x 50 mL SPE extract at three sampling dates, 5 injections of each sample extract).

Toxins <sup>a</sup> (ng mL <sup>-1</sup> ) <sup>c</sup>	BSX-1			BSX-2			BSX-3 <sup>b</sup>			BSX-4			BSX-5		
	Day 3	Day 14	Day 28	Day 3	Day 14	Day 28	Day 3	Day 14	Day 28	Day 3	Day 14	Day 28	Day 3	Day 14	Day 28
Injection 1	31.8	258.2	791.3	6.2	61.9	546.0	39.4	298.5	40.7	25.4	32.8	8.7	2.1	5.2	6.1
Injection 2	35.4	267.7	791.1	4.9	65.3	534.8	39.7	311.7	36.3	26.2	31.6	8.8	2.1	5.6	5.0
Injection 3	32.2	268.0	783.6	7.2	70.5	518.4	40.7	298.9	38.6	26.6	34.0	9.3	2.8	5.6	5.7
Injection 4	30.8	264.5	779.2	5.6	70.6	530.3	40.4	310.0	40.5	27.4	35.4	8.5	2.5	6.5	5.1
Injection 5	34.5	258.3	778.5	7.0	71.2	536.9	41.3	304.6	39.3	23.3	36.5	9.3	2.7	6.2	5.6
<b>Mean</b>	33.0	263.4	784.7	6.2	67.9	533.3	40.3	304.7	39.1	25.8	34.1	8.9	2.4	5.8	5.5
<b>SD<sup>d</sup></b>	1.93	4.84	6.22	0.97	4.12	10.09	0.76	6.10	1.81	1.58	1.96	0.37	0.31	0.52	0.44
<b>%RSD<sup>d</sup></b>	5.9	1.8	0.8	15.7	6.1	1.9	1.9	2.0	4.6	6.1	5.8	4.1	12.7	8.9	7.9

**Table 4-7.** (continued)

Toxins <sup>1</sup> (ng mL <sup>-1</sup> )	BSX-6			KBT-F			KBT-G			KBT-H			KBT-I		
	Day 3	Day 14	Day 28	Day 3	Day 14	Day 28	Day 3	Day 14	Day 28	Day 3	Day 14	Day 28	Day 3	Day 14	Day 28
Injection 1	27.9	47.2	2.5	25.0	174.3	65.6	5.6	63.4	19.1	26.32	156.21	43.72	5.2	61.0	19.9
Injection 2	31.3	44.4	2.0	25.0	170.5	66.9	6.4	65.0	23.0	22.47	175.46	46.71	5.2	59.2	15.4
Injection 3	29.4	44.3	1.7	24.8	178.5	67.0	4.9	61.1	21.1	27.2	167.36	40.27	5.7	65.2	13.2
Injection 4	28.4	43.4	1.8	26.7	175.4	69.1	6.2	66.9	23.1	29.63	165.75	39.24	6.4	66.4	18.4
Injection 5	28.4	42.9	1.2	23.7	177.4	68.9	5.1	65.5	23.7	24.76	169.89	42.04	5.1	64.4	14.7
<b>Mean</b>	29.1	44.4	1.8	25.0	175.2	67.5	5.7	64.4	22.0	26.1	166.9	42.4	5.5	63.3	16.8
<b>SD</b>	1.34	1.67	0.46	1.10	3.10	1.46	0.65	2.20	1.87	2.68	7.04	2.96	0.54	3.03	2.60
<b>%RSD</b>	4.6	3.7	25.0	4.4	1.8	2.2	11.6	3.4	8.5	10.3	4.2	7.0	9.8	4.8	15.5

<sup>a</sup> BSX, brevisulcatic acid; KBT, brevisulcinal;

<sup>b</sup> BSX-3 and BSX-6 were calibrated using BSX-1 and BSX-4 respectively;

<sup>c</sup> Toxin concentrations present in final SPE extract as prepared for LC-MS determination (concentration factor from culture 13.3x);

<sup>d</sup> SD, standard deviation; RSD, relative standard deviation.

#### 4.3.3 Determination of brevetoxin profile in *K. brevis* extract

Toxicity of *K. brevis* is dependent on production of brevetoxins. At least nine brevetoxins have been identified as the metabolites of *K. brevis* by previous studies (Lin *et al.*, 1981; Morohashi *et al.*, 1995; Quilliam, 2003a; Ramsdell, 2008; Shimizu *et al.*, 1986). These brevetoxins can be simply classified into two types according to their different backbone structures (Ramsdell, 2008): Type A brevetoxins with 10 fused cyclic ether rings (5,8,6,7,9,8,8,6,6,6) (Shimizu *et al.*, 1986), and Type B brevetoxins with 11 fused cyclic ether rings (6,6,6,7,7,6,6,8,6,6,6) (Lin *et al.*, 1981). The previous abbreviations for the parent brevetoxins brevetoxin-A and -B are now brevetoxin-1 and -2 respectively. Toxicity of brevetoxins is dependent on i) the backbone structure e.g. brevetoxin-1 being more potent than brevetoxin-2 in several bioassays (Roth *et al.*, 2007); and ii) the “tail” structure, e.g. brevetoxin-B5 (carboxylated tail) being less toxic i.p. than brevetoxin-2 (aldehyde tail) (Figure 2-10) (Ishida *et al.*, 2004a).

The LC-MS scanning experiments (Method 3) showed SPE extract of cultures of *K. brevis* (CAWD 122) produced four brevetoxins but did not produce BSXs or KBTs (Table 4-8). The lactone ring-A closed brevetoxin-1 and brevetoxin-2 were the main toxins produced. However, the lactone ring-A opened (ROd) brevetoxin-3 and ROd brevetoxin-B5 were predominant in SPE extracts (Figure 4-10). The presence of ROd brevetoxins supports the previous studies that the A ring of brevetoxins can be easily hydrolysed both under natural and laboratory conditions (Abraham *et al.*, 2006; Hua & Cole, 1999; Roth *et al.*, 2007). The polarities are ROd brevetoxin-3 > ROd brevetoxin-B5 > ROd brevetoxin-2 > ROd brevetoxin-1 > brevetoxin-3 > brevetoxin-B5 > brevetoxin-2 > brevetoxin-1 (Figure 4-10).

All brevetoxins were predominantly ionised to form  $[M+H]^+$  by both Ultima and Premier MS. An eight channel SIR method was further developed using uPLC-Premier MS to quantitatively analyse the concentrations of four parent brevetoxins and their ROd derivatives in the *K. brevis* cultures used for the fish acute toxicity tests described in Section 7.2.5. Calibration was achieved with solutions of RSMs of brevetoxin-1, -2, -3 and -B5 (UNCW). The response factors for ROd toxins were assumed to be the same as for the respective parent brevetoxins.

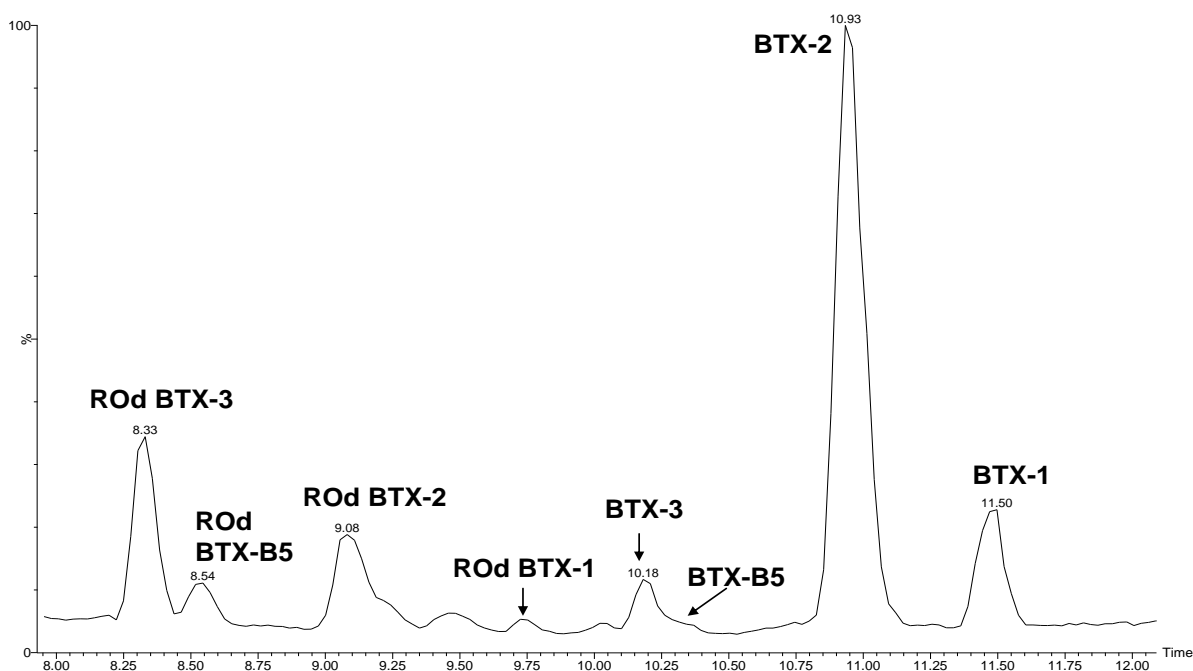


**Figure 4-10.** TIC from 8 to 12 min (Method 3, scanning) of an SPE extract of a *K. brevis* culture at  $m/z$  500-1000. BTX represents brevetoxin, and ROb BTX indicates ring opened brevetoxin.

**Table 4-8.** Toxins detected in a *K. brevis* (CAWD 122) extract using LC-MS (Method 3, scanning).

Toxin <sup>a</sup>	Retention time (min)	[M+H-H <sub>2</sub> O] <sup>+</sup> ( $m/z$ )	[M+H] <sup>+</sup> ( $m/z$ )	[M+NH <sub>4</sub> ] <sup>+</sup> ( $m/z$ )	[M+Na] <sup>+</sup> ( $m/z$ )
<b>BTX-1</b>	11.5	849.4	867.5	884.5	889.5
<b>BTX-2</b>	10.9	877.4	895.7	912.7	ND <sup>b</sup>
<b>BTX-3</b>	10.2	879.4	897.7	ND	919.7
<b>BTX-B5</b>	10.3	ND	911.1	ND	ND
<b>ROd BTX-1</b>	9.7	867.4	885.4	902.2	907.3
<b>ROd BTX-2</b>	9.1	895.4	913.5	ND	ND
<b>ROd BTX-3</b>	8.3	897.5	915.7	ND	ND
<b>ROd BTX-5</b>	8.5	911.4	929.4	ND	ND

<sup>a</sup> BTX, brevetoxin; ROb BTX, ring opened brevetoxin

<sup>b</sup> ND, not detected

#### 4.3.4 Detection of novel compounds produced by *K. mikimotoi*

The fish-killing mechanisms of *K. mikimotoi* are still unclear, but may involve novel biotoxins, ROS, haemolysins or environmental stressors e.g. dissolved oxygen depletion (Landsberg, 2002). In this study, LC-MS (Method 3, scanning) was used to investigate *K. mikimotoi* extracts prepared from the cell pellets of mass cultures. Table 4-9 summarises the novel compounds produced by different strains. No brevetoxins, BSXs and KBTs were found in any extracts of three *K. mikimotoi* strains. Four novel compounds were detected in the extract of CAWD 63, and can be classified into two classes of compounds according to their molecular weights (Table 4-9). However, no gymnocins were detected and this strain was non-toxic in the bioassays conducted at Cawthron Institute (Chapter 7). For CAWD 134, no significant compounds were detected by LC-MS (Table 4-9).

Four *K. mikimotoi* strains produced several interesting novel compounds including gymnocins and the TIC are shown in Figure 4-11. The Japan strain (CAWD 05) produces several potential polycyclic ether compounds in which gymnocin A (Figures 4-11A, 4-12A) was confirmed using the RSM of gymnocin-A kindly provided by Prof. Satake (Satake *et al.*, 2002). Additionally, two unknown compounds were also observed, giving spectra with  $[M+H]^+$  of  $m/z$  927 and  $m/z$  1126 respectively (Figure 4-11A, Table 4-9).

*K. mikimotoi* China strain was isolated from South China Sea in 2009, and is believed to have caused several fish-killing events (C.L. Gao, pers. comm.). The LC-MS scanning shows two significant peaks with  $[M+H]^+$  spectra of  $m/z$  1173 and  $m/z$  1157 (Figure 4-11B, Table 4-9) respectively. The latter ion was consistent with gymnocin-B with molecular mass of 1156 Da (Figures 2-12, 4-12B) (Satake *et al.*, 2005).

NZ strains CAWD 117 and 133 were isolated from Marlborough Sounds and Kennedy Bay, Coromandel respectively, which are both important shellfish production areas. Both these strains gave the same significant peak (8.6 min) which has a spectrum with an  $[M+H]^+$  of  $m/z$  1143 and a strong fragment ion at  $m/z$  1125, corresponding to  $[M+H-H_2O]^+$  (Figures 4-11C, 4-12C). The protonated mass is the same as for gymnocin-C, a new analogue of gymnocin-A (Figure 2-12; Y. Oshima, pers. comm.). However, without the standard materials, it was not possible to confirm the assignments for  $[M+H]^+$  1157 (gymnocin-B?) and  $[M+H]^+$  1143 (gymnocin-C?).

Ruakaka Bay, Marlborough Sounds experienced a severe HAB event during 2010 in which more than 20,000 adult Chinook salmon were killed (MacKenzie *et al.*, in press). This

bloom was dominated by *Pseudochattonella verruculosa*, but a strain of *K. mikimotoi* was also isolated from that bloom. Ruakaka spp 1 was found to produce several novel compounds but mainly with relatively low molecular weights (600-1103 Da) (data not shown). A novel compound M927 (Rt 7.9 min,  $[M+H]^+$   $m/z$  927) was observed in extracts of CAWD 05 and Ruakaka spp1 (Figures 4-11A, D, 4-12D; Table 4-9). The molecular weight of 926 Da is closer to those for brevetoxins (m.w. 800-1000 Da) than those for gymnocins, and the spectrum is characteristic of polycyclic ethers with strong  $[M+H]^+$  and multiple water loss ions. This compound is similar to BSX-1 and BSX-2 in polarity (Figures 4-1A, 4-11A), suggesting that M927 is less likely to bioaccumulate in shellfish tissues. However, both CAWD 05 and Ruakaka spp 1 were suspected to cause several fish killing events in Japan and New Zealand (L. MacKenzie, pers. comm.). The isolation of this brevetoxin-like M927 in further studies will be helpful to better understanding fish killing mechanisms of *K. mikimotoi*, which appears to be a diverse species with respect to the types and concentrations of polyether compounds produced.

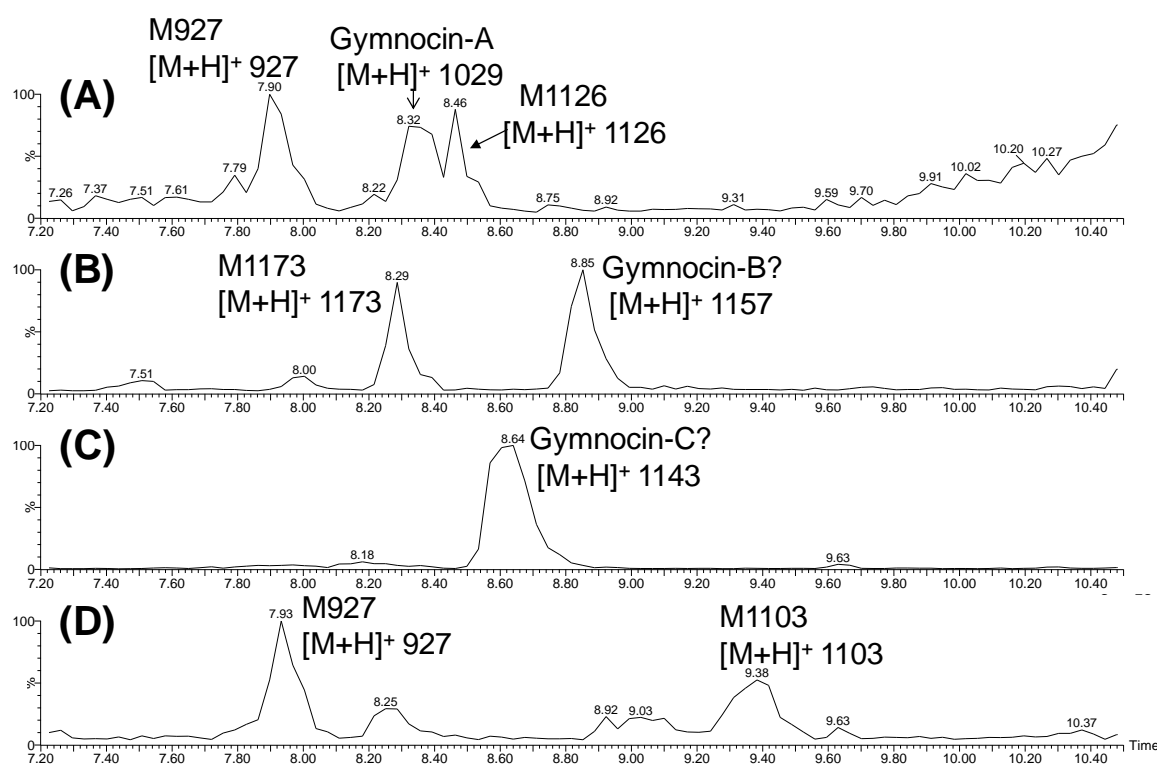


**Figure 4-11.** TIC from 7.2 to 10.5 min (Method 3, scanning) of extracts of *K. mikimotoi* cultures at  $m/z$  900-2150: (A) Japanese strain, CAWD 05; (B) South China Sea strain; (C) NZ strains, CAWD 117 and 133 and (D) NZ strain isolated from Ruakaka Bay, Marlborough Sounds.

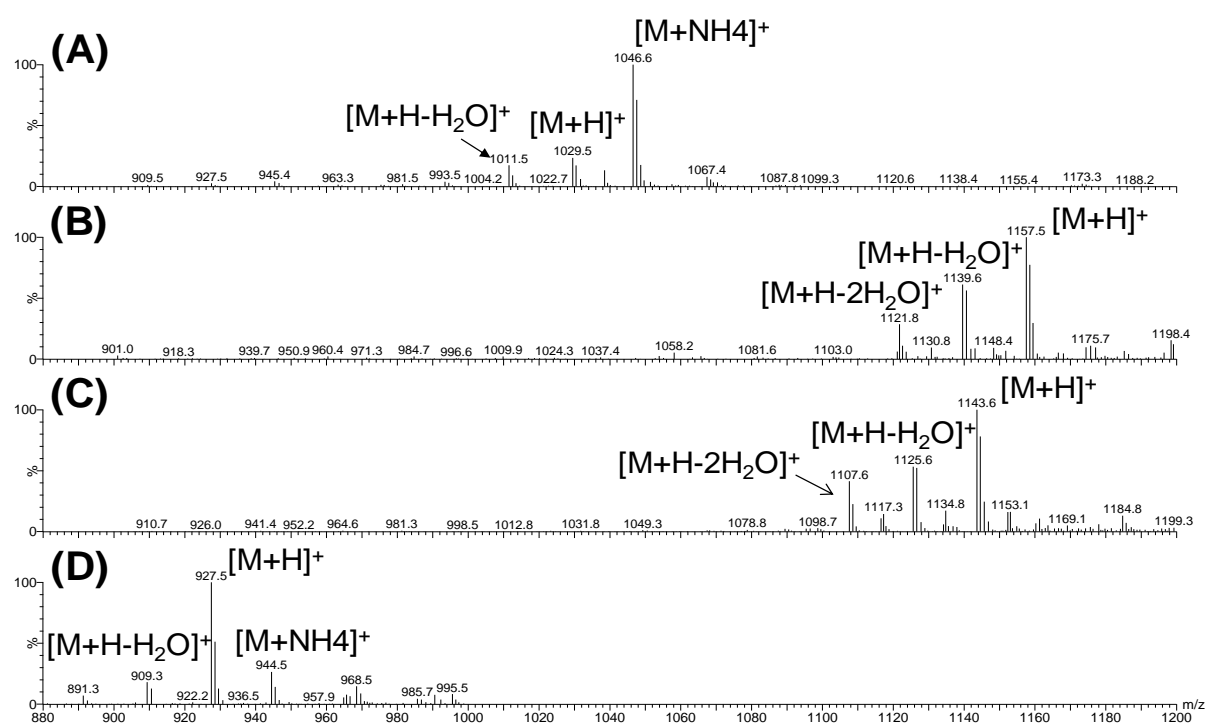


**Figure 4-12.** Mass spectra (ESI<sup>+</sup>) of (A) gymnocin-A, (B) M1157 (gymnocin-B?), (C) M1143 (gymnocin-C?), and (D) component M927.

**Table 4-9.** Novel compounds detected in *K. mikimotoi* extracts by LC-MS (Method 3, scanning).

Strain	Potential toxins	Retention time (min)	[M+H-H <sub>2</sub> O] <sup>+</sup> (m/z)	[M+H] <sup>+</sup> (m/z)	[M+NH <sub>4</sub> ) <sup>+</sup> (m/z)	[M+Na] <sup>+</sup> (m/z)
CAWD 05	M927	7.9	909.3	927.5	944.6	ND
	gymnocin-A	8.36	1011.5	1029.4	1046.5	1051.4
	M1126	8.46	1108.3	1126.5	1143.7	ND
	M1309	11.6	NA	1309.7	1326.8	1331.7
CAWD 63	M1361	7.47	1343.5	1361.7	1378.8	ND
	M1227	8.89	1209.6	1227.6	ND	ND
	M703	9.84	685.4	703.4	720.4	725.4
	M701	10.4	683.3	701.4	718.4	723.4
CAWD 117 & CAWD 133	gymnocin-C? M1157	8.6	1125.7	1143.7	ND	ND
CAWD 134	ND	-	-	-	-	-
Ruakaka spp1	M927	7.9	909.3	927.5	944.6	ND
	M1103	9.03	1085.6	1103.1	NA	ND
China strain	M1173	8.29	ND	1173.6	1190.9	ND
	gymnocin-B? M1143	8.85	1139.6	1157.5	ND	ND

ND, not detected

## 4.4 Summary

*K. brevisulcata* isolated from Wellington Harbour, New Zealand is similar to other *Karenia* species in cell morphology but is vastly different in toxin production. LC-MS scanning of SPE extracts of *K. brevisulcata* cultures shows this species can produce six BSXs and at least seven KBTs. BSXs are a group of polycyclic ether compounds with m.w. 800-950 Da. Six BSXs are named according their polarity under acidic separation conditions, and can be simply divided into ring-opened BSXs (-1 to -3) and ring-closed BSXs (-4 to -6). KBTs are larger novel compounds with m.w. >1800 Da. There were eight KBTs detected by LC-MS including four known KBTs (-F, -G, -H & -I) and unknown KBT-related compounds (M1917, M2135, M2165 & M2181)

A fast and sensitive LC-MS SIR method using uPLC-Premier MS was developed to monitor BSXs production in *K. brevisulcata* cultures. However, KBTs could not be quantitatively analysed by uPLC-Premier MS because of poor reliable and repeatable  $[M+Na]^+$  ionisation. The breakthrough came with the isolation and purification of RSMs of BSXs and KBTs (Sections 5.3.2 & 5.3.4.1). It enabled the development of MRM quantitation to provide a more sensitive and selective LC-MS method for quantitatively analysis of six BSXs and four KBTs. Calibration using 5-points standard solutions is highly linear for all toxins tested over the concentration range of 5-200 ng mL<sup>-1</sup> with  $R^2 > 0.99$ . Validation data has been gathered for culture media via fortification with toxins from standard solutions and an SPE extract of *K. brevisulcata* culture. Fortification levels were 0.15–15.6 µg L<sup>-1</sup> in culture media, which represents the expected range in *K. brevisulcata* cultures. Recoveries were 46-102% and repeatabilities were excellent (RSDs < 10%) except for a few of the toxins at the low concentration. LOQs for both BSXs and KBTs were ca. 2 ng mL<sup>-1</sup> in 80% methanol, which correspond to 0.15 µg L<sup>-1</sup> algal culture.

*K. brevis* and *K. mikimotoi* were also investigated by LC-MS in this study. The former produces four brevetoxins which are present in both ring-opened and ring-closed forms in the SPE extracts and have similar LC-MS appearances to BSXs e.g. m.w. and polarity. Seven strains of *K. mikimotoi* were tested by LC-MS scanning. Several novel compounds were identified such as gymnocin-A, M1157 (gymnocin-B?), M1143 (gymnocin-C?) and M927 (Table 4-9), which may also be ichthyotoxic and/or cytotoxic (Satake *et al.*, 2002; Satake *et al.*, 2005). Thus isolation and purification of these novel compounds in the future will be helpful to a better understanding of fish killing mechanism of *K. mikimotoi*.

## Chapter 5

### Chemical investigations of BSXs and KBTs

#### 5.1 Introduction

*K. brevisulcata* isolated from Wellington Harbour, New Zealand in 1998 is a toxic dinoflagellate that proved lethal to many marine vertebrates, marine invertebrates, and marine flora following a major bloom event (Chang, 1999a, b). Ecological damage and over 500 cases of human respiratory distress were reported (Chang, 1999b; Chang *et al.*, 2001; Gardner & Wear, 2006; Wear & Gardner, 2001). This species can produce complex toxic agents which are strongly toxic to mouse, haemolytic and cytotoxic (Chang, 1999b; Keyzers, pers. comm.; Truman *et al.*, 2005). Neuro2a cell cytotoxicity was partially attributed to blocking of sodium channels (Truman, 2007). However, the responses of Neuro2a cells treated with *K. brevisulcata* extracts were different to the known VGSC-dependent algal toxins such as brevetoxins, CTX and STX (Truman *et al.*, 2005). LC-MS screening of *K. brevisulcata* cultures did not detect brevetoxins -1, -2, -3 and -9 (McNabb *et al.*, 2006) or metabolites brevetoxin-B2 and brevetoxin-B5, but did find several acidic compounds with molecular weights similar to brevetoxins which were subsequently named brevisulcatic acids (BSXs). Researchers at Tohoku University, Japan identified and partially isolated 6-8 novel bioactive polyether compounds with m.w. 1900 to 2200 Da from the lipophilic extract of *K. brevisulcata* cultures produced at Cawthron Institute (Y. Oshima, pers. comm.). These lipophilic toxins were initially named Karenia brevisulcata toxins (KBTs). Following further structural studies by a research group at the University of Tokyo, Japan, led by Prof. Masayuki Satake, these toxins were named brevisulcenals but the acronym KBT was retained (Hamamoto *et al.*, 2012).

NMR is the most powerful tool for chemical structure elucidation of organic compounds. It can study a wide variety of nuclei with net spin of  $\frac{1}{2}$ , including  $^1\text{H}$ ,  $^{13}\text{C}$ ,  $^{15}\text{N}$ ,  $^{19}\text{F}$  and  $^{31}\text{P}$ .  $^1\text{H}$  and  $^{13}\text{C}$  NMR are the most useful for natural product chemists because hydrogen and carbon are major components of most organic compounds. The chemical shifts for individual atoms in a molecule are exquisitely linked to their proton environment (number and configuration of neighbouring protons), and carbon environment (number and type of carbon atoms) in an organic molecule. These 1D chemical shift spectra can be interpreted to provide structural information as to the molecular architecture. 2D spectra which correlate atoms within a spin system enable more detailed probing of connectivity. Heteronuclear Single Quantum



correlation (HSQC) experiments correlate the chemical shift of each proton with the chemical shift of a direct bonded heteronucleus (an atomic nucleus other than proton), most often  $^{13}\text{C}$  or  $^{15}\text{N}$ .  $^1\text{H}$ - $^{13}\text{C}$  HSQC experiments are frequently used as part of structural elucidation of algal toxins by NMR (Morohashi *et al.*, 1995; Satake *et al.*, 2002; Satake *et al.*, 2005). The resulting spectrum is 2D with x axis for  $^1\text{H}$  and y axis for  $^{13}\text{C}$ , determining the  $\text{CH}_n$  groups in an organic compound. Correlation spectroscopy (COSY) and total correlation spectroscopy (TOCSY) are 2D spectra that correlate protons on adjacent and further carbons respectively. Heteronuclear multiple-bond correlation spectroscopy (HMBC) is also widely used in NMR experiments of algal toxins (Morohashi *et al.*, 1995; Satake *et al.*, 1995; Satake *et al.*, 2002; Satake *et al.*, 2005; Seki *et al.*, 1995), which can detect correlations of  $^{13}\text{C}$  atoms over longer ranges of 2-4 bonds. In combination with  $^1\text{H}$  and  $^{13}\text{C}$  1D spectra, 2D NMR experiments such as HSQC, COSY, TOCSY and HMBC allows the complete elucidation of the carbon connectivity and 3-dimensional chemical structure of complex organic molecules. The principal problems with NMR are i) the relative insensitivity of the technique especially for  $^{13}\text{C}$  where the natural abundance is only 1.1%; ii) the long time frames to acquire data of sufficiently high signal/noise (partially arising from i). Typically 1-5 mg of a highly purified compound is required to acquire a full range of 1D and 2D spectra. Acquisition of data can take 12 hours or longer for a typical 2D experiment. These limitations can be somewhat overcome by employing instruments of higher field/higher frequency (600-800 MHz) and by producing toxins enriched in  $^{13}\text{C}$ .

In this study, four BSX and four KBT toxins including  $^{13}\text{C}$  labelled toxins were isolated at Cawthron and the University of Tokyo respectively using multiple stages of column chromatography and were characterised by spectroscopy and micro-derivatisation. Data obtained from UV, MS, MS/MS and NMR spectra enabled the preliminary structural elucidation of BSXs and KBTs.

## **5.2 Materials and methods**

### **5.2.1 Crude extracts of *K. brevisulcata* cultures**

The crude HP20 extracts used for all the following experiments were obtained from mass cultures of *K. brevisulcata* produced at Cawthron Institute, Nelson, New Zealand (Section 3.3.5).

## **5.2.2 Isolation and purification of toxins**

### **5.2.2.1 Separation of BSX toxins from neutral KBTs**

The crude HP20 extract was dissolved in methanol and diluted to 55% v/v with pH 7.2 phosphate buffer. Typically, the volume was 500 mL for each 100 L culture. This solution was partitioned with chloroform (CHCl<sub>3</sub>; 2x 250 mL) and the combined CHCl<sub>3</sub> fraction containing neutral toxins (KBTs and BSX-3 to -6) was evaporated. The aqueous fraction was adjusted to pH 4 with 1M HCl and partitioned with dichloromethane (DCM; 3x 200 mL). The combined DCM fraction enriched in acidic toxins (BSX-1 & -2) was evaporated.

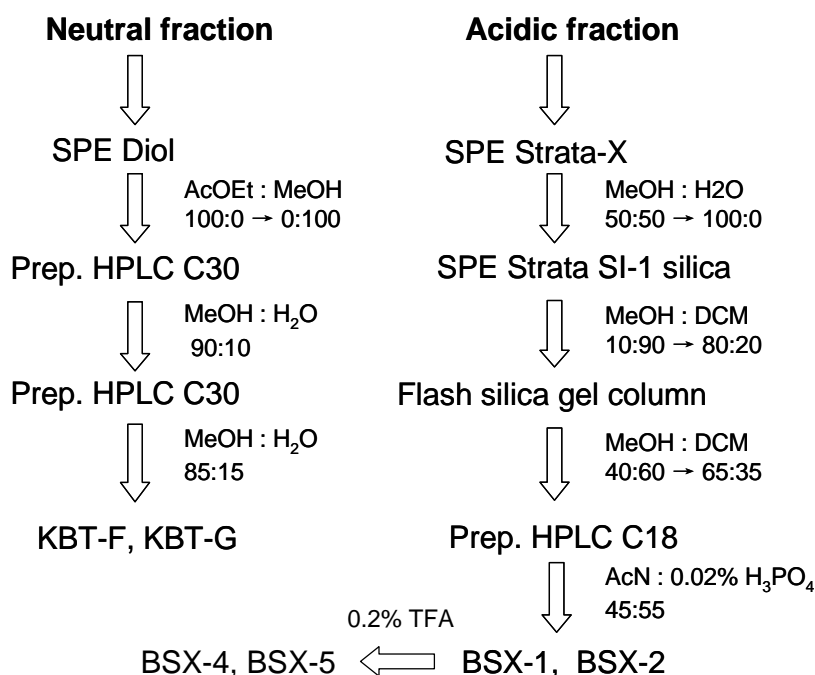
### **5.2.2.2 Isolation and purification of KBT-F & -G (collaboration with Prof. Satake at the University of Tokyo)**

Figure 5-1 shows a schema of the chromatographic isolation procedures for KBTs and BSXs. KBT-F and KBT-G were isolated at the University of Tokyo from the neutral fractions of bulk cultures by column chromatography using diol-silica (SepPak 500mg, Waters Corp, MA) with stepwise elution (ethyl acetate to methanol) and guided by the mammalian cell cytotoxicity assay. Final purification was by two stages of preparative HPLC (250 mm x 4.6 mm id Develosil C30-UG-5, Nomura Chemical Co., Japan) with isocratic elution (90% methanol/H<sub>2</sub>O followed by 85% methanol/H<sub>2</sub>O) and guided by UV absorbance at 230 nm (Hamamoto *et al.*, 2012).

### **5.2.2.3 Isolation and purification of BSX-1 and BSX-2 (ring-opened)**

BSX-1 and BSX-2 were isolated (Figure 5-1) from the acidic fraction of bulk cultures using SPE for desalting (1g/20mL Strata-X cartridges, Phenomenex Inc, CA) and defatting (1g/6mL Strata-Si cartridges, Phenomenex Inc, CA) followed by normal phase silica flash chromatography. The glass column (20 x 1 cm, i.d.) was packed with flash silica gel (particle size 32-63 µm; pore size 60 Å) purchased from Scientific Absorbents Inc. (GA, USA). The column was conditioned with DCM (50 mL). Defatted extracts were applied in DCM followed by elution with a step-wise gradient (methanol/DCM, 40:50 to 65:25). Toxins in the fractions were monitored by LC-MS using Method 1 (SIR) for unlabelled BSXs and Method 2 (scanning) for <sup>13</sup>C labeled BSXs. Final purification of BSX-1 and BSX-2 in milligram quantities was achieved using preparative HPLC (Shimadzu, Japan) with a reverse phase column (250 x 10 mm id Luna C18(2), Phenomenex Inc, CA) with isocratic elution (0.05% phosphoric acid in acetonitrile/water 45:55 v/v) and monitoring by UVD (200 nm) (Figure 5-

1). The combined toxin fractions from multiple injections were diluted with water and deacidified and concentrated using Strata-X SPE (1g/20 mL) with methanol elution. Pure BSX-1 and BSX-2 were obtained after gentle evaporation of methanol.



**Figure 5-1.** Chromatographic isolation procedures for KBT and BSX toxins from cultures of *K. brevisulcata*.

#### 5.2.2.4 Acidic catalysed lactone ring-closed of BSXs

Preliminary work showed the lactone BSXs (-4 & -5) were easily formed from BSX-1 and BSX-2 respectively under acidic condition and were detectable by LC-MS as peaks eluting after the ring-opened toxins. Small scale lactone formation experiments were carried out using subsamples of purified ring-opened BSXs (10 µg each BSX-1 or -2 in separate vials) dissolved in various solvents (1 mL) including CHCl<sub>3</sub>, DCM and acetone respectively. TFA (20 µL) was added to each vial as an acidic catalyst (Figure 5-1). The capped vials were held at room temperature for 1 hr and solvents were then removed under a gentle stream of nitrogen at room temperature. The residue was dissolved in 80% methanol (1 mL) before LC-MS testing (Method 1, SIR & Method 2, scanning). After determination of the optimum acid catalytic conditions, large amounts of BSX-1 (1.8 mg) and BSX-2 (0.6 mg) were converted to their lactones ring-closed BSX-4 and BSX-5 for analytical, chemical and toxicological studies.

### 5.2.3 LC-UV, LC-MS and HRMS

#### 5.2.3.1 LC-UV plus Premier MS (SIR, scanning, MS/MS)

UV and mass spectra for KBT and BSX toxins were obtained from extracts of *K. brevisulcata* cultures and toxin fractions using a Waters Acquity Ultra-Performance Liquid Chromatography (uPLC) system coupled with a Waters Acquity PDA detector in-line with a Waters-Micromass Quattro Premier XE TSQ MS. Masslynx Ver.4.1 software was used for instrument control, data acquisition and data processing. The electrospray ionisation source was operated in positive- or negative-ion mode ( $\text{ESI}^+$  or  $\text{ESI}^-$ ) at 100 °C, capillary 4 kV, cone 30-70 V, nitrogen gas desolvation 800 L hr<sup>-1</sup> (400 °C). Separation of BSXs was achieved using the same column and gradient as described in Section 4.2.3.1. KBT toxins were analyzed using the same gradient but with 0.1% FA rather than buffer in the mobile phase.

For quantitative analysis of BSXs during toxin purification, SIR operating mode was used with the seven channels (Method 1, Table 4-2, Section 4.2.3.1). The concentrations of BSX-1, -2, -4 and -5 were estimated from the area responses calibrated using a RSM solution of brevetoxin-2 (UNCW). MS spectra for each toxin were achieved using MS scan operating mode at  $m/z$  700-1100 for BSXs or  $m/z$  1900-2200 for KBTs (Method 2, Section 4.2.3.1). Daughter ion spectra (MS/MS) were collected following low energy fragmentation of the appropriate molecular ion species (30-50 eV collision energy, argon gas  $2 \times 10^{-3}$  mBar).

#### 5.2.3.2 HRMS

Accurate mass measurements were obtained for BSXs at the University of Waikato, Hamilton using a MicroTOF instrument (Bruker Daltonics GmbH) with sample infusion and  $\text{ESI}^+$ . High resolution mass spectra were acquired with the time-flight analyser over  $m/z$  500-1500. For KBTs, a Spiral TOF-TOF instrument was used (JEOL, Tokyo) with MALDI ionisation (Hamamoto *et al.*, 2012).

### 5.2.4 Micro-chemistry of BSXs and KBT-F

#### 5.2.4.1 Base hydrolysis assay

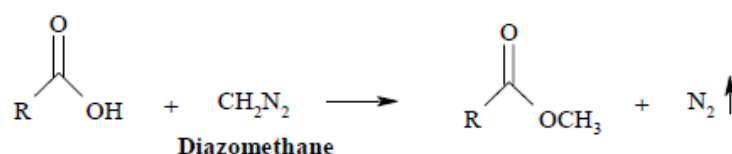
The base hydrolysis of marine algal toxins containing carboxylic acid esters including 7-acyl OA esters and the lactone ring in brevetoxins have been reported in several studies (Hua & Cole, 1999; Suzuki *et al.*, 2004). Preliminary experiments on hydrolysis of lactone BSXs to their respective parent toxin used the strong bases 25% ammonia solution or 2.5M sodium

hydroxide (NaOH) solution. Further experiments were carried out with weaker solutions (0 to 12.5 mM NaOH solution) at room temperature for 30 min. The samples were neutralised using 2.5 M acetic acid prior to LC-MS testing (Method 1, SIR & Method 2, scanning).

To study the kinetics of base hydrolysis, subsamples of BSX-4 and BSX-5 were dissolved in methanol containing 1.0 mM NaOH to concentrations of  $10\text{ }\mu\text{g mL}^{-1}$ . The capped vials were incubated at 20 °C. Aliquots (20  $\mu\text{L}$ ) were taken from each vial at 0, 5, 10, 15, 30, 60, 120 and 180 min of incubation and diluted with 160  $\mu\text{L}$  80% methanol plus 20  $\mu\text{L}$  of 0.1 mM acetic acid for LC-MS testing (duplicate analyses; Method 1, SIR & Method 2, scanning). The rate equations for base hydrolysis of the lactones were established based on the area responses for each lactone and parent toxin at each reaction time.

#### 5.2.4.2 Methylation and acetylation of BSXs

Micro-reactions were carried out on 10-20  $\mu\text{g}$  of each BSX toxin. Methylation used ethereal diazomethane followed by evaporation under nitrogen and reconstitution in 80% methanol:



Diazomethane is a carcinogen and explosive in the form of a gas. However, it is safe to use in a fume hood when dissolved in dilute solutions and in small volumes. The preparation of diazomethane was carried out on a microscale in a sealed apparatus in a fume hood (Figure 5-2). Diazomethane was generated by the reaction between Diazald (*N*-methyl-*N*-nitroso-*p*-toluenesulfonamide) and potassium hydroxide (Hashimoto *et al.*, 1981). Diazald (ca. 300 mg) was dissolved in a mixture of diethylether (3 mL) and 2-ethoxyethanol (2 mL) in the glass reaction tube. 30% aq. KOH (1 mL) was injected through the septum. Nitrogen was bubbled into the reaction tube to transfer the generated diazomethane into a 15 mL polypropylene conical tube (Falcon, Becton & Dickinson, USA) containing 5 mL diethylether to trap the diazomethane. Dissolved diazomethane was apparent from the generation of a pale yellow colouration and the aliquots (1 mL) were added immediately to BSX vials to allow reaction at room temperature for 10 min. Reaction products were studied by LC-MS (Method 2, scanning).

Acetylation used redistilled acetic anhydride and dry pyridine (1:2 v/v) at 60 °C for 1 hr followed by dilution into 80% methanol. The acetylated derivatives were detected by LC-MS (Method 2, scanning).

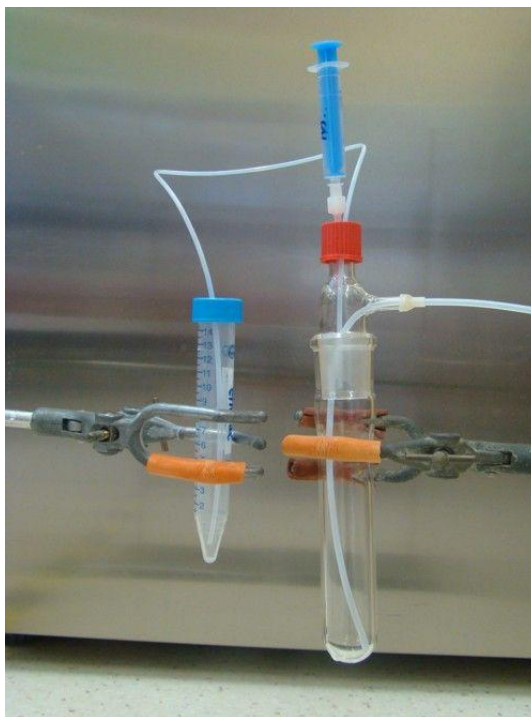


**Figure 5-2.** Apparatus for preparation of diazomethane.

#### **5.2.4.3 Preparation of a KBT-F benzene sulfonate derivative**

The KBT-F benzene sulfonate derivative (BSD) was prepared by Professor Masayuki Satake at the University of Tokyo (Hamamoto *et al.*, 2012). KBT-F (10 µg) was reacted with an excess of 3-(hydrazinecarbonyl)-benzene sulfonate sodium salt (HBSS) for 2 hours in 80% pyridine. The produced KBT-BSD was extracted by solvent elimination and partitioning between CHCl<sub>3</sub> and MQ. The CHCl<sub>3</sub> fraction was used for the MALDI-SpiralTOF-TOF measurements (Section 5.2.3.2).

#### **5.2.5 NMR spectroscopy (collaborations with Prof Satake and Dr Patrick Edwards)**

For BSXs, 500 and 700 MHz Advance spectrometers with cryoprobe (Bruker Biospin GmbH) and 3 mm sample tubes were used (collaboration with Dr Patrick Edwards, Institute for Fundamental Science, Massey University, Palmerston North). The solvents were deuterio-methanol (CD<sub>3</sub>OD). For KBTs, 500 and 800 MHz JEOL ECA spectrometers were used (Hamamoto *et al.*, 2012). The solvent was deuterio-pyridine.

## 5.3 Results and discussion

### 5.3.1 Separation of crude toxins (solvent partitioning)

Preliminary partitioning experiments with the crude HP20 extracts followed by LC-MS analysis and bioassay investigation revealed that the highest toxicity to mice was in neutral fractions while the acidic fractions were less toxic but contained novel polyether compounds (BSX-1,  $[M+H]^+$  917 Da, and BSX-2  $[M+H]^+$  899 Da in ESI+). These two compounds were deduced to be moderately polar and acidic in nature because they eluted early in HPLC, especially with a neutral rather than an acidic mobile phase, and gave prominent  $[M-H]^-$  ions in ESI-.  $CHCl_3$  is a suitable solvent to extract lipophilic toxins from crude algal extracts solubilised in aqueous methanol. The optimum aqueous phase composition was determined by small scale experiments. Four solutions containing different concentrations of methanol in MQ (20%, 40%, 60% and 80%) were partitioned with  $CHCl_3$  and monitored by LC-MS (Method 1, SIR). The lactones BSX-4 and BSX-5 had not been identified when this experiment was conducted. Thus this partitioning condition was based on separation effectiveness of BSX-1 and BSX-2 from the neutral fraction ( $CHCl_3$ ).

The recovery of BSX-1 in the aqueous phase following partitioning increased with increasing concentrations of methanol in MQ (Figure 5-3A). 80% methanol did not separate from  $CHCl_3$  (homogenous mixture). The highest recovery of BSX-1 was observed using 60% methanol and no BSX-1 and BSX-2 were found in the  $CHCl_3$  fraction (Figure 5-3A). BSX-2 recovery was 93% in 20% methanol after partitioning with  $CHCl_3$  fraction and the recoveries were similar in 40% and 60% methanol (Figure 5-3A). As BSXs exhibited some acidic character and were moderately water soluble, a buffer was tested for pH control of the aqueous phase in the presence of crude extract. Using 60% methanol with pH 7.2 phosphate buffer gave high recoveries of both BSX-1 and BSX-2. These observations suggested the aqueous solvent for the initial partition should be of medium polarity (40-60% methanol) buffered to pH 7.2. The partitioning system of 55% methanol with pH 7.2 phosphate buffer and  $CHCl_3$  was chosen for processing bulk extracts to separate water-soluble BSX-1 and BSX-2 from a lipophilic fraction containing KBTs.

Recovery of BSX-1 and BSX-2 from the aqueous fraction was carried out through a second partition using DCM following pH adjustment to protonate carboxylic acid groups. After the partitioning with  $CHCl_3$ , small scale 55% methanol fractions were adjusted to pH at 3, 4, 5 or 8 using 1M HCl or phosphate buffer, and then partitioned with DCM (Figure 5-3B). Highest recovery of BSXs into the DCM phase (63-72%) occurred at pH 4 with only 13%

BSXs recovered at pH 3 and 17% of BSX-2 plus 3% of BSX-1 at pH 5. No toxins were detected in the DCM phase at pH 8. The optimised procedure for the second partitioning employed adjustment of the 55% methanol fraction to pH 4 using 1M HCl followed by three successive partitions with DCM. The large scale bulk toxin isolation from approximately 864 litres unlabelled and 245 litres  $^{13}\text{C}$  labelled cultures followed these optimised procedures for solvent partitioning. The solvent fractions were concentrated and dried by rotary evaporation. The neutral  $\text{CHCl}_3$  fractions were sent to the University of Tokyo (Prof. Masayuki Satake) for isolation of KBTs. The crude BSX-1 and BSX-2 sourced from total 1109 litres of unlabelled and labelled cultures were then isolated and purified at Cawthron Institute. Additionally, the HP20 crude extract of 234 litres  $^{13}\text{C}$ -labelled cultures (WHT 11-2, Table 3-3) was also sent to the University of Tokyo for further isolation and purification of KBTs and BSXs.

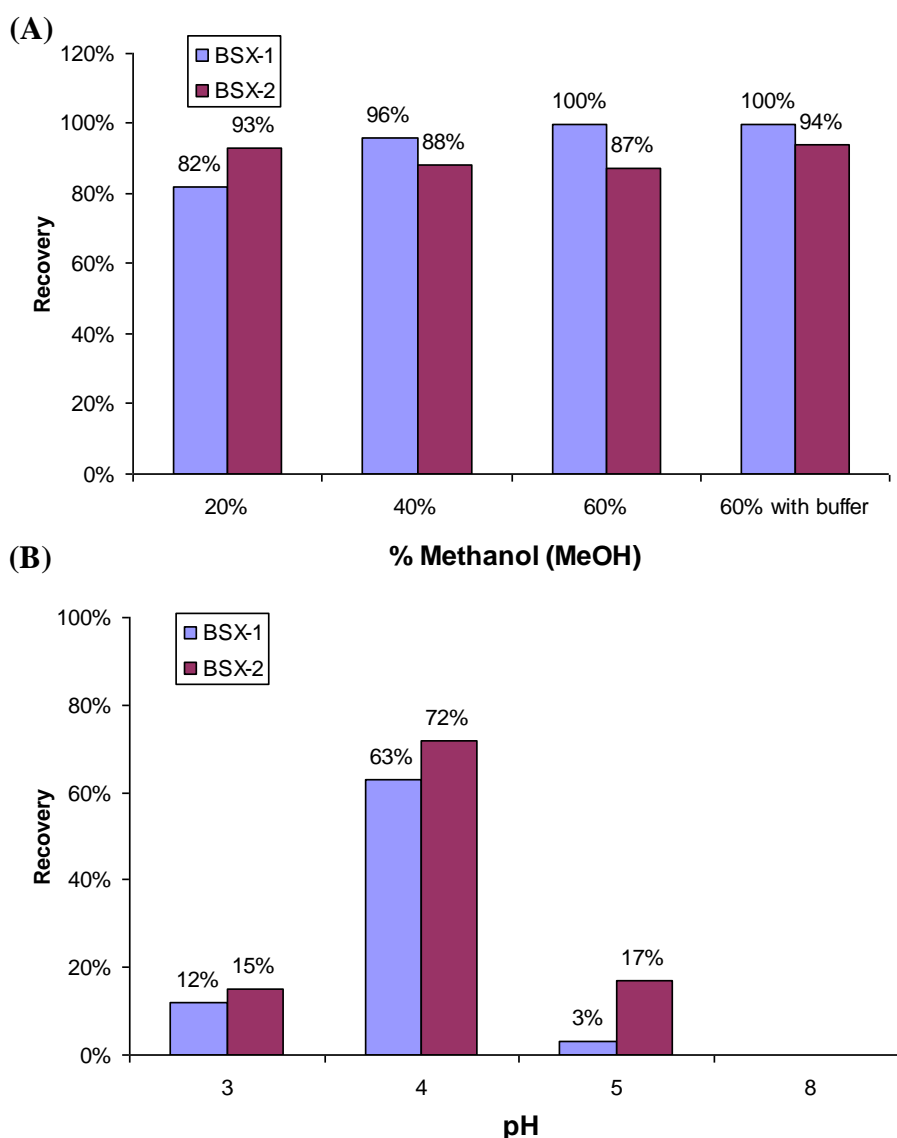


**Figure 5-3.** Determination of optimal conditions for solvent partitioning: (A) the effects of aqueous phase composition in the first partition, and (B) pH of aqueous phase in the second partition. BSX-1 and BSX-2 were monitored using LC-MS (Method 1, SIR).



### 5.3.2 Isolation and purification of BSX

BSX-1 and BSX-2 were isolated in milligram quantities and high purity from the acidic fraction of crude extracts by multi-step chromatographic cleanups and separations (Figure 5-1). Minor amounts of BSX-4 and BSX-5 were also isolated and further quantities were generated by acid-catalysed lactone ring closure of BSX-1 and BSX-2 respectively. These materials were used for analytical, structural and toxicology studies.

#### 5.3.2.1 Semi-purification BSXs

Strata-X (reverse phase) and silica gel (normal phase) were effective at separating BSX-1 and BSX-2 from co-extractives such as salts and lipophilic pigments.

Reverse phase SPE with and without buffering were conducted to determine optimum conditions for i) retention of BSXs on Strata-X while salts and other polar materials were eluted to waste, and ii) elution of BSXs while retaining some lipophilic co-extractives on the cartridge. Strata-X retained BSXs applied in 20% methanol with or without buffering. The cartridge loaded without buffering was eluted using increasing concentrations of methanol in MQ and approximately 85% of BSXs were recovered in the 30-100% methanol fractions. Two experiments controlling the pH showed that with the loading fraction at pH 4-5, 70% BSXs were recovered in the 70% and 80% methanol fractions. Adjustment of the load to pH < 4 resulted in > 95% BSXs eluting in the 90% and 100% methanol fractions. However, LC-MS tests showed that 90-100% methanol also eluted some co-extractives and contaminants such as ethoxylate surfactants ( $R-(C_2H_4O)_n-R'$ ). These compounds were detected in crude HP20 extracts by LC-MS (Method 2, scanning) as broad peaks containing series of mass peaks separated by 44, 22, 14.7 or 11 Da (single to quadruple charged oligimers). They may be introduced at large-scale culture harvesting through contamination of the drum acetone, filters or pumping system. Thus, SPE load adjustment to pH 4-5 was used for separation of BSXs from contaminants. The optimised SPE conditions used with the 1 g Strata-X cartridges were MQ as wash solvent and 50-100% methanol as eluting solvents (50 mL each, Figure 5-4). The 90% methanol fraction contained substantial amounts of ethoxylate contaminants with small amounts of BSXs (1% BSX-1 and 8% BSX-2) and was therefore not suited for further purification. Overall, 76% of both BSX-1 and -2 were recovered from Strata-X in the two 80% methanol eluant fractions which were combined and subjected to rotary evaporation for defatting. The 50% and 70% methanol fractions containing ca. 20% of the applied BSX-1 and

15% BSX-2 were finally combined from various batch cultures and recycled using Strata-X SPE to increase the overall toxin yields from this desalting step.

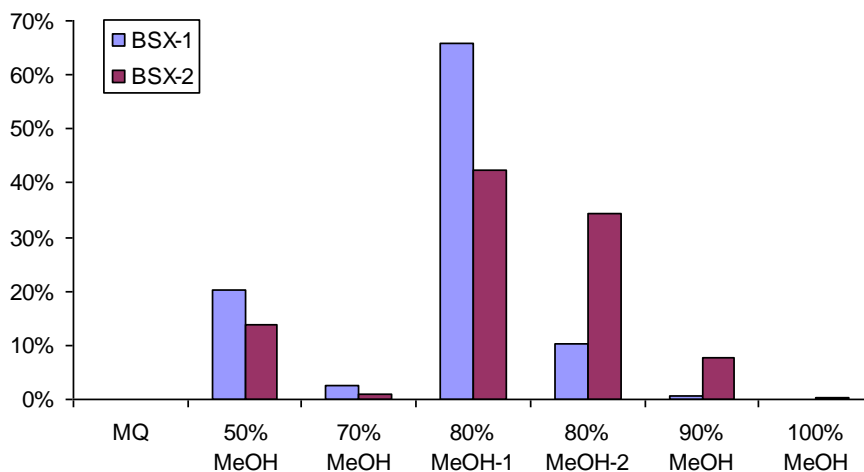


**Figure 5-4.** The elution profile of BSX toxins from a reserve phase SPE (1g/20 mL Strata-X, 50 mL fractions) preconditioned with methanol and MQ water. BSXs were monitored using LC-MS (Method 1, SIR).

A Strata Si-1 (normal phase) SPE cartridge was used to separate lipophilic compounds such as triglycerides from medium polarity BSXs (defatting semi-purification). BSX-1 and -2 showed low solubility in most solvents except methanol so the desalted fraction was dissolved in methanol and then diluted to 5% v/v in DCM for loading onto the SPE cartridges. Large amounts (> 1 mg) of BSXs were not soluble in 5% methanol in DCM. The low solubility resulted in the poor separation and streaking of BSXs from the column. Thus, the loading of BSXs was limited to ca. 1mg per column. Small amounts of BSX-5 were eluted in the load fraction, while BSX-4 was eluted in 10-20% methanol/DCM. 80% of BSX-2 was recovered in 30% methanol/DCM and 95% of BSX-1 in the 40-70% methanol/DCM fractions. The results of normal phase SPE implied the following polarity order: BSX-5 < BSX-4 < BSX-2 < BSX-1. This matches the polarities observed with reversed phase HPLC (LC-MS) except in the inverse separation order, as expected (Figure 4-1A). The 30-70% methanol/DCM fractions were combined for final isolation. The toxicological studies revealed that the less polar BSX-4 and BSX-5 were more interesting than the more polar BSX-1 and BSX-2 (Section 6.3.8). However, BSX-4 and BSX-5 could not be completely separated from lipophilic co-contaminants by column chromatography and preparative HPLC. Therefore, BSX-4 and BSX-5 collected from Strata-Si-1 SPE were hydrolysed by addition of base (section 5.3.3.2). The ring-opened BSX-1 and -2 hydrolysis products were desalted and combined with the semi-purified BSX-1 and BSX-2 fraction. After removal of solvents, a

total of 55 mg dry weight (dw) semi-purified unlabelled toxins (Table 5-1) were separated from a total of 179 mg dw of material from the partitioning step. The final separation and isolation used normal phase column chromatography.

#### **5.3.2.2 Final isolation and purification of BSX-1 and BSX-2**

Semi-purified BSXs after SPE were dissolved in methanol and then diluted to 20% methanol in DCM (total 10 mL loading solution each column) for loading onto a flash silica gel column (20 cm x 10 mm i.d). The column was eluted with increasing concentrations of methanol in DCM (5% increments). 36 fractions, 10 mL each, were generated and each was tested by LC-MS (aliquots diluted 1:100, Method 1). BSX-1 and BSX-2 were eluted from the column in fractions 18-20 and 22-25, respectively (Figure 5-5). Following evaporation of the combined fractions, 6.52 mg BSX-1 and 5.09 mg BSX-2 were isolated from 55 mg semi-purified fraction (Table 5-1). Fraction 21, containing small amounts of both BSX toxins, was retained separately.

Preparative HPLC under C18 reversed phase conditions was used to further purify isolated BSX-1 and BSX-2. The toxins dissolved in 80% methanol were injected onto a 250 x10 mm C18 column with mobile phase 45% acetonitrile with 0.05% phosphoric acid. Repeated injections of 100-200 µL were made each containing 100-200 µg toxin. Fractions were collected containing BSX-1 and BSX-2, guided by UVD at 200 nm (each totalling ca. 50 mL), and were diluted 1:5 with MQ and adjusted to pH 4 for concentration/desalting by Strata-X SPE. After removal of the eluting solvent (methanol), 4.21 mg dw BSX-1 and 1.75 mg dw BSX-2 were obtained from the unlabelled *K. brevisulcata* cultures (Table 5-1).

The purity of the toxins was assessed using LC-MS and LC-UVD. A subsample (10 µg) of each purified toxin was taken up in 1 mL 80 % methanol and studied by LC-MS (Method 2, scanning) and LC-UVD (190-360 nm). Figure 5-6 shows four graphs from MS and UVD. The top two graphs are the chromatograms for BSX-1 and the bottom two are for BSX-2. Both toxins had >98% purity with no impurity peaks being observed by MS or UV detection.

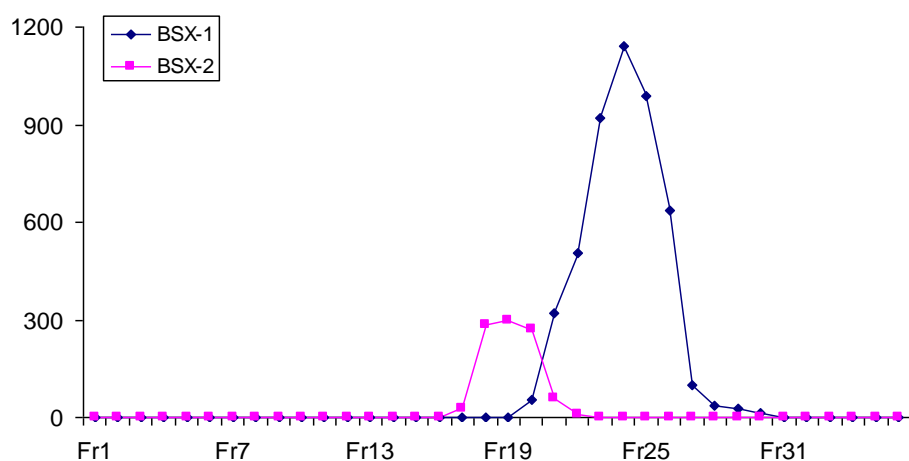


**Figure 5-5.** Elution profile of BSX-1 and BSX-2 from a silica gel column (20 cm x 10 mm i.d., 10 mL fractions) with methanol in dichloromethane.

**Table 5-1.** The isolation and purification of BSX toxins.

	BSX-1	BSX-2
Isolated toxin after flash silica by weight <sup>a</sup> (mg)	6.52	5.09
Expected toxin, from LC-MS data <sup>b</sup> (mg)	3.97	1.40
Purified toxin after preparative HPLC by weight <sup>a</sup> (mg)	4.21	1.75

<sup>a</sup> dry weight, data from five-place balance

<sup>b</sup> Data from LC-MS calibrated with brevetoxin-2 standard solution (Method 1, SIR)

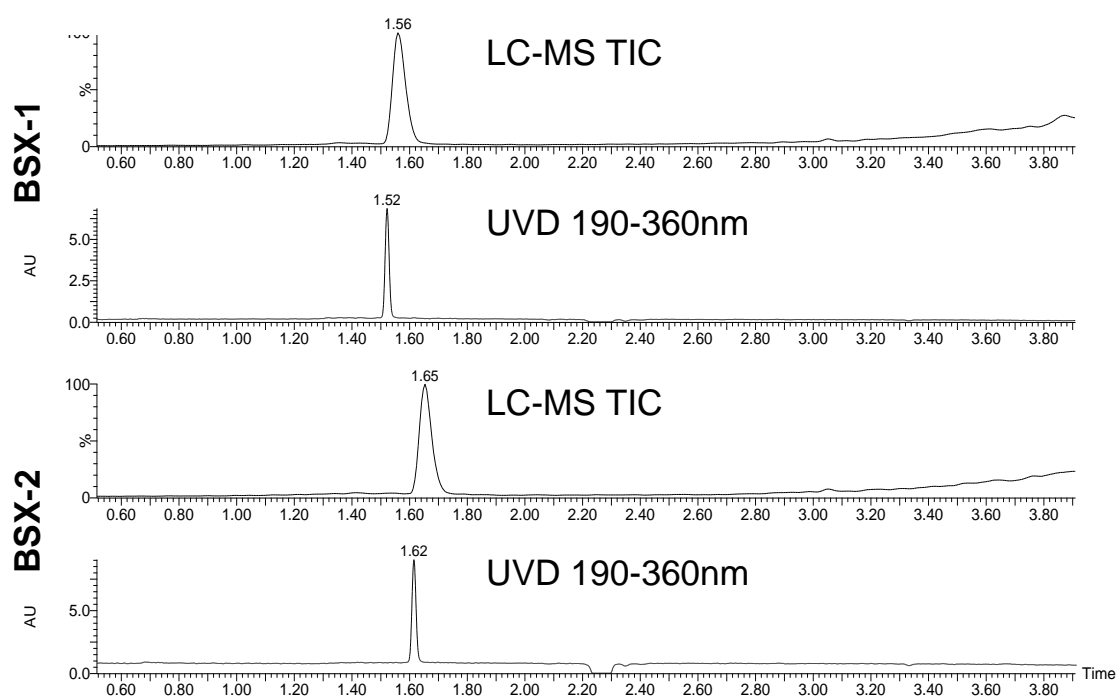


**Figure 5-6.** LC chromatograms of purified BSXs using MS and UV detection.

### 5.3.2.3 Production of ring-closed BSX-4 & -5 from ring-opened BSX-1 & -2

The ring opened/lactone inter-conversions (Figure 5-7) were confirmed chemically using the isolated toxins. BSX-1 and BSX-2 are compounds containing two carboxyl groups, one of which can react with a labile hydroxyl to form a lactone ring. The di-lactone derivatives of ring opened BSXs were not observed by LC-MS, indicating that the second carboxyl group is stable. Lactone formation is most likely to occur at the terminal ring of BSXs and produce a ring-closed structure (Figure 5-7). The efficiency of acidic catalytic lactone formation is solvent dependent for different BSX toxins (Figure 5-8). After incubation for 1 hr at room temperature followed by evaporation under nitrogen, conversion of BSX-1 to BSX-4 was >95% in  $\text{CHCl}_3$  and DCM, and 85% in acetone. LC-MS testing (Method 2, scanning) showed BSX-1 was mostly converted to BSX-4 but some BSX-4 methyl ester ( $[\text{M}+\text{H}]^+$  913 Da) was formed in  $\text{CHCl}_3$ . The highest efficiency of conversion of BSX-2 to BSX-5 was observed in acetone (90% versus 35-55% in  $\text{CHCl}_3$  or DCM). Increased evaporation temperature enhanced the production of methyl ester derivatives. Therefore, quantitative formation of the lactones was obtained using 0.2% TFA in DCM (11 mL) for BSX-1 (1.8 mg) or in acetone (7 mL) for BSX-2 (0.6 mg) followed by gentle evaporation under nitrogen without heating.

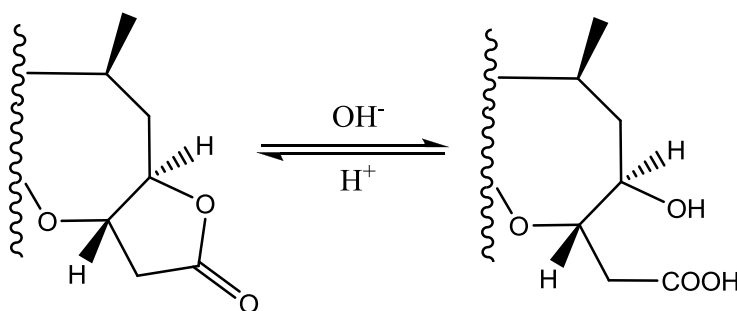


**Figure 5-7.** Inter-conversions of ring-opened and lactone BSX toxins.

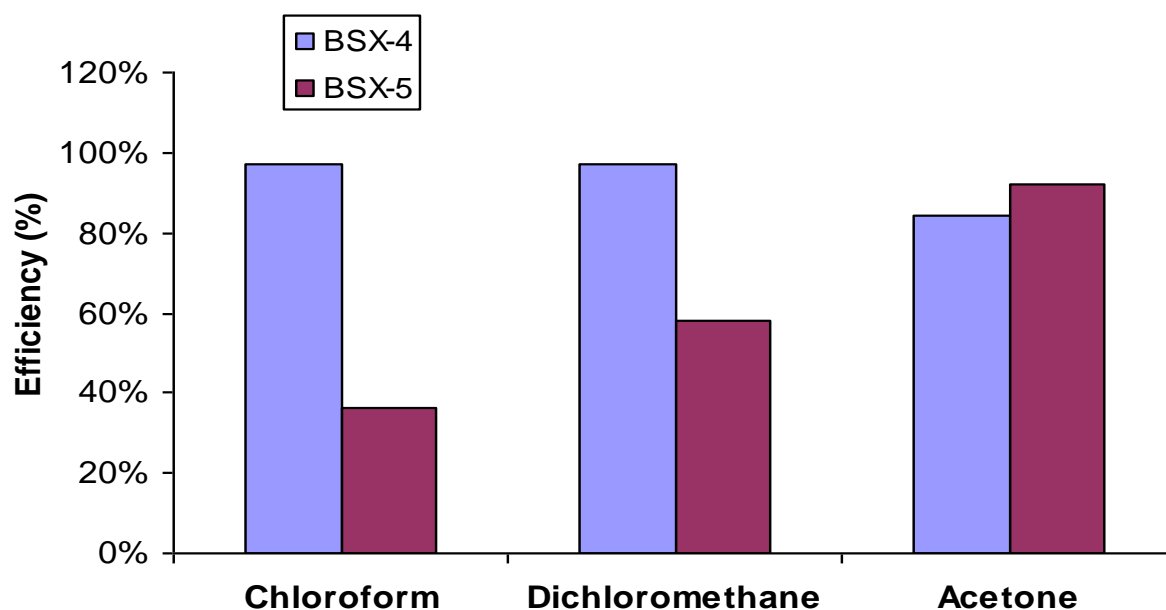


**Figure 5-8.** The efficiency of ring-closed BSX compounds (BSX-4 & -5) formation in different solvents with added trifluoroacetic acid (unreplicated experiment).

#### 5.3.2.4 Isolation and purification of $^{13}\text{C}$ -labelled BSX-4 and BSX-5

$^{13}\text{C}$ -labelled BSXs were isolated and purified from 245 litres labelled *K. brevisulcata* culture (WHT 10-2). These toxins cannot be monitored using LC-MS method 1 (SIR) because of complex mass spectra arising from the multiple  $^{13}\text{C}$  contributions. Thus, LC-MS scanning (Method 2) was used to guide the isolation of these labelled BSXs. After desalting, defatting, and isolation using the flash silica gel column chromatography, BSX-1 and BSX-2 were subjected to acid-catalysed ring closure to generate BSX-4 and BSX-5 respectively (Figure 5-1). The ring-closed BSXs were further purified by preparative HPLC. Finally, 1.06 mg  $^{13}\text{C}$ -labelled BSX-4 and 0.5 mg  $^{13}\text{C}$ -labelled BSX-5 were isolated and purified for  $^{13}\text{C}$ -NMR studies.

### 5.3.3 Structural characterisation of BSXs

#### 5.3.3.1 UV- and mass spectrometry of BSXs

The molecular formula established by HRMS ( $[\text{M}+\text{H}]^+$  found, required) were: BSX-1  $\text{C}_{49}\text{H}_{72}\text{O}_{16}$  (917.4827, 917.4899); BSX-2  $\text{C}_{47}\text{H}_{68}\text{O}_{15}$  (873.4578, 873.4636); BSX-4  $\text{C}_{49}\text{H}_{70}\text{O}_{15}$  (899.4747, 899.4793); BSX-5  $\text{C}_{47}\text{H}_{66}\text{O}_{14}$  (855.4593, 855.4530). Thus BSX-1 has an additional  $\text{C}_2\text{H}_4\text{O}$  over BSX-2. The rings plus double bond count ( $r+\text{db} = \#\text{C} - \frac{1}{2}\#\text{H} + 1$ ) is 14 for BSX-1 & -2, and 15 for BSX-4 & -5. BSXs are similar to other polycyclic ether toxins

such as brevetoxins in molecular formula and rdb: e.g.  $C_{49}H_{70}O_{15}$  rdb=15 for BSX-4 versus  $C_{49}H_{70}O_{13}$  rdb=15 for brevetoxin-1,  $C_{50}H_{70}O_{14}$  rdb=16 for brevetoxin-2 and  $C_{50}H_{70}O_{15}$  rdb=16 for brevetoxin-B5, an acidic metabolite of brevetoxin-2 (Ishida *et al.*, 2004a; Ishida *et al.*, 2004b; Ishida *et al.*, 2004c; Lin *et al.*, 1981; Shimizu *et al.*, 1986).

The UV absorbance  $\lambda_{max}$  was 196 nm for both BSX-1 and BSX-2 toxins but BSX-2 has a broader tail to longer wavelengths (Figure 5-9). Both toxins probably have carbonyl groups and BSX-2 may also have conjugated unsaturation, e.g. conjugated diene or double bond beta to a carbonyl (expected  $\lambda_{max}$  220-235 nm). Isolated olefinic groups are also possible.

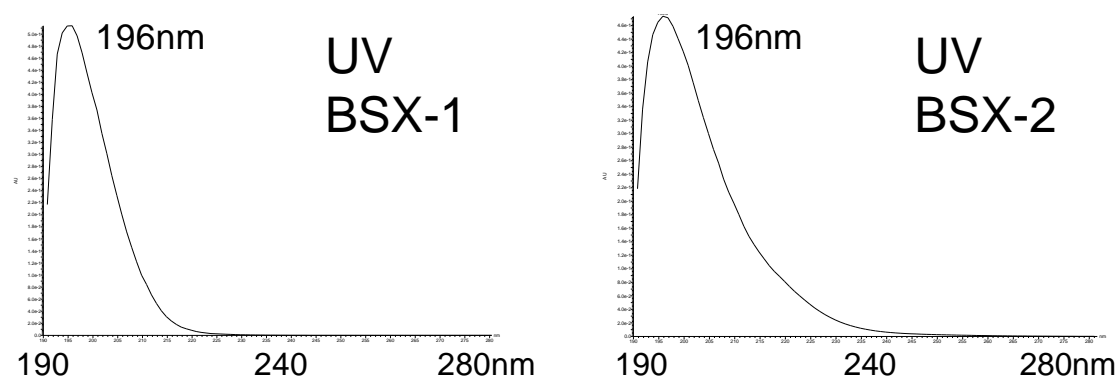
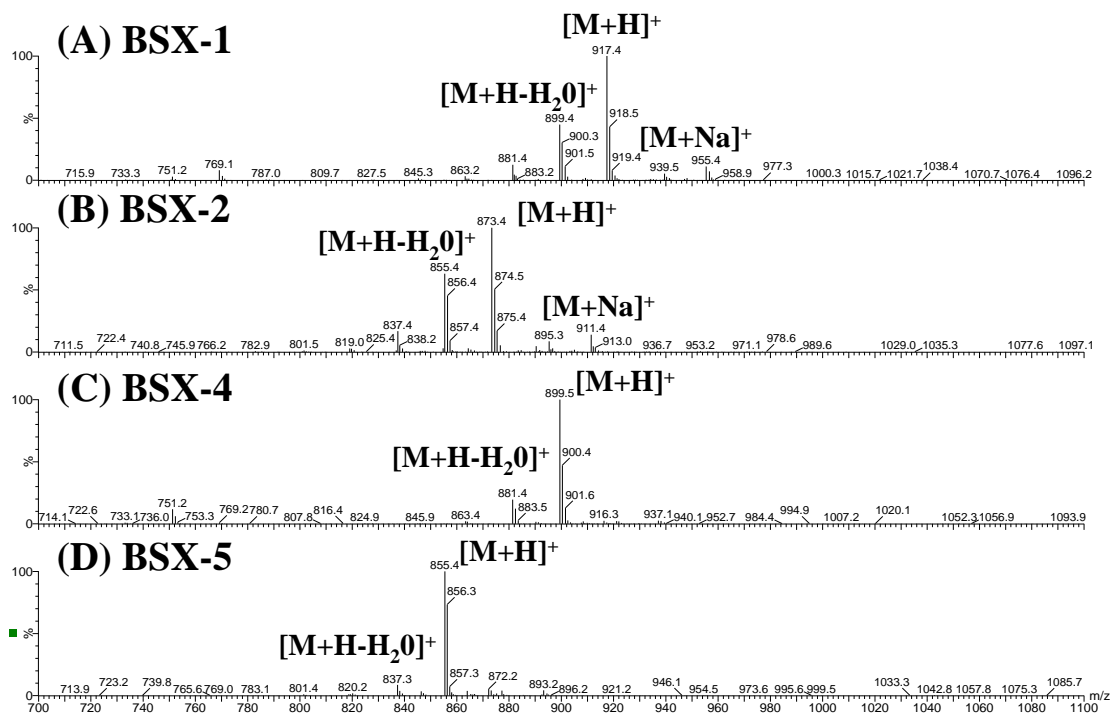


**Figure 5-9.** UV spectra of BSX-1 (left) and BSX-2 (right).

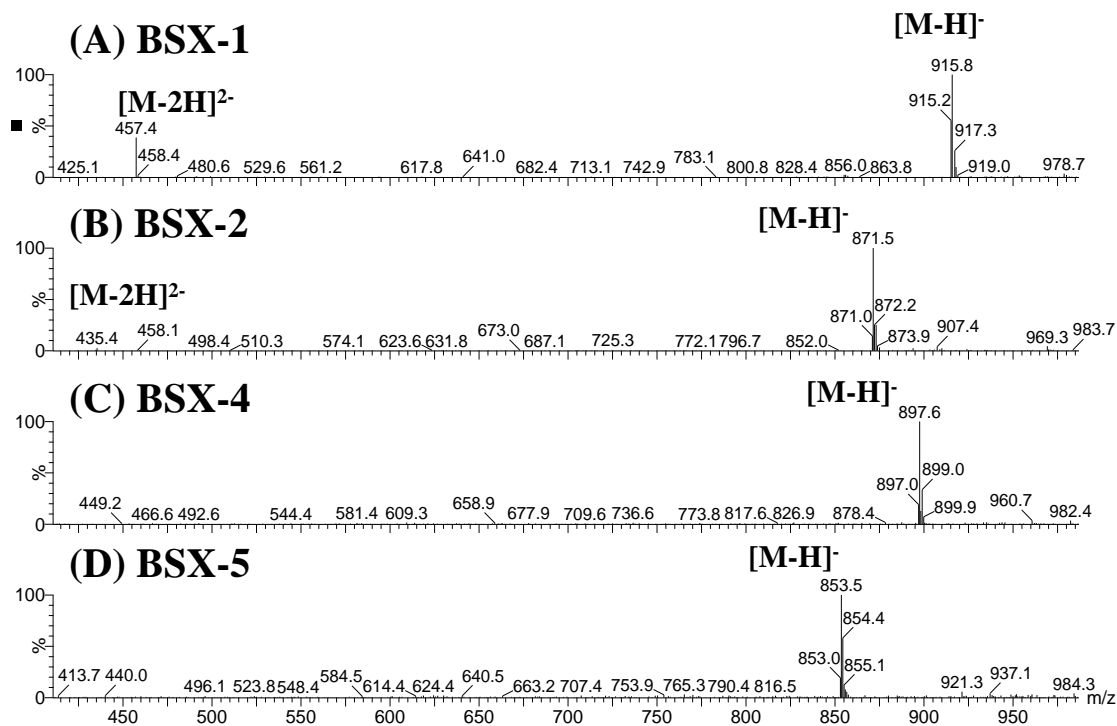
Figure 5-10 shows MS spectra ( $ESI^+$ ) for BSX-1, BSX-2, BSX-4 and BSX-5. BSX-1 and -2 each showed an high abundant water loss ion  $[M+H-H_2O]^+$  indicating a labile hydroxyl. MS spectra of the two lactones (Figure 5-9C, D) show  $[M+H]^+$  at lower masses than for that the ring-opened BSXs compounds by 18 Da. The lactones gave much weaker  $[M+H-H_2O]^+$  ions than ring-opened BSXs, indicating absence of very labile hydroxyl groups. The loss of water from the parent ions of the ring-opened BSX-1 and BSX-2 corresponds to gas phase formation of the lactones in the ESI source.

Figure 5-11 shows the MS spectra of the four compounds using negative ionisation mode with an acidic mobile phase. The  $[M-H]^-$  molecular anions are 2 Da lower than the corresponding  $[M+H]^+$  ions in  $ESI^+$ . Doubly charged anions  $[M-2H]^{2-}$  at  $m/z$  457 and 435 were observed in the spectra of BSX-1 and BSX-2 respectively (Figure 5-11 A, B). These peaks were relatively much stronger when a neutral mobile phase was used which facilitates deprotonation in  $ESI^-$  (data not shown) but reduces the retention and separation of the toxins by reversed phase LC. No double charged anions were produced by BSX-4 and BSX-5 (Figure 5-11 C, D).  $[M-2H]^{2-}$  arises from loss of two protons confirming BSX-1 and BSX-2

contain two acidic groups such as carboxyls while the lactones (BSX-4 & BSX-5) only contain one acidic group.



**Figure 5-10.** Mass spectra (ESI<sup>+</sup>) of BSX-1 (A), BSX-2 (B), BSX-4 (C) and BSX-5 (D).



**Figure 5-11.** Mass spectra (ESI<sup>-</sup>) of (A) BSX-1, (B) BSX-2, (C) BSX-4 and (D) BSX-5.



### 5.3.3.2 Kinetics of hydrolysis of BSX-4 and BSX-5

A preliminary experiment used 25% ammonia solvent to hydrolyse BSX-4 and BSX-5 dissolved in aqueous methanol. In addition to the parent toxins, two amide derivatives were detected by LC-MS (Method 2, scanning): BSX-1 amide ( $[M+H]^+$ ,  $m/z$  916) and BSX-2 amide ( $[M+H]^+$ ,  $m/z$  872). To avoid amide formation, aqueous NaOH was used to hydrolyse BSX-4 and BSX-5. Figure 5-12 shows the base hydrolysis of BSX-4 at different concentrations of NaOH at room temperature for 30 min. BSX-4 was completely converted to BSX-1 at NaOH concentrations  $> 7.5$  mM. The speed of hydrolysis of BSX-5 was similar to that of BSX-4.

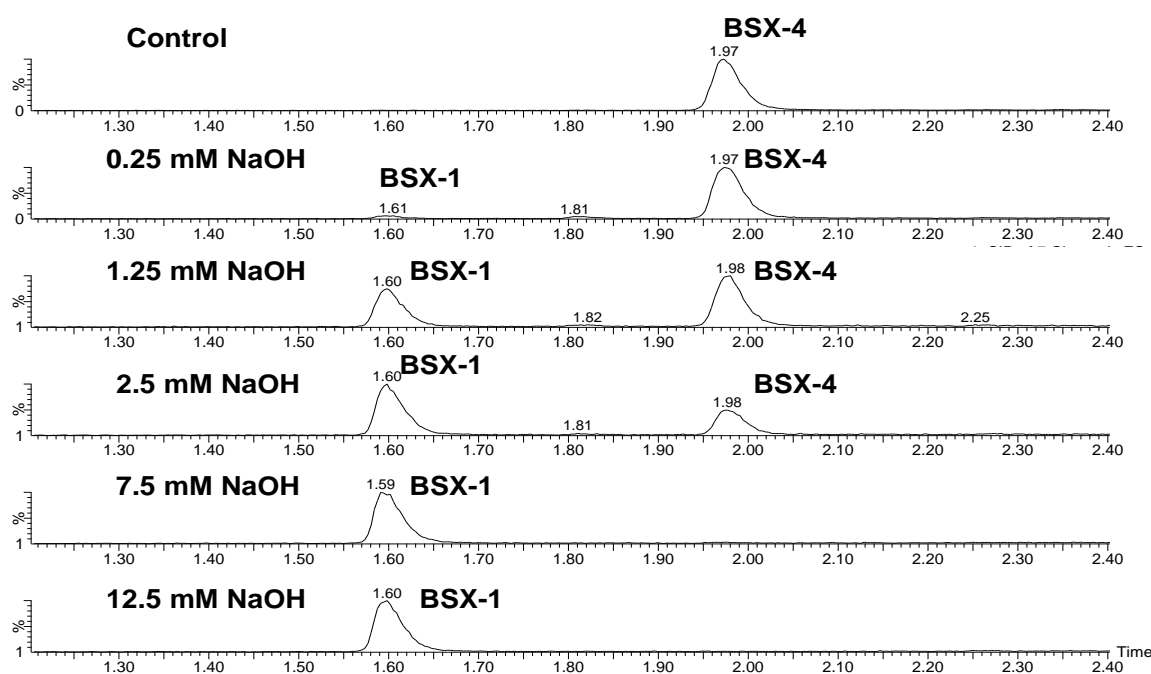


**Figure 5-12.** Base hydrolysis of BSX-4 to BSX-1 in 80% methanol at different concentrations of NaOH (30 min at room temperature).

The rates at which the lactones BSX-4 and BSX-5 were hydrolysed to their ring-opened BSX-1 and BSX-2, were studied using 1 mM NaOH with analysis by LC-MS Method 1 (SIR) to quantify the toxins. The bimolecular reaction of the lactone ester bond with base reduces to pseudo first order kinetics because of the large excess of base with rate equation:

$$C_t/C_0 = B e^{-kt}$$

Therefore the experimental data was fitted to the linear equation:

$$\text{Log}_e((A_{\text{inf}} - A_t)/(A_{\text{inf}} - A_0)) = -k(A_t - A_{t_0})$$

Where:  $t_0 = 0$  min

$A_0$  is the initial peak area of the lactone

$A_{inf}$  is the peak area of the lactone at infinite time (estimated from  $t = 180$  min)

$A_t$  is the peak area of the lactone at time  $t$ ;  $k$  is the pseudo-first-order rate constant.

The plots of this data (Figure 5-13) were highly linear indicating that a pseudo-first order reaction was taking place. After 180 min, equilibrium status was reached, as the peaks for both BSX-4 and -5 reduced to low and rather constant levels. The correlation coefficients for hydrolysis of BSX-4 and BSX-5 were 0.9932 and 0.9783, respectively. The slope of the line represents the pseudo-first-order rate constant  $k$  for lactone hydrolysis to BSX-1 and BSX-2. The rate constants of  $0.0115$  and  $0.0112 \text{ min}^{-1}$  are comparable to those obtained for hydrolysis of brevetoxin-1, brevetoxin-2 and brevetoxin-3 (Hua & Cole, 1999).

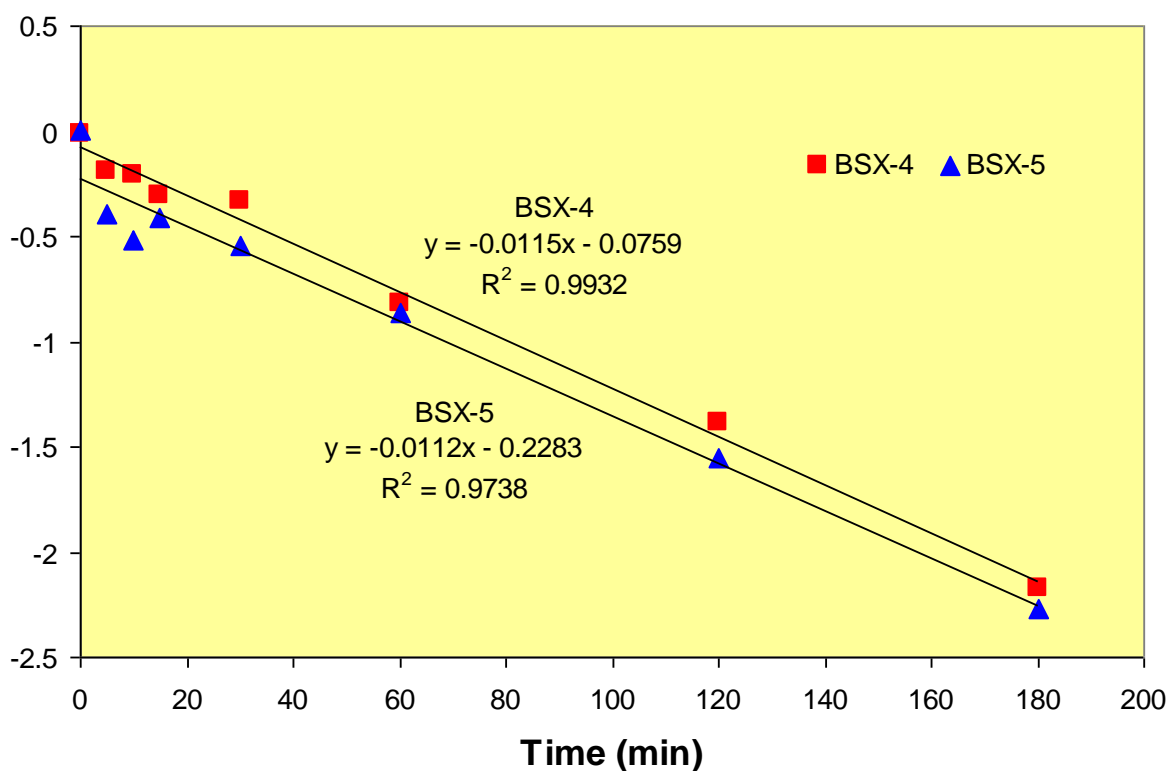


**Figure 5-13.** First order reaction plots of hydrolysis of BSX-4 and BSX-5 (9  $\mu\text{g}$  each in 1 mM NaOH in 80% methanol at 50  $^{\circ}\text{C}$ ).

### 5.3.3.3 Microchemistry of BSXs (methylation; acetylation)

The presence of carboxyl and hydroxyl groups in the BSXs was confirmed by methylation with diazomethane and acetylation respectively followed by LC-MS analysis. The toxins dissolved in methanol were treated with diazomethane in diethyl ether (generated from Diazald). The methylated products detected by LC-MS (Method 2, scanning) are shown

in Figure 5-14 and summarised Table 5-2. The dimethyl esters were observed for BSX-1 ( $[M+H]^+$  945 Da) and BSX-2 ( $[M+H]^+$  901 Da), and the monomethyl esters for the lactones BSX-4 ( $[M+H]^+$  913 Da) and BSX-5 ( $[M+H]^+$  869 Da). There was substantial lactone formation during methylation of BSX-1 and BSX-2. No unmethylated starting materials were observed. These derivatives support the hypothesis that the structures of BSX-1 and BSX-2 include two carboxyl groups, one of which readily forms a lactone. Several minor additional peaks were also detected by LC-MS in the methylated extracts, particularly for BSX-2, which were derived from the parent BSXs. From their  $[M+H]^+$  masses they appear to be BSX-1 Me<sub>3</sub>, BSX-4 Me<sub>2</sub>, BSX-2 Me<sub>5</sub>, BSX-2 Me<sub>6</sub>, BSX-5 Me<sub>4</sub>, and BSX-5 Me<sub>5</sub> (Table 5-2). Artifacts from diazomethane methylation are well known and can include methylation of some hydroxyl groups and double bonds to produce these over-methylated products.

**Table 5-2.** Products observed from methylation of BSXs with diazomethane. Note: the over-methylated products for BSX-2 and BSX-5 have not been fully characterised.

Parent compound	Derivative	Rt (min)	$[M+H]^+$	$[M+Na]^+$	$[M+H-H_2O]^+$
BSX-1	BSX-1 Me <sub>2</sub>	1.99	945	967	927
	BSX-1 Me <sub>3</sub>	2.10	959	981	941
BSX-4	BSX-4 Me	2.16	913	935	895
	BSX-4 Me <sub>2</sub>	2.27	927	949	909
BSX-2	BSX-2 Me <sub>2</sub>	2.19	901	923	883
	BSX-2 Me <sub>5</sub>	2.02	943	965	ND
	BSX-2 Me <sub>6</sub>	2.13	976	979	ND
BSX-5	BSX-5 Me	2.37	869	891	ND
	BSX-5 Me <sub>4</sub>	2.19	911	nd	ND
	BSX-5 Me <sub>5</sub>	2.30	925	947	ND

ND, not detected

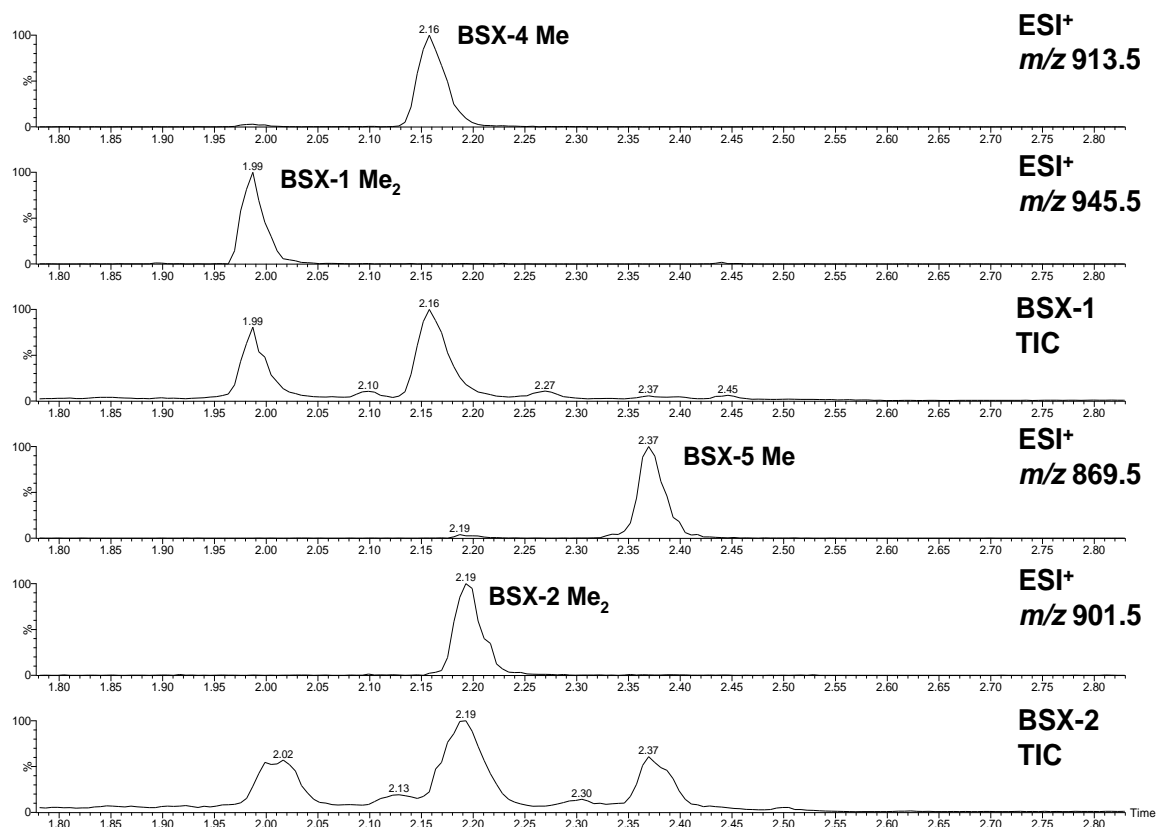


**Figure 5-14.** LC-MS chromatograms of methylation products of BSX-1 and BSX-2 by diazomethane (scanning TIC plus selected masses).

In the acetylation experiments, BSX-4 rapidly formed a monoacetate at 20 °C but the diacetate remained a minor product even after 1 h at 60 °C. BSX-5 was mainly unacetylated but minor amounts of a mono-acetate appeared after 1 h at 60 °C. Acetylation of BSX-1 and -2 led to immediate formation of the respective lactones with the acetylated products being the same as for BSX-4 and BSX-5. These results indicate that there is a single secondary OH on ether rings of BSX-4 and BSX-5 which is not very reactive, probably due to a sterically hindered conformation. BSX-4 also contains a reactive hydroxyl group, probably on the terminal side chain.

#### 5.3.3.4 Daughter ion spectra of BSXs and their analogues

Daughter ion scanning (LC-MS/MS) to obtain collisional activation spectra for the parent ions was used to probe the molecular structures of the toxins and derivatives. Each parent ion ( $[M+H]^+$  or  $[M-H]^-$ ) was selected in MS1 and the daughter ions formed in the collision cell were scanned in MS2 (100-920 Da). Figure 5-15 shows the daughter ion spectra for  $[M+H]^+$  of the four BSX toxins (855 for BSX-1, 873 for BSX-2, 899 for BSX-4 and 917 for BSX-5) and the equivalent daughter ion spectra for  $[M+H]^+$  857 (BSX-3) and 839 (BSX-

6) using semi-purified materials are shown in Figure 5-16. Three methylated toxins (945, 913 and 869 respectively) were also investigated and the daughter ion spectra are exhibited in Figure 5-17. The significant fragment ions are summarised in Table 5-3.

A series of water loss ions  $[M+H-(H_2O)_n]^+$  were observed in all MS/MS spectra: BSX-1,  $n = 1$  to 7; BSX-2,  $n = 1$  to 5; BSX-3,  $n = 1$  to 6; BSX-4  $n = 1$  to 5; BSX-5,  $n = 1$  to 3; and BSX-6,  $n = 1$  to 5 (Figures 5-15, 5-16; Table 5-3). Water loss ions are commonly observed for polycyclic ether toxins e.g. brevetoxins (Abraham *et al.*, 2006) and can arise from hydroxyl groups (water elimination to form an olefin) or ring ether groups (water elimination after ring opening).

Daughter ions (F1) are also seen at 769, 751, 783 and 751 Da in the spectra of BSX-1, BSX-4, BSX-1 dimethyl ester and BSX-4 methyl ester, respectively (Table 5-3). The mass shifts between these daughter masses indicate that this F1 fragment retains the lactone-forming carboxyl plus labile hydroxyl or the lactone ring but has lost the second carboxyl. This fragment was not observed for BSX-2, BSX-3 or their lactone ring-closed derivatives indicating that the cleavage is facilitated by the additional functional group specific to BSX-1.

A significant fragment ion (F2) was observed at 531 Da for ring-opened BSXs which shifted to 545 for the dimethyl ester and to 513 Da for the ring-closed derivatives (Figures 5-15 to 5-17). This suggests that the F2 fragment is common to ring-opened BSXs and retains the lactone-forming carboxyl plus labile hydroxyl but has lost the second carboxyl. Another fragment ion F3 at 381 Da for BSX-1 and its lactone (BSX-4) shifted to 337 Da for BSX-2 and its lactone (BSX-5), or 321 Da for BSX-3 and its lactone (BSX-6). The mass shifts suggest that F3 does not contain the lactone portion but does contain chemical characteristics specific to each individual BSX. The mass shifts for the methylated derivatives suggest that F3 for BSXs (-1, -2, -4, & -5) also contains the second carboxyl group.

A range of other fragment ions were evident in the complex low mass region which cannot be interpreted currently e.g. F4 at 219 Da in BSX-1 and its lactone BSX-4 versus 191 Da in BSX-2 and its lactone BSX-5. However, the corresponding F4 fragment ions were not observed for BSX-3 and BSX-6 in Figure 5-16 and may be arisen due to the relatively low purity of semi-purified materials.

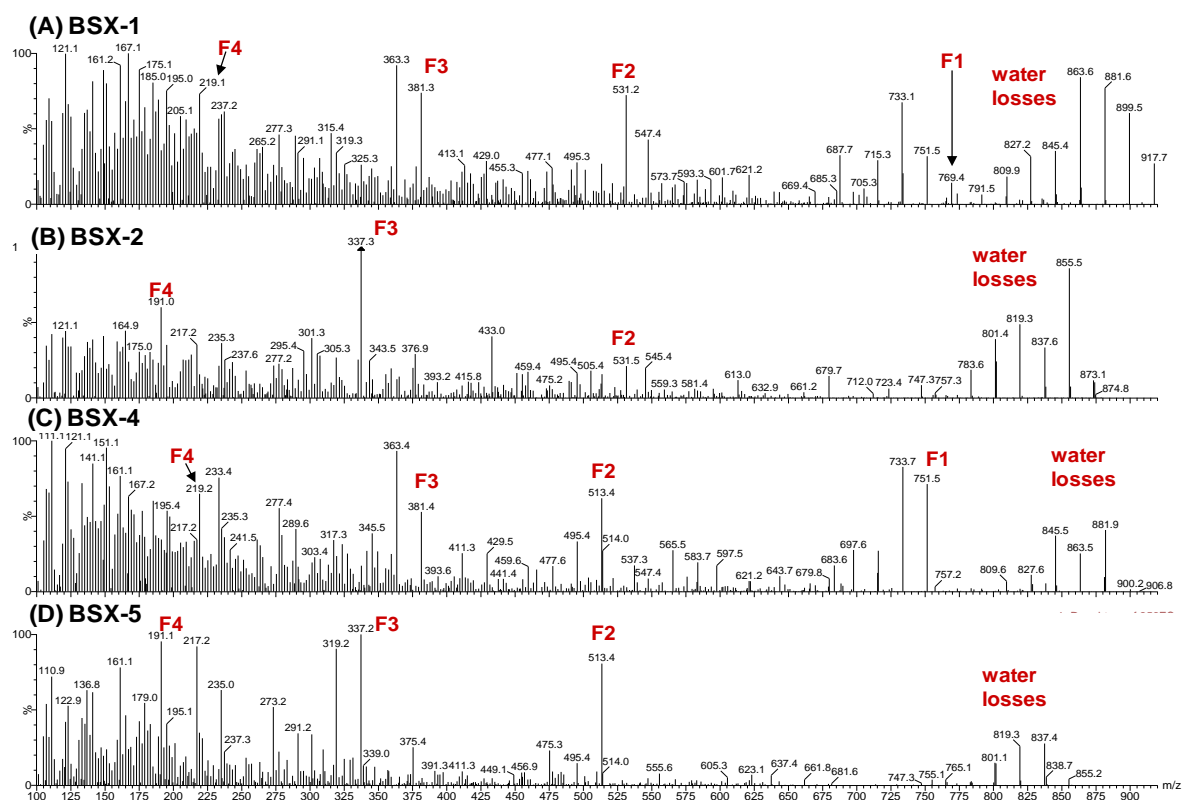


**Figure 5-15.** Daughter ion spectra ( $\text{ESI}^+$ ) for  $[\text{M}+\text{H}]^+$  (A) BSX-1 917; (B) BSX-2 873; (C) BSX-4 899; (D) BSX-5 855 at collision energy 30 eV.

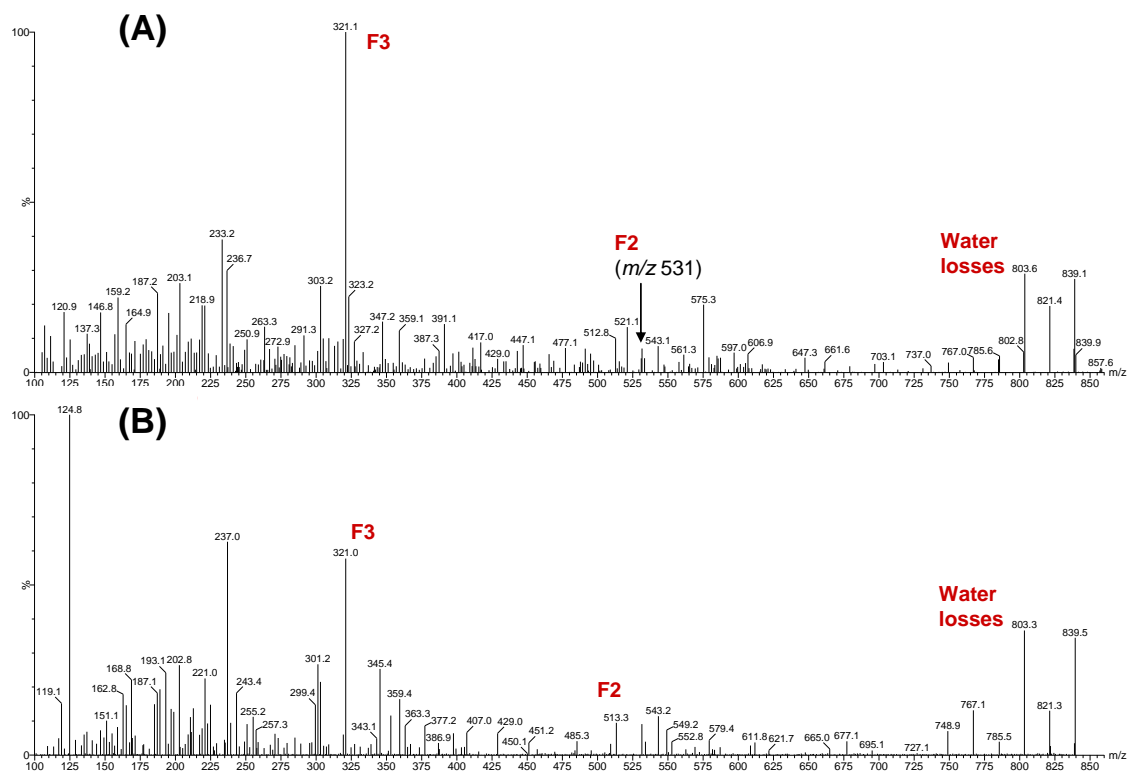


**Figure 5-16.** Daughter ion spectra ( $\text{ESI}^+$ ) for  $[\text{M}+\text{H}]^+$  of (A) BSX-3 857 and (B) BSX-6 839 at collision energy 30 eV.

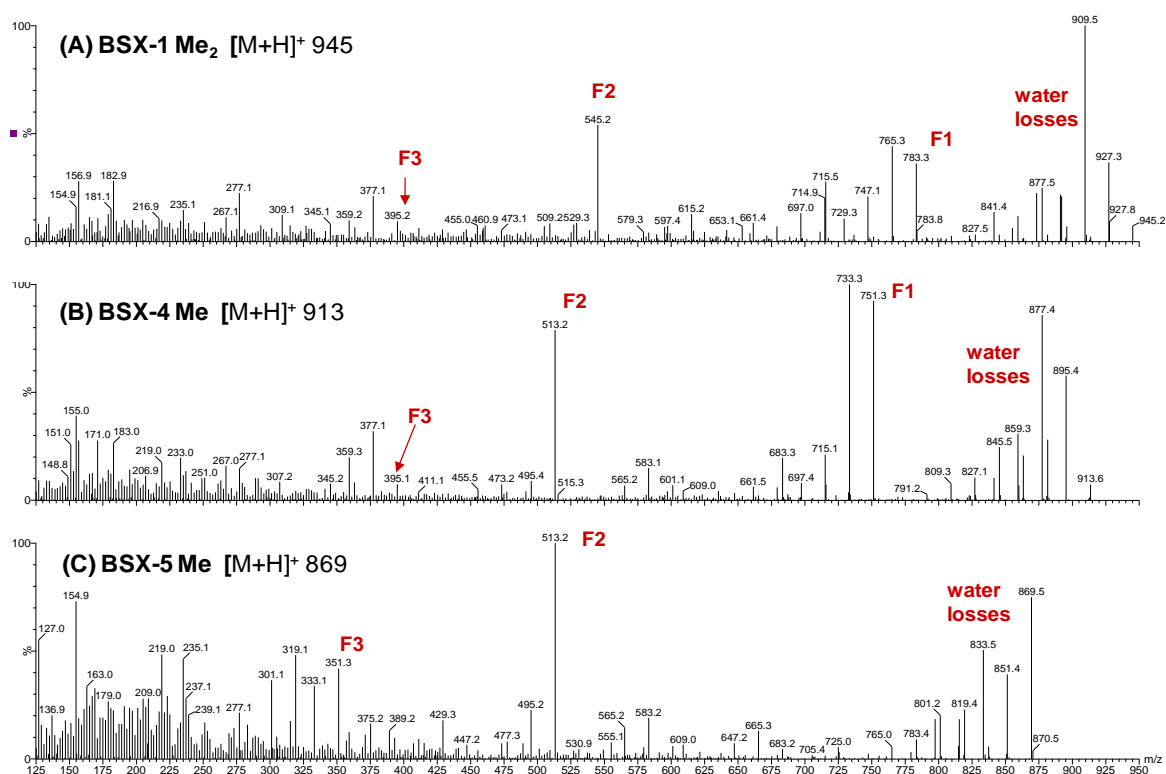


**Figure 5-17.** Daughter ion spectra (ESI<sup>+</sup>) for [M+H]<sup>+</sup> of methylated BSX compounds: (A) BSX-1 Me<sub>2</sub>, (B) BSX-4 Me, and (C) BSX-5 Me at collision energy 27 eV.

**Table 5-3.** Significant MS/MS fragment ions (ESI<sup>+</sup>) for four BSX toxins and their methyl esters.

Parent compound	[M+H] <sup>+</sup>	Fragment ions						
		water losses <sup>a</sup>	F1	water losses <sup>b</sup>	F2	F3	water loss <sup>c</sup>	F4
BSX-1	917	7	769	3	531	381	2	219
BSX-4	899	5	751	2	513	381	1	219
BSX-2	873	5	-	-	531	337	1	191
BSX-5	855	3	-	-	513	337	1	191
BSX-3	857	6	-	-	531	321	1	-
BSX-6	839	5	-	-	513	321	1	-
BSX-1 Me <sub>2</sub>	945	5	783	3	545	395	2	?
BSX-4 Me	914	4	751	2	513	395	1	?
BSX-5 Me	869	3	-	-	513	351	1	?

<sup>a</sup> Number of water losses from [M+H]<sup>+</sup>

<sup>b</sup> Number of water losses from F1

<sup>c</sup> Number of water losses from F3

Daughter ion spectra were also gathered in ESI<sup>-</sup> mode for the molecular anion of BSX-1 (Figure 5-18). At collision energy 25 eV, little fragmentation was observed but at 45 eV there was a strong loss of 60 Da and other fragment ions at 759 Da and 292 Da were evident. Loss

of 60 Da corresponds to elimination of the elements of acetic acid and indicates that at least one of the carboxyl groups is terminal on a methylene unit ( $-\text{CH}_2\text{-COOH}$ ).

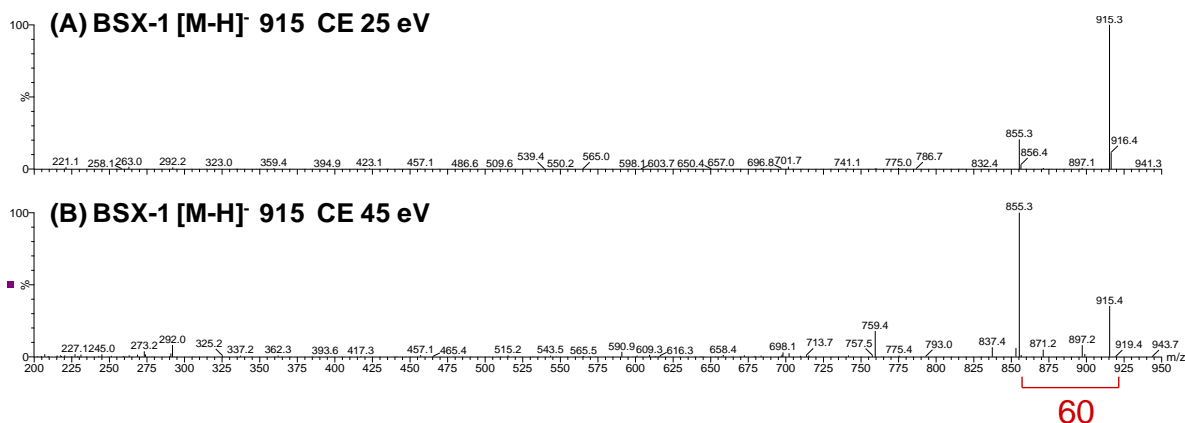


**Figure 5-18.** Daughter ion spectra (ESI-) for  $[\text{M-H}]^-$  of BSX-1 at collision energy 25 eV (A) and 45 eV (B).

Figure 5-19 shows the ESI- daughter ion spectra for  $[\text{M-H}]^-$  of BSX-4 and BSX-5. The base peak at  $m/z$  111 for BSX-5 is postulated to arise from a cleavage across the terminal ether ring. This fragment ion is also observed for brevetoxin-B5 (Ishida *et al.*, 2004a) which contains a carboxylate side chain. In BSX-4, this base peak is shifted to  $m/z$  137, arising from the same cleavage to give  $m/z$  155 followed by facile loss of the hydroxyl group as water. These results confirm the hypothesis from the ESI+ daughter spectra that the difference between BSX-4 and BSX-5 is in a terminal carboxyl side chain incorporating the unit ( $-\text{CH}_2\text{-CHOH}-$ ).

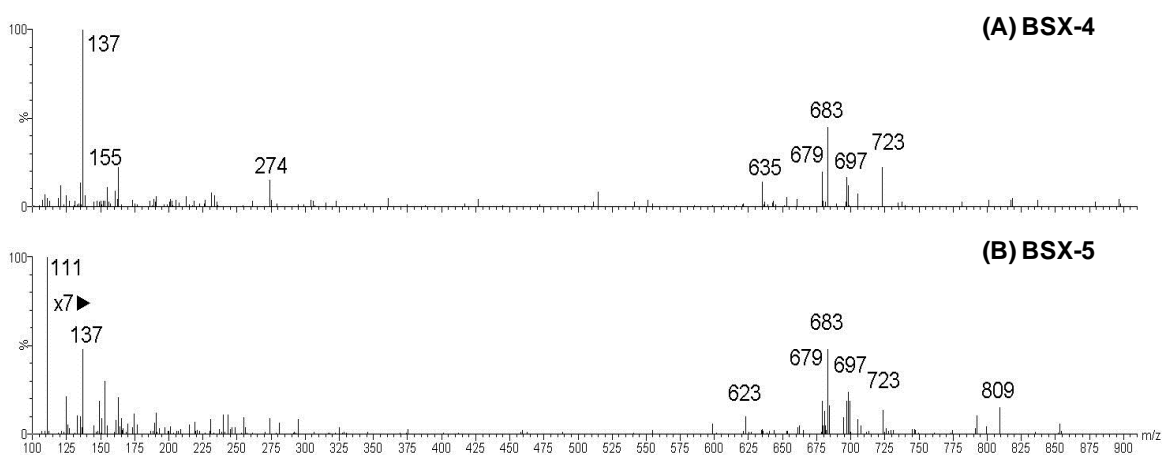


**Figure 5-19.** Daughter ion mass spectra (ESI-) for  $[\text{M-H}]^-$  of (A) BSX-4 897 and (B) BSX-5 853 at collision energy 45 eV.



#### **5.3.3.5 Probable structures of BSX toxins (collaboration with Prof Satake and Dr Patrick Edwards)**

NMR spectra were obtained for BSX-1 and BSX-4 by Dr Patrick Edwards, Massey University. Both BSXs gave spectra of typical of polycyclic ether compounds with ladder-frame structures. Prof. Satake (University of Tokyo) assisted with interpretation of the complex spectra and he has provided the probable structures for BSX-1 and BSX-4 (Figure 5-20). Preliminary NMR studies were undertaken on BSX-1 at 300K. The  $^1\text{H}$ ,  $^{13}\text{C}$  and HSQC spectra clearly showed the presence of two carbonyl groups, a sharp doublet methyl, an olefinic double bond and a methylenic double bond plus a suite of oxy-methine signals. The structures for the opened five-membered ring-A plus rings-B and -C were deduced from the HSQC, HMBC and COSY spectra. Carboxylic acids at both termini of BSX-1 were confirmed by HMBC correlations from methylene protons to carboxylic carbons and the side chain also contains an unconjugated methylenic double bond and a hydroxyl group.

However, only approximately 2/3 of the carbons and protons could be accounted for in the HSQC spectra (Figure 5-21) and many signals for the middle part of the molecule were missing. The methylenic side chain carbon is accounted for at 112.3 ppm (red, 2 protons) but only one olefinic double bond (blue, 2 carbons at 127.3 and 135.4 ppm). Some broad peaks were present in the  $^1\text{H}$  spectrum. Slow conformation changes in the time frame of NMR pulse sequences are known to affect the spin couplings and broaden or eliminate peaks. In the case of brevetoxin-1 and ciguatoxin, conformer effects involving the flexible central 8- and 9-membered rings were overcome by obtaining NMR spectra at lower temperatures (Murata *et al.*, 1990; Pawlak *et al.*, 1987). Further spectra for BSX-1 were obtained at 273K, the lowest probe temperature obtainable on the 700 MHz instrument. Although there was some sharpening of the broad  $^1\text{H}$  peaks, and the number of peaks in the HSQC spectrum increased, many important signals involving the central part of the molecule were still missing.

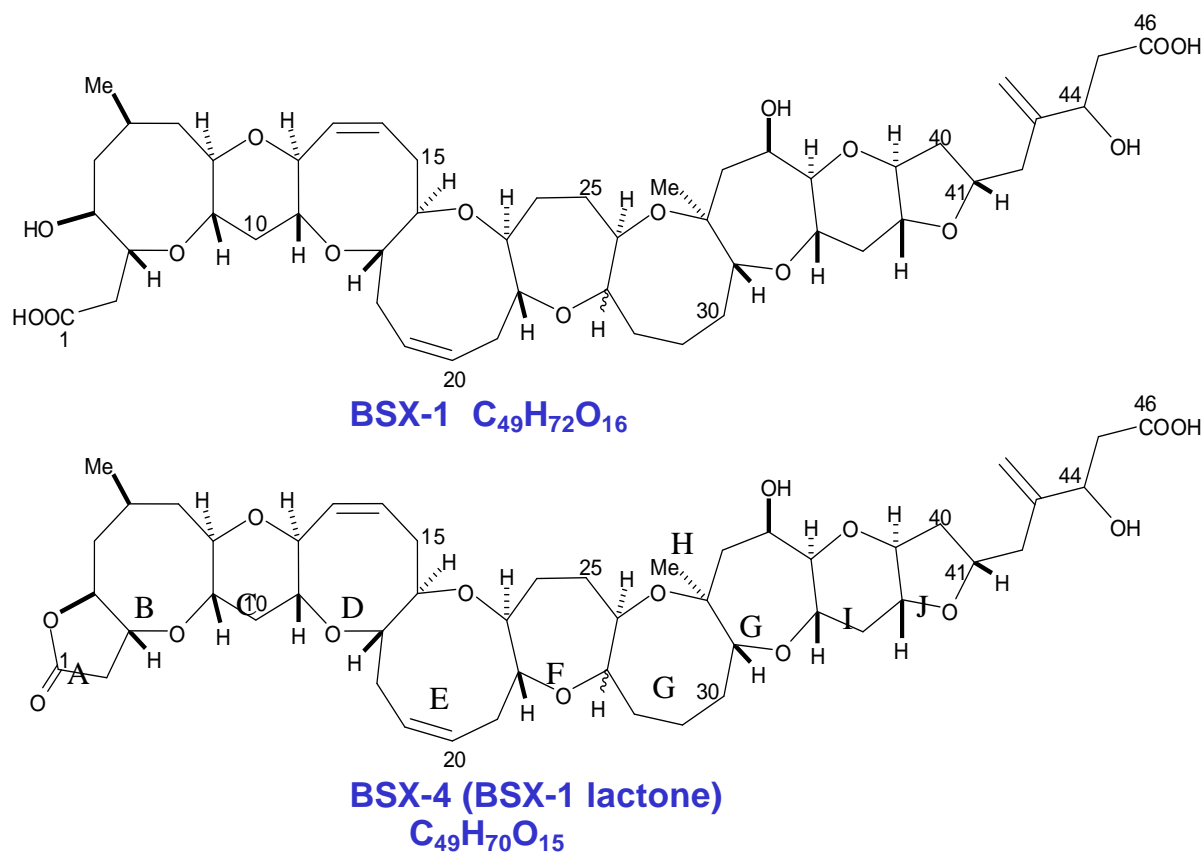


**Figure 5-20.** The probable structures of BSX-1 and BSX-4 elucidated by NMR (at Massey University and University of Tokyo).

The 500 MHz instrument has a probe that can be maintained at lower temperatures. The sensitivity loss at 500 MHz was offset by using toxins with  $^{13}C$  incorporation. The lactone analogue BSX-4 was generated from BSX-1 containing ca. 10%  $^{13}C$  (Figure 5-20; Sections 3.3.4 & 5.3.2.4). NMR spectra were obtained for  $^{13}C$ -BSX-4 (Section 5.3.2.4) using 500 and 700 MHz instruments and deuterio-methanol as solvent. Overall the spectra at 273K using the 700 MHz instrument were very similar to those for BSX-1 with the expected changes in chemical shifts in ring A due to the lactone ring closure e.g. a lower  $^1H$  chemical shift for H4. Further peaks were observed in the HSQC spectra at 243K (Figure 5-22) and some broad bands in the  $^1H$  spectra at 273K become discrete peaks. Although the overall resolution of the  $^1H$  spectra were reduced as the temperature was lowered from 300K to 243K, the number of discrete carbons observed in the HSQC spectra increased. In the olefin region of the spectra (Figures 5-21, 5-22;  $^1H$  region 4.4 – 5.7 ppm), the number of peaks increased from 2 to 6. However, the r+db count of the molecular formula indicates there should be only two ring olefin groups i.e. four olefinic protons. The conclusion is that at 243K the molecule is spending about equal amounts of time in two conformations, each involving the 9-membered ring E and with slightly different chemical shifts that provide two pairs of peaks for the ring E olefin in the HSQC spectrum. The number of HSQC peaks corresponding to the ring junction

O-C-H's also increased (Figures 5-22, 5-22;  $^1\text{H}$  region 3.0 – 4.5 ppm). Corresponding increases in the  $-\text{CH}_2$  signals (not shown) were also observed. Although the HSQC spectra at 243K now contained peaks for most of the 49 carbons, conformer effects had not been sufficiently eliminated to allow all spin couplings to be observed in the HMBC and COSY spectra. Therefore some ambiguities remain regarding rings D to H. The A, B and C rings for BSX-4 are the same as those of brevetoxin-1 except for the lack of the ring-junction tertiary methyl group (Figure 2-9, 5-20). The terminal H, I and J rings appear to be different from brevetoxin-1 and include a secondary hydroxyl group.

The structures for BSX-2 and BSX-5 are postulated, on the basis of micro-reactions and MS/MS data (Sections 5.3.3.3 & 5.3.3.4), to be the same as BSX-1 and BSX-4 respectively but with a shorter side chain by the  $\text{CH}_2\text{CHOH}$  formulae difference and conjugation of the carboxyl group as in brevetoxin-B5 (Ishida *et al.*, 2004a). This remains to be confirmed by NMR.

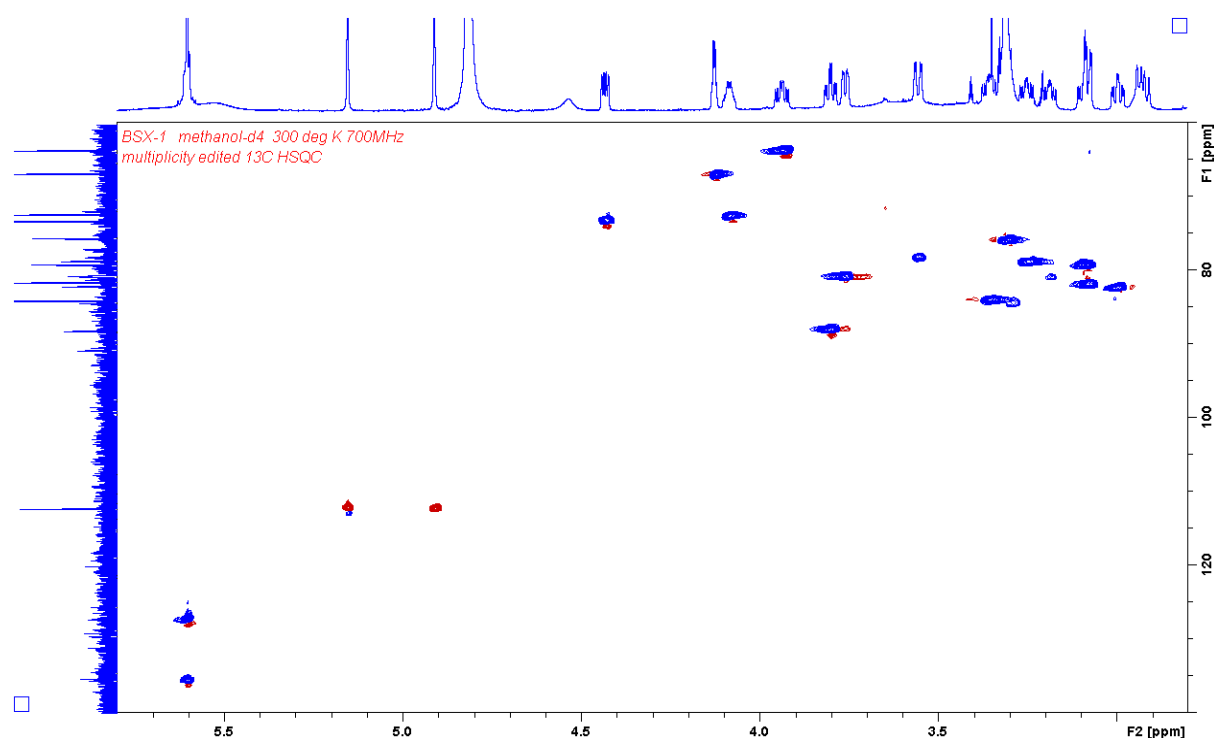


**Figure 5-21.**  $^1\text{H}$ - $^{13}\text{C}$  HSQC spectrum (partial) of BSX-1. The spectrum was obtained in deuterio-methanol at 300K using a 700 MHz instrument.

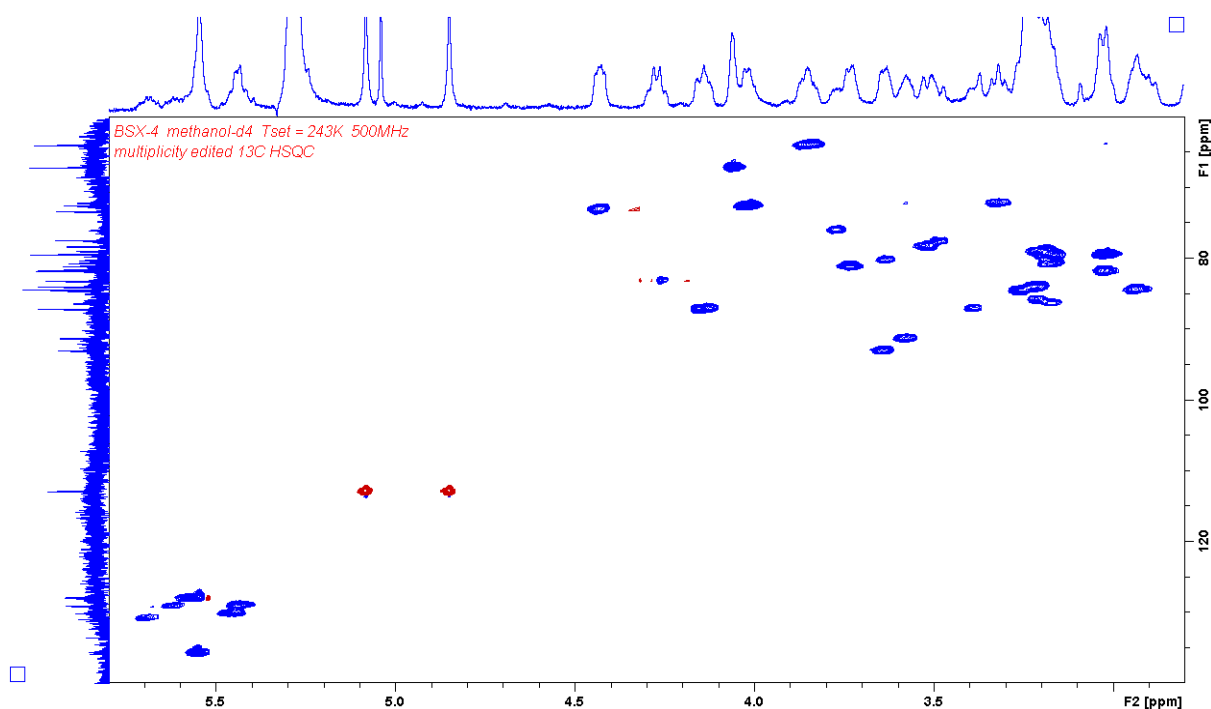


**Figure 5-22.**  $^1\text{H}$ - $^{13}\text{C}$  HSQC spectrum (partial) of  $^{13}\text{C}$ -labelled BSX-4. The spectrum was obtained in deuterio-methanol at 243K using a 500 MHz instrument.

### 5.3.4 Chemical investigations of KBTs

This section summarises the studies conducted at University of Tokyo by the team led by Prof. Satake using crude extracts of *K. brevisulcata* bulk cultures prepared at Cawthron Institute (Hamamoto *et al.*, 2012).

#### 5.3.4.1 Isolation of KBT-F and KBT-G

KBTs, large molecular toxins with 1800-2200 Dalton, were isolated and purified at University of Tokyo. The initial isolations were guided by mouse bioassay and murine P388 lymphocytic leukemia cell assay. The neutral toxic fraction from less than 5000 *K. brevisulcata* cells was sufficient to kill mice under 24 hr. The P388 assay was used to guide initial chromatographic fractionations. The most cytotoxic fractions were associated with UV absorbance at 230nm and the latter property was used to guide the final isolation and purification of KBT-F and KBT-G (Figure 4-3). These toxins coeluted under C18 reversed phase conditions. Two stages of chromatography using a C30 phase were required to purify and separate them preparatively. KBT-F (3.1 mg) and KBT-G (1.3 mg) were isolated in high purity from crude extracts of 1450 litres of culture. In addition, KBT-H (1.2 mg) and KBT-I (0.6 mg) were also isolated and purified from the same extracts (M. Satake, pers. comm.).

Small amounts of these two KBTs were provided and used for analytic studies using LC-MS at Cawthron Institute (Sections 4.3.1.3 & 4.3.2.2).

#### 5.3.4.2 Structural characterisation of KBT-F

The molecular formulae established by HR-MALDI-TOF were ( $[M+Na]^+$  required, found, rings plus double bonds): KBT-F  $C_{107}H_{160}O_{38}$  (2076.0485, 2076.0476, r+db=28), KBT-G  $C_{108}H_{162}O_{39}$  (2106.0591, 2106.0596, r+db=28). NMR spectra for KBT-F were extremely complex but large numbers of protons on oxygenated carbons observed in the  $^1H$  spectra suggested that KBT-F is a ladder chain polycyclic ether compound.

The chemical structure of KBT-F was elucidated from detailed interpretation of 2D NMR spectra and confirmed by MS/MS data (Figures 5-23, 5-24) (Hamamoto *et al.*, 2012). The  $^1H$ ,  $^{13}C$  and HSQC spectra showed signals for 13 methyls (2 for doublets and 11 for singlets), one methine and 25 methylene aliphatic carbons, 51 oxygenated methine and 10 oxygenated quaternary carbons, five methine and a quaternary olefinic carbons, and an aldehyde carbon (total 107 carbon atoms). A 2-methyl-2-butenal side chain was characterised by 2D NMR spectra including  $^1H$ - $^1H$  correlation spectroscopy (COSY), HSQC and HMBC. The signals match those of the 2-methyl-2-butenal side chain in gymnocin-A and gymnocin-B (Satake *et al.*, 2002; Satake *et al.*, 2005). The UVmax of 227 nm for KBT-F and KBT-G also matched that for the gymnocins. KBT-F contains less ether rings (24 versus 32) and hydroxyl groups (13 versus 28) than MTX (Satake *et al.*, 1995). However, it contains a large number of smaller polyether rings with a higher proportion of methyl groups at ring junctions than in the BSXs, brevetoxins or gymnocins (Figures 2-9, 2-11, 5-24). KBT-F does not contain 8- or 9-membered ring systems and therefore did not give conformer problems in the NMR unlike BSXs and brevetoxin-1 (Figures 2-9, 5-20, 5-24).

The complex ether rings of KBT-F were confirmed using negative ion MALDI TOF MS/MS with high collision energy (Hamamoto *et al.*, 2012). KBT-F does not contain a suitable functional group for charge remote fragmentation. To introduce a charge site into the molecule, KBT-F was reacted with HBSS to chemically synthesise KBT-F BSD. This derivative contains a sulphate group at the terminus which is easily charged under negative ionisation (Figure 5-23A) (Murata *et al.*, 1994; Naoki *et al.*, 1993). The prominent fragment ions in the TOF-TOF spectra correspond to cleavages at the characteristic sites of ether rings. These confirmed the sequence in KBT-F of cyclic ethers for rings A-Q and S-W (Figure 5-22B, C). These MS/MS and TOF-TOF spectra supported the KBT-F planar structure

elucidated from NMR experiments (Hamamoto *et al.*, 2012). The diastereoisomer relationships of the central sections connecting the two main ring systems remain to be determined.

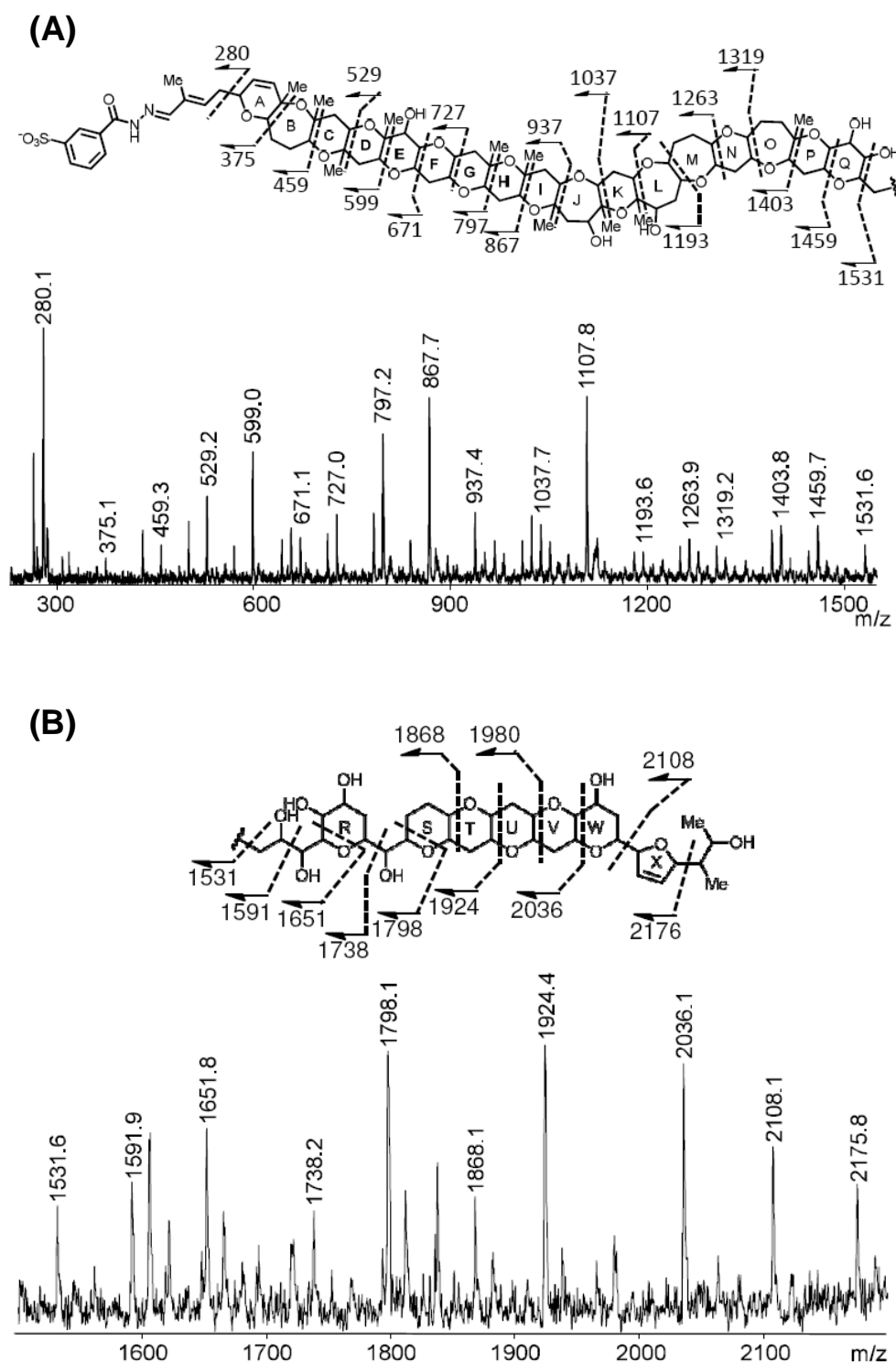


**Figure 5-23.** MALDI Spiral TOF-TOF MS/MS spectrum of KBT-F BSD [modified from Hamamoto *et al.* (2012)]. The spectrum was taken for the parent ion  $[M-Na]^+$  at  $m/z$  2250 and is shown in two parts: (A)  $m/z$  250-1550 (C1-C63) and (B)  $m/z$  1500-2200 (C63-C95).

Daughter ion spectra for  $[M+H]^+$  of KBT-F ( $ESI^+$ ) were also gathered at Cawthron Institute using TSQ MS/MS as the part of development of MRM quantitation (Figure 5-24, Section 4.3.2.2). At 50 eV collision energy, the major fragmentation  $[M+H-84]^+$  at 1971 Da was observed but no other significant high mass fragments were evident. In the TSQ collision cell (Figure 2-7), fragment ions are generated by multiple low energy collisions. This is not advantageous for generation of ether ring cleavages compared to the single high energy collisions (10 kV) obtainable in TOF-TOF instruments. Loss of 84 Da corresponds to elimination of the 2-methyl-2-butenal side chain ( $C_5H_8O$ ) and confirms that the side chain of KBT-F is the same as that in gymnocin-A and -B (Satake *et al.*, 2002; Satake *et al.*, 2005). The equivalent side chain cleavage fragment ion ( $[M+H-84]^+$  or  $[M+H-100]^+$ ) was also observed in the daughter ion spectra for KBT-G, -H and -I (data not shown). These significant  $[M+H-84]^+$  or  $[M+H-100]^+$  fragment ions were developed for quantitative analysis of KBTs using TSQ MS/MS in MRM mode (Section 4.3.2.2).

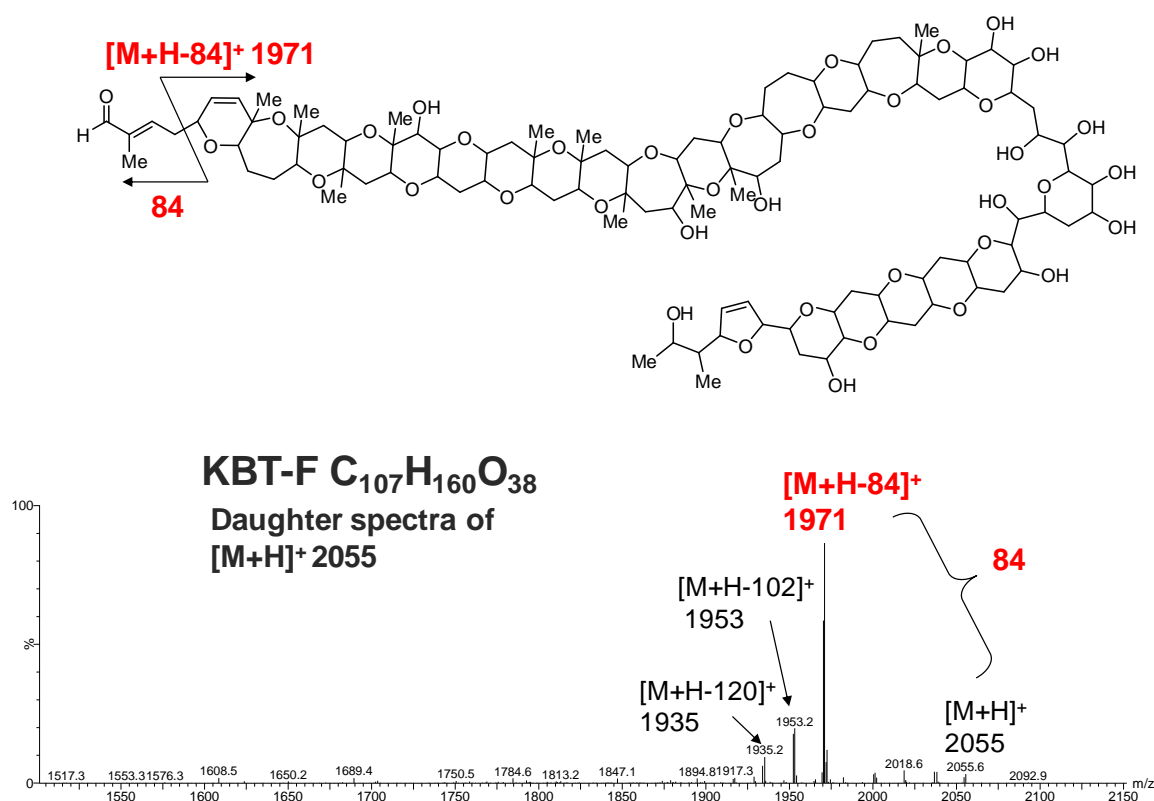


**Figure 5-24.** Structure and TSQ ( $ESI^+$ ) daughter ion spectrum of KBT-F ( $C_{107}H_{160}O_{38}$ ) at collision energy 50 eV. The main daughter ions from  $[M+H]^+$  2055 are generated by cleavage of the 2-methyl-2-butenal side chain ( $m/z$  1971,  $[M+H-84]^+$ ) and associated water losses ions.

## 5.4 Summary

Procedures for isolation and purification of BSXs were developed and optimised by small scale experiments. An LC-MS method using uPLC for rapid separations was developed to guide isolation and purification of BSXs (Section 4.3.2.1). Large scale isolation and purification of the toxins followed the optimised procedure: solvent partitioning to separate BSX-1 and BSX-2 from a neutral fraction containing KBTs; desalting and defatting using SPE (reverse and normal phase SPE); separation of BSX-1 and BSX-2 using silica gel flash chromatography; final purification by preparative C18 reverse phased HPLC and generation of BSX-4 and BSX-5 by lactone ring closure. 4.21 mg BSX-1 and 1.75 mg BSX-2 were isolated in high purity from unlabelled mass cultures of *K. brevisulcata*. Subsamples of pure BSX-1 and -2 were used to prepare the lactone derivatives (1.8 mg BSX-4 and 0.6 mg BSX-5) by acid catalysed dehydration. Methylation and acetylation provide information about the number of labile hydroxyls in the BSXs. BSX-1 (M 916 C<sub>49</sub>H<sub>72</sub>O<sub>16</sub>) and BSX-2 (M872 C<sub>47</sub>H<sub>68</sub>O<sub>15</sub>) are polycyclic ether dicarboxylates with UVmax 196 nm. The molecular formulae and MS/MS data suggest that BSX-1 and BSX-2 are very closely related structurally and differ only by a C<sub>2</sub>H<sub>4</sub>O unit that is remote from the lactone ring A. The biosynthetic pathways are likely to be related. BSX-4 and BSX-5 are the lactone ring-closed derivatives of BSX-1 and BSX-2 respectively and are presumed to be the primary toxins in the algal cells. Experiments with BSX-4 and -5 using dilute base showed that the base hydrolysis of the lactone ring proceeded rapidly with pseudo-first order kinetics. In addition to unlabelled materials, <sup>13</sup>C-labelled toxins were also isolated and purified for <sup>13</sup>C NMR and 2D NMR experiments. Structural information from UV, MS, MS/MS and NMR showed BSXs have some similarities to brevetoxin-1 and Prof. Satake has proposed a probable structure for BSX-4 (Figure 5-20). However, complete structural elucidation by NMR has been prevented thus far by conformer effects presumed to arise from very flexible 8- or 9- membered rings. In addition, two further novel compounds [M+H]<sup>+</sup> 857 and 839 Da named BSX-3 and its putative lactone BSX-6 were detected in culture extracts using LC-MS (Figure 4-1A, Section 4.3.1.2). The daughter ion spectra showed these BSXs gave equivalent fragment ions to the other BSXs (Table 6-3), suggesting structural similarities. However, isolation, purification and NMR studies for BSX-3 and BSX-6 were not conducted in this PhD study.

Isolation, purification and structural elucidation of KBTs were carried out by researchers at the University of Tokyo using crude extracts provided by Cawthron Institute. Four KBTs were isolated from 1450 L of bulk cultures and purified in quantities of 0.6-31 mg. Preliminary chemical investigations show that KBT-F (m.w. 2054 C<sub>107</sub>H<sub>160</sub>O<sub>38</sub>) and KBT-G



(m.w. 2084 C<sub>108</sub>H<sub>162</sub>O<sub>39</sub>) are complex polycyclic ethers with UV<sub>max</sub> at 227nm. NMR and MS/MS data has provided the structure for KBT-F which has a ladder frame polyether structures with 24 ether rings (17 of them contiguous) and a 2-methyl-2-butenal side-chain, similar to gymnocins (Hamamoto *et al.*, 2012; Satake *et al.*, 2002; Satake *et al.*, 2005). However, the chemical structures of KBT-G, -H, and -I are still not confirmed, and related chemical studies are being completed at University of Tokyo.

## Chapter 6

# Toxicological investigations of novel biotoxins isolated from the dinoflagellate *Karenia brevisulcata*

### 6.1 Introduction

The toxicological investigations of newly purified toxins are based on *in vivo* and *in vitro* bioassays. Mouse bioassays using i.p. injection (MBA) are used in routine monitoring of PSP, NSP and NSP toxins (APHA, 1985; Cembella *et al.*, 1995; Yasumoto *et al.*, 1978). MBA has also been developed to study toxicokinetics of unknown toxins based on dose response curves and dose-death time relationships using multiple tests with increasing doses (OECD, 2001). However, there are shortcomings including low sensitivity, low selectivity/specificity, large amount of material required, and animal ethical concerns (Holland, 2008).

*In vitro* cell based assays are a subtype of *in vitro* functional assays, and are based on biological response of viable cells. They do not require prior knowledge of the initial cellular target for toxins (Fairey *et al.*, 1999). Therefore they are recommended for studies of new toxins for (i) cytotoxicity assessment, (ii) mode-of-action identification, and (iii) method development for detection/monitoring. Several mammalian cell lines were studied for their usefulness in evaluating of compounds produced by toxic algae: Neuro2a (mouse neuroblastoma cell), P388 (murine lymphoid macrophage), Vero (African green monkey kidney epithelial cell) and primary mouse erythrocytes cells (Swiss albino mice).

*K. brevisulcata* was isolated from a severe HAB event which occurred in Wellington Harbour, New Zealand, in 1998 that caused mass mortalities of marine biota and flora (Chang, 1999a, b; Chang *et al.*, 2001). Although it is similar to *K. brevis* and *K. mikimotoi* in morphology (Chang, 1999a), this dinoflagellate does not produce brevetoxins or gymnocins (Section 4.3). Further research identified that *K. brevisulcata* produced two suites of complex polyether compounds, BSXs and KBTs. Milligram quantities of the following toxins were isolated from mass cultures: KBT-F, KBT-G; BSX-1, BSX-2, BSX-4 and BSX-5 (Sections 5.3.2 & 5.3.4.1).

A novel cyclic imine compound C402 was isolated from the cultures of another dinoflagellate species and the structure has been elucidated by NMR spectrometry (A.I. Selwood, pers. comm.). The toxicity and the mode-of-action of C402 have not been previously assessed.

Some algal toxins e.g. DA and OA can induce cell death via apoptosis (programmed cell death). Cell viability assays measuring mitochondrial activity of viable cells (MTS reduction) is of limited use in quantitation of apoptotic cell death and evaluation of cytotoxicity of an apoptosis inducer (Lobner, 2000). The enzyme caspase-3 is critical in caspase dependent apoptosis. Activation of caspase-3 leads to cleavage of number of cellular substrates (e.g. Bid, caspase-7, ICAD and PARP), and triggers cells to undergo irreversible apoptosis (D'Amelio *et al.*, 2010; Slee *et al.*, 2001; Walsh *et al.*, 2008). Thus caspase-3 was developed as a biomarker for apoptosis identification.

In this study, several toxicological bioassays were used to evaluate toxicities of the novel compounds motioned above (BSXs, KBTs and C402), including MBA, Bignami assay, and Neuro2a, P388 and Vero cell based bioassays. The *in vitro* cell-based assays were also developed for measurement of multiple end-points including cell viability (MTS reduction), cell membrane integrity (LDH release), and caspase-3 activity. The data obtained from bioassays conducted on algal toxins in this study will provide preliminary information about their modes-of-action: VGSC toxin, apoptosis inducer or haemolysin (cell membrane destroyer).

## **6.2 Materials and methods**

### **6.2.1 Pure biotoxins**

KBTs (-F & -G) and BSXs (-1, -2, -4 & -5) were isolated and purified from *K. brevisulcata* (CAWD 82) cultures by Japanese researchers at the University of Tokyo and New Zealand researchers at Cawthron Institute respectively (Sections 5.3.2 & 5.3.4.1). Palytoxin and OA were purchased from Wako, Japan, and Calbiochem, Merck (Darmstadt, Germany) respectively. A semi-purified mixture of the diol esters of OA was isolated from cultures of *Prorocentrum lima* (CAWD 69) by Dr Patrick Holland at Cawthron. C402 was isolated and purified by Andy Selwood from a peridinoid dinoflagellate. Staurosporine was purchased from Sigma-Aldrich (USA).

### **6.2.2 Mammalian Toxicology**

MBA were conducted by Dr Rex Munday, AgResearch, Hamilton. Female Swiss albino mice, with initial body weight of 18–22 g, were used in all experiments. The animals were allowed free access to food (Laboratory Chow, Sharpes Animal Feeds, Carterton, NZ) and tap

water throughout the experimental period. Acute toxicities were determined according to the principles of OECD Guideline 425 (OECD, 2001) and LD<sub>50</sub> values with 95% confidence limits calculated on a live-weight basis. Test materials were dissolved in ethanol and aliquots diluted with 1% Tween-60 in saline. The diluted solution (1 mL), containing 0.5% v/v ethanol, was injected i.p.. The mice were closely observed throughout the day of dosing (for ca. 8 hr). Survivors were examined and weighed each day for the next 13 days, and sacrificed at day 14. A gross pathological examination was carried out on all mice.

### 6.2.3 P388 and Vero cell culturing

P388 and Vero were obtained from the ECACC through Sigma-Aldrich (Sigma, Castle Hill, NSW). Both were grown in tissue flasks (25 or 75 cm<sup>2</sup>, Nunc, Denmark) in a CO<sub>2</sub> (5%)-incubator (Galaxy 170S, New Brunswick, USA) at 37 °C.

P388 cell growth required minimum essential medium (MEM, Sigma) supplemented with 10% foetal bovine serum (FBS, Gibco, Invitrogen, USA), NaHCO<sub>3</sub> (4.2 mg mL<sup>-1</sup>), streptomycin (132 µg mL<sup>-1</sup>, Sigma), penicillin (132 units mL<sup>-1</sup>, Sigma), L-glutamine (2 mM, Sigma) and Hepes buffer (7.4 mM, Sigma). Sub-culturing or harvesting of cells was conducted at an interval of 2 or 3 days. The cell suspension was gently transferred to a Falcon centrifuge tube (50 mL, Becton, Dickinson, UJ, USA) and reminding attached cells were released from tissue flasks through washing twice with Ca<sup>2+</sup> and Mg<sup>2+</sup>-free phosphate buffered saline (PBS, Sigma; 10 mL each per tissue flask) and trypsinization (trypsin-EDTA solution, Sigma) at room temperature for 30 seconds. Combined cell suspensions with detached cells in Falcon tubes were centrifuged at 300g for 10 min. The P388 cell pellets were re-suspended in fresh MEM and sub-cultured or diluted to desired cell concentration for *in vitro* cell-based assays.

Vero cells were grown in Dulbecco's Modified Eagle's Medium (DMEM, Sigma) supplemented with 10% FBS, NaHCO<sub>3</sub> (3.7 mg mL<sup>-1</sup>), streptomycin (132 µg mL<sup>-1</sup>), penicillin (132 units mL<sup>-1</sup>) and L-glutamine (2 mM). When cell confluency reached 80-90%, the cells were washed twice with PBS and then trypsinized at 37 °C for two min. Fresh DMEM (with 10% FBS) was then immediately added to protect cell plasma membrane proteins from trypsin proteolysis and to re-suspend cells for sub-culturing or cell bioassays. To assist detachment of cells from tissue flasks, mechanical agitation was conducted e.g. tapping the sides of flask or gentle scraping.

Cell concentrations were determined using trypan-blue dye (0.4%, 100  $\mu$ L dye per 100  $\mu$ L cells) and counting using haemocytometry (dilution factor 2x).

#### **6.2.4 Cell viability assay (MTS reduction)**

Cell viability was determined by measurement of mitochondrial activity (metabolic activity) of cells, using the MTS assay. The assay in 96 well plates (Nunc Denmark) followed the instructions of the manufacturer (Promega Corp., WI, USA). MTS is a clear yellow coloured liquid used with an electron coupling reagent (phenazine methosulfate; PMS, Sigma, USA) at the ratio of 1:20 (v/v). Pure toxins were dissolved in ethanol and aliquots were diluted with MEM or DMEM. Preliminary experiments using MTS assay and inverted microscope confirmed that up to 1% (v/v) of ethanol in cell growth media did not cause observable toxic effects on morphology or growth of P388 or Vero cells. The final ethanol concentration in each well was controlled at < 0.5%. Where ethanol concentrations > 0.5% were required, ethanol controls were used (n=3 or 4). For a positive control, palytoxin was used at 5 ng mL<sup>-1</sup> (n=3 or 4) in both P388 and Vero cell assays.

P388 cell bioassays do not require a pre-incubation stage prior to exposure of cells to toxin. The cell seeding concentrations were  $2.5 \times 10^4$  and  $1 \times 10^4$  cells/well (50  $\mu$ L per well) for 24 and 72 hr exposure experiments respectively. Toxin solutions in ethanol were diluted 100 times with MEM and 50  $\mu$ L aliquots were added into wells containing 50  $\mu$ L cell suspension (n = 4). MEM containing 1 % ethanol was added into wells with and without cells (n=3 or 4), as negative control or blank respectively.

As an adherent cell line, Vero cells required several hours to stabilise and attach to flat-bottomed 96 well plates. In this study, Vero cells were seeded at  $1 \times 10^4$  and  $0.5 \times 10^4$  cells/well (100  $\mu$ L per well) for 24 and 72 hr exposure experiments respectively. The plates were pre-incubated for 24 hr at 37 °C and the media then decanted from the wells. Toxin solutions in ethanol were diluted 200 times with DMEM and the aliquots of 100  $\mu$ L were added into wells containing cells (n = 4). DMEM containing 0.5% ethanol was added into wells with or without cells (n=3 or 4) as negative control and blank respectively.

For P388 and Vero cells, 20  $\mu$ L of MTS/PMS solution was added to each well containing 100  $\mu$ L suspension after 24 or 72 hr exposure. The plates were re-incubated for 1 to 4 hr at 37 °C and the absorbance was measured at 492 nm using a FluoStar microplate reader (BMG Lab Technologies).

Cell viability was calculated from the absorbance data based on the following equation:

$$\text{Cell viability \%} = 100 \times [\text{AB}_{\text{sam}} - \text{AB}_{\text{bl}}]/(\text{AB}_{\text{nc}} - \text{AB}_{\text{pc}})$$

Where:  $\text{AB}_{\text{sam}}$  is the absorbance of each sample

$\text{AB}_{\text{bl}}$  is the mean absorbance of blanks.

$\text{AB}_{\text{nc}}$  and  $\text{AB}_{\text{pc}}$  are the mean absorbances of negative controls and positive controls.

$\text{EC}_{50}$  values were determined by fitting a sigmoidal dose-response curve to the mean cell viability, plotted against toxin concentration ( $\log \text{ ng mL}^{-1}$ ) using Prism 4 software (Graphpad, CA).

### 6.2.5 Cell membrane integrity assay (LDH)

Cell membrane integrity was assessed by a homogenous assay kit that measures activity of LDH released from leaky cells. In the presence of lactate,  $\text{NAD}^+$  and diaphorase, coupled enzymatic reactions are triggered by LDH to generate a fluorescent resorufin compound (Figure 2-6). LDH release percent represents the percent of membrane integrity loss. The kit was used according to the manufacturer's instruction (Promega Corp., WI, USA).

P388 cells were selected for LDH assays. After harvesting and dilution of P388 cells to  $2.77 \times 10^5 \text{ cells mL}^{-1}$ , 90  $\mu\text{L}$  of the cell suspensions were added into flat-bottomed 96 well plates (clear, Nunc, Denmark), corresponding to  $2.5 \times 10^4 \text{ cells/well}$ . KBT-F and C402 were diluted to 1  $\mu\text{M}$  in ethanol and further diluted to 50 nM with MEM. To investigate the mode-of-action of KBT-F and C402, staurosporine (1 mM in DMSO) was diluted by 100 times with MEM and was used as apoptosis control in this assay. 10  $\mu\text{L}$  of toxin or staurosporine samples were added into plates ( $n=5$ ) at time 0, 12, 18, 21, and 24 hr to expose the cells to the toxins for 24, 12, 6, 3, and 0 hr respectively prior to measurement of LDH release. Ethanol and DMSO were diluted to 5% and 1% with MEM respectively as control solutions. Aliquots (10  $\mu\text{L}$ ) of each control solution were added into ten wells containing cells at time 0. Five wells were used as negative control and the remaining five wells were treated with lysis buffer (2  $\mu\text{L}$  per well) at the end of experiment as positive control (Maximal LDH activity). The data from positive controls was not used in calculation of LDH release %, but as blank data for coupled assays (MTS or caspase-3/7 fluorescent assay, Section 6.2.7)

At the end of exposure time, the 96 well plates and LDH reagents were incubated for 20-30 minutes at 22  $^{\circ}\text{C}$  prior to initiating the reaction. 50  $\mu\text{L}$  of cell suspension were gently

removed from each well to a separate 96 well fluorescent plate (Black, NUNC, Denmark) following addition of 50  $\mu$ L of LDH reagent. After shaking for at least 30 seconds at 300-500 rpm using a mini plate shaker (MSI, IKA), the fluorescent plate were incubated at 22  $^{\circ}$ C for 5 min. Stop solution (25  $\mu$ L) was added into each well, and the fluorescent signal was measured at excitation/emission wavelengths of 544 nm/590 nm using the FluoStar plate reader.

LDH release was calculated from the fluorescence data by the following equation:

$$\text{LDH release \%} = 100 \times [\text{FL}_{\text{sam}} - \text{FL}_{\text{nc}}] / (\text{FL}_{\text{pc}} - \text{FL}_{\text{nc}})$$

Where:  $\text{FL}_{\text{sam}}$  is the fluorescence of each sample,

$\text{FL}_{\text{nc}}$  and  $\text{FL}_{\text{pc}}$  are the mean fluorescence of negative and positive controls, respectively.

The cell membrane integrity assay was usually coupled with a cell viability assay (Section 6.2.4) or a caspase-3/7 fluorescent assay (Section 6.2.7). The clear 96-well plates containing the remaining 50  $\mu$ L of treated P388 cells were incubated with 10  $\mu$ L of MTS/PMS at 37  $^{\circ}$ C for 1-4 hr. The absorbance was read at 492 nm to calculate cell viability %. Vero cells were not used for these mode-of-action studies because P388 cells proved to be more sensitive to the toxins studied.

### 6.2.6 Caspase-3 colorimetric assay

Caspase-3 activity was measured using a colorimetric protease assay modified from Alkhalaf *et al.* (2008) and Hunt *et al.* (2011). Lysis and assay buffer stocks were prepared (Table 6-1) and stored at -20  $^{\circ}$ C. Aliquots of the two buffer stocks were diluted to 1 x with 17 megohm water (Merck, Germany). The caspase-3 substrate [Acetyl-Asp-Glu-Val-Asp p-nitroanilide (Ac-DEVD-pNA)] and caspase-3 inhibitor [(Acetyl-Asp-Glu-Val-Asp-al (Ac-DEVD-CHO)] were purchased from Sigma-Aldrich (Castle Hill, NSW, Australia) and dissolved in DMSO to 20 and 2 mM respectively. Aliquots of the stock reagents were diluted 10 times with 1 x assay buffer prior to adding to 96 well plates. All stock solutions were stored at -20 $^{\circ}$ C and brought to room temperature immediately before use.

P388 cells were used to investigate the modes of action of KBT-F and C402 because of their higher sensitivity to these toxins than Vero cells (Section 6.3.4). P388 cells were diluted with MEM to  $1.1 \times 10^6$  cells  $\text{mL}^{-1}$ . 9 mL of the cell suspensions were seeded into 25  $\text{cm}^2$  tissue flasks ( $1 \times 10^7$  cells/flask). This was followed by the addition of 1 mL of 5% ethanol in MEM (control), 50 nM KBT-F, 50 nM C402, or 10  $\mu$ M staurosporine (apoptosis control).

After 12 or 24 hr exposure time, the cells were harvested by centrifuging at 300g for 10 min at 4 °C. After gently removing the supernatants, cells were removed with cold PBS into mini centrifuge tubes (1mL; Labcon, CA, USA), and re-centrifuged at 300g for 10 min at 4 °C. After removing PBS, the cell pellets were re-suspended in 100 µL of 1 x lysis buffer and incubated on ice for 20 min. The mini-tubes were centrifuged at 16,100 g for 15 min at 4 °C and the supernatants (cell lysates) were assayed (n=3) for detection of caspase-3 activity in 96 well plates (Table 6-2). The plates were incubated at 37 °C for 8-12 hr and the absorbance was measured at 405 nm using the FluoStar.

**Table 6-1.** Buffer compositions for caspase-3 colorimetric assay (based on the instruction of Sigma CASP-3-C kit).

<b>Buffer</b>	<b>Chemical</b>	<b>Concentration</b>	<b>Producer</b>
5 x lysis buffer	HEPES	250 mM	Sigma, USA
	CHAPS	25 mM	Biovision, USA
	DTT	25 mM	Merck, Germany
10 x assay buffer	HEPES	200 mM	Sigma, USA
	CHAPS	1%	Biovision, USA
	DTT	50 mM	Merck, Germany
	EDTA	20 mM	Merck, Germany

**Table 6-2.** Pipetting scheme for caspase-3 colorimetric assay (96 well-plate, triplicate wells).

	<b>Cell lysate</b>	<b>Caspase-3 substrate Ac-DEVD-pNA 2 mM</b>	<b>1 x Assay buffer</b>	<b>Caspase 3 inhibitor Ac-DEVD-CHO 200 µM</b>
<b>Reagent blank</b>	---	10 µL	90 µL	---
<b>Sample or control without inhibitor</b>	15 µL	10 µL	75 µL	---
<b>Sample or control with inhibitor</b>	15 µL	10 µL	65 µL	10 µL



The absolute absorbance at 492 nm represents caspase-3 activity of each treatment after 12 or 24 hr exposure and was calculated based on the following equation:

$$\text{Absorbance at 492 nm} = \text{Ab}_{\text{without}} - \text{Ab}_{\text{with}}$$

Where:  $\text{Ab}_{\text{without}}$  is the mean absorbance of samples or controls without caspase-3 inhibitor,

$\text{Ab}_{\text{with}}$  is the mean absorbance of samples or controls with caspase-3 inhibitor.

### 6.2.7 Caspase-3/7 fluorescent activity assay

The caspase-3/7 activity was measured using a kit based on the homogeneous fluorescent method described in Riss and Moravec (2004) (Promega Apo-ONE assay). The 96 well plates/samples for this assay were also used for LDH assay (Section 6.2.5). The blank/control solutions (5% ethanol for KBT-F and C402, and 1% DMSO for staurosporine) and sample solutions (50 nM KBT-F and 50 nM C402) and apoptosis control solution (10  $\mu\text{M}$  staurosporine) were prepared as described in Section 6.2.5. After harvesting, P388 cells were re-suspended in fresh MEM and adjusted to  $2.77 \times 10^5 \text{ cells mL}^{-1}$ . Cells were seeded into a 96 well fluorescence plate (Plate I, black; Nunc, Denmark) at 90  $\mu\text{L}$ /well containing  $2.5 \times 10^4$  cells. 10  $\mu\text{L}$  of each control solution was immediately added into blank wells ( $n=3$ ) containing 90  $\mu\text{L}$  fresh MEM, and six wells containing 90  $\mu\text{L}$  cells, half as negative control ( $n=3$ ) and half as positive control for LDH assay (maximal LDH activity,  $n=3$ ). 10  $\mu\text{L}$  of each sample solution was added into plates ( $n=3$ ) at time 0, 12, 18, and 21 hr to provide cell exposure times of 24, 12, 6 and 3 hr. After treatment, the plates were incubated for 20-30 min at 22  $^{\circ}\text{C}$  and positive controls were treated with lysis buffer (2  $\mu\text{L}$ /well) to release maximal LDH activity (Section 6.2.5). 50  $\mu\text{L}$  of culture suspension from each well of blank, sample and controls were gently removed to a separate 96-well fluorescent plate (Plate II, black, Nunc, Denmark) for LDH assay (Section 6.2.5).

50  $\mu\text{L}$  of caspase-3/7 reagent containing  $[\text{Z-DEVD}]_2\text{-R110}$  was added to the remaining solution in the wells for Plate I. After gently shaking at 300-500 rpm for 1-2 min using a mini plate shaker, the plate was incubated at room temperature for 2 hr and the cleaved fluorescent products were measured at excitation/emission wavelengths of 485 nm/538 nm using the FluoStar.

The % max caspase-3/7 activity was calculated from the fluorescence data using the following equation:

$$\% \text{ max caspase-3/7 activity} = 100 \times [\text{FL}_{\text{sam}} - \text{FL}_{\text{bl}}] / (\text{FL}_{\text{max}} - \text{FL}_{\text{nc}})$$

Where:  $\text{FL}_{\text{sam}}$  is the fluorescence of each sample.

$\text{FL}_{\text{bl}}$  is the mean fluorescence of blanks.

$\text{FL}_{\text{max}}$  is the mean fluorescence of treatment with maximal caspase-3/7 activity observed in this experiment.

$\text{FL}_{\text{nc}}$  is the mean fluorescence of negative controls.

### 6.2.8 Haemolysis assay

The assay was conducted by Dr Lyn Briggs, AgResearch, Hamilton. Samples in ethanol were diluted into media (RPMI 1640). Aliquots were assayed with mouse erythrocytes in 96-well plates according to the protocol of Bignami (Bignami, 1993) with cell exposure of 5 hr in a humidified CO<sub>2</sub> incubator at 37 °C followed by overnight at 21 °C. The absorbance of wells was determined at 405 nm using a Versa<sub>max</sub> microplate reader (Molecular Devices Corp, CA). Standard solutions of palytoxin were used to generate reference curves and data analysis was performed with SOFTmax PRO data analysis software (Molecular Devices Corp, CA). Four-parameter curve fits of mean absorbance versus the logarithm of palytoxin concentration provided the EC<sub>50</sub> values.

### 6.2.9 Neuro2a cytotoxicity assay

The Neuro2a cytotoxicity assay was conducted by Dr Penelope Truman, ESR, Porirua, following the method described previously (Truman, 2007). Neuro2a mouse neuroblastoma cells (ATCC CCL-131) were cultured in RPMI 1640 medium supplemented with glutamine, sodium pyruvate, 10% foetal calf serum, and antibiotics. The cells were maintained in culture flasks (25 or 75 cm<sup>2</sup>; Nunc, Denmark) and incubated in a CO<sub>2</sub> (5%)-incubator at 37 °C. Cells were detached from the flasks by treatment with Mg<sup>2+</sup> and Ca<sup>2+</sup>-free PBS for 5 min at 37 °C. Detached cells were seeded into 96-well plates at density of 1.2-1.6 x10<sup>5</sup> cell mL<sup>-1</sup> of culture medium and allowed to re-attach overnight. 10 µg of individual toxins (BSX-1, -2, -4 and -5 and KBT-F & -G) were dissolved in ethanol, and dilutions were made into cell culture medium (minimum 10-fold). Eight replicates of untreated controls, with and without ouabain (0.083 mM) and veratridine (0.017 mM), and with no sample added, were set in the outer

wells. The diluted samples (10  $\mu$ L) were added in triplicate to inner wells with and without ouabain and veratridine. The plates were incubated for 18–20 hr at 37  $^{\circ}$ C and cell viability assessed using MTT (Truman, 2007). EC<sub>50</sub> values for Neuro2a cells in the presence of ouabain and veratridine were determined as described in Section 6.2.4.

## **6.3 Results and discussion**

### **6.3.1 Mouse bioassay**

KBT-F and KBT-G were very toxic to mice i.p. with LD<sub>50</sub> values of 32 and 40  $\mu$ g kg<sup>-1</sup> bw respectively. These values are lower than for brevetoxin-2 and much lower than for the four BSXs (Table 6-3). Signs of discomfort were observed immediately after injection of KBT-F or KBT-G, indicating an irritant effect. Abdominal breathing was seen soon after dosing, with little or no effect on the respiration rate. The animals became very lethargic, and showed staggering gait when stimulated. Their appearance and behaviour normalised after 1.3–3.3 hr, and then remained normal throughout the day of dosing. By next day, however, mice receiving the higher doses of the test compounds were again very lethargic and such animals died or were humanely sacrificed between 24 and 48 hr after dosing. At necropsy, renal and pulmonary enlargement was noted. At lower doses, mice suffered significant weight loss 24 hr after dosing, but their appearance and behaviour was normal at this time, and they regained the weight over the subsequent 13-day observation period. The water intake of surviving mice was abnormally high for several days after dosing, indicative of kidney damage by KBTs. At necropsy, some surviving mice showed adhesions between the liver, diaphragm, kidney, spleen, pancreas and stomach. The organ weights of surviving mice were within the normal range. Preliminary histological studies showed pulmonary haemorrhage, dilatation of renal tubules, oedema and erosion of the stomach, and areas of necrosis in the thymus.

BSX-4 and BSX-5 were more toxic to mice than BSX-1 and BSX-2 (Table 6-3). At sub-lethal doses of these compounds, mice were initially hyperactive, but became immobile within minutes after dosing, with abdominal breathing. All aspects of appearance and behaviour returned to normal 2–4 hr after dosing, and remained normal throughout the subsequent 13-day observation period. At lethal doses, mice became prostrate within 3 minutes after dosing. They showed rapid abdominal breathing at this time, and were unresponsive to stimulation. The symptoms were typical of those observed for brevetoxins. Respiration suddenly ceased after ~ 20 minutes. Although the oral toxicities of KBTs and

BSXs via diet or gastric gavage have not been investigated due to insufficient pure toxins, these toxins are not expected to be of major risk to humans through the seafood chain because their bioaccumulation is predicted to be low. Shellfish may not accumulate significant levels of BSXs because of their relatively high polarity. KBTs severely affected marine organisms (Chapter 7) which showed avoidance behaviour e.g. cessation of feeding at sub-lethal doses.

C402 is less acutely toxic than some other cyclic imine toxins. The LD<sub>50</sub> of C402 is 1570 µg kg<sup>-1</sup> dw, with 95% confidence limits between 1269 and 3080 µg kg<sup>-1</sup> bw (Table 6-3). The acute toxic dose was 16-fold higher than for gymnodimine, 35-fold higher than for pinnatoxin-E, and 100-fold higher than for pinnatoxin-G (Munday *et al.*, 2004; Selwood *et al.*, 2010).

**Table 6-3.** Toxicity of toxins from *K. brevisulcata* to mice by i.p. administration.

<b>Toxin</b>	<b>KBT-F</b>	<b>KBT-G</b>	<b>BSX-1</b>	<b>BSX-2</b>
<b>LD<sub>50</sub> (µg kg<sup>-1</sup> bw)<sup>a</sup></b>	32 (22-43) <sup>b</sup>	40 (28-53)	3900 (3280-4150)	>6600 <sup>c</sup>
<b>Toxin</b>	<b>BSX-4</b>	<b>BSX-5</b>	<b>BTX-B<sup>d</sup></b>	<b>C402</b>
<b>LD<sub>50</sub> (µg kg<sup>-1</sup> bw)</b>	1880 (1580-2000)	1590 (1396-2110)	200	1570 (1269-3080)

<sup>a</sup> micrograms per kilogram live body weight

<sup>b</sup> 95% confidence interval

<sup>c</sup> highest dose tested

<sup>d</sup> brevetoxin-2 (Baden & Mende, 1982)

### 6.3.2 Culturing and harvesting of P388 and Vero cells

Vero and P388 cells were obtained from ECACC through Sigma-Aldrich (Castle Hill, NSW). The frozen cells were immediately stored in liquid nitrogen on arrival at Cawthron Institute. To eliminate cross-contamination, the two cell lines were not incubated together at the stage of “working cell bank” establishment. The working vials were frozen at -80 °C for storage periods of < 12 weeks and in liquid nitrogen for long-term storage. The medium for Vero cells followed the recommendation by ECACC. However, for P388 cells the medium described in the previous study of Lang *et al.* (2006) was used.

Trypsin-EDTA solution was used to remove all cell surface proteins/receptors and detach adhering cells from tissue flasks. As adherent cells, Vero cells required a longer incubation time of trypsinization (2 min at 37 °C) than P388 cells (30 sec at room temperature). Because P388 cells are semi-adherent, harvesting is through trypsinization and

centrifugation (suspension and adherent cells). Different relative centrifuge forces (rcf) from 100 to 600 g for 10 min centrifuging were tested. The results showed that  $\text{rcf} > 500$  g reduced the cell viability as determined using trypan blue haemocytometry. Thus 300g for 10 min was chosen as suitable centrifugation.

More than 50 subcultures of each individual cell line were prepared over a 10 month period and no contamination by bacteria or fungi occurred.

### **6.3.3 Determination of the initial cell population for cell viability assay**

*In vitro* cell bioassays require cells to grow over a period of time. However, different cell lines have different growth rates and levels of metabolic activity. Therefore, it is necessary to choose an initial cell population that ensures sufficient sensitivity but does not give rise to signals at the end of the treatment period exceeding the linear range of the assay. In this study, P388 and Vero cell lines were developed to establish cell bioassays for algal toxin investigations. Absorbance was measured at 492 nm after 4 hr treatment with MTS/PMS reagent at 37 °C. Figure 6-1 shows the effects of initial cell populations on absorbance and the data is summarized in Table 6-4.

P388 cells do not require pre-incubating and were directly added into 96 well plates. A linear increase of absorbance was observed at 0 -  $2.5 \times 10^4$  cells/well ( $R^2 = 0.962$ ) for 24 hr and at 0 -  $1 \times 10^4$  cells/well ( $R^2 = 0.911$ ) for 72 hr.

Vero cells were seeded into 96 well plates and incubated for 24 hr to allow cells to attach. The culture media was decanted and replaced with fresh DMEM. The cells were re-incubated for another 24 or 72 hr prior to adding MTS/PMS reagent. The correlations of absorbance and Vero cell population were linear up to  $1 \times 10^4$  and  $0.5 \times 10^4$  cells/well for 24 hr and 72 hr experiments respectively.

The lower initial populations for Vero cells than those for P388 cells in both 24 and 72 hr exposure experiments arose from the need for longer incubation periods (24 + 24/72 hr) for adherent cells. The background signals for MEM and DMEM media were both approximately 0.1 - 0.3 absorbance units after 4 hr incubation. The initial cell populations were selected to produce an absorbance between 0.75 and 1.25 in the MTS cell viability assay. This gave an adequate range and reduced errors in absorbance readings using the FluoStar microplate reader.

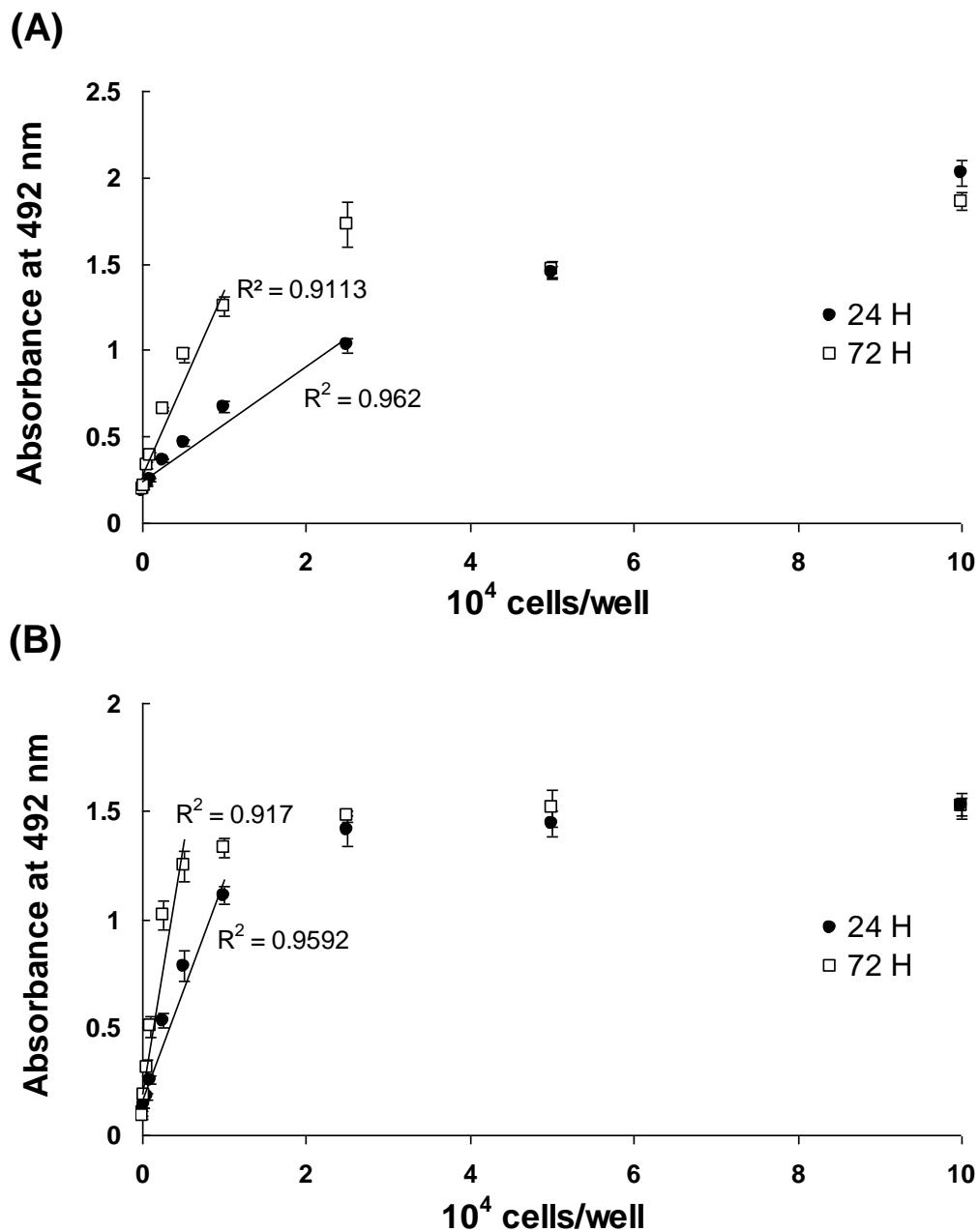


**Figure 6-1.** Effect of initial P388 (A) and Vero (B) cell population on cell viability measured using the MTS assay (absorbance at 492 nm). The cell populations seeded into 96 well plates were determined using trypan blue haemocytometry. The data are shown as Mean  $\pm$  SD (n=6).

**Table 6-4.** Determination of initial cell populations for P388 and Vero cell bioassays for different experimental periods.

Cell line	Experimental period	Linear range ( $10^4$ cells/well)	Correlation coefficient ( $R^2$ )	Initial cell population ( $10^4$ cells/well)	Average absorbance <sup>a</sup>
<b>P388</b>	24 hr	0 - 2.5	0.962	2.5	1.03 $\pm$ 0.04
	72 hr	0 - 1	0.9113	1	1.26 $\pm$ 0.05
<b>Vero</b>	24 hr	0 - 1	0.9592	1	1.11 $\pm$ 0.04
	72 hr	0 - 0.5	0.917	0.5	1.02 $\pm$ 0.07

<sup>a</sup> MTS assay; Values are means of six replicate samples  $\pm$  SD.

#### 6.3.4 Cytotoxicity of novel algal toxins using P388 and Vero cell viability assays

Based on the preliminary experiments, concentration ranges for each toxin were chosen and the assays repeated. The cytotoxicity data is summarised in Table 6-5, and the dose-response curves for KBT-F, KBT-G and C402 are shown in Figure 6-2. All compounds showed cytotoxicity to P388 and Vero cells.

For KBTs, the step-wise reductions in viability for each cell line were dose-dependent. Maximal cytotoxicity occurred at the concentration of 10 nM (20 ng mL<sup>-1</sup>) for KBT-F (Figures 6-2A, D) and 5 nM (10 ng mL<sup>-1</sup>) for KBT-G (Figures 6-2B, E). The longer exposure of 72 hr with KBTs did not significantly shift the dose-response curves to the left in P388 bioassays (Figures 6-2A, B), but decreased viability of Vero cells (Figures 6-2D, E). P388 cells were more sensitive to KBTs than Vero cells. The dose-response curve of KBT-G (Figures 6-2B, E) was steeper than that of KBT-F (Figures 6-2A, D) in each cell bioassay (24 or 72 hr exposure). The EC<sub>50</sub>'s for KBT-G are lower than those of KBT-F in both P388 and Vero bioassays after the same exposure time (Table 6-5). These results support the data obtained from other toxicological bioassays e.g. MBA, Neuro2a assay and Bignami bioassay (Sections 6.3.1 & 6.3.8), and show that KBT-G is more potent than KBT-F. Japanese researchers also used P388 cells to investigate KBTs and reported EC<sub>50</sub>'s of 2.7 nM for KBT-F and 0.82 nM KBT-G respectively (Holland *et al.*, 2012). The lower EC<sub>50</sub>s than that obtained from my experiments (3.0 - 4.8 nM for KBT-F and 4.3-5.6 nM for KBT-G) may be explained by some of the differences between the two assays: (i) cell line sources (ATCC versus ECACC), (ii) the exposure time (96 hr versus 24 or 72 hr), and (iii) initial cell population (500 cells/well versus 1 or 2.5 x 10<sup>4</sup> cells/well).

C402 (Figure 6-1) is a cyclic imine related to pinnatoxins and spirolides in chemical structure but is only weakly toxic by i.p. injection to mice (Section 6.3.1). However, it was highly cytotoxic and this was confirmed in P388 and Vero bioassays (Table 6-5). For 72 hr exposure, the dose-response curves were similar and 100% reduction in cell viability was observed at the C402 concentration of  $10 \text{ ng mL}^{-1}$  (2.5 nM) in both cell bioassays (Figures 6-2C, F). For 24 hr exposure, P388 cells were completely killed with C402 at  $10 \text{ ng mL}^{-1}$  (Figure 6-2C), and there was a 25% reduction in cell viability with Vero cells (Figure 6-2F). The dose-response curves of C402 in Vero cell bioassays (Figure 6-2F) mimic that of OA (Figure 6-3), a known apoptosis inducer. The similar observations for cellular appearance 24 hr post treatment with C402, OA and staurosporine (photographs not shown) suggest that C402 is an apoptosis inducer.

BSXs are less cytotoxic than KBTs (Table 6-5). 24 hr  $\text{EC}_{50}$ 's of greater than 8000 nM were measured for all four BSXs in both P388 and Vero cell bioassays. Ring-closed BSXs (-4 & -5) were more potent than ring opened BSXs (-1 & -2) in Neuro2a assay (Section 6.3.8). However, the similarly high  $\text{EC}_{50}$ 's for the four BSXs in these cell assays suggested that toxic actions of these toxins at VGSC may be minor.

OA is a typical DSP toxin and the mode-of-action has been well investigated (Dounay & Forsyth, 2002; McNabb, 2008; Vale & Botana, 2008). Also, it has been reported as a tumour promoter/initiator based on its apoptosis-inducing, genotoxic and immunotoxic activities (Jayaraj *et al.*, 2009; Toyofuku, 2006). After treatment with OA at 1-150 nM for 24 hr, inverted microscopy showed significant morphological changes in P388 and Vero cells (photographs not shown). Most of the morphological abnormalities e.g. rounded or flattened cells, detachment and loss of microvilli and focal adhesion structure, were similar to those described previously (Amzil *et al.*, 1992; Aune *et al.*, 1991; Oteri *et al.*, 1998; Perez-Gomez *et al.*, 2004; Tubaro *et al.*, 1996). However, reduction in cell viability could not be detected using the MTS assay (Figure 6-3), indicating that the cells may be in early stages of apoptosis but the mitochondrial functions of the cells were still intact. Interestingly, Vero cells showed higher sensitivity to OA than P388 cells. The 72 hr  $\text{EC}_{50}$  against Vero cells (34 nM) was 2.2-fold lower than that against P388 cells (Table 6-5). The 72 hr  $\text{EC}_{50}$  for OA diol esters in P388 cell bioassay was approximately 90 nM, which was slightly lower than that for OA (74 nM). The cytotoxicity of OA diol esters was not evaluated after 24 hr exposure due to lack of semi-purified materials.



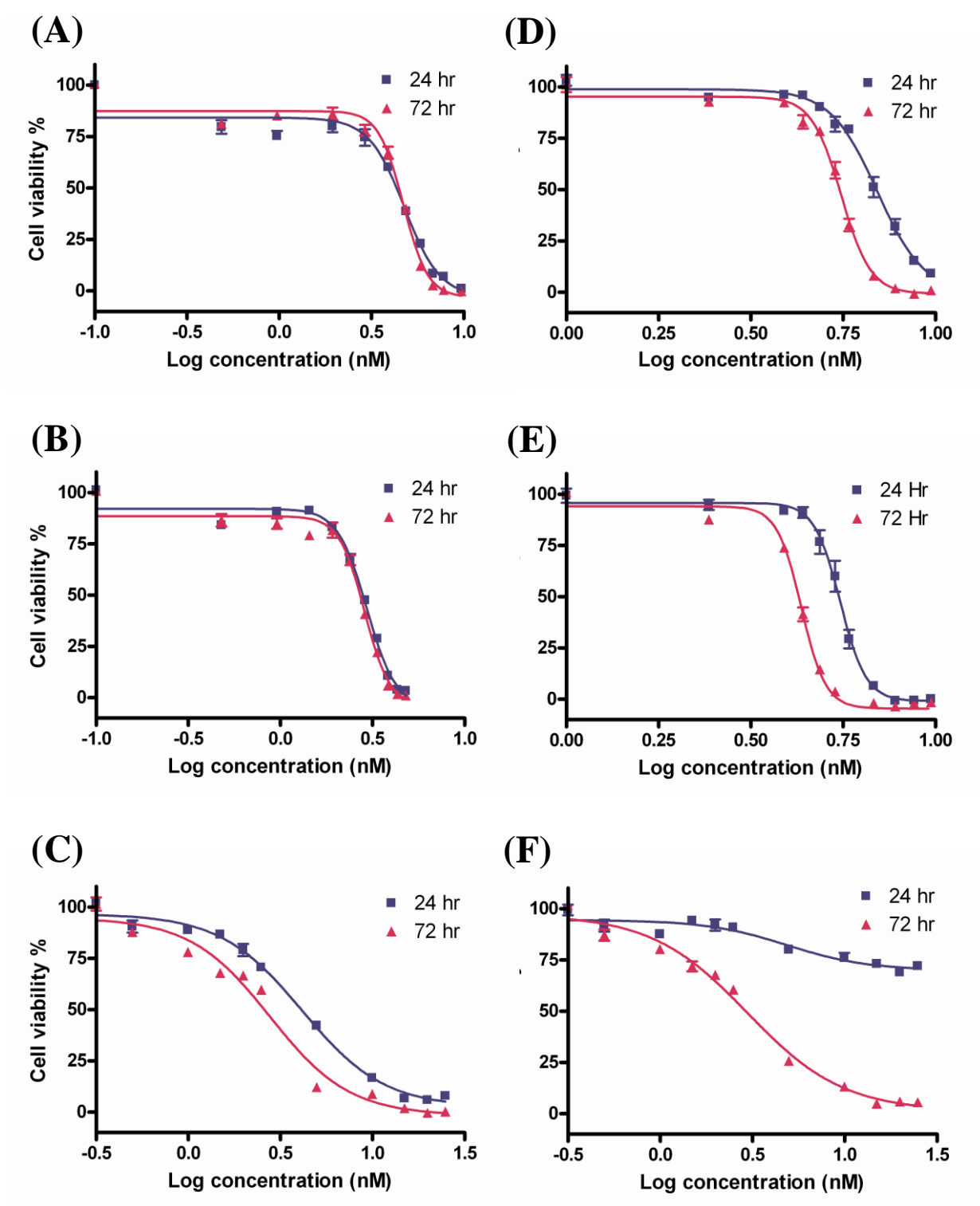


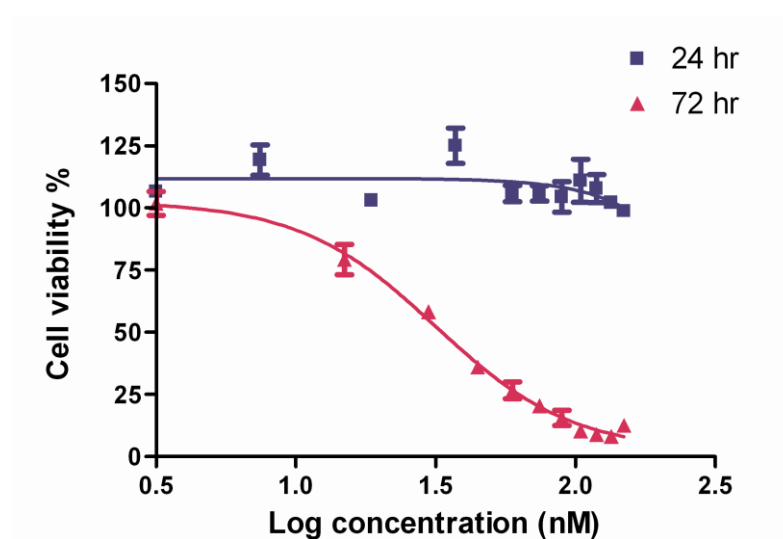
**Figure 6-2.** Dose-response curves of KBT-F (A, D), KBT-G (B, E) and C402 (C, F) against P388 (A-C) and Vero cells (D-F) bioassays after 24 hr and 72 hr exposure. The cell viability % was determined using MTS assay.

**Table 6-5.** Cytotoxicities of novel toxins against P388 and Vero cells.

	MW (Da)	EC <sub>50</sub> against P388 (nM)			EC <sub>50</sub> against Vero (nM)		
		4 hr	24hr	72 hr	4 hr	24hr	72 hr
<b>KBT-F</b>	2055	NT	4.8	4.7	15.7	7.0	5.6
<b>KBT-G</b>	2085	NT	3.0	2.9	11.8	5.5	4.3
<b>BSX-1</b>	917	NT	>10905	>10905	NT	>10905	>10905
<b>BSX-2</b>	873	NT	>11455	ca. 10309	NT	>11455	ca. 8591
<b>BSX-4</b>	899	NT	>11123	ca. 11123	NT	>11123	ca. 8343
<b>BSX-5</b>	855	NT	>11696	>11696	NT	>11696	>11696
<b>C402</b>	402	NT	4.2	2.7		N/A	3
<b>OA</b>	805	NT	N/A	74	NT	N/A	34
<b>OA diol esters</b>	854	NT	NT	ca. 90	NT	NT	NT

NT, not tested

N/A not available

**Figure 6-3.** Dose-responses of okadaic acid against Vero cell bioassays after 24 hr and 72 hr exposure. The cell viability % was determined using MTS assay.

### 6.3.5 Cell membrane integrity assay

The loss of membrane integrity can be quantitatively analysed by measurement of LDH that leaks from the cytoplasm into the surrounding culture medium. It is possible to measure multiple kinetic endpoints using treated cells from a single 96-well plate. A cell bioassay model was designed to investigate the mode-of-action of novel biotoxins through measurement of double endpoints, LDH/MTS or LDH/caspase-3/7 (Section 6.3.7). The model used P388 cells because these cells were more sensitive to KBTs and C402 than Vero cells and could be significantly affected by all tested compounds using an exposure period of 24 hr. In preliminary experiments, a time-dependent reduction in LDH activity was observed in the wells of the negative control, but there was no fluorescence change over time in the blank

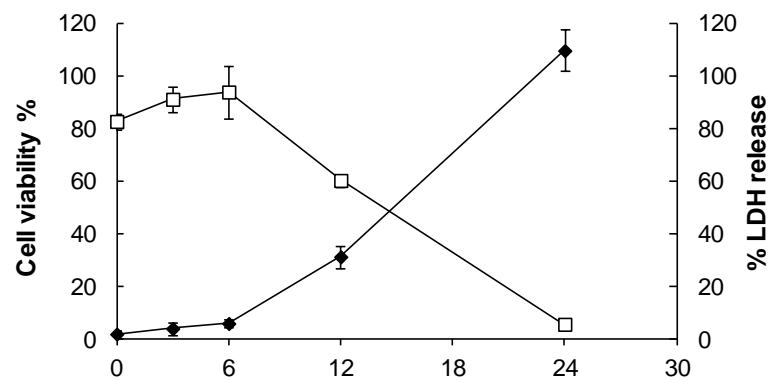
wells (medium without cells). This suggested that some enzymes in media supplemented by FBS, important for cell growth, can react with LDH reagent and produce a fluorescent signal. Therefore, the blank response was not used to calculate loss of membrane integrity. Instead, the mean fluorescence of negative controls was taken as the background activity of LDH, and used for calculation of percent loss of membrane integrity.

Two newly isolated algal toxins, KBT-F and C402, were investigated by measurement of double endpoints. The 5 nM concentration of KBT-F and C402 was chosen according to the data obtained from the P388 cell viability assays (24 hr exposure, Table 6-5). In addition, the effects of 1  $\mu$ M staurosporine, an apoptosis inducer, were also investigated.

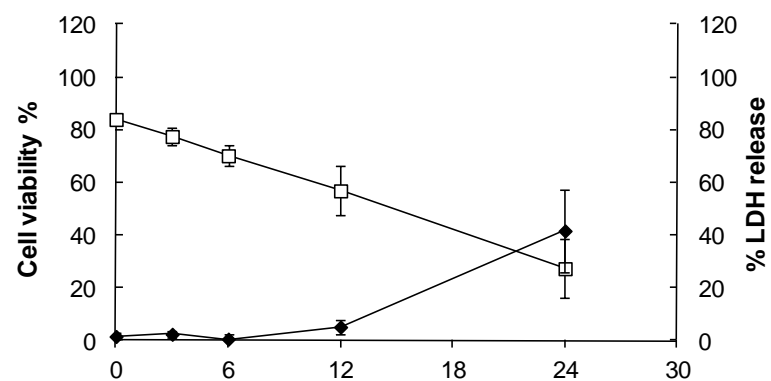
Figure 6-4 shows the time-response curves of KBT-F (5 nM), C402 (5 nM), and staurosporine (1  $\mu$ M) for the LDH and MTS assays. KBT-F did not cause significant changes in LDH release and MTS reduction during the initial 6 hr exposure (Figure 6-4A). The cell membrane integrity assay showed a time-dependent increase in LDH after 6 hr exposure (Figure 6-4A) with 100% LDH release observed after 24 hr of exposure. Consistently, there was a time-dependent reduction in cell viability after 6 hr exposure (Figure 6-4A). At 24 hr after exposure, no viable cells were observed by MTS assay. At each time point of the LDH and MTS assays with KBT-F, the summed values were close to 100%, indicating that cell membrane disintegration is strongly associated with mitochondrial dysfunction.

The time-response curves of C402 and staurosporine were similar to each other, but both differed from that of KBT-F. C402 and staurosporine did not cause significant increases in LDH leakage (> 20%) up to 12 hrs after exposure. However, time-dependent reductions in cell viability were observed after treatment with the both toxins (Figures 6-4B, C). The summed values of cell viability and LDH release were < 85% at each time point, suggesting that C402 and staurosporine are different from KBT-F in their mode-of-action. Cell death can be classified into necrosis and apoptosis. During apoptosis, mitochondrial dysfunction occurs earlier than cell membrane disintegration with release of LDH (Renz *et al.*, 2001). Staurosporine has been used in many previous studies to induce cell apoptosis, which can induce programmed cell death through multiple pathways (Bertrand *et al.*, 1994; Chae *et al.*, 2000; Jantas-Skotniczna *et al.*, 2006; Kruman *et al.*, 1998; Yue *et al.*, 1998; Zhang *et al.*, 2004). It is also likely that the mode-of-action of C402 is similar to that for staurosporine, also involving apoptosis. However, KBT-F is unlikely to cause cell death via apoptosis pathways. Caspase-3 is a critical enzyme in the caspase cascade, cleavage of which will trigger irreversible apoptosis. To further investigate the mode of action of KBT-F and C402, two caspase-3 assays were established using P388 cells.

**(A) KBT-F 5 nM**



**(B) C402 5 nM**



**(C) Staurosporine 1  $\mu$ M**

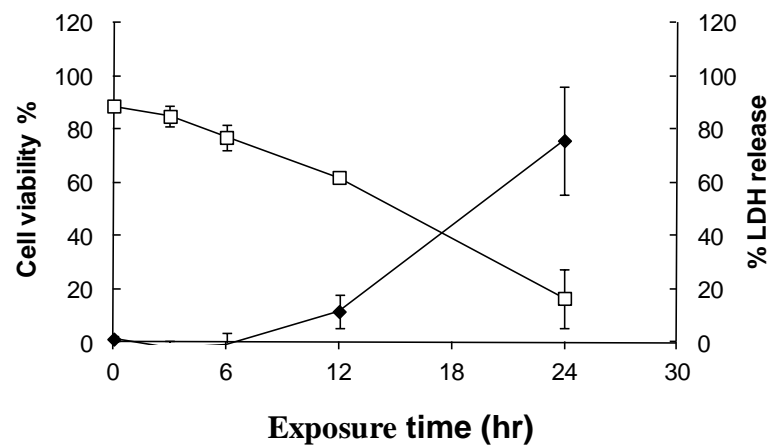


**Figure 6-4.** Time-response curves of (A) KBT-F 5 nM, (B) C402 5 nM and (C) staurosporine 1  $\mu$ M for the cell membrane integrity (◆, LDH release) and cell viability (□, MTS) assays. The values are mean  $\pm$  SD of five replicates.

### 6.3.6 Caspase-3 colorimetric assay

To investigate the mode-of-action of KBTs and C402, caspase-3 activity, a critical apoptosis indicator, was determined using a colorimetric assay modified from Alkhalaf *et al.* (2008) and Hunt *et al.* (2011). The presence of caspase-3 can catalyse the caspase-3 substrate (Ac-DEVD-pNA) to release coloured pNA which is yellow and can be measured at a wavelength of 405 nm. Ac-DEVD-CHO (caspase-3 inhibitor) was used to inhibit caspase-3 induced cleavage of pNA from Ac-DEVD-pNA at the C-terminal side of the aspartate residue of the sequence DEVD (Nicholson *et al.*, 1995). The absorbance value from wells with the inhibitor represented the blank (Table 6-2).

Preliminary experiments found that this colorimetric assay requires at least  $5 \times 10^5$  apoptotic cells to provide sufficient caspase-3 (Sigma protocol suggestion). It was quite difficult to induce and rapidly harvest sufficient apoptotic P388 cells in microtiter plates. Therefore, P388 cells were treated in small tissue flasks ( $25 \text{ cm}^2$ ,  $1 \times 10^7$  cells) with KBT-F (5 nM), C402 (5 nM), and staurosporine (1  $\mu\text{M}$ ) for 12 and 24 hr and 0.5 % ethanol in MEM was used as control. The cell lysates were prepared under temperature control at 4°C and used immediately to reduce experimental errors caused by caspase-3 degradation.

Figure 6-5 shows the effects of KBT-F (5 nM), C402 (5 nM) and staurosporine (1  $\mu\text{M}$ ) on caspase-3 activity in treated P388 cells after 12 and 24 hr exposure. All three compounds induced significantly higher activity than the control after 12 hr exposure: 2.5-fold higher for KBT-F, 10.5-fold higher for C402, and 14-fold higher for staurosporine. However, after 24 hr exposure, the caspase-3 activity reduced by 28%, 58% and 16% in cells treated with KBT-F, C402, and staurosporine, respectively, indicating that cleaved caspase-3 was being degraded. Interestingly, there was a 6-fold increase in caspase-3 activity in the control wells between 12 hr and 24 hr exposures (Figure 6-5). This can be explained as due to P388 cells undergoing apoptosis induced by increasing environmental stressors at periods longer than 12 hr (high cell densities and low nutrient environment. Together the data obtained from MTS, LDH, and caspase-3 colorimetric assays strongly suggested that the mode-of-action of C402 was similar to staurosporine and involved the caspase-3 dependent apoptosis pathway.

For the mode-of-action of KBT-F, it was still unclear whether cell death involved apoptosis via the caspase cascade. The caspase-3 activity was higher than the control at 12 hr after exposure but the absorbance at 405 nm was lower than 0.1 unit which was difficult to identify as activity or noise in the colorimetric assay (Figure 6-5). Caspase-3 activity at shorter exposure times was not tested by this assay due to the non-availability of adequate

KBT toxins for the assay. A faster and more sensitive fluorescent caspase-3/7 activity assay was used to directly assess the involvement of caspase-3 cleavage in treated P388 cells after shorter exposure times (Section 6.3.7).

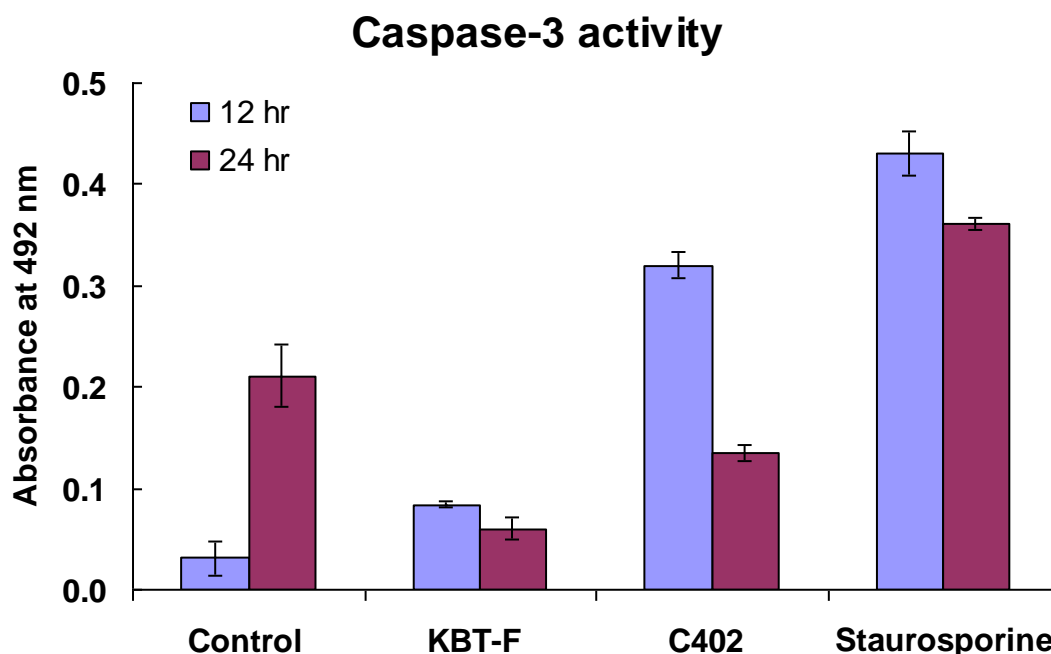


**Figure 6-5.** Effects of KBT-F 5 nM, C402 5 nM and staurosporine 1  $\mu$ M on caspase-3 activity in treated P388 cells after 12 and 24 hr exposure. Control is 0.5% ethanol in MEM. The values are mean  $\pm$ SD of triplicates.

### 6.3.7 Fluorescent caspase-3/7 activity assay

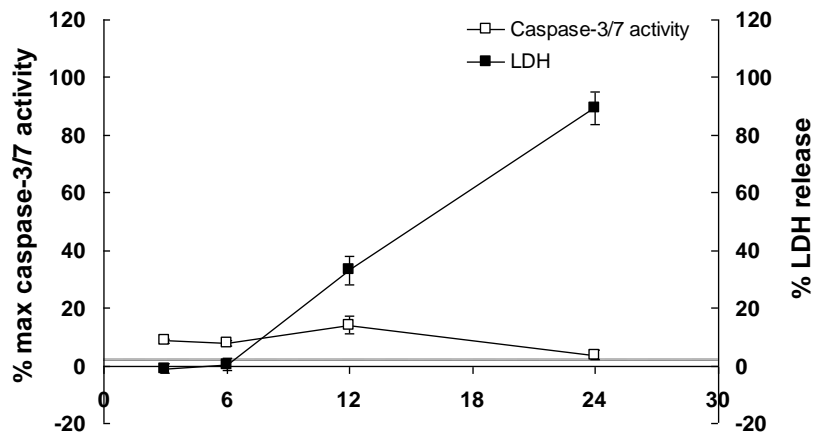
The fluorescent caspase-3/7 activity assay can provide a simpler, faster, more sensitive, higher throughput and a more reliable method to measure caspase-3/7 activity in purified caspase enzymes, treated cells, or fresh tissues. It can detect caspase-3/7 activity from as few as several hundred cells and can be performed in 96-well plates. However, the expensive commercial reagents limited large scale use in cell assays. An experiment was designed to investigate both LDH release and caspase-3/7 activity over time, using treated cells from a single 96 well plate. Negative controls (n=3), P388 cells treated with either 0.5% ethanol or 0.1% DMSO for 24 hr produced similarly low fluorescent signal in both LDH and caspase-3/7 assays, indicating neither “vehicle” affected cell growth. According to this data and previous observations, it was assumed that the cells in negative controls were healthy during 24 hr exposure and the highest caspase-3/7 activity would be produced at 24 hrs.

Figure 6-6 shows the time-response curves of KBT-F (5 nM), C402 (5 nM), and staurosporine (1  $\mu$ M) for the fluorescence caspase-3/7 activity and LDH assays. The caspase-

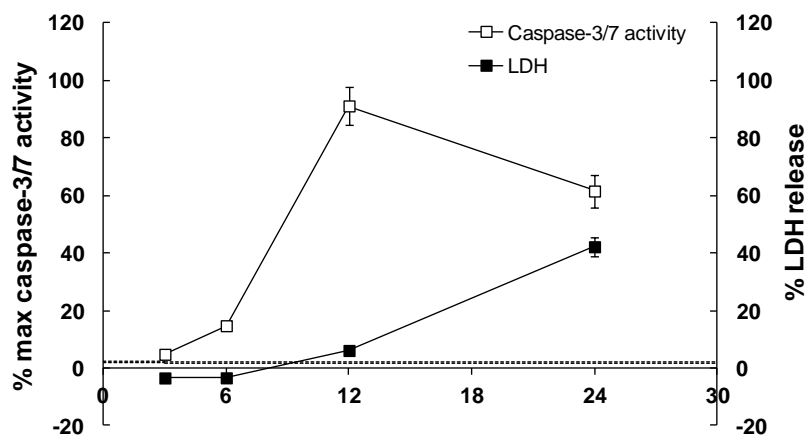
3/7 activity was low in KBT-F treated cells over the 24 hr exposure (Figure 6-6A). However, a time-dependent increase in LDH release was observed after 6 hr exposure and 83% of cells lost their membrane integrity after 24 hr exposure (Figure 6-6A). This supports that the mode of action of KBT-F in P388 cell death is unlikely to involve a caspase-3 dependent apoptosis pathway.

The patterns for caspase-3/7 activity of C402 and staurosporine are similar (Figures 6-6B, C). The time-response curves of LDH release matched that observed in LDH/MTS assays (Section 6.3.5), revealing that the data from both assays are reliable and repeatable. There was no significant increase in LDH release over the initial 12 hr exposure to C402 or staurosporine. However, both toxins produced a time-dependent increase in caspase-3/7 activity during 0-12 hr exposure. Caspase-3/7 activity was observed to peak after 12 hr exposure to staurosporine and this was used as the reference maximal activity (Figure 6-6C). The peak caspase-3/7 activity induced by C402 was approximately 90% of the reference maximal activity and was 45-fold higher than control (Figure 6-6B). Together, data obtained from three independent experiments (Sections 6.3.5 to 6.3.7) strongly suggested that C402 can induce cell apoptosis through a caspase-3 dependent pathway. There was a gradual reduction of caspase-3/7 activity as measured by the both colorimetric and fluorescent assays during 12–24 hr exposure to C402 and staurosporine (Figure 6-5; 6-6B, C). This was consistent with increasing degradation of cleaved caspase-3/7 and a significant increase of LDH released from apoptotic cells undergoing secondary necrosis *in vitro*.

**(A) KBT-F 5 nM**



**(B) C402 5 nM**



**(C) Staurosporine 1  $\mu$ M**

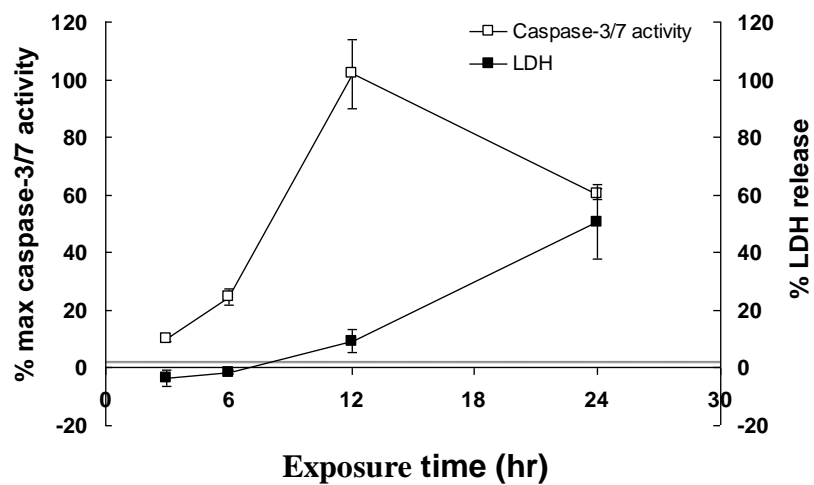


**Figure 6-6.** Time-response curves of KBT-F 5 nM, C402 5 nM and staurosporine 1  $\mu$ M for the fluorescent caspase-3/7 activity and cell membrane integrity (LDH) assays. The dash line (----) represents the caspase-3 activity of control. The values are mean  $\pm$  SD of triplicates.



### 6.3.8 Haemolytic and Neuro2a cell assays

KBT-F and KBT-G were highly haemolytic with  $EC_{50}$  values of  $5.5 \text{ ng mL}^{-1}$  (3.7 nM) and  $1.7 \text{ ng mL}^{-1}$  (2.6 nM), respectively (Table 6-6), although palytoxin was 200x more haemolytic under these assay conditions. These toxins were also active in the potentiated Neuro2a assay (Table 6-6, Figure 6-7A) but were active in this assay without added ouabain/veratridine. A steep reduction in cell viability was observed at toxin concentrations 1.5x and 3x higher respectively than the  $EC_{50}$  value in the potentiated assay. This indicates general (non sodium-channel-dependent) cytotoxicity for these toxins, although some interaction at the VGSC could be not ruled out.

The BSXs were only weakly haemolytic but were active in the Neuro2a assay potentiated for VGSC activity (Figure 6-7B, C). Activities of BSX-4 and BSX-5 were ca. 10% that of brevetoxin-3 (Table 6-6). These toxins did not exhibit cytotoxicity in the absence of ouabain/veratridine and the potentiated activity was antagonised by saxitoxin (Figure 6-7D) which, at approximately twice the  $EC_{50}$ , reversed the effect of ouabain and veratridine. The cell viability actually increased to >100% because saxitoxin also counteracted some toxic effects of veratridine which is also a VGSC opener (Catterall & Risk, 1981). Thus, these toxins act as VGSC agonists, similar to brevetoxins. BSX-1 and BSX-2 were less active as might be expected based on the relative activities of parent and ring-opened brevetoxins in the Neuro2a assay (Roth *et al.*, 2007).

The original research on cytotoxicity of *K. brevisulcata* (Truman, 2007; Truman *et al.*, 2005) used crude extracts of cultures which contained mixtures of the full suite of KBTs and BSXs. In general, the characteristics of the crude, mixed toxins followed the pattern of Neuro2a toxicity observed for the pure KBT toxins. The relatively small amounts of brevetoxin-type activity from BSXs would have been difficult to discern. However, the effects of pure BSX and KBT toxins in combination have not yet been examined in this cellular model. The combined activities of KBT-F plus KBT-G can explain only ca. 10-20% of the cytotoxicity and the toxicity to mice of a crude culture extract. Thus the other unidentified KBTs (Figures 4-1B; 4-3) and potentially synergistic activities of the BSXs may contribute substantially to the overall toxicity of *K. brevisulcata*.

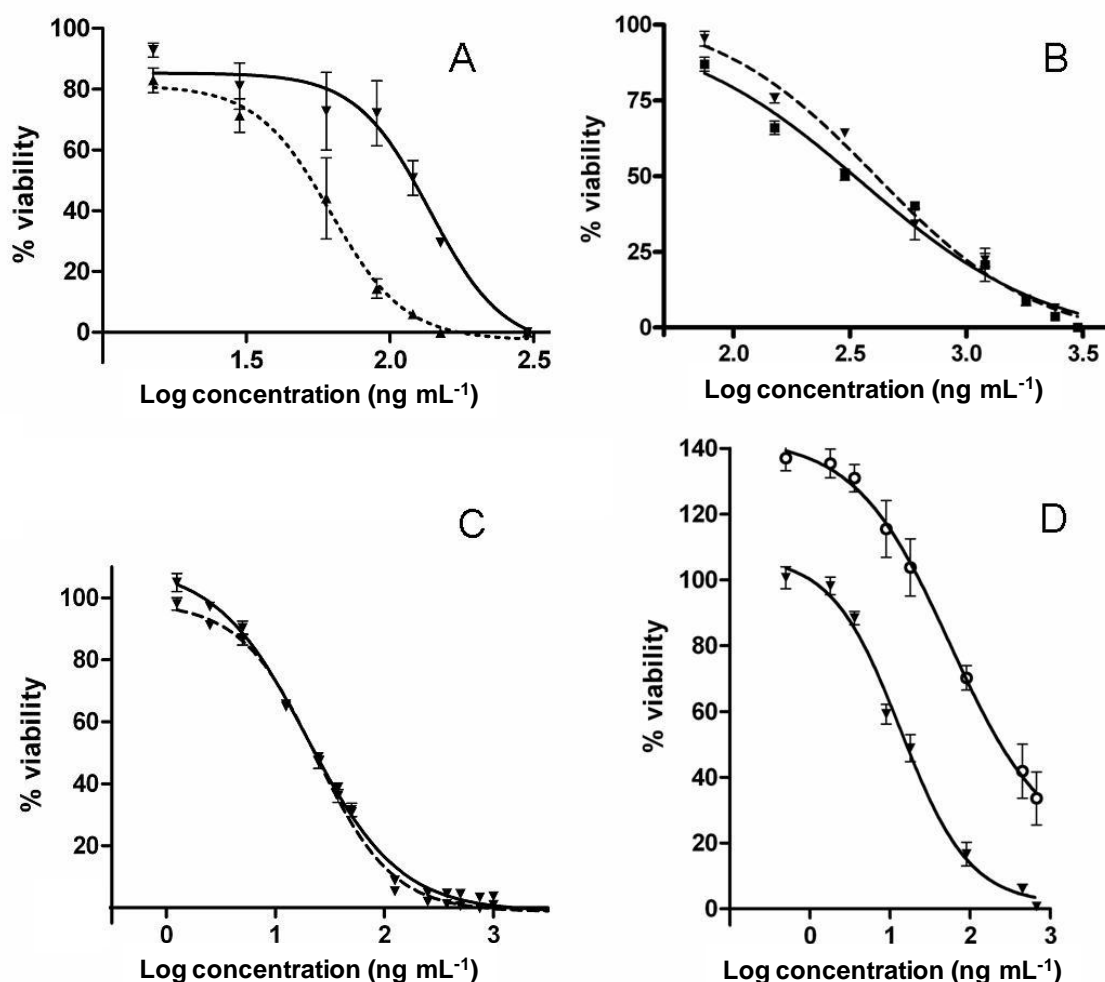


**Figure 6-7.** Dose-response curves of toxins from *K. brevisulcata* in the Neuro2a cell assay potentiated for VGSC activity with ouabain/veratridine: (A) KBT-F (—) and KBT-G (----); (B) BSX-1 (—) and BSX-2 (----); (C) BSX-4 (—) and BSX-5 (----); (D) BSX-5 with (o) and without (▼) the VGSC antagonist saxitoxin (3.2 nM). Assays were conducted by Penny Truman (ESR).

**Table 6-6.** Cytotoxicities of BSX and KBT toxins based on Bignami and Neuro2a cell assays.

Toxins	Haemolysis <sup>a</sup> EC <sub>50</sub> nM	Neuro2a <sup>d</sup> EC <sub>50</sub> nM <sup>e</sup>	Mode of action
KBT-F	3.7	73 (32-175)	Strongly haemolytic, cytotoxic
KBT-G	2.6	30 (24-37)	Strongly haemolytic, cytotoxic
BSX-1	nd <sup>b</sup>	390 (230-640)	Weak brevetoxin-like VGSC agonist
BSX-2	nd <sup>b</sup>	370 (355-620)	Weak brevetoxin-like VGSC agonist
BSX-4	6660	24.5 (22-27)	Brevetoxin-like VGSC agonist
BSX-5	nd <sup>b</sup>	26.9 (22-27)	Brevetoxin-like VGSC agonist
Brevetoxin-3	Negative <sup>c</sup>	2.8 (2.3-3.4)	Strong VGSC agonist

<sup>a</sup> mouse erythrocytes

<sup>b</sup> no determined, >10 μM

<sup>c</sup> negative against human erythrocytes and red drum erythrocytes (Neely & Campbell, 2006; Tatters *et al.*, 2009)

<sup>d</sup> Neuro2a neuroblastoma cells potentiated with ouabain/veratridine

<sup>e</sup> 95% confidence limits (in brackets)

## 6.4 Summary

*K. brevisulcata* produced two novel classes of toxins. The BSXs are VGSC agonists and have some structural similarities to brevetoxin-1. The potencies of BSX toxins are lower than brevetoxins in mammalian toxicity and Neuro2a cytotoxicity. KBT-F and KBT-G are high molecular weight polyether toxins with strongly haemolytic activity, cytotoxicity to mammalian cells, and high i.p. toxicity to mice. The mode-of-action of KBT-F still remains unclear but is unlikely to induce cell apoptosis through caspase-3 cleavage. C402, a novel cyclic imine compound recently isolated from a peridinoid dinoflagellate, is weakly toxic by i.p. injection to mice but is highly cytotoxic to both P388 and Vero cells. A significant increase in caspase-3 activity observed after 12 hr exposure indicated that C402 is a potential apoptosis inducer with a stronger activity than staurosporine. To better understand the mode-of-action of C402, further studies such as Annexin-V staining assay, TUNEL or DNA ladder electrophoresis, and mitochondrial assays are required.

## Chapter 7

# Toxic effects of *Karenia* species on fish, invertebrate larvae and mammalian cells

### 7.1 Introduction

*Karenia* blooms have been observed in New Zealand over the past 20 years that damaged or threatened marine ecosystems and aquaculture (molluscan shellfish and cage fisheries). The toxic species reported have included *K. cf. brevis*, *K. mikimotoi*, *K. selliformis*, *K. concordia* and *K. brevisulcata*. These toxic species appear similar under the microscope but they differ in the suites of toxins produced and their effects on marine species. In 1992/93, *K. cf. brevis* was identified as the dominant species in the 1992/1993 harmful algal bloom and caused more than 180 cases of human illness with symptoms mostly of NSP (Chang, 1995; Chang *et al.*, 1995; Jasperse, 1993; MacKenzie, 2008; MacKenzie *et al.*, 1995). High levels of several metabolites of brevetoxins were identified in shellfish samples collected at that time (Ishida *et al.*, 1995; Morohashi *et al.*, 1995; Morohashi *et al.*, 1999; Murata *et al.*, 1998). This species was considered the cause of the shellfish contamination and mass mortalities of marine fauna via production of ichthyotoxic brevetoxins but unfortunately the algae was not isolated at that time. However, a range of other *Karenia* species isolated from New Zealand waters have tested negative for brevetoxins by LC-MS/MS (McNabb *et al.*, 2006).

*K. mikimotoi* is one of the most common fish-killing toxic dinoflagellates in both the Atlantic and Pacific regions (Gentien *et al.*, 2007; Honjo, 1995; Silke *et al.*, 2005; Zou *et al.*, 2010). The cell concentration in a typical *K. mikimotoi* bloom can easily reach millions of cells per litre ( $1\text{--}20 \times 10^6$  cells L<sup>-1</sup>) (Davidson *et al.*, 2009; ICES, 2006; Silke *et al.*, 2005; Ulrich *et al.*, 2010). This species was responsible for several severe HAB events in New Zealand waters in the past two decades and some of these blooms have been characterised (Chang *et al.*, 2003). Mass mortalities of fin-fish and eels were reported during a bloom dominated by *K. mikimotoi* (highest cell density  $> 2.1 \times 10^6$  cells L<sup>-1</sup>), which occurred at Te Puna Inlet, Northland, New Zealand in 2007 (Smith *et al.*, 2007). No brevetoxins were detected in oysters collected from marine farms in the area using LC-MS/MS analysis for brevetoxin-2 and brevetoxin-3, and the fish kills were associated with mechanical gill damage or environmental stressors e.g. anoxia. *K. mikimotoi* produces several classes of compounds, including gymnocins, haemolytic glycolipids, and polyunsaturated fatty acids, which have cytotoxic, haemolytic, and ichthyotoxic properties (Gentien *et al.*, 2007; Marshall *et al.*, 2005;

Satake *et al.*, 2002; Satake *et al.*, 2005; Yasumoto *et al.*, 1990). However, there is currently no clear understanding of the roles of any of these compounds in marine mortalities caused by *K. mikimotoi*.

*K. brevisulcata* (Chang) was isolated in 1998 from the severe HAB that devastated almost all of the marine biota in Wellington Harbour, New Zealand, (Chang, 1999a, b; Chang *et al.*, 2001). This species was very damaging to a wide range of marine organisms including fish, invertebrates, and macroalgae (Chang, 1999b). Ecosystem studies in Wellington Harbour confirmed the widespread and long-term damage caused to the benthos, particularly to marine invertebrate populations (Gardner & Wear, 2006; Kröger, 2008). In addition, over 500 cases of human respiratory illnesses were reported during the bloom event, suggesting that *K. brevisulcata* may also pose a potential risk to human health. Our chemical research has revealed that *K. brevisulcata* can produce two suites of complex polyether compounds, including 6-8 KBTs with molecular weights of 1900-2200 Da and 6 BSXs with molecular weights 800-950 Da (Holland *et al.*, 2012). Preliminary toxicological studies have been completed using several bioassays. However, the toxic potencies of these compounds and the overall toxicity of *K. brevisulcata* algae to marine organisms have not been established. In this study, three *Karenia* species were investigated for the toxic potencies of cell cultures against aquatic organisms. Bioassays combined with LC-MS determination of toxin production will contribute to evaluating the toxic potency and mode-of-action of biotoxins produced by the three *Karenia* species. This research will provide shellfish aquaculture and fish farmers with some guidance should harmful *Karenia* species bloom in marine farming areas. The research reported in this chapter on effects of *Karenia* species on fish, invertebrate larvae species on fish, invertebrate larvae has been accepted for publication (Shi *et al.*, 2012).

## 7.2 Materials and methods

### 7.2.1 Microalgae cultures and growth conditions

The *Karenia* cultures used in this study are maintained in the Cawthron Institute Culture Collection of Micro-algae (CICCM) and their characteristics are summarised in Table 4-1: *K. brevis* (CAWD122), *K. brevisulcata* (CAWD82), and *K. mikimotoi* (CAWD05). *K. brevis* was grown in modified L1 medium (Guillard & Hargraves, 1993) at  $25 \pm 1$  °C. *K. brevisulcata* and *K. mikimotoi* were grown at  $19 \pm 1$  °C in 100% GP+Se medium (Beuzenberg *et al.*, 2012; Loeblich & Smith, 1968) and 50% GP medium respectively (Loeblich, 1975). Mass cultures were grown in glass flasks (2 L) or plastic barrels (15 L) with  $90 \mu\text{Ein.m}^{-2}\text{s}^{-1}$  (12:12 hr L:D)

and sparged with filtered air (0.22  $\mu\text{m}$ ). Previous studies showed maximum production of BSX toxins in *K. brevisulcata* cultures occurred at ca. 20 days before cell numbers collapsed. All three species were grown for 18-22 days. Respiratory masks were worn to prevent exposure to aerosolised cultures. The number of cells per litre of each mass culture (cell density) was calculated from microalgal counts of 25  $\mu\text{L}$  samples in Utermöhl chambers with 1 mL seawater/ Lugols solution and using an inverted microscope (Olympus TMT-2) at 100x magnification and counting of three random fields.

### **7.2.2 Algal toxin extraction for LC-MS analysis and invertebrate bioassay**

Mass culture samples and cell-free medium (control) of *K. brevis* (CAWD122), *K. brevisulcata* (CAWD82), and *K. mikimotoi* (CAWD63) were extracted using polymeric solid phase extraction (SPE) cartridges (Strata-X 60mg/3mL, Phenomenex, USA) pre-conditioned with Methanol (3 mL) and MQ water (3 mL). The SPE cartridges were loaded with culture or medium (50 mL), washed with MQ (3 mL) and 20% methanol (3 mL) and eluted with methanol (3 mL). An aliquot of the methanol eluant (0.8 mL) was diluted to 1 mL with MQ for LC-MS determination of brevetoxins and BSX toxins. Aliquots of the methanol eluant (0.6 mL) were dried under a gentle flow of nitrogen (40  $^{\circ}\text{C}$ ) and dissolved in sterile seawater (10 mL) to provide SPE extracts for the invertebrate larvae bioassays (equivalent concentration to raw cultures on a cell basis). Purified BSX-1, -2, -4 and -5 toxins from *K. brevisulcata* (Section 5.3.2) were individually dissolved in sterile seawater to concentrations of 100  $\mu\text{g L}^{-1}$ .

### **7.2.3 Preparation of algal extracts and cell-free culture supernatants for cell bioassays**

The algal extracts of *K. brevisulcata*, *K. brevis* and *K. mikimotoi* were prepared following the methods described in Section 4.2.2. The dry methanol eluants or cell pellets were reconstituted in ethanol for P388 and Vero cell bioassays (Section 7.2.7).

The cell-free culture supernatants of *K. brevisulcata* and *K. mikimotoi* were prepared using the same procedure. Cultures (50 mL) at late log phase of each *Karenia* species were centrifuged at 1000g for 10 min. The cell-free culture supernatants were gently removed and diluted with seawater media to use immediately in direct exposure bioassays (Section 7.2.8).

## 7.2.4 Chemical analyses

SPE extracts of cultures were tested for brevetoxins (-1, -2, -3, -B5 and their hydrolysed lactone ring-opened derivatives) and BSXs (-1, -2, -4 and -5) using a Waters Acquity UPLC system coupled with a Waters-Micromass Quattro Premier XE MS with ESI. Toxin separation was achieved based on the same column and gradient as described in Section 4.2.3.1. The electrospray ionisation source was operated in positive-ion mode (ESI<sup>+</sup>) with the same parameters for SIR quantitation (Section 4.2.3.1). SIR operating mode used channels for [M+H]<sup>+</sup> ions at 867.5, 885.4, 895.7, 897.7, 911.1, 913.5, 915.7 and 929.4 for brevetoxins monitoring and *m/z* 855.5, 873.5, 899.5 and 917.5 for BSXs monitoring. Concentrations were estimated from the area responses calibrated using brevetoxin-2 for BSXs and using brevetoxin-1, -2, -3 and -B5 for brevetoxins (standards supplied by NRCC Halifax, Canada). The LC-MS LOQs were similar for brevetoxins and BSXs at ca. 5 ng mL<sup>-1</sup> solution for each toxin as injected into the LC-MS. These LOQs correspond to 0.4 µg L<sup>-1</sup> algal culture (Section 4.3.2.1).

## 7.2.5 Fish acute toxicity tests

Juvenile Chinook salmon (*Oncorhynchus tshawytscha*; 50 g) were obtained from King Salmon Ltd., Marlborough Sounds and juvenile New Zealand snapper (*Pagrus auratus*; 60 g) from Plant and Food Ltd, Nelson. Both species were held in aquaria at the Cawthron Institute for 12 days to habituate them to laboratory conditions. Feeding was ceased 1 day before exposure to *Karenia* cultures. Fish were transferred gently to cylindrical glass aquaria (4 fish per aquarium per treatment) containing 10 L of seawater plus *Karenia* mass culture. The control treatment was seawater (salinity 32 ppt; ammonia stable at approximately 0.25 mg/L). The aquaria were maintained in dim light at 18 °C. For the salmon experiment, a single addition of culture was made to provide each of the cell densities (3 for *K. brevis* and 2 for *K. brevisulcata*; Table 7-1). For the snapper experiment, three stepwise additions of culture were made over several hours to provide sufficient cells to produce a response in this less sensitive species. The cell densities of initial cell additions were ca. 10% of the final cell densities (Table 7-1). Stress responses in both species were observed and included colour change, dorsal fin position (relaxed or upright), balance, gasping, gill condition, and panic. The health index was: healthy (6), slight loss of balance (5), agitation (4), gasping (3), leaping (2), extreme loss of balance (1), dead or moribund (fish floating, no response to touching) (0). The times at which the above changes occurred were recorded for establishment of time-response

curves.  $LT_{50}$  is defined as the time for 50% of the fish to become moribund as determined from semi-log plots of the data. When fish were showing acute stress, they were euthanised by transferring into a plastic bag and covering with crushed ice. Autopsies were immediately conducted. Animal Welfare Ethics approval was gained for all *in vivo* fish experiments from the Ministry of Agriculture and Forestry through the Bioethics Committee of the Nelson Marlborough Institute of Technology, under the New Zealand Animal Welfare Act (1993).

## 7.2.6 Invertebrate larvae bioassays

Brine shrimp (*Artemia salina*) cysts were obtained from a local pet shop and hatched at room temperature in filtered seawater. The larvae were used at 24-48 h post hatching. Four to six day old larvae of Greenshell<sup>TM</sup> mussel (*Perna canaliculus*), Pacific oyster (*Crassostrea gigas*), sea urchin (*Evechinus chloroticus*), and paua (New Zealand abalone, *Haliotis iris*) were raised at the Glenhaven hatchery, Nelson, were used. Sea slug larvae (*Pleurobranchia maculata*) were raised at the Cawthron Institute from adults collected from the Hauraki Gulf, New Zealand [species responsible for dog killing events in Auckland in 2009 (McNabb *et al.*, 2010)]. Larvae (6-10 of each test species) were transferred with minimal carryover of seawater, into wells of 24-well tissue culture plates (3.5 mL/well, Becton Dickinson, USA). *Karenia* cultures (18-22 days post sub-culturing), sea water fractions from SPE extracts or individual BSX toxins in seawater were added at 1000, 100, 10 or 0 (control)  $\mu$ l per well following larval addition (Table 7-2, triplicate wells per treatment). Larvae were observed using an inverted microscope (Olympus TMT-2) at 6 time intervals over 24 hr and health scores were assigned: 0 Death: larvae disintegrated, tissue appears amorphous and decayed; 1 Moribund: cilia gone, larvae disintegrating, still some jerking movement; 2 Severe stress: larvae located at bottom and retracted into cell but cilia movement still occurring inside shell; 3 Stressed: larvae at the bottom, cilia healthy, but not moving; 4 Static: larvae with cilia movement, but not swimming; 5 Healthy: swimming larvae with healthy veligers. A mean health score at each exposure time was calculated for each well and then each treatment ( $n=3$ ; mean  $\pm$  SEM). The time course of toxic effects was studied using plots of the mean health scores versus time.  $MLT_{50}$  (median time for 50% of larvae being moribund) were calculated from quadratic curves fitted to the data points for individual larvae at specified cell concentrations.  $MLC_{50}$  (median cell concentration for 50% of larvae being moribund) was calculated for each species at specified observation times. A mean health score of 2.5 was defined as 50% moribund.



### 7.2.7 P388 and Vero cell bioassays

P388 and Vero cells were cultured as described in Section 6.2.3. The cytotoxicities of algal extracts were assessed using MTS assay (Section 6.2.4).

### 7.2.8 Cytotoxicity assay for direct exposure to dinoflagellates

To determine a suitable cell line, P388 and Vero cells were directly exposed to sterile seawater and two seawater media (100% GP+Se & 50% GP). Vero cells were found to be highly resistant to seawater (Section 7.3.6) and were used in the exposure experiments according to the procedure described by Katsuo *et al.* (2007). Detached cells were seeded into 96 well plates at  $1 \times 10^4$  cells/well. After 24 hr incubation to allow Vero cells to attach, the cell growth DMEM was decanted and cells were washed twice with PBS. Negative and positive controls in at least four replicates were exposed to seawater media. Vero cells were directly exposed to serially dilute algal cultures or the cell-free culture supernatants for 2 hr with photon flux of  $90 \mu\text{Ein.m}^{-2}\text{s}^{-1}$  at  $18 \pm 1^\circ\text{C}$ . Seawater media in each well was removed by gentle aspiration. Fresh DMEM was added to the wells of samples and negative control, and palytoxin ( $5 \text{ ng mL}^{-1}$ ) in fresh DMEM was added to positive control wells. The plates were incubated in a humidified  $37^\circ\text{C}$  incubator, supplemented with 5%  $\text{CO}_2$  for 24 hr. Cell viability was assessed using the MTS assay (Section 6.2.4).

## 7.3 Results

### 7.3.1 Algal cultures and toxin production

*Karenia brevis*: The mass culture used for fish and larvae assays was grown in a plastic carboy for 20 days and contained  $8.7 - 9.3 \times 10^6$  cells  $\text{L}^{-1}$ . The strain of *K. brevis* used in this study was from Florida and produced four main brevetoxins which were each present in the SPE extracts as the parent toxin and the lactone ring-opened hydrolysis product (Abraham *et al.*, 2006). The total concentration of these brevetoxins in the culture at 20 d was  $490 \mu\text{g L}^{-1}$  ( $52 \text{ pg cell}^{-1}$ ). Brevetoxin-2 was the predominant toxin ( $370 \mu\text{g L}^{-1}$ ). The ratios of parent to ring-opened brevetoxin were 15 for brevetoxin-1, 20 for brevetoxin-2, 0.3 for brevetoxin-3 and 0.6 for brevetoxin-B5 (Figure 7-1A), similar to those reported by Roth *et al.* (2007)

*Karenia brevisulcata*: An LC-MS (SIR) method was validated to detect and quantify four BSXs in SPE extracts of cultures (Method 1, Section 4.2.3.1). The mass culture used for fish assays was grown in a carboy for 19 days and contained  $26 \times 10^6$  cells L<sup>-1</sup> with a total concentration of BSXs of  $12 \mu\text{g L}^{-1}$  ( $0.5 \text{ pg cell}^{-1}$ ). The flask cultures of *K. brevisulcata* used for invertebrate larvae bioassays contained  $84 \times 10^6$  cells L<sup>-1</sup> with a total concentration of BSXs of  $22 \mu\text{g L}^{-1}$  ( $0.26 \text{ pg cell}^{-1}$ ). No brevetoxins were detected in SPE extracts of *K. brevisulcata* cultures. The spectroscopic and microchemical data showed that the BSXs have similarities to brevetoxin-1 in ring structure and included a carboxylic acid on the terminal side chain (Section 5.3.3). BSX-4 and BSX-5 are ring-closed lactone derivatives of BSX-1 and BSX-2 respectively and have appreciable activity as sodium channel agonists (Section 6.3.8). The ratios of BSX-4 to BSX-1, and BSX-5 to BSX-2, were 0.05 and 0.1 respectively. Thus the BSX toxins from *K. brevisulcata* were mainly present in the lactone-A ring opened, less active hydrolysed forms (Figure 7-1B) in contrast to *K. brevis* where the ring-closed parent brevetoxins predominated. The KBTs were difficult to monitor by LC-MS when this experiment was conducted due to their complexity of structure, lack of standards, and limitations in the method. However, preliminary data from large-scale isolations and LC-MS indicated that two of the key toxins, KBT-F and KBT-G, were present in *K. brevisulcata* cultures at similar concentrations to BSX-1 and BSX-2 respectively.

*Karenia mikimotoi*: The cultures used for fish and larvae assays were grown in carboys ( $5.4 \times 10^6$  cells L<sup>-1</sup>) and glass flasks ( $56\text{-}118 \times 10^6$  cells L<sup>-1</sup>) respectively for 28-30 days. No brevetoxins or BSXs were detected by LC-MS of SPE extracts. Several novel compounds were detected in the extract by LC-MS. However, these compounds were not further investigated nor quantitatively analysed in this study (Section 4.3.4).

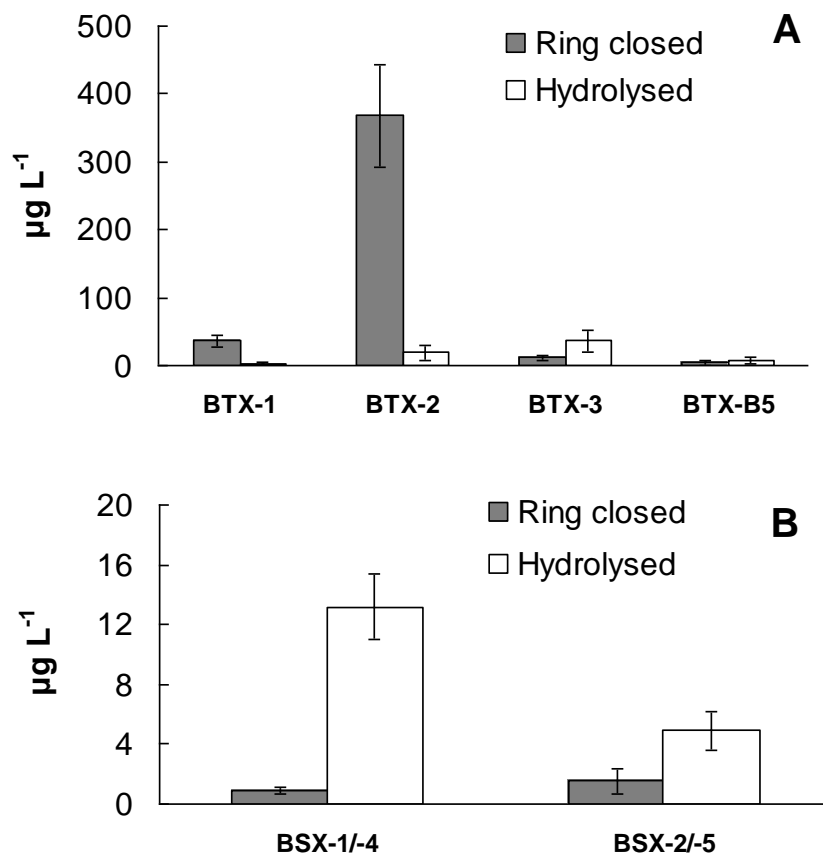


**Figure 7-1.** Biotoxins produced by (A) *K. brevis* and (B) *K. brevisulcata*. Batch carboy cultures grown for 19-20 days and extracted by SPE for LC-MS determination. BSX concentrations in brevetoxin-2 response equivalents. The points/bars depict the Mean  $\pm$  SEM (n=3). Note different concentration scales on Y-axis.

### 7.3.2 Ichthyotoxicity of *Karenia* microalgae

All fish survived after 48 hr when sterile seawater (control) or *K. mikimotoi* ( $3.4 \times 10^6$  cells L<sup>-1</sup>) were added. The concentration of *K. mikimotoi* in this study matches the range of maximum cell population ( $0.5\text{--}4 \times 10^6$  cells L<sup>-1</sup>) reported for most *K. mikimotoi* blooms. Strains of *K. mikimotoi* vary in toxicity and mode of action (Zou *et al.*, 2010) and there may be a range of sub-species. The strain tested for ichthyotoxicity was isolated from Northland in 1993, and was believed to have contributed to the severe 1992/93 *Karenia* bloom. It is a producer of several novel polyethers compounds with similar molecular weights to gymnocins (Section 4.3.4). Gymnocin-A and gymnocin-B are weakly cytotoxic and ichthyotoxic (Satake *et al.*, 2002; Satake *et al.*, 2005). However, no known gymnocins were detected. ROS and other potential toxins were not tested in this study. However, the autopsy found no observable tissue damage in treated snapper. These observations support the hypothesis that fish kills by *K. mikimotoi* may be mainly due to environmental stressors (Landsberg, 2002; Silke *et al.*, 2005; Yamasaki *et al.*, 2004).

Both *K. brevis* and *K. brevisulcata* were toxic to juvenile salmon and snapper (Figure 7-2, Table 7-1). Panic, gasping, and loss of balance were observed in all fish exposed to either *K. brevis* or *K. brevisulcata* with effects being apparent soon after exposure. Figure 7-2 shows the time-response curves of juvenile salmon to two *Karenia* species. Exposure of salmon to *K. brevis* at  $4.6 \times 10^6$  cells L<sup>-1</sup> immediately led to a slight loss of balance. After 4 min, two fish completely lost balance, and at 10 min, three fish were euthanised. All fish had died or were euthanised by 18 min. Exposure of salmon to *K. brevis* at  $0.9 \times 10^6$  cells L<sup>-1</sup> led to stress symptoms at 2-18 min, including loss of balance, tilting, gasping, leaping, and panicking. Four salmon were euthanised at 20, 25, 30 and 35 min, respectively. Exposure of salmon to *K. brevisulcata* at  $11 \times 10^6$  cells L<sup>-1</sup>, led to a loss of balance at 5 min in one fish which died at 29 min. The other fish began to gasp at 30 min and were euthanised at 40 min. At  $1.3 \times 10^6$  cells L<sup>-1</sup>, salmon started gasping at 44 min and two fish lost balance. All fish had died or were euthanised by 112 min. The autopsy did not reveal any signs of damage or stress to the gill, kidney, or liver of the experimental salmon. The LT<sub>50</sub> for salmon in the presence of *K. brevisulcata* was 0.48 hr with  $11 \times 10^6$  cells L<sup>-1</sup> and 0.93 hr at  $1.3 \times 10^6$  cells L<sup>-1</sup> (Table 7-1). In comparison, the LT<sub>50</sub> for *K. brevis* at 4.6, 0.9 and  $0.18 \times 10^6$  cells L<sup>-1</sup> were 0.17, 0.42 and 0.75 hr respectively (Table 7-1).

The time course of toxic effects in snapper from *K. brevis* and *K. brevisulcata* were slower than for salmon and only became evident at higher cell densities. The LT<sub>50</sub> for snapper were calculated as 4.5 h for *K. brevis* ( $6 \times 10^6$  cells L<sup>-1</sup>) and 7.5 hr for *K. brevisulcata* ( $16 \times 10^6$  cells L<sup>-1</sup>; Table 7-1). Salmon is more sensitive to both *Karenia* dinoflagellates than snapper. Autopsy revealed that only the snapper exposed to *K. brevisulcata* exhibited any signs of damage, that being minor sloughing of the gill tissue cells.

The findings confirm that *K. brevis* is more toxic than *K. brevisulcata* to juvenile fish. Brevetoxins produced by *K. brevis* are ichthyotoxic and are absorbed directly across the gill membranes of fish (Baden, 1989). It was confirmed that the strain used in this study produced two types of brevetoxins: Type A, brevetoxin-1; and Type B, brevetoxins -2, -3 and -B5 (Ishida *et al.*, 2004a; Ishida *et al.*, 2004b; Ishida *et al.*, 2004c; Ramsdell, 2008). Type A are more potent than Type B brevetoxins (Abraham *et al.*, 2006; Baden, 1989; Landsberg, 2002). Brevetoxin-2 is the predominant toxin (14-95 nM) produced by the Florida strain and may have been responsible for mortalities of juvenile salmon and snapper. The concentrations of brevetoxin-1 and -3 in our fish bioassays with *K. brevis* were 0.1-2 nM and 0.1-4 nM respectively. These LC<sub>50</sub>'s are much lower than reported for mosquitofish (*Gambusia affinis*)

with exposure to brevetoxin-1 (3-4 nM) and brevetoxin-3 (10-37 nM) for 24 hr (Baden, 1989; Landsberg, 2002).

**Table 7-1.** Ichthyotoxicity of *Karenia* species against juvenile Chinook salmon (*Oncorhynchus tshawytscha*) and juvenile New Zealand snapper (*Pagrus auratus*) (For all experiments, n=4 fish).

Fish tested	<i>Karenia</i> species	Cell density (10 <sup>6</sup> cells L <sup>-1</sup> )	LT <sub>50</sub> <sup>a</sup> (hr)
Salmon	<i>K. brevis</i>	4.6	0.17
	<i>K. brevis</i>	0.9	0.42
	<i>K. brevis</i>	0.18	0.75
	<i>K. brevisulcata</i>	11	0.48
	<i>K. brevisulcata</i>	1.3	0.93
Snapper	<i>K. brevis</i>	5.9 <sup>b</sup>	4.5
	<i>K. brevisulcata</i>	16.1 <sup>b</sup>	7.5
	<i>K. mikimotoi</i>	3.4 <sup>b</sup>	N <sup>c</sup>

<sup>a</sup> Time to 50% fish being moribund.

<sup>b</sup> Final cell density after step-wise addition of 8 litres of microalgal mass culture over 2.5 h.

<sup>c</sup> No morbidity after 24 hr observation.

Mass mortalities of marine life were reported in the *K. brevisulcata* bloom in Wellington Harbour, 1998 before algal cell populations reached 33 x 10<sup>6</sup> cells L<sup>-1</sup> (Chang, 1999b; Chang *et al.*, 2001). The fish bioassays indicated that both species of juvenile fish can be killed in a short exposure time (< 12 hr) by *K. brevisulcata* at 11-16 x 10<sup>6</sup> cells L<sup>-1</sup>. Four BSX toxins were monitored and the predominant toxins were A-ring opened hydrolysis products BSX-1 and BSX-2 (Figure 7-1B). BSXs are similar to brevetoxins in chemistry, toxicology, and biology, but are less potent. Roth *et al.* (2007) suggested that brevetoxins are present within *K. brevis* cells in the form of A ring closed toxins, but can also be released to seawater as hydrolysed (A ring opened) forms. It is probable that BSX-4 and BSX-5 are the parent toxins produced by *K. brevisulcata* and the hypothesis is that this species is more leaky or fragile than *K. brevis*, and therefore can lead to higher toxin levels in the medium where hydrolysis of the lactone ring takes place. The ichthyotoxicity of pure KBT and BSX were not tested. KBTs are much more potent in MBA and cell bioassays (Chapter 6), and may be highly toxic to marine life. KBTs are also haemolytic but salmon death without gill injury indicates that fish gill damage is not likely to be a major mechanism leading to fish morbidity. KBTs are

difficult to monitor by LC-MS without standards, and they may also be easily released from cells to seawater at similar concentrations to BSXs (preliminary LC-MS data). However, they lack readily hydrolysed lactone rings. KBTs are proposed as the main contributors to toxicity in these bioassays and to fish kills in the Wellington Harbour bloom event in 1998. During this outbreak, ozone was used to eliminate *K. brevisulcata* toxicity and protect the NIWA hatchery facilities (Chang, 1999b). The environmental stability and metabolism by target species of these potent biotoxins is of interest in future investigations of long term ecological effects of *K. brevisulcata* blooms.

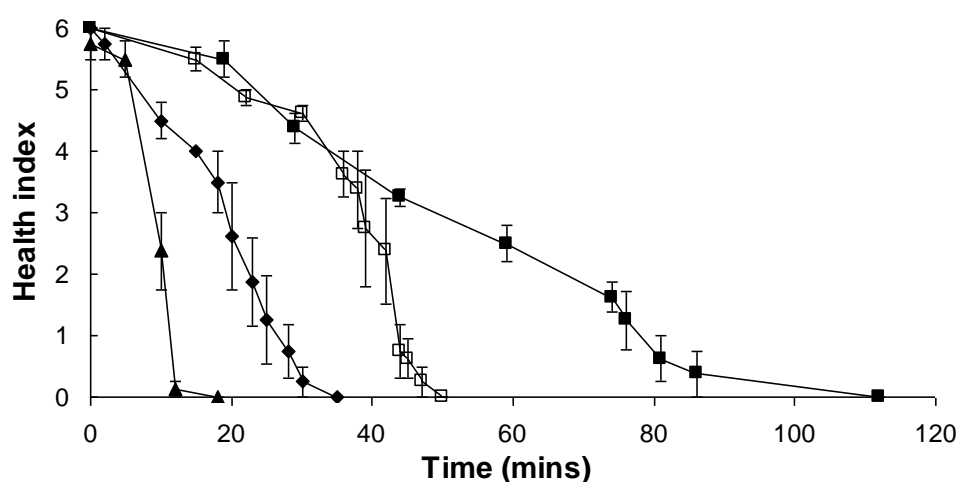


**Figure 7-2.** Responses of juvenile salmon (*Oncorhynchus tshawytscha*) to two *Karenia* species versus time: *K. brevis* 4.6 x 10<sup>6</sup> cells L<sup>-1</sup> (▲) and 0.9 x 10<sup>6</sup> cells L<sup>-1</sup> (◆), *K. brevisulcata* 11 x 10<sup>6</sup> cells L<sup>-1</sup> (□) and *K. brevisulcata* 1.3 x 10<sup>6</sup> cells L<sup>-1</sup> (■). The points/bars depict the Mean ± SEM (n=4). Health index: 0 death, 1 extreme loss of balance, 2 leaping, 3 gasping, 4 agitation, 5 slight loss of balance, 6 healthy. Untreated fish remained healthy over the experimental time period and survived for at least 2 days under these conditions.

### 7.3.3 Toxicity of *Karenia* to marine invertebrate larvae

*K. brevis*, *K. brevisulcata* and *K. mikimotoi* (CAWD 63) were tested for toxicity to the larvae of six invertebrate species (Table 7-2) in a 24-well plate bioassay. The responses of larvae to *Karenia* species over 0-24 hr were observed using an inverted microscope, and recorded using a similar health score system to that described in Section 7.2.6.

No mortality or sublethal effects on brine shrimp were observed following exposure to any of the three *Karenia* species tested. The results match the report of Botes *et al.* (2003) where *A. salina* larvae were not sensitive to *Karenia* dinoflagellates. However, preliminary

studies at the time of the bloom showed that *A. salina* was seriously affected by the seawater collected from the bloom area in Wellington Harbour, in 1998. *K. brevisulcata* maintained by sub-culturing in the CICCMM may have changed in the toxin profile or toxin quota over the past 13 years.

**Table 7-2.** Toxic effects of fresh cultures and SPE extracts of *Karenia* species and of BSX<sup>a</sup> toxins, on invertebrate larvae (6 day old)<sup>b</sup> over 24 hr observation period. For all experiments, there were 3 replicates of 6 – 10 larvae.

<i>Karenia</i> species	Concentration	Invertebrates Tested	Affected
<i>K. brevis</i>	0.1 x 10 <sup>6</sup> cells L <sup>-1</sup>	All	None
	0.9 x 10 <sup>6</sup> cells L <sup>-1</sup>	All	None
	8.7 x 10 <sup>6</sup> cells L <sup>-1</sup>	All	None
	SPE extract 9 x 10 <sup>6</sup> cells L <sup>-1</sup>	GM	No
<i>K. brevisulcata</i>	0.8 x 10 <sup>6</sup> cells L <sup>-1</sup>	All	None
	8.4 x 10 <sup>6</sup> cells L <sup>-1</sup>	All	GM, sea urchin, paua
	84 x 10 <sup>6</sup> cells L <sup>-1</sup>	All	All except brine shrimp
	Cell-free, 56 old	GM	Yes
	SPE extract 72 x 10 <sup>6</sup> cells L <sup>-1</sup>	GM	Yes
	BSX toxins 1-100 µg L <sup>-1</sup>	GM	No
	0.5 x 10 <sup>6</sup> cells L <sup>-1</sup>	All except paua	None
<i>K. mikimotoi</i>	6 x 10 <sup>6</sup> cells L <sup>-1</sup>	All except paua	None
	56 x 10 <sup>6</sup> cells L <sup>-1</sup>	All except paua	None
	1.2 x 10 <sup>6</sup> cells L <sup>-1</sup>	Paua	No
	12 x 10 <sup>6</sup> cells L <sup>-1</sup>	Paua	Yes
	118 x 10 <sup>6</sup> cells L <sup>-1</sup>	Paua	Yes
	SPE extract 85 x 10 <sup>6</sup> cells L <sup>-1</sup>	GM	No

<sup>a</sup> brevisulcatic acid-1, -2, -4, & -5.

<sup>b</sup> Brine shrimp, Greenshell<sup>TM</sup> mussel (GM), Pacific oyster, Paua (New Zealand abalone), Sea slug and Sea urchin.

Greenshell<sup>TM</sup> mussel, Pacific oyster, sea urchin, and sea slug were not significantly affected by *K. brevis* or *K. mikimotoi* at the highest cell densities tested of 8.7 and 56 x 10<sup>6</sup> cells L<sup>-1</sup> respectively (Table 7-2). These cell densities can be reached in a real *K. brevis* or *K. mikimotoi* HAB event. Paua larvae were not affected by *K. brevis* but were sensitive to *K. mikimotoi* (Table 7-2, Figure 7-3A) with 100% mortality after 24 hr exposure to cell densities at 118 x 10<sup>6</sup> and 12 x 10<sup>6</sup> cells L<sup>-1</sup>. Our data agreed with the South African research that abalone (*Haliotis midae*) larvae were not significantly affected by *K. mikimotoi* at the highest concentration tested (< 10 x 10<sup>6</sup> cells L<sup>-1</sup>) (Botes *et al.*, 2003). Paua requires higher quality seawater than Greenshell<sup>TM</sup> mussel and Pacific oyster (N. Ragg pers. comm.). The death of paua larvae in *K. mikimotoi* HAB events is most likely due to environmental degradation e.g. hypoxia or ROS. The bioassay data indicate low direct risks to paua from *K. brevis*. However, paua may be indirectly affected by *K. brevis* blooms and the potential risk of brevetoxin contamination in abalone species is still unknown. The areas of major abalone production around the world have not reported experiencing *K. brevis* dominant HAB events. A future study to evaluate the risk of NSP through abalone consumption would be interesting and probably necessary for New Zealand because of the harvesting of wild paua and also the past experience of a NSP event linked to a dominant *K. cf. brevis* bloom that occurred in North Island, New Zealand in 1993 (Chang, 1995; MacKenzie *et al.*, 1995).

*K. brevisulcata* at a cell density of 84 x 10<sup>6</sup> cells L<sup>-1</sup> severely affected Greenshell<sup>TM</sup> mussel, Pacific oyster, sea urchin, paua and sea slug larvae (Table 7-2, Figures 7-3B-F) with sea urchin being the most sensitive and Pacific oyster the least sensitive. The results supported the reports from the 1998 Wellington Harbour bloom event which devastated almost all marine invertebrates (Chang, 1999b). *K. brevisulcata* at 8.4 x 10<sup>6</sup> cells L<sup>-1</sup> resulted in complete mortality of paua after 24 hr (Figure 7-3F), and almost complete mortality of sea urchin within 24 hr (Figure 7-3E) but there were no apparent effects on Pacific oyster (Figure 7-3C) or sea slug (Figure 7-3D). At this cell concentration, *K. brevisulcata* did not appear to affect Greenshell<sup>TM</sup> mussel larvae after 0-1 hr exposure (Score 5, Figure 7-3B; Score 4, Figure 7-4A) but the larvae became stressed after 1-2 hr (Score 3, Figure 7-4B). At 2 hr, most larvae retracted into their shell with cilia moving (Score 2, Figure 7-4C), but some began disintegrating (Score 1, Figure 7-4D). At 4 hr, all larvae were moribund as identified by larval disintegration and damage to cilia (Figure 7-4D). At 8 hr, larval death began to occur and all larvae were dead by 24 hr (Score 0, Figure 7-4E). No symptoms were observed after 24 hr exposure to 0.84 x 10<sup>6</sup> cells L<sup>-1</sup> (Table 7-2).





Paua, but not other species, was similarly severely affected by *K. mikimotoi* (24 hr LC<sub>50</sub> of approximately 2 x 10<sup>6</sup> cells L<sup>-1</sup>).

The effects of HAB on shellfish usually include reduced feeding, mortality due to hypoxia, or other physical mechanisms and shellfish toxin accumulation. Unlike *K. brevis*, *K. brevisulcata* is more likely to directly kill shellfish by toxin release (Section 7.3.7) and this can lead to unacceptable economic losses. Therefore, establishment of a trigger cell concentration for *K. brevisulcata* is required for early warning. The observations at the time of the 1998 Wellington Harbour bloom revealed that marine life kills began in late February when the cell population was approximately 1 x 10<sup>5</sup> cells L<sup>-1</sup> (Chang *et al.*, 2001). A provisional trigger of 1 x 10<sup>4</sup> cells L<sup>-1</sup> is recommended according to the data from this study, which can provide an early warning of 5-7 days for a *K. brevisulcata* bloom similar to that which occurred in Wellington Harbour in 1998.

**Table 7-3.** Toxicity of cultures of *Karenia* species to invertebrate larvae. MLT<sub>50</sub> = Median time for 50% of larvae to become moribund after exposure to specified cell concentration (Mean ± SEM from curve fit). MLC<sub>50</sub> = Median cell concentration for 50% of larvae to become moribund after exposure time of 2 or 24 hours (estimate; 50% moribund defined as mean toxicity score 2.5). > survival of all larvae at the longest observation time or highest cell concentration used.

Invertebrate		MLT <sub>50</sub> Hours	Concentration 10 <sup>6</sup> cells/L	MLC <sub>50</sub> (10 <sup>6</sup> cells/L)	
				2 hours	24 hours
<i>K. brevisulcata</i>	P.oyster	9.2 ±1.5	34	>35	10
	G. mussel	1.9 ±0.5	7.5	10	2
	Sea Slug	6 <sup>a</sup>	84	>90	10
	Sea Urchin	6.1 ±0.3	7.8	12	2
	Paua	1 <sup>a</sup>	9.6	5	2
	Brine shrimp	>24	84	>90	>90
<i>K. mikimotoi</i>	P.oyster	>24	100	>100	>100
	G. mussel	>24	39	>40	>40
	Sea Slug	>24	22	>25	>25
	Sea Urchin	>24	64	>70	>70
	Paua	10.0 ±2.2	12	20	2
	Brine shrimp	>24	56	>60	>60
<i>K. brevis</i>	P.oyster	>24	7	>7	>7
	G. mussel	>24	13	>13	>13
	Sea Slug	>24	3	>3	>3
	Sea Urchin	>24	13	>13	>13
	Paua	>24	13	>13	>13
	Brine shrimp	>24	8.7	>9	>9

<sup>a</sup> Estimate (insufficient data for curve fit)

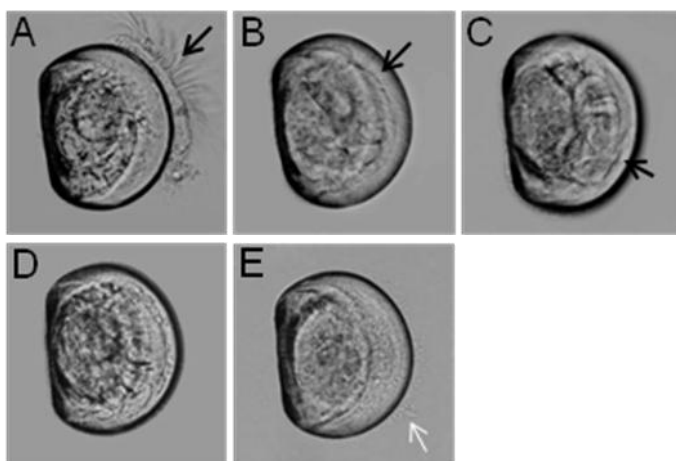


**Figure 7-4.** Photomicrographs of Greenshell™ mussel (*Perna canaliculus*) larvae affected by *K. brevisulcata* during exposure over 24 hr to  $8.4 \times 10^6$  cells  $L^{-1}$ : (A) healthy and static, score 4; (B) stressed the velum started to disintegrate, and cilia withdrawn but healthy and moving, score 3; (C) severely stressed, larvae retracted into shell and cilia moving inside shell, score 2; (D) moribund, cilia gone, larvae disintegrating, still some jerking movement, score 1; (E) dead, disintegrated larvae appeared amorphous, decayed and jelly-like, and cells were being discharged from the dead animal, score 0. Black arrow in A-C shows cilia and white arrow in E shows leaked tissue. The shell diameter for larvae at day 4-6 is around 100-120  $\mu m$ .

#### 7.3.4 Toxicity of BSXs and SPE extracts of *Karenia* cultures, against Greenshell™ mussel larvae

Greenshell™ mussel (*Perna canaliculus*) is a species of filter-feeding shellfish, which is a potential good model to investigate harmful algae and shellfish toxins. In the 24-well plate bioassays used in this study, all larvae survived for 24 hr with control extract as did those challenged with SPE extracts of *K. mikimotoi* (CAWD 63) and *K. brevis*. The *K. brevis* extract (re-suspended in seawater) contained a high concentration of brevetoxins (total 255  $\mu g L^{-1}$  as determined by LC-MS) but no harmful effects were observed on the mussel larvae. The results support the previous studies that brevetoxins can accumulate in living Greenshell™ mussel without affecting their survival (Ishida *et al.*, 2004b; Ishida *et al.*, 2004c; Ishida *et al.*, 1995).

Exposure of Greenshell™ mussel larvae to the SPE extract of a *K. brevisulcata* bulk culture ( $72 \times 10^6$  cells  $L^{-1}$  29 d old; total BSXs 31  $\mu g L^{-1}$ ) gave a consistent increase in the severity of adverse symptoms with time (Figure 7-5). The larvae exhibited stress after a 2 hr exposure to the extract. At 8 hr, all larvae were moribund, and at 24 hr, most were dead. The response curve was very similar to that for an older *K. brevisulcata* culture (56 d; total BSXs 28  $\mu g L^{-1}$ ), where motile, dividing cells had disappeared (Figure 7-5). Toxicities of pure BSX toxins against Greenshell™ mussel larvae were also evaluated. No acute symptoms were observed following exposure to the four individual BSX toxins at concentrations in seawater

of up to 100  $\mu\text{g L}^{-1}$  (Table 7-2). The Neuro2a cell bioassay showed that BSXs are brevetoxin-like sodium channel agonists (Section 6.3.8). Accumulation of BSX toxins is possible in Greenshell<sup>TM</sup> mussels although the predominant ring opened forms are less lipophilic and therefore exhibit a lower bioaccumulation potential. KBT toxins are much more toxic than BSXs in MBA, Bignami assays, and multiple cell cytotoxicity assays. Although these large compounds are difficult to monitor in cultures, the concentrations of KBT-F and KBT-G in *K. brevisulcata* cultures as estimated by LC-MS were similar to those of BSX-1 and BSX-2. It is more likely that KBT toxins are the main toxic agents responsible for deaths of fish and marine invertebrates which occur before significant accumulation of toxins in tissues.

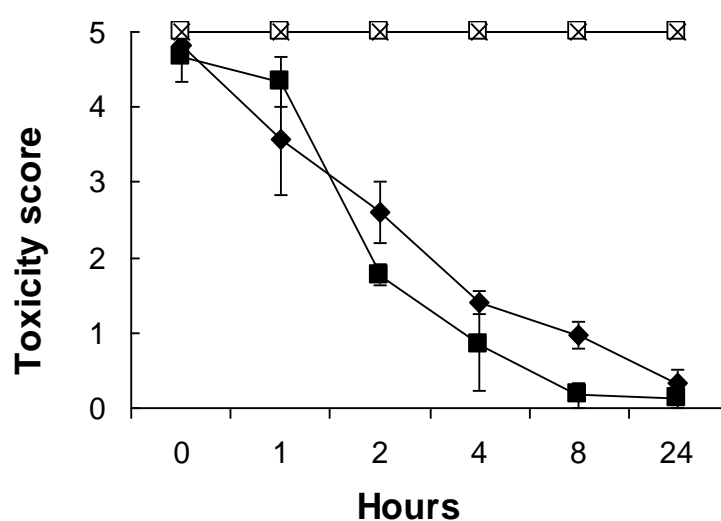


**Figure 7-5.** Responses of Greenshell<sup>TM</sup> mussel (*Perna canaliculus*) larvae against a 56 d *K. brevisulcata* mass culture without living cells (■) and SPE extracts of 20-30 d *Karenia* mass cultures: *K. mikimotoi* (x,  $85 \times 10^6$  cells  $\text{L}^{-1}$ ), *K. brevis* (□,  $9 \times 10^6$  cells  $\text{L}^{-1}$ ) and *K. brevisulcata* (◆,  $72 \times 10^6$  cells  $\text{L}^{-1}$ ). The points/bars depict the Mean  $\pm$  SEM (n=3).

### 7.3.5 Cytotoxicity of *Karenia* extracts

The cytotoxicity of *Karenia* cultures was evaluated using P388 and Vero cell bioassays (Table 7-4). A significant reduction in cell viability was observed in P388 cell bioassay after exposure to both *K. brevis* and *K. brevisulcata* extracts. At the same algal cell concentration of  $4 \times 10^6$  cells  $\text{L}^{-1}$ , the cell viability in *K. brevisulcata* was approximately 5% and was significantly lower than that in *K. brevis*. The results showed that *K. brevisulcata* was more cytotoxic than *K. brevis* to P388 cells. The Florida strain of *K. brevis* investigated in this study contained a high level of brevetoxins. The low effect of *K. brevis* extracts on P388 cell viability suggested that this cell line was less sensitive to VGSC toxins and not a good model for such cytotoxicity research.

Four isolates of *K. mikimotoi* were investigated by P388 cell bioassays. Two strains (CAWD 63 and CAWD 134) obtained from NZ waters did not produce any toxic effects. However, two positive responses were observed in the P388 assays after 72 hr treatment with the extracts of Japan strain (CAWD 05) and NZ strain (CAWD 133). These two strains were further investigated by direct exposure experiments for their toxic potency (Section 7.3.7).

Vero cells were also used to evaluate cytotoxicity of *Karenia* extracts except *K. brevis*. The similar EC<sub>50</sub>'s of BSXs in P388 or Vero cell bioassays suggested that Vero cells are also not sensitive to VGSC toxins. *K. brevisulcata* cultures also showed high cytotoxicity to Vero cells. No viable Vero cells were observed after 72 hr exposure to the extract from  $> 1 \times 10^6$  cells L<sup>-1</sup> *K. brevisulcata* culture. Seven isolates of *K. mikimotoi* were tested using Vero cells, but only the Japanese strain (CAWD 05) produced cytotoxic effects. CAWD 117 and CAWD133 were not cytotoxic to Vero cells up to the equivalent cell concentration of  $50 \times 10^6$  cells L<sup>-1</sup> (Table 7-4). The cytotoxicity of CAWD 117 was not evaluated against P388 cells, but LC-MS studies showed that CAWD 117 may produce the same novel compounds as CAWD 133. The two strains of *K. mikimotoi* recently isolated from the salmon killing event in Ruakaka Bay, Marlborough Sound, New Zealand in 2010, were not found to be cytotoxic to Vero cells.

**Table 7-4.** Cytotoxicities of *Karenia* extracts evaluated using P388 and Vero cell bioassays after 72 hr exposure.

Cell line tested	<i>Karenia</i> species	Strains	Maximal algal cell concentration (10 <sup>6</sup> cells L <sup>-1</sup> )	Cytotoxicity evaluated by MTS assay
<b>P388</b>	<i>K. brevis</i>	CAWD 122	4.1	Toxic
	<i>K. brevisulcata</i>	CAWD 82	5.0	Highly toxic
	<i>K. mikimotoi</i>	CAWD 05	32.3	Toxic
		CAWD 63	31.1	Not
		CAWD 133	25.1	Toxic
		CAWD 134	45.5	Not
<b>Vero</b>	<i>K. brevisulcata</i>	CAWD 82	5.0	Highly toxic
	<i>K. mikimotoi</i>	CAWD 05	50	Toxic
		CAWD 63	50	Not
		CAWD 117	50	Not
		CAWD 133	50	Not
		CAWD 134	50	Not
		Ruakaka spp 1	50	Not
		Ruakaka spp 2	50	Not

### **7.3.6 Resistance of two mammalian cell lines two seawater media**

ATCC Vero cells are reported to survive in seawater medium for at least three hours and were used to investigate cytotoxicity of toxic *Alexandrium* species (Katsuo *et al.*, 2007). To determine suitable exposure times for *Karenia* studies, the viabilities of P388 and Vero cell lines (ECACC) were examined after exposure to cell media (control), sterile seawater and two artificial sea water media (100% GP+Se & 50% GP) for 1-6 hr under the conditions for microalgae growth. As shown in Figure 7-6A, P388 cells appeared stressed under the conditions compatible with dinoflagellate growth. A reduction in absorbance over 0-3 hr was observed in control and two seawater media. However, high resistance of Vero cells to seawater media and low temperature conditions for the initial 2-3 hr was observed (Figure 7-6B). Thus, in the next experiments, Vero cells were used to develop a toxicological model for direct investigation of marine microalgae.

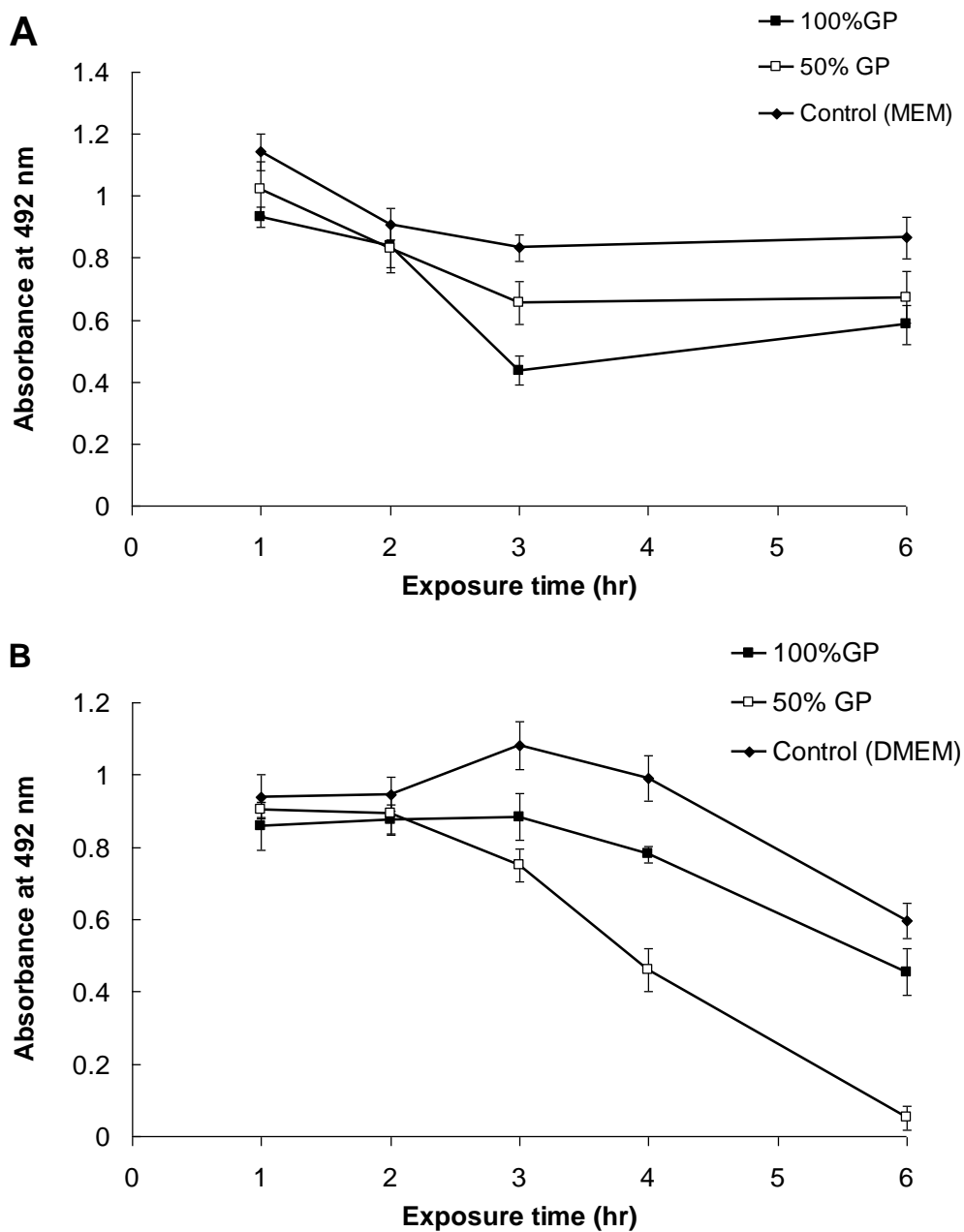


**Figure 7-6.** Viability of P388 (A) and Vero (B) cells in control (MEM or DMEM) and seawater media (100% GP+Se or 50% GP) after the indicated periods of times. The cell viability was determined using MTS assay. Each point represents the mean of at least triplicate measurements. Each bar represents standard deviation.

### 7.3.7 Comparison of cytotoxic potentials of *Karenia* species by the direct exposure bioassay using Vero cells

Previous studies have suggested that some species of *Karenia* dinoflagellates can directly threaten many marine organisms via various mechanisms (Landsberg, 2002). In some cases, such effects are suspected to be mediated by the production of biotoxins. To investigate toxic potentials and the mechanisms involved, three CICC strains of *Karenia* dinoflagellates, *K. mikimotoi* (CAWD 05 and 133) and *K. brevisulcata* (CAWD 82), were directly tested using Vero cells. The cytotoxic potentials were CAWD 82 > CAWD 05 > CAWD 133 (Figure 7-7). *K. brevisulcata* showed high cell-killing activity. Even the algal culture diluted to  $0.5 \times 10^6$  cells mL<sup>-1</sup> reduced the viability of Vero cells by 95% (Figure 7-7). For *K. mikimotoi*, the Japanese strain (CAWD 05) showed cytotoxicity to Vero cells in a cell-concentration dependent manner with a EC<sub>50</sub> value of  $12 \times 10^6$  cells L<sup>-1</sup>, but no cytotoxicity of NZ strain (CAWD 133) was observed at over a range of concentrations up to  $39 \times 10^6$  cells L<sup>-1</sup> (Figure 7-7).

The cytotoxicity of the cell-free supernatants and fresh algal cultures of two *Karenia* species were compared (Figure 7-8). Both supernatants and culture of *K. brevisulcata* showed increased cytotoxicity in algal concentration-dependent manner, supporting the idea that the biotoxins are easily released from leaky *K. brevisulcata* cells and are stable in seawater for at least 2 hr (Figure 7-8A).

The algal culture of *K. mikimotoi* (CAWD 05) produced cytotoxicity in the direct exposure experiments (Figure 7-8B). However, there was no significant effect observed after Vero cells were exposed to the cell-free supernatants of CAWD 05. ROS, gymnocins, and haemolysis are potential toxic agents produced by *K. mikimotoi*. The results from this experiment (Figure 7-8B) suggested that the toxic agents responsible for Vero cell death are unlikely to be present at high concentrations in cell-free supernatants. This is supported by a previous study of *K. mikimotoi* (Zou *et al.*, 2010). Certain cytotoxic metabolites may mainly accumulate in the intracellular compartment of this dinoflagellate. The cytotoxicity of *K. mikimotoi* is possibly mediated through direct cell-to-cell exposure which damages cell membranes of algal cells and releases toxins to Vero cells or fish gill cells.



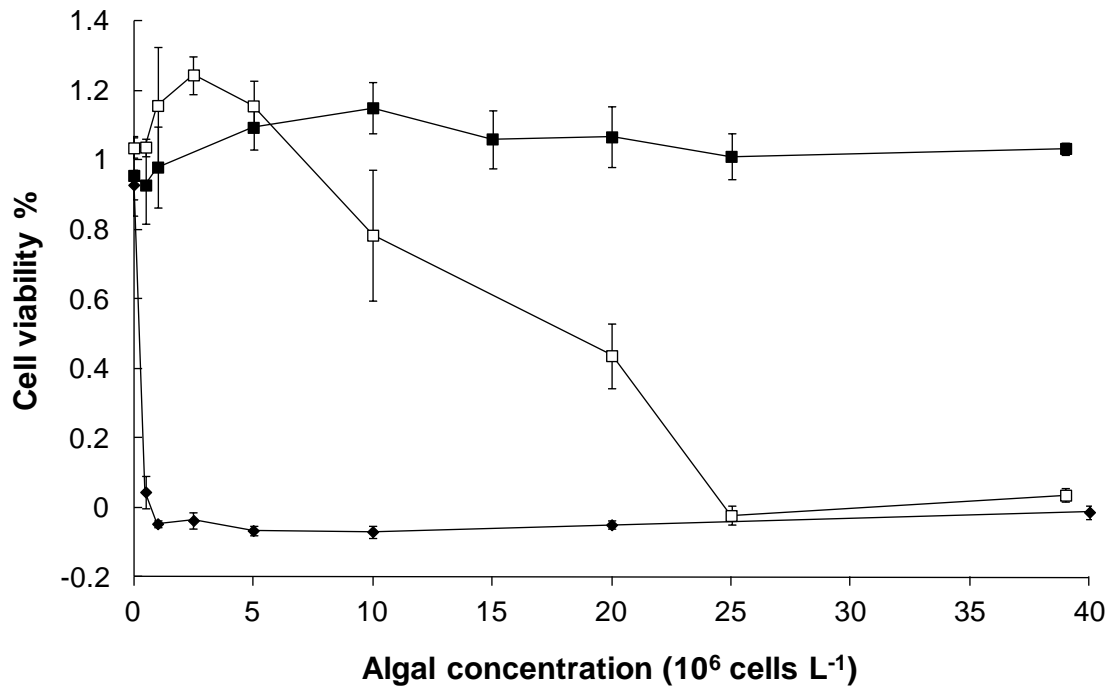


**Figure 7-7.** Viability of Vero cells after direct exposure to algal cultures of three *Karenia* species: *K. brevisulcata* (CAWD 82, ♦), Japan strain of *K. mikimotoi* (CAWD 05, □) and New Zealand strain of *K. mikimotoi* (CAWD 133, ■). The Vero cells were exposed for 2 hr at 18 °C in the light ( $100 \mu\text{mol photons m}^{-2} \text{s}^{-1}$ ), and then the seawater media of each well was replaced with the cell culture medium (DMEM). After 24 hr incubation at 37 °C with 5%  $\text{CO}_2$ , the viability of the cells was examined by MTS assay as described in the text. Each point represents the mean of at least four replicate measurements. Each bar represents standard deviation.

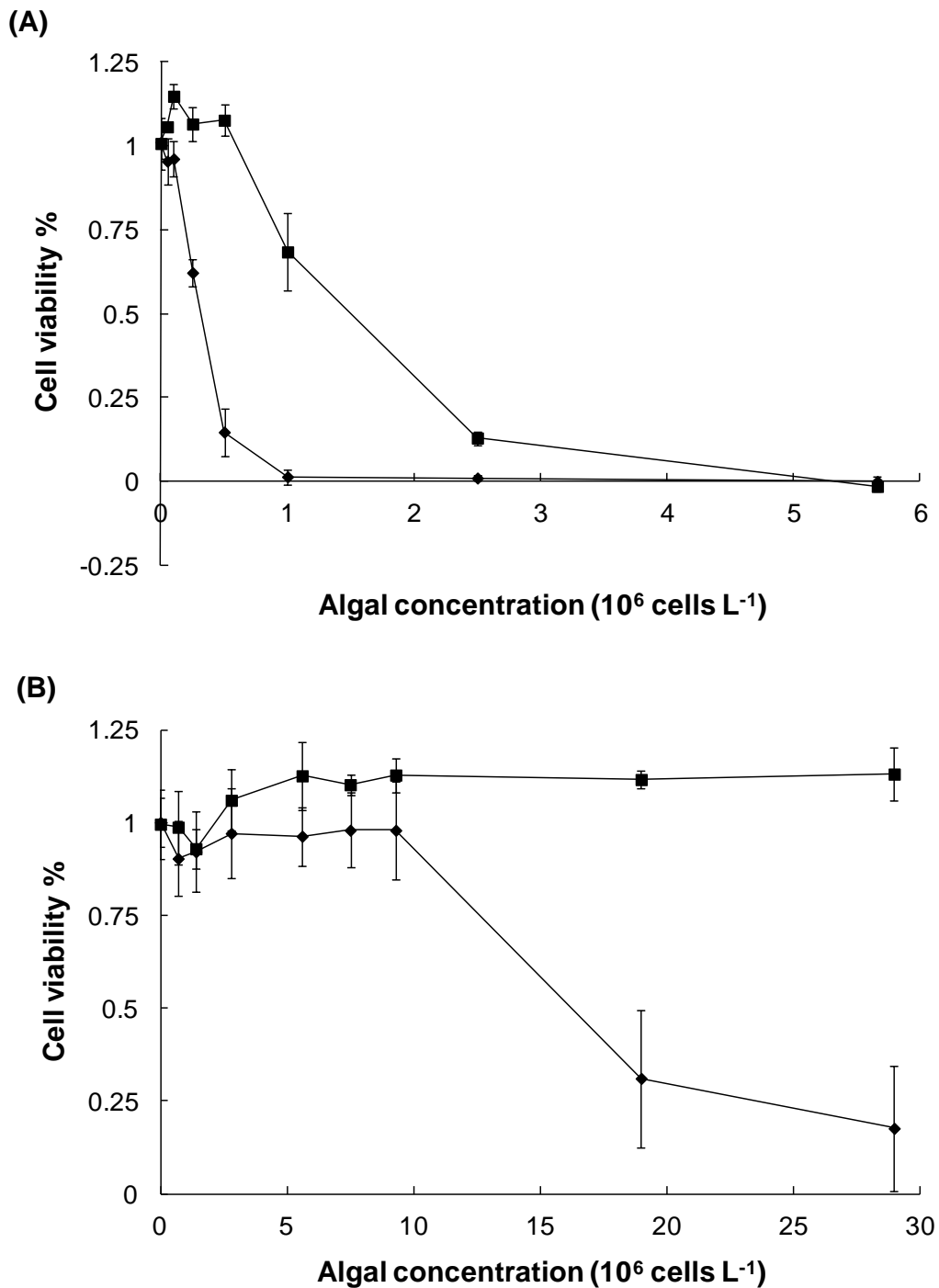


**Figure 7-8.** Viability of Vero cells after direct exposure to algal cultures (◆) and cell-free supernatants (■) of: (A) *K. brevisulcata* (CAWD 82) and (B) *K. mikimotoi* (CAWD 05). The Vero cells were exposed for 2 hr at 18 °C in the light ( $100 \mu\text{mol photons m}^{-2} \text{s}^{-1}$ ), and then the seawater media of each well was replaced with the cell culture medium (DMEM). After 24 hr incubation at 37 °C with 5%  $\text{CO}_2$ , the viability of the cells was examined by MTS assay as described in the text. Each point represents the mean of at least four replicate measurements. Each bar represents standard deviation.

## 7.4 Summary

This study used several bioassays to investigate the toxicity and potential modes-of-action of three *Karenia* species. Both fish and invertebrate larvae bioassays confirmed field observations of the high ecotoxic risks posed by blooms of *K. brevisulcata*. The data showed that  $1 \times 10^4$  cells L<sup>-1</sup> can be recommended as the cell concentration to trigger an early warning in a *K. brevisulcata* HAB event. KBTs are most likely to be the main toxic agents. However, KBTs and BSXs are not predicted to bioaccumulate in shellfish tissues and cause human intoxication through the food chain. The Vero cell direct exposure assay supported that mechanisms for fish and invertebrate kills differ for *K. brevisulcata* and those for *K. brevis* or *K. mikimotoi*, and are more likely to depend on release of toxins into seawater. More detailed studies are required, using isolated toxins and as mixtures, to better understand the mode of action of KBTs, potential synergism with BSXs, and risks to mammals from dietary or aerosol exposures.

## Chapter 8

### Discussion, future directions and summary

HABs caused by dinoflagellates in the genus *Karenia* are increasing in frequency, intensity, duration and geographic distribution and are often associated with mass mortalities of marine vertebrates and invertebrates (Gentien *et al.*, 2007; Landsberg, 2002; Magaña *et al.*, 2003; Wear & Gardner, 2001). *K. brevisulcata* is a newly identified dinoflagellate isolated from the Wellington Harbour during a major bloom event in 1998. Several investigations of this event, the dinoflagellate and the toxins produced have been reported in the literature (Chang, 1999a, b; Chang *et al.*, 2001; Truman *et al.*, 2005). *K. brevisulcata* was extremely toxic to marine fauna and flora. Extracts of *K. brevisulcata* produced a variety of toxic effects in bioassays (mouse, biota) and cell assays (Neuro2a), and the name WHT was assigned to the causative compound (Keyzers, pers. comm.; Truman, 2007; Truman *et al.*, 2005). More recent research has revealed that WHT is a toxin complex containing multiple toxins.

Further studies in a collaboration between Japanese and New Zealand researchers revealed that the toxins produced by *K. brevisulcata* can be classified into two suites: brevisulcatic acids (BSXs) and brevisulcenals (KBTs) (Holland *et al.*, 2012; Oshima, 2007). However, detailed studies on these toxins were not conducted due to a lack of pure materials. In this PhD study, *K. brevisulcata* was grown in different culturing system to maximize production of BSXs and KBTs. LC-MS was used to investigate toxin production in cultures of *K. brevisulcata*, *K. brevis* and *K. mikimotoi* and to guide BSXs isolation. Four BSXs and four KBTs, including <sup>13</sup>C-labelled materials, were isolated and purified using multiple-steps of chromatography at Cawthron and the University of Tokyo respectively. These pure toxins were used for analytical, chemical and toxicological studies. Cytotoxicity assays with mammalian cells (P388, Vero, Neuro-2a and erythrocytes) were used to investigate the modes-of-action of the isolated toxins. The toxicities of *Karenia* cultures were also compared using whole fish bioassays and a novel bioassay in multi-well plates with larvae of several marine invertebrates.

## 8.1 LC-MS analysis of biotoxins produced by *Karenia* dinoflagellates

LC-MS was used in this PhD study to identify and compare qualitatively and quantitatively the biotoxins produced by *K. brevisulcata*, *K. brevis*, and *K. mikimotoi*. The significant differences in toxin production between *K. brevisulcata* and other *Karenia* species support previous studies (Chang, 1999a, b; Haywood *et al.*, 2004) that *K. brevisulcata* is a new species of the dinoflagellate genus *Karenia*, which produces novel bioactive compounds of great interest.

The LC-MS of *K. brevisulcata* SPE extracts with scanning to  $m/z$  1100 revealed the presence of six BSXs with  $[M+H]^+$  in the range 839 to 917 Da. The numbering of these BSXs was based on their polarities under acidic separation conditions (Figure 4-1A), and can be simply classified into two groups: lactone ring-opened (BSX-1, -2, and -3) and lactone ring-closed BSXs (BSX-4, -5 and -6). Ring-closed/ring-opened inter-conversions for BSXs were reversible and are similar to those for the A-ring lactone of brevetoxins (Abraham *et al.*, 2006; Hua & Cole, 1999; Roth *et al.*, 2007). However, *K. brevisulcata* cultures are dominated by the ring-opened products BSX-1 and BSX-2 (Figure 7-1B), whilst brevetoxins are mainly in the lactone ring-closed forms, with only ca. 10-20% of the ring-opened hydrolysis forms (Figure 7-1A) (Abraham *et al.*, 2006). The LC-MS analyses confirmed the absence of brevetoxins (1, -2, -3 or -9) production by *K. brevisulcata* (McNabb *et al.*, 2006).

Japanese research collaborators have isolated and purified four KBTs (-F, -G, -H & -I) from the neutral fractions of *K. brevisulcata* cultures produced at Cawthron Institute. Microgram quantities of KBTs were kindly provided by Prof Satake and were used as RSMs in LC-MS studies. The LC-MS of *K. brevisulcata* SPE extracts with scanning of  $m/z$  1000 to 2300 found 7-8 large novel compounds (Figures 4-1B, 4-3; Tables 4-4, 4-5). These compounds with  $m.w. > 1900$  Da have complex spectra (Figures 4-4 to 4-6) which are difficult to differentiate from some contaminants e.g. ethoxylates or lipids. To overcome this problem,  $^{13}\text{C}$ -labelled toxins were produced by addition of  $\text{NaH}^{13}\text{CO}_3$  into mass cultures. Comparison of SPE extracts of both unlabelled and labelled cultures by LC-MS scanning confirmed that there were four KBTs (-F, -G, -H & -I) and four KBT-related compounds incorporating  $^{13}\text{C}$  atoms (Table 4-5). These eight KBTs when ordered according to their polarity under acidic separation conditions are:  $\text{M2181} > \text{M2135/KBT-H/-I} > \text{M2165} > \text{M1917} > \text{KBT-F/-G}$  (Figure 4-1B). The data obtained from this LC-MS study revealed there may be inter-relationships amongst these KBTs, which will be discussed in Section 8.5.

*K. brevis* and *K. mikimotoi* do not produce BSXs and KBTs. *K. brevis* (Florida strain, CAWD 122) tested in this study produces brevetoxins with four predominating analogues (Table 4-8). No compounds with m.w. > 1500 Da were detected by LC-MS in the SPE extracts. *K. mikimotoi* strains produce several 700-1200 Da metabolites with characteristics of polycyclic ethers but not brevetoxins or BSXs (Table 4-9). The LC-MS study showed that the toxin profiles are different between individual strains except CAWD 117 that has the same toxin production as CAWD 133 (Figures 4-11C, 4-12C, Table 4-9). Gymnocin-A was confirmed in CAWD 05 using the RSM of gymnocin-A kindly provided by our Japanese co-workers (Satake *et al.*, 2002). However, several interesting compounds such as M927, “gymnocin-B (m.w. 1156)”, and “gymnocin-C (m.w. 1142)” could not be confirmed as reported toxins (e.g. gymnocin-B and -C) (Satake *et al.*, 2005) (Y. Oshima, pers. comm.) because of lack of pure reference standard materials. The Japanese research group led by Prof. Oshima at the Tohoku University, Sendai, isolated a large polycyclic ether compound, gymnocin-F (m.w. 2076 Da) from mass cultures of a *K. mikimotoi* strain collected from the Japanese coast (Y. Oshima, pers. comm.). This large compound has a higher potency to P388 cells than reported gymnocins (Satake *et al.*, 2002; Satake *et al.*, 2005). LC-MS scanning of seven strains of *K. mikimotoi* identified the absence of gymnocin-F or other polycyclic ethers m.w. > 1200 Da in the extracts. These findings support the finding that biotoxin production by *K. mikimotoi* is unusually strain dependent. Therefore the isolation and purification of some key compounds identified by LC-MS (Table 4-9) will be critical for further investigations of the fish killing mechanism(s) of *K. mikimotoi*.

## **8.2 Development of LC-MS methods for quantitative analysis of BSXs and KBTs**

One of the key tasks in the isolation and purification of BSXs at Cawthron Institute was the development of an efficient method to separate the small amounts of toxins from bulk algal co-extractives, and then from each other. Sensitive and specific LC-MS techniques (Quilliam, 2003b) were developed in this study to guide the isolation rather than using the bioassays which were used in the initial research on toxins from *K. brevisulcata* (Keyzers, pers. comm.). Much of the quantitative work in this thesis was obtained with LC-MS (SIR) methods, developed for BSXs. A further more sensitive method based on MS/MS (MRM) was developed to determine 6 BSXs and 4 KBTs within a single run.

Compared to KBTs (m.w. 1900-2200), BSXs are medium size molecules that are more suitable for preliminary LC-MS determination. Monitoring of fractions by LC-MS during the isolation of BSXs used SIR operating mode, because SIR requires little information about the new compounds and calibrations can be established with a single standard of a similar compound. In SIR mode, MS1 and collision cell are not used, and only specified masses are selected in MS2 for detection (Figure 2-7). Thus SIR is more sensitive and selective than full scan mode which scans MS2 over a set mass range. The uPLC-Premier MS system was used because it provided a rapid separation of BSXs (total run time of 5 minutes). The electrospray ionisation source was operated in the positive mode ( $\text{ESI}^+$ ). The dominant  $[\text{M}+\text{H}]^+$  was observed in the MS spectra for all six BSXs. Ring-opened BSXs also gave a strong peak for  $[\text{M}+\text{H}-\text{H}_2\text{O}]^+$ , indicating the presence of a labile hydroxyl in the molecules (Figures 4-3, 5-10). A seven channel SIR method (Method 1, Section 4.3.2.1; Table 4-2) was developed based on the MS scan experiments (Section 4.3.1.1). Brevetoxin-2 (RSM, UNCW) was used to calibrate and quantify the responses of the six BSXs.

This LC-MS SIR method was intensively used for quantitatively analysing toxin production in different culturing systems (Sections 3.3.1 & 3.3.2) and guiding isolation and purification of unlabelled BSXs (Sections 5.3.1 & 5.3.2). The response of the LC-MS system for BSXs and the calibrant was compared using standard solutions of pure BSX-1, BSX-2 and brevetoxin-2, which gave highly linear calibrations (Figure 4-7). The LC-MS sensitivity of BSX-1 was shown to be higher than brevetoxin-2 but BSX-2 was less sensitive than brevetoxin-2. LOQs for BSXs were low ( $< 0.5 \mu\text{g L}^{-1}$  algal culture). The precision of this SIR method was demonstrated obtained from replicate measurements using batch carboy cultures. Measurements for ring-opened BSXs showed good repeatability with  $<15\%$  RSD, but ring-closed BSXs showed relatively less repeatability with 10-40% RSD.

KBTs were not routinely monitored using the uPLC-Premier MS because the dominant  $[\text{M}+\text{Na}]^+$  mass ions showed poor repeatability. Further LC-MS studies were carried out using The HPLC-Ultima MS. The Waters 2695 HPLC uses one pump to drive three mobile phase solutions which were combined in the mixing reservoir to generate linear gradients. The maximal pressure for the HPLC was 5000 psi, which is much lower than 15000 psi for the uPLC system. Thus, toxins separation on the HPLC system required coarser packing materials and a longer running time (15 min). The mobile phase was optimised and an acidic mobile phase was selected because it was suited for toxins separation and dominant  $[\text{M}+\text{H}]^+$  ionisation. C8 and C18 reversed phase columns were compared. Both provided good toxin separation but the C8 column was more efficient and faster. This system was used in scanning

mode (ESI<sup>+</sup> and ESI<sup>-</sup>) to study profiles and daughter ion spectra of toxins in *Karenia* cultures, including <sup>13</sup>C-labelled *K. brevisulcata*.

An MS/MS method using MRM mode (Method 4) was developed to quantitatively analyse six BSXs and four KBTs. This method was more specific and selective quantitation than SIR. In MRM experiments, dominant [M+H]<sup>+</sup> mass ions for each toxin are selected in MS1, the ions are fragmented in the collision cell using a gas (argon) plus electrostatic energy and the fragment ions are selected in MS2 for detection. For each BSX, two transitions were monitored: one for quantitative analysis and another for toxin confirmation (Table 4-3). Only a single transition was used for each KBT. The toxin concentrations were calibrated with RSMs of four BSXs (-1, -2, -4, & -5) and four KBTs (-F, -G, -H & -I). BSX-3 and BSX-6 have not yet been isolated and purified. Their LC-MS characteristics were similar to those of BSX-1 and BSX-4. Thus RSMs of BSX-1 and BSX-4 were used to calibrate BSX-3 and BSX-6 respectively.

The calibration curves for all toxins standards (4 BSXs and 4 KBTs) were linear with R<sup>2</sup> > 0.99 over the concentration range of 5–200 ng mL<sup>-1</sup>. A preliminary validation study was conducted using culture media fortified with two concentrations of pure toxins and with a single level of algal extract. Recoveries were 46-73% for BSX-1, 60-87% for BSX-2, 73-95% for BSX-4, 58-102% for BSX-5, 61-63% for KBT-F, 50-71% for KBT-G, 77-85% for KBT-H, and 53-90% for KBT-I respectively (Table 4-6). Ionisation suppression by co-extractives from SPE was eliminated as a significant cause of apparent low recoveries because recoveries did not increase when extracts were rerun following dilution. Toxins losses in SPE sampling were also tracked which showed that no toxins were eluted in the load or wash solutions and toxin retention in the SPE cartridge after the elution was negligible for BSXs and minimal for KBTs. The low LOQs for BSXs by MRM (2 ng mL<sup>-1</sup> in 80% methanol) confirmed that this methodology is more sensitive and specific than SIR (Method 1). The precision of the method established using subsamples of batch carboy cultures extracted by SPE was excellent with RSDs for all toxins of 2-15% at concentrations > 10 ng mL<sup>-1</sup>. This MRM method is reliable and reproducible for quantitative analysis of BSXs and KBTs at concentrations greater than the LOQs (2 ng mL<sup>-1</sup> in 80% methanol or 0.15 µg L<sup>-1</sup> algal culture). Toxin production over time in *K. brevisulcata* cultures was monitored using the SIR method because the laboratory culturing phase of this research was completed before the MRM method was developed and KBT standards became available from Japanese co-workers. This MRM method is suited for quantitative analysis of BSXs and KBTs in seawater and could be used for environmental



monitoring, particularly during development of *K. brevisulcata* blooms. It could be further developed for analysis of biota and also used in studies of bioaccumulation.

### 8.3 Laboratory culturing of *K. brevisulcata*

Isolation and purification of milligram quantities of BSXs was a major objective of this PhD study. To obtain sufficient crude toxins, 1428 litres of *K. brevisulcata* were grown under laboratory conditions at Cawthron Institute. Three culturing systems were investigated to optimise *K. brevisulcata* growth and toxin production. Barrels, carboys and photobioreactor required 14, 24 and 26 days to reach  $G_{\max}$  respectively. The highest  $G_{\max}$  observed in batch bioreactor culture was 5-fold higher than that in barrels and 4-fold higher than that in carboys and that reported in Wellington Harbour Bloom, 1998 (Beuzenberg *et al.*, 2012; Chang, 1999a, b; Holland *et al.*, 2012). Carboys were the most efficient in batch culture mode with the highest growth rate ( $\mu=0.086 \text{ day}^{-1}$  versus  $0.050\text{-}0.057 \text{ day}^{-1}$  for barrels and photobioreactor). Thus, most mass cultures of *K. brevisulcata* were grown in carboys. *K. brevisulcata* grew better in continuous culture with 1.3-fold and 2-fold higher growth rates than batch carboy and batch bioreactor cultures respectively. Photobioreactors have potential for large scale culturing of *K. brevisulcata* and other toxic dinoflagellates.

The concentration of total BSX toxins was highest in bioreactor batch culture at  $G_{\max}$  (Table 3-1). The production of ring-closed BSXs appeared to be cell concentration-dependent. Previous studies have revealed that brevetoxins in *K. brevis* are mainly the ring-closed structures, and can be hydrolysed when released from algal cells into seawater (Abraham *et al.*, 2006; Roth *et al.*, 2007). A similar process may also occur in *K. brevisulcata* which may have more fragile cells. The concentrations of BSX-1 and BSX-2 increased over time, even after culture collapse, suggesting that these two BSXs are stable in seawater and may be end products of BSX metabolism (Figure 8-1). The concentration of BSX-3 increased during the early stages of batch carboy cultures and suddenly declined when the medium pH exceeded 9 at day  $15 \pm 1$  (data not shown). This BSX may be more easily degraded due to reactive chemical properties (Figure 8-1). Comparison of cell growth and BSX production curves for different batch cultures of *K. brevisulcata* (Figure 3-2) suggested that maximal cell division and BSX biosynthesis may require different culture conditions.

The LC-MS MRM method was used to determine the concentrations of ten toxins (6 BSXs and 4 KBTs) at three different stages in a batch carboy culture (Table 4-7). The data for

BSXs (Table 4-7) matched the preliminary research (Figure 3-2B) in that (i) the highest productions for lipophilic BSXs (-3 to -6) occur at  $G_{\max}$ , and (ii) the concentrations of BSX-1 and BSX-2 at the late stage when the culture had collapsed are multiple-fold higher than those at  $G_{\max}$  (day 14). For KBTs, the concentrations reached peak at  $G_{\max}$  (Table 4-7) and were 2.5-4 fold higher than those at day 28 when the culture collapsed. The data suggests that productions of KBTs and ring-closed BSXs are closely associated during cell proliferation, but the concentration of KBTs in *K. brevisulcata* cultures at  $G_{\max}$  were 5.6-fold higher than that of ring-closed BSXs.

These studies contributed to a better understanding of the fate of cell growth, and BSX and KBT metabolism. The results are helpful to provide an insight into *K. brevisulcata* bloom dynamics and future laboratory bulk culturing. For BSX-1 and -2, the mass cultures could be harvested at a later culturing stage when more ring-closed BSXs will be hydrolysed to their ring-opened derivatives. However, for lipophilic BSXs (-3 to -6) and KBTs, culture harvesting should be conducted on the day of  $G_{\max}$  when the highest yield of these parent toxins are achieved.

## 8.4 Chemical and toxicological studies of BSXs

Milligram quantities of two ring-opened BSXs (-1 & -2) were isolated and purified from crude HP20 extracts (from a total 1109 litres cultures) following the steps of solvent partitioning, SPE desalting and defatting, separation of BSXs by normal phase column chromatography, and final purification using preparative HPLC. An increase (ca. 10-20%) in ring closed BSXs from ring opened analogues were observed after removal of solvents by rotary evaporation at  $> 40^{\circ}\text{C}$  (data not shown). The inter-conversion of ring-closed and ring-opened toxins was a significant problem during isolation and purification of the toxins. Triethylamine added prior to evaporation was initially used to prevent lactone formation during evaporation. However, the traces of triethylamine caused problems in further testing such as NMR. Thus concentration of toxin fractions was carried out with temperature control ( $\leq 40^{\circ}\text{C}$ ). Dry BSXs which are stored at  $-20^{\circ}\text{C}$  are stable up to 12 month and less than 5% of ring-opened BSXs were converted to ring-closed analogues. Milligram amounts of the ring-closed BSXs were produced from BSX-1 and BSX-2 by acid-catalysis for NMR experiments and toxicological studies.

Hydrolysis experiments showed the lactone ring closure reaction is reversible. Hydrolysis of BSX-4 and BSX-5 in 1 mM NaOH at 50 °C gave highly linear pseudo-first order reaction plots with rate constants of ca 0.12 min<sup>-1</sup>, similar to those reported for hydrolysis of brevetoxins (Hua & Cole, 1999). This indicates that the lactone ring for BSX-4 or BSX-5 is similar to that in brevetoxins (Figure 5-7). LC-MS experiments revealed that ring-opened BSXs (-1 and -2) are predominant in *K. brevisulcata* culture (Figure 7-1B). In contrast, *K. brevis* cultures produced mainly the lactone ring-closed brevetoxins (Figure 7-1A). Roth *et al.* (2007) suggested that the ring-closed brevetoxins were the parent toxins produced in *K. brevis* cells and the hydrolysed toxins were formed following leakage into the media. It is probable that BSX-4 and BSX-5 are the parent toxins produced by *K. brevisulcata* which appears to have more leaky or fragile cells than *K. brevis*, leading to higher toxin levels in the culture medium where hydrolysis of the lactone ring takes place (Holland *et al.*, 2012; Shi *et al.*, 2012).

One of the key goals for harmful algae research is to elucidate the chemical structure of novel algal toxins. Milligram quantities of four BSXs (-1,-2, -4 & -5) were purified and applied for structural determination using UV, MR and NMR spectroscopic techniques. HRMS data revealed the chemical formulae of BSXs were similar to those of brevetoxins. NMR spectra for unlabelled BSX-1 and <sup>13</sup>C-labelled BSX-4 were obtained by Dr Patrick Edwards using 500 and 700 MHz instruments at Massey University, and the complex spectra were interpreted with assistance of Professor Satake (University of Tokyo). The partial structures of BSX-1 and BSX-4 have been elucidated with several confirmed chemical characteristics including two carbonyl groups, a sharp doublet methyl, an olefinic double bond, and a methyleneic double bond plus a suite of oxy-methine carbons. These BSXs have a typical ladder-frame polycyclic ether structure with similarities to brevetoxins, yessotoxin, CTX, MTX and gymnocins (Holland *et al.*, 2012; Lin *et al.*, 1981; Murata *et al.*, 1987; Murata *et al.*, 1990; Satake *et al.*, 1995; Satake *et al.*, 2002; Satake *et al.*, 2005; Shimizu *et al.*, 1986). The daughter ion mass spectra for BSXs and their derivatives did not contain the ring cleavage fragments at *m/z* 473 or 611 observed for brevetoxins, indicating the carbon backbones of BSXs are unlikely to be A-type or B-type brevetoxin-like. BSX-4 may have the same A, B and C rings as brevetoxin-1 except for the lack of the ring-junction tertiary methyl group (Figures 2-9, 5-20). HMBC correlations from methylene protons to carboxylic carbons confirmed that carboxylic acids are in both termini of BSX-1 and that A ring closure provides BSX-4 with a 5-membered lactone ring.

The structure of the side chain for BSX-1 and BSX-4 was elucidated on the basis of UV, MS/MS, and NMR data. In addition to a terminal carboxylic acid group, there is also an unconjugated methylene double bond and a hydroxyl group. The main ring structure for BSX-2 and BSX-5 is postulated to be the same as for BSX-1 and BSX-4, with a shorter side chain by the CH<sub>2</sub>CHOH formulae difference and conjugation of the carboxyl group as in brevetoxin-B5 (Ishida *et al.*, 2004a) (Figure 8-1), giving the broader tail to longer wavelengths observed in the UV spectra (Figure 5-9) and a prominent daughter ion at *m/z* 873 or 855.

The structures of BSX-1 and BSX-4 have not been completely elucidated because of missing NMR peaks due to conformation changes in the time frame of the NMR pulse sequences. Approximately 1/3 of the carbons and protons could not be accounted for in the spectra for BSX-1 obtained at 300K using 700 MHz instrument. Similar effects were observed in NMR spectra for brevetoxin-1 and CTX and involved missing signals for the flexible central 8- and 9-membered rings. These conformer effects were successfully overcome by obtaining NMR spectra at lower temperatures (Murata *et al.*, 1990; Pawlak *et al.*, 1987). Further spectra for BSX-1 and <sup>13</sup>C-BSX-4 were obtained at lower temperatures (to 273K on the 700 MHz instrument; to 243K on the 500 MHz instrument). However, the conformer effects were not completely eliminated with some important signals still missing. The conformer effects appeared to involve three flexible 7-, 8- and 9-membered ether rings with one double bond and a tertiary methyl group in the central part of the molecule (Figure 5-20). The pure BSXs have been sent to the University of Tokyo and more NMR spectra will be obtained at lower temperatures. This will hopefully confirm the proposed structure. However, the NMR and MS/MS data have proven that BSX-1 and BSX-4 have different ring systems to the known polycyclic ether toxins. There are structural similarities to brevetoxin-1, but there are also significant differences (Figures 2-9, 5-20).

Toxicological studies were conducted for BSXs using several bioassays. Aside from studies with P388 and Vero cells, this research was conducted through collaborations but using materials isolated as a part of this PhD. The MBA with i.p. administration showed that BSXs (-1, -2, -4 & -5) are weakly toxic to animals with LD<sub>50</sub>'s of >1500 µg kg<sup>-1</sup> bw, and are 8-33 fold less potent than brevetoxin-2 (Baden & Mende, 1982). Oral administration of BSXs was not carried out because of lack of sufficient material. The BSXs are weakly haemolytic with EC<sub>50</sub>'s with 6-10 µM (Section 6.3.8) and weakly cytotoxic to P388 and Vero cells. However, BSXs are cytotoxic to Neuro2a cells in the presence of ouabain and veratridine. BSX-4 and BSX-5 are more cytotoxic in the Neuro2a cell assay than the ring-opened

analogues (Table 6-6), and their activity was antagonised by saxitoxin. Ring-closed brevetoxins were also reported to be more potent agonists of sodium channels than their hydrolysed analogues in receptor binding and cytotoxicity bioassays (Roth *et al.*, 2007). These BSXs are brevetoxin-like sodium channel agonists, especially BSX-4 and BSX-5, but with a lower activity than brevetoxin-3 (Table 6-6). The chemical characteristics indicate that parent BSXs could potentially bioaccumulate in shellfish tissues, but these weak toxins are also more polar than ring-closed brevetoxins (Figures 4-1B, 4-9), and therefore are not expected to be of high risk to human health through the food chain. Hundreds of cases of human respiratory illness were reported during the *K. brevisulcata* bloom from late January to early March in 1998 (Chang, 1999b), with similar symptoms to those caused by aerosolised brevetoxins (Benson *et al.*, 2005; Benson *et al.*, 2002; Cheng *et al.*, 2005; Fleming *et al.*, 2005a; Fleming *et al.*, 2005b; Fleming *et al.*, 2007; Kirkpatrick *et al.*, 2004). The respiratory distress was believed to be caused by direct exposure to sea-spray aerosols containing biotoxins or toxic algal cells (Chang *et al.*, 2001; Cheng *et al.*, 2005). An aerosol collection system using preconditioned Strata-X SPE cartridges were designed and used when *K. brevisulcata* was cultured in carboys. However, technical difficulties prevented adequate sampling of aerosols. I believe that optimisation of an effective and efficient aerosol collection system is critical for repeating this experiment in the future.

BSX-3 ( $[M+H]^+$  857 Da) is a novel toxin detected in cultures during the studies and another peak named BSX-6 ( $[M+H]^+$  839 Da) is postulated as its ring-closed lactone derivative. These two compounds were more lipophilic than BSX-1 and BSX-2 under acidic-neutral separation conditions ( $pH \leq 7$ ) and appear to be unstable under alkaline conditions ( $pH > 9$ ). Keyzers (pers, comm.) reported that WHT lost toxic activity at pH 9, which may indicate that BSX-3 and -6 also contribute to the toxicity of WHT. The LC-MS studies showed that BSX-3 has a similar structure to BSX-1. The 60 Da difference in mass is consistent with the carboxylated side chain for BSX-1/4 being substituted with an unsaturated aldehyde terminal for BSX-3/6 (Figure 8-1) of the same structure as for brevetoxin-1 and brevetoxin-2 (Lin *et al.*, 1981; Shimizu *et al.*, 1986) (Figure 8-1). In the cases of brevetoxin metabolism, brevetoxin-B5 is produced from brevetoxin-2 through oxidation of the terminal aldehyde to form the carboxylic acid (Ishida *et al.*, 2004a; Ishida *et al.*, 2004b; Ishida *et al.*, 2004c). It is also possible that BSX-6 is an important intermediate in the biosynthesis and metabolism of BSXs (Figure 8-1). BSX-6 can be hydrolysed to BSX-3, and is also likely to be the precursor of BSX-4 and BSX-5. The oxidation of the terminal aldehyde in BSX-6 could produce BSX-5. Selwood *et al.* (2008) developed a simple method to convert brevetoxin-2 to brevetoxin-B2 through Michael addition of cysteine. It is possible that the terminal aldehyde

for BSX-6 is metabolised to BSX-4 in *K. brevisulcata* cells through enzymatic addition of acetate (Figure 8-1). However, the equivalent brevetoxin addition products to BSX-1 or BSX-4 have not been observed in *K. brevis*.

In the case of brevetoxins, brevetoxin-2 (aldehyde side chain) has a lower LD<sub>50</sub> than brevetoxin-B5 (carboxylated side chain) (Ishida *et al.*, 2004a). It is suggested that BSX-3 and BSX-6 are possibly more toxic than BSX-2 and BSX-5 respectively because of the reactive aldehyde terminus. The lipophilic nature, similar to brevetoxins (ring-closed, Figures 4-1B, 4-10), indicates BSX-6 is more likely than other BSXs to bioaccumulate in shellfish tissue and cause human health issues through consumption of contaminated seafood.

The biosynthetic and metabolic pathways for BSXs have not been fully confirmed. The isolation of BSX-3 and BSX-6 in the future is critical for establishment of the pathway for toxin biosynthesis in *K. brevisulcata* cells. BSX-3 and -6 were not isolated as a part of this PhD project because all neutral (CHCl<sub>3</sub>) fractions containing lipophilic BSXs (-3 to -6) were sent to the University of Tokyo for isolation of KBTs. The following isolation stages for BSX-3/-6 are proposed using cultures harvested before G<sub>max</sub>: (i) hydrolysis of ring closed BSXs to ring opened BSXs, (ii) separation of BSX-3 from more polar BSX-1 and -2 by solvent partitioning (55% MeOH/CHCl<sub>3</sub>), (iii) acid-catalysed formation of BSX-6; (iv) separation of BSX-6 from the more polar KBTs using solvent partitioning or column chromatography, (v) formation of BSX-3 by hydrolysis of BSX-6, and (vi) purification of BSX-3 and -6 using preparative HPLC. Chemical synthesis of BSX-3/6 from BSX-1/4 or BSX-2/5 is another option for future work.

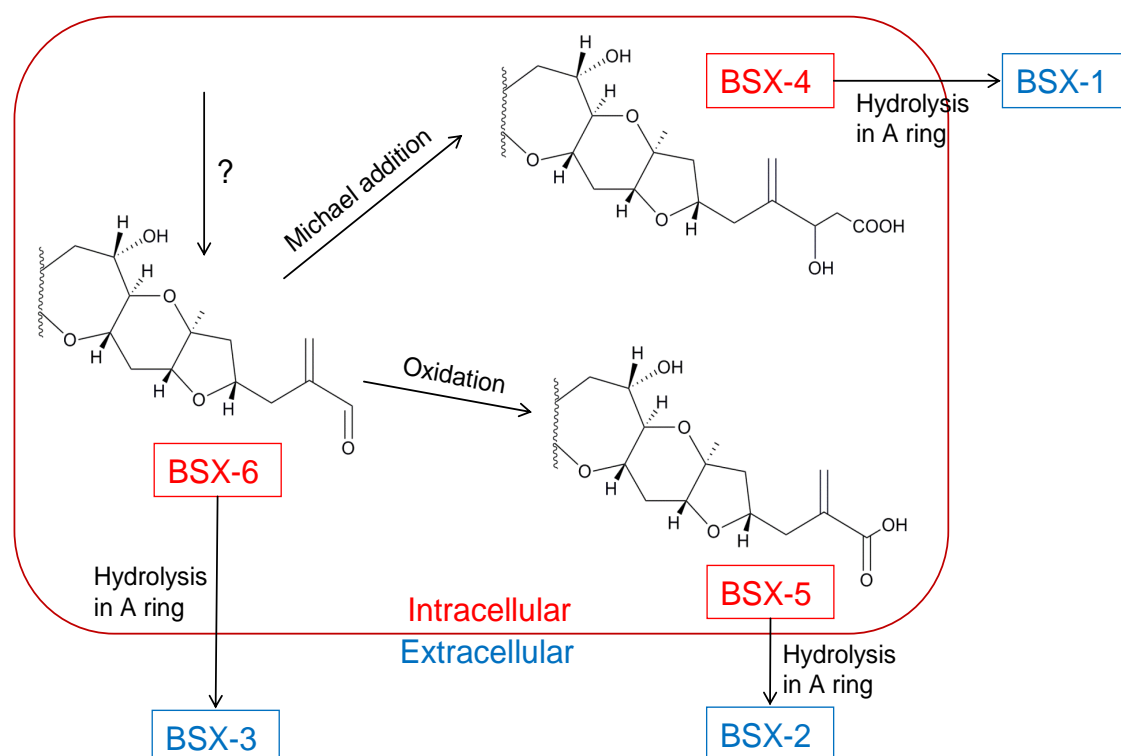


**Figure 8-1.** Hypothesised inter-relationships of six BSXs: (i) within *K. brevisulcata* cell, BSX-6 is the primary BSX that forms BSX-4 through a Michael addition with acetate or is oxidised to BSX-5; (ii) released into seawater, the lactone BSXs (-4, -5, & -6) are hydrolysed to ring-opened BSXs (-1, -2, & -3).

## 8.5 Chemical and toxicological studies of KBTs

KBTs are a novel group of large polycyclic ether toxins produced by *K. brevisulcata* (Hamamoto *et al.*, 2012; Holland *et al.*, 2012). These compounds are lipophilic and can be separated from acidic toxins (BSX-1 and BSX-2) by solvent partitioning between aqueous methanol and  $\text{CHCl}_3$ . The neutral  $\text{CHCl}_3$  fractions were sent for isolation and purification of KBTs at the University of Tokyo. Milligram quantities of KBT-F ( $\text{C}_{107}\text{H}_{160}\text{O}_{38}$ ), KBT-G ( $\text{C}_{108}\text{H}_{162}\text{O}_{39}$ ), KBT-H ( $\text{C}_{107}\text{H}_{160}\text{O}_{39}$ ) and KBT-I ( $\text{C}_{108}\text{H}_{162}\text{O}_{40}$ ) have been isolated using column chromatography and two stages of preparative HPLC purification (Hashimoto *et al.*, 1981). The m.w. of KBT-H and KBT-I are 16 Da higher than those of KBT-F and KBT-G respectively, indicating KBT-H and KBT-I may be the oxidative analogues of KBT-F and KBT-G respectively, (M. Satake, per. comm.). The difference in formulae between KBT-F / -H and KBT-G / -I is  $\text{CH}_2\text{O}$ . The unsaturation ( $r+\text{db} = \#C - \frac{1}{2}\#H + 1$ ) is 28 for all four KBTs, which is 2-fold higher than for BSXs but is lower than for MTX ( $r+\text{db} = 37$ ) (Satake *et al.*, 1995). The Japanese group has determined the full structure of KBT-F by  $^1\text{H}$ ,  $^{13}\text{C}$  and 2D NMR experiments with MS/MS confirmation (Hamamoto *et al.*, 2012). The NMR spectra for

KBT-F did not exhibit conformer problems because KBT-F does not contain 8- or 9-membered ring systems (Holland *et al.*, 2012; Murata *et al.*, 1990; Pawlak *et al.*, 1987). However, the large molecular formula and many C-H's with similar spin systems required great interpretative skills by the Japanese researchers. KBT-F is a novel ladder frame polycyclic ether compound with a 2-methyl-2-butenal side chain that is the same as that in gymnocin-A and gymnocin-B (Figures 2-12, 5-24) (Satake *et al.*, 2002; Satake *et al.*, 2005). The total number of ether rings for KBT-F is less than MTX (24 versus 32), but KBT-F has the 17 CER (rings A-Q), the largest number amongst known polycyclic ethers, e.g. 10 CERs for MTX (Satake *et al.*, 1995), 10-11 CERs for brevetoxins (Lin *et al.*, 1981; Shimizu *et al.*, 1986), and 14-15 CERs for gymnocins (Satake *et al.*, 2002; Satake *et al.*, 2005). The sequence of ether rings in KBT-F was confirmed by MS/MS spectra (MALDI-TOF-TOF, high collision energy) of a KBT-F benzene sulphonate derivative which contains a ready ionisable group ( $-\text{SO}_3\text{Na}$ ) and gave a sequence of distinctive ions arising from cleavages at each ether ring junction (Hamamoto *et al.*, 2012). The many structural differences between BSXs and KBTs indicate that these toxin groups are unlikely to share the same biosynthetic pathways. The structures of other KBTs have not yet been determined. The UV absorbance  $\lambda_{\text{max}}$  for KBT-G, -H, and -I is the same as that for KBT-F and gymnocins (Hamamoto *et al.*, 2012; Satake *et al.*, 2002; Satake *et al.*, 2005). The daughter ion spectra using TSQ MS/MS show that the major fragment ion at  $[\text{M}+\text{H}-84]^+$  for KBT-F is the same as that for KBT-G, while it is shifted to  $[\text{M}+\text{H}-100]^+$  for KBT-H or -I. Together this data suggests that the  $\text{CH}_2\text{O}$  difference between KBT-F and KBT-G is somewhere within the ether rings, but the difference between KBT-F / -G and their oxidative analogues (KBT-H/-I) is hydroxylation of the methyl group on the butenal side chain (Figure 8-2).

In addition to the four KBTs (-F, -G, -H & -I) which have been isolated, there were four other novel compounds also identified by LC-MS in SPE extracts of *K. brevisulcata* cultures (Table 4-5, Figure 4-1B). Except M1917, all three compounds plus KBT-H and KBT-I show interesting relationships to KBT-F or KBT-G which may be the parent compounds for other KBTs. A possible metabolism for the side chain of these KBTs in *K. brevisulcata* cells is proposed in Figure 8-2. The m.w. for M2135, M2165 and M2181 are 80 Da higher than that of KBT-F, -G and -I respectively, and the  $\text{ESI}^+$  mass spectra (Figure 4-6) show a peak corresponding to  $[\text{M}+\text{H}-\text{SO}_3]^+$ , suggesting that they are sulphated analogues (Figure 8-2). The sulphate of KBT-H ( $[\text{M}+\text{H}]^+$  2151) may be produced by *K. brevisulcata*. However, the corresponding peak was not detected in the SPE extracts by LC-MS. More detailed studies for these sulphated KBT analogues are required in the future to determine the positions of sulphation and their toxicities. M1917 is the smallest compound isolated with the m.w. >1200



Da. The UV and LC-MS studies show that this compound does not contain an acidic group or  $\beta$ -unsaturated carbonyl group which is on the terminal side chain of known KBTs. M1917 may be a breakdown fragment from KBTs, an intermediate in KBT metabolism or some other polycyclic ether compound not directly related to KBTs.

Toxicological studies were conducted with KBT-F and KBT-G using several bioassays. Aside from studies with P388 and Vero cells, this research was conducted through collaborations but using material isolated from culture extracts prepared as a part of this PhD. KBT-F and KBT-G are 50-200 fold more potent in mouse bioassays with i.p. administration than BSXs, and 5-fold more potent than brevetoxin-2 (Baden & Mende, 1982). Liver, diaphragm, spleen, pancreas and stomach are primary target tissues for KBTs. Preliminary histological studies showed pulmonary haemorrhage, dilatation of renal tubules, oedema and erosion of the stomach, and areas of necrosis in the thymus. The preliminary MBA with oral gavage (Y. Ito, pers. comm.) showed KBTs can pass through the gastrointestinal lining and may be of risk to human health from the seafood chain. However, the distribution of KBTs in mouse plasma and the oral LD<sub>50</sub>'s for KBT-F and KBT-G have not been determined because of lack of sufficient research material. High cytotoxicities for KBT-F and KBT-G were observed in P388, Vero and Neuro2a assays. Neuro2a cells treated with ouabain/veratridine are widely used for VGSC toxins. The EC<sub>50</sub>'s for KBTs against sensitised Neuro2a cells were 30-73 nM, higher than that for BSX-4 and BSX-5 (Table 6-6) and the cytotoxicity of KBTs was maintained in the absence of ouabain/veratridine. These studies revealed that the mode-of-action of KBTs differs from BSXs and brevetoxins, and does not involve sodium channels. The positive VGSC toxicity in neutral extracts of *K. brevisulcata* cultures reported in a previous study (Truman, 2007) is more likely to be caused by lipophilic BSXs (-3 to -6, Section 6.3.8) (Holland *et al.*, 2012). The Bignami assay confirmed that KBTs are strongly haemolytic, although the activities were 200x less than palytoxin, the positive control in this assay. Toxicological studies for KBT-H and KBT-I have not been completed due to lack of pure materials. A preliminary study by Japanese co-workers using mouse leukemia cells revealed that KBT-H and KBT-I were 2-4 fold more cytotoxic than KBT-F and KBT-G respectively. More detailed studies for these oxidative analogues and their sulphates are necessary in the future.

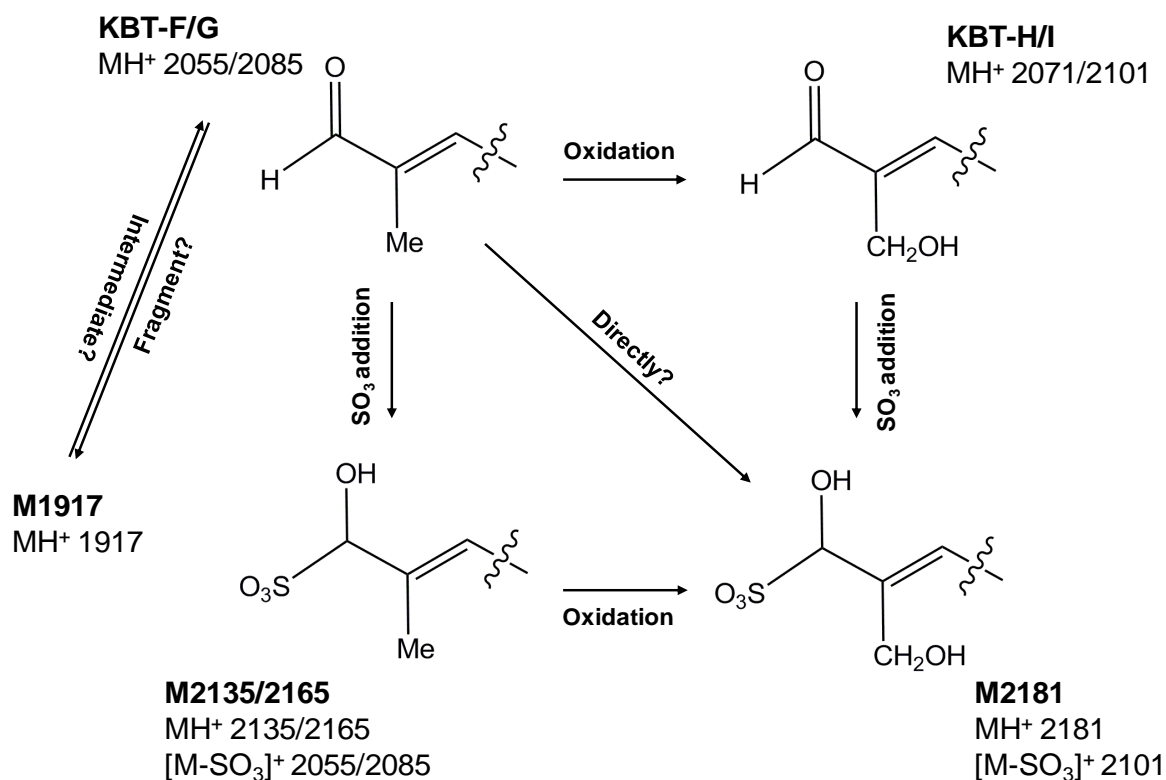


**Figure 8-2.** Possible metabolism of the side-chain of KBTs in *K. brevisulcata* cells. Information on the position of sulphation is conjectural and this could be on one of the OH groups in the ether ring systems.

## 8.6 *In vitro* cell bioassays for algal toxin research

*In vitro* cell bioassays have been widely used for algal toxin research over the past three decades (Bellocci *et al.*, 2008; Dragunow *et al.*, 2005; Katsuo *et al.*, 2007; Kharrat *et al.*, 2008; Manger *et al.*, 2003; Manger *et al.*, 1993; Roth *et al.*, 2007; Tachibana *et al.*, 1981; Truman *et al.*, 2002; Xia *et al.*, 2008; Yasumoto & Satake, 1998). In this PhD project, two mammalian cell lines were selected and used to establish *in vitro* cell bioassays at Cawthron Institute for (i) direct evaluation of cytotoxicity of marine microalgae, (ii) guiding biotoxin isolation, (iii) cytotoxicity assessment for pure algal toxins and (iv) investigation of mode-of-action of biotoxins.

P388 and Vero cell lines were selected due to their ease of culture and specific characteristics. P388 cells (murine lymphoid macrophage) have a broad specificity and high sensitivity to toxins, and are suited for investigation of multiple classes of biotoxins. Japanese researchers have used P388 cell line (ATCC) to guide the isolation of many algal toxins e.g. gymnocins, KBTs, OA and pinnatoxins (Hamamoto *et al.*, 2012; Kita & Uemura, 2005; Satake *et al.*, 2002; Satake *et al.*, 2005; Tachibana *et al.*, 1981; Yasumoto & Satake, 1998).

Higher sensitivity to algal toxins was observed for P388 cells than Vero cells (Table 6-5). Therefore, cell assays based on P388 were developed for investigation of mode-of-action in this study. Vero cell line (African green monkey kidney epithelial cells) is more resistant to seawater than other mammalian cells and was used to develop direct exposure experiments for *Alexandrium* and *Heterocapsa* species (Katsuo *et al.*, 2007). In this toxicological study, Vero cells were directly exposed to *K. brevisulcata* and *K. mikimotoi* for studying fish killing mechanisms of different *Karenia* species (Section 7.3.7), which will be discussed in the next section (Section 8.7).

A total of nine algal toxins were evaluated by both P388 and Vero cell bioassays using measurement of cell viability with MTS reagent (Table 6-5). Compared to MTT reagent which is commonly used in cytotoxicity studies (Table 2-4), MTS assay is simpler to use (water soluble versus water insoluble) and time saving (1-4 hr versus overnight) (Twiner *et al.*, 2007; Twiner *et al.*, 2005). The cytotoxicities of the toxins tested by MTS cell viability assay are summarised in Table 6-5. The cytotoxicity order established was KBT-G > C402 > KBT-F > OA/OA diol esters > BSXs. The four BSXs showed the weakest cytotoxicities to both P388 and Vero cells (Table 6-5), but were relatively high cytotoxic to Neuro2a cells in the presence of ouabain and veratridine (Table 6-6). Unlike Neuro2a, neither P388 nor Vero cells are good models for investigation of VGSC toxins such as STX, CTX and brevetoxins.

KBT-F and KBT-G were highly cytotoxic with EC<sub>50</sub>'s of 3-7 nM after 24 or 72 hr exposure (Table 6-5). Cell membrane disintegration of both P388 and Vero cells was observed by inverted microscopy after exposure to either KBTs or palytoxin (positive control). This matched previous studies that biotoxins produced from *K. brevisulcata* could "dissolve" the cell membrane of Neuro2a cells, and disintegrate both the cell wall and the cell membrane of dinoflagellate cells (Chang, 2011; Truman *et al.*, 2005).

C402 is a novel compound isolated from the dinoflagellate which is widely distributed in Pacific area. In contrast to KBTs, C402 showed weaker toxicity in MBA (Table 6-3), but similar strong cytotoxicity to P388 and Vero cells (Table 6-5). The cell morphological changes induced on exposure to C402 are similar to those caused by OA (potent inhibitor of protein phosphatases and an apoptosis inducer) e.g. rounded or flattened cells, detachment and loss of microvilli and focal adhesion structure (Amzil *et al.*, 1992; Aune *et al.*, 1991; Oteri *et al.*, 1998; Perez-Gomez *et al.*, 2004; Tubaro *et al.*, 1996). The morphological differences to those caused by KBTs (disintegration of cell membranes) indicate different modes-of-action for C402 and KBTs.

To further investigate the modes-of-action of these algal toxins, P388 cell assays were developed for multiple end-point measurements including LDH release/cell viability (Section 6.3.5), caspase-3 colorimetric assay (Section 6.3.6), and LDH release/caspase-3/7 activity (Section 6.3.7). The results suggested that C402 is likely to be an apoptosis inducer similar to staurosporine that induces cell death through a caspase-3 dependent apoptosis pathway (Jantas-Skotniczna *et al.*, 2006; Yue *et al.*, 1998). KBT-F caused cell membrane disintegration and this loss of cell viability is strongly associated with mitochondrial dysfunction (Section 6.3.5). The increase of caspase-3/7 activity, the critical biomarker of apoptosis, was not detected in P388 cell bioassays over 24 hr exposure with 5 nM KBT-F (Sections 6.3.6 & 6.3.7), indicating that KBT-F induced cell death does not involve caspase-3 cleavage. The cytotoxicity of KBTs may be cell membrane targeted rather than apoptotic. Future research may need to consider whether KBTs have a similar mode-of-action to palytoxin (haemolysin, Na<sup>+</sup>/K<sup>+</sup> ATPase disruptor) (Bellocci *et al.*, 2008; Guennoun-Lehmann *et al.*, 2007; Habermann, 1989) or MTX (voltage gated calcium channel toxin) (Trevino *et al.*, 2008; Xi *et al.*, 1992).

## 8.7 Effects of *Karenia* species on marine biota and implications for ecotoxicology

The toxic effects of *Karenia* on marine biota vary depending on the species, strains, growth stage, test organisms and exposure conditions. Often it has been unclear which particular toxins have been present and what mode-of-action led to the observed effects in exposed organisms. In this study, toxicity investigations for cultures of three *Karenia* species were conducted on two commercial fish species and the larvae of six representative coastal invertebrate species.

*K. mikimotoi* caused no short-term effects on snapper at a concentration of  $3.4 \times 10^6$  cells L<sup>-1</sup>, which is at the higher end of cell densities reported for fish-killing *K. mikimotoi* blooms in Ireland and New Zealand ( $0.5\text{--}4 \times 10^6$  cells L<sup>-1</sup>) (Silke *et al.*, 2005; Smith *et al.*, 2007). In a recent study of Kareniaceae ichthyotoxicity, live or lysed cells of *K. mikimotoi* (up to  $10 \times 10^6$  cells L<sup>-1</sup>) were also found to be non-toxic to sheepshead minnow larvae (*Cyprinodon variegatus*) (Mooney *et al.*, 2010). *Karenia mikimotoi* can produce several potentially toxic compounds, including gymnocins, haemolysins and ROS (Haywood *et al.*, 2004; Munday *et al.*, 2004; Satake *et al.*, 2002; Satake *et al.*, 2005; Yamasaki *et al.*, 2004; Yasumoto *et al.*, 1990). It is a cosmopolitan species and there may be a range of sub-species with varying

toxicities and modes-of-action (Zou *et al.*, 2010). The strain of *K. mikimotoi* used in this fish study (CAWD 63) was isolated from the northern coast of New Zealand in 1993 and is suspected to be one of the toxic dinoflagellates which caused the severe 1993 HAB event. The LC-MS studies of cell extracts showed that this strain of *K. mikimotoi* is a producer of several novel polyether compounds (Table 4-9). The toxicity and mode-of-action of these novel compounds are still unclear, but cytotoxicity bioassays using P388 and Vero cells showed that these novel compounds were unlikely to be highly cytotoxic (Table 7-4). Yamasaki *et al.* (2004) reported that *K. mikimotoi* isolated from Western Japan can produce ROS similar to raphidophyceae flagellates involved in fish kills e.g. *Chattonella marina* and *Heterosigma akashiwo* (Ishimatsu *et al.*, 1996; Oda *et al.*, 1997; Yang *et al.*, 1995). Zou *et al.* (2010) indicated that ROS production depended on the *K. mikimotoi* strain and two other Japanese strains did not generate ROS. In this study, ROS and haemolysins were not investigated. Hallegraeff (1995) classified *K. mikimotoi* as a red tide causative species that was non-toxic to humans but harmful to fish and invertebrates through a gill-damage mechanism. However, the histological study presented here did not show significant fish gill damage in snapper after 48 h exposure to *K. mikimotoi*. These results support the toxicity mechanism proposed in some previous studies, namely, fish mortality in *K. mikimotoi* HABs is mainly due to environmental stressors resulting from high cell densities, such as depletion of dissolved oxygen (Landsberg 2002; Yamasaki *et al.* 2004; Silke *et al.* 2005), although roles of other toxic agents have not been ruled out.

*K. brevis* and *K. brevisulcata* were both toxic to juvenile snapper and salmon. *K. brevis* is the representative red-tide causative dinoflagellate and has been responsible for many mass mortalities of fish in the Gulf of Mexico over the decades (Magaña *et al.*, 2003). HAB events involving this alga have been widespread and have affected hundreds of species of marine vertebrates and invertebrates (Landsberg, 2002). Quick and Henderson (1974) suggested exposure of fish to *K. brevis* at  $0.005\text{--}0.25 \times 10^6$  cells L<sup>-1</sup> for days or weeks usually triggers fish morbidity. In my study, salmon were killed in less than one hour after exposure to a similar concentration ( $0.18 \times 10^6$  cells L<sup>-1</sup>, Table 1). The sensitivities of snapper and salmon to *K. brevis* were different. Exposure of juvenile fish to  $4.6\text{--}5.9 \times 10^6$  cells L<sup>-1</sup>, resulted in LT<sub>50</sub> of 4.5 hr for snapper and 0.17 hr for salmon. Salmon therefore seem to be more sensitive than snapper to *K. brevis*. The signs of intoxication observed in snapper and salmon, including panic and loss of balance, were similar to those reported previously for fish exposed to *K. brevis* (Baden, 1989; Landsberg, 2002). Brevetoxins produced by *K. brevis* are potent ichthyotoxins and, as with mammals, the toxicity is strongly associated with binding to VGSC leading to uncontrolled sodium flux and disruption of neural transmission (Baden, 1989). The

toxic mechanism of *K. brevis* in fish is believed to relate to brevetoxins from cells or water being absorbed directly across the gill membranes of fish. Type A brevetoxins such as brevetoxin-1 are more potent than Type B brevetoxins (brevetoxin-2, brevetoxin-3) (Abraham *et al.*, 2006; Baden, 1989; Landsberg, 2002).

The only reported *K. brevisulcata* bloom occurred in New Zealand during the austral summer of 1998 along the SE coast of the North Island and in Wellington Harbour. Cell concentrations reached  $33 \times 10^6$  cells L<sup>-1</sup> and this red tide event severely impacted on the local marine ecosystem with mass mortalities of vertebrates and invertebrates (Chang 1999b; Wear & Gardner 2001; Gardner & Wear 2006; Kröger *et al.* 2006). It is an interesting question as to the origin of this species and factors that might give rise to another bloom are not well understood, although very particular water conditions were measured during the 1998 bloom (Chang *et al.*, 2001). Visible blooms dominated by *Karenia* dinoflagellates, especially *K. mikimotoi*, regularly occur in the Hauraki Gulf. Chang (2003) reported *K. brevisulcata* as a minor component of one of these *Karenia* blooms. However, *K. brevisulcata* has not been reported over the past 14 years of phytoplankton monitoring by NZ MoH/MAF.

In the *in vivo* bioassays with *K. brevisulcata* at ca.  $11 - 16 \times 10^6$  cells L<sup>-1</sup> the LT<sub>50</sub> was 7.5 and 0.5 hr with juvenile snapper and salmon respectively. Both fish species showed similar signs of intoxication to those observed in the *K. brevis* bioassays. In the fish bioassays, only snapper exposed to *K. brevisulcata* for 7.5 – 10.5 hr had minor disintegration of the gill filaments. The lack of observable gill damage in salmon may be due to the shorter experimental period (< 1 hr). Fish gill damage by *K. brevisulcata* is not likely to be the major toxic mechanism leading to fish morbidity. While longer exposures of fish to lower cell concentrations would be of interest, bioethical considerations preclude such experiments.

*K. brevisulcata* produces two classes of novel complex polycyclic ether biotoxins: KBTs and BSXs. The toxicological studies showed that KBTs are 50-200 fold more potent in mouse bioassays (i.p. administration) than BSXs and are also cytotoxic and haemolytic (Holland *et al.*, 2012). These high molecular weight KBT toxins could not be accurately monitored by LC-MS when this experiment was conducted. However, some preliminary analytical data showed that concentrations of KBT-F and KBT-G in *K. brevisulcata* cultures were of similar order of magnitude to those of BSX-1 and BSX-2 respectively (Table 4-7) (Holland *et al.*, 2012; Shi *et al.*, 2012). Subsequent validation of the LC-MS MRM method (Method 4) for KBTs and BSXs showed that *K. brevisulcata* culture at G<sub>max</sub> do indeed produce comparable concentrations of these toxins (Table 4-7). The total concentration of each class was ca. 2.5 pg cell<sup>-1</sup> for BSXs and 1.2 pg cell<sup>-1</sup> for KBTs respectively. The main contributors to toxicity in

these bioassays and to fish kills in the Wellington Harbour bloom event may have been KBTs rather than BSXs. However, the tested fish showed the similar neurotoxic symptoms after exposure to *K. brevis* and *K. brevisulcata*, suggesting that potentially synergistic activities of BSXs and KBTs may contribute substantially to the overall neurotoxicity of *K. brevisulcata*.

Marine invertebrate larvae have been widely used in ecotoxicology, and more recently were used for toxic microalgae research (Botes *et al.*, 2003; Rhodes *et al.*, 2006). These bioassays are cheap, simple, reproducible, and more relevant to “actual” toxic effects of microalgae in blooms. In this PhD study, an assay using six NZ invertebrate larvae was developed in multi-well plates to evaluate toxicities of three *Karenia* species and investigate their potential mechanisms of toxic effects.

Brine shrimp were unaffected by any of the three *Karenia* species tested. This confirms the data reported by Botes *et al.* (2003) where *A. salina* larvae were unaffected by exposure to a range of toxic dinoflagellates including *K. brevis*, *K. mikimotoi* and *K. cristata* (<10% mortality at 24 h for cell concentrations  $1-10 \times 10^6$  cells L<sup>-1</sup>). This hardy organism, commonly used for ecotoxicology assessments, may not be sensitive to many algal toxins. However, seawater collected during the *K. brevisulcata* bloom event in 1998 did show quite strong effects on *A. salina* (F.H. Chang, pers. comm.). It cannot be ruled out that the toxin profile has changed or the toxin quota is now reduced in the strain of *K. brevisulcata* maintained due to sub-culturing in the CICCM over the decade since it was collected.

No acute effects of *K. brevis* or *K. mikimotoi* were observed with the two bivalve mollusc species tested. However, Greenshell<sup>TM</sup> mussel larvae (5-6 d old) gave a consistent increase in the severity of symptoms over 24 h when exposed to a *K. brevisulcata* concentration of  $8.4 \times 10^6$  cells L<sup>-1</sup> (Figure 7-3B). Pacific oyster larvae were less sensitive to *K. brevisulcata*, but still exhibited severe symptoms at high cell densities. The main reported effect of HABs on shellfish is reduced feeding, with mortality generally only occurring at very high cell densities where anoxia and other physical mechanisms may predominate. Shellfish appear well adapted to the common algal toxins and can accumulate them to levels that are harmful to predatory vertebrates, including humans. Therefore, the high toxicity of *K. brevisulcata* is unusual. The similar effects on mussel larvae of the lipophilic SPE extract of a young mass culture (29d, equivalent well concentration  $72 \times 10^6$  cells L<sup>-1</sup>) and an old *K. brevisulcata* mass culture (56 d, living cell free) confirm that the toxic agents against invertebrates can be extracted from water and cells by absorption to polymeric material and that these toxins are still present in the medium after algal cells decay. BSXs were at similar concentrations in the older cell free culture and the SPE extract of a live culture (28 versus 31

$\mu\text{g L}^{-1}$ ). However, no acute effects on Greenshell<sup>TM</sup> mussel larvae were observed following exposure to the four individual BSX toxins at a dose of  $100 \mu\text{g L}^{-1}$ . KBTs are also recovered from mass cultures by the SPE method (Holland *et al.*, 2012) (Section 4.3.2.2). From their higher acute toxicity to mice and mammalian cells, it is concluded that KBT toxins are likely to be the main toxic agents against invertebrates following exposure to *K. brevisulcata*. KBTs may also leak into seawater medium from dead or damaged *K. brevisulcata* cells, similar to BSX toxins. In direct exposure experiments, Vero cells were 100% killed by either cell free supernatants or mass cultures of *K. brevisulcata* as the cell concentrations were  $> 5 \times 10^6 \text{ cells L}^{-1}$  (Figure 7-8A). In contrast, no cytotoxicity was detected in cell free supernatants of *K. mikimotoi* cultures even when the cell concentrations were up to  $30 \times 10^6 \text{ cells L}^{-1}$  (Figure 7-3B). The results confirmed the proposal that highly toxic agents, which may be mainly KBTs, can be directly released from *K. brevisulcata* cells into seawater and can lead to mass mortalities of marine animals (Holland *et al.*, 2012; Shi *et al.*, 2012). However, the toxic agents of *K. mikimotoi* are mainly in the algal cells. Thus fish are more likely to be killed in *K. mikimotoi* blooms by direct contact of gill cells with algal cells which may release haemolytic toxins and induce gill damage. Synergistic effects may also be important whereby damage to gills from toxins make fish more sensitive to low oxygen potentials resulting from algal blooms.

Paua larvae were also very sensitive to *K. brevisulcata*, supporting observations at the time of the 1998 bloom (Chang, 1999b). Paua larvae were also the only invertebrate tested that was sensitive to *K. mikimotoi* (24 h  $\text{LC}_{50}$  of  $2 \times 10^6 \text{ cells L}^{-1}$ ). Effects on paua were observed at a hatchery in Northland during a major bloom of *K. mikimotoi* in 2002 (F.H. Chang, pers. comm.). Botes *et al.* (2003) have reported bioassay data (24 hr) for *Haloitidis midae* larvae where *K. mikimotoi* gave a  $\text{LC}_{50}$  of  $1.1 \times 10^6 \text{ cells L}^{-1}$  and *K. brevis* gave  $<10\%$  mortality at the highest concentration tested ( $<10 \times 10^6 \text{ cells L}^{-1}$ ). These data for South African abalone larvae match our data for the New Zealand species. The South African study also included abalone spat and this growth stage was very sensitive to all the *Karenia* species tested (Botes *et al.*, 2003). There is increasing cultivation of abalone species worldwide and blooms of these *Karenia* species are therefore a threat to abalone aquaculture industry.

*K. brevisulcata* blooms occurring near commercial aquaculture farms may directly cause unacceptable economic losses. For *K. brevis*, the early warning trigger for potential shellfish contamination and closure of growing areas for harvesting is when cell concentrations reach  $0.5 \times 10^4 \text{ cells L}^{-1}$  (Haywood *et al.*, 2007). A trigger for *K. brevisulcata* is also required for



bivalve mollusc farms and cage fisheries to provide early warning of potential damage from blooms of this unusual *Karenia* species. Although accumulation of toxins in seafood from this species has not been established, the present data indicates direct toxicity may be more of an issue, especially for juvenile salmon, shellfish, and paua larvae. From the data gathered in this study, a provisional trigger of  $1 \times 10^4$  cells  $L^{-1}$  is recommended.

## 8.8 Future directions

My studies on *K. brevisulcata* and the two suites of biotoxins have raised numerous interesting questions. It would be valuable to address these with further investigations.

To obtain sufficient crude toxins, *K. brevisulcata* was cultured under laboratory conditions. The fate of BSXs in *K. brevisulcata* cultures have been investigated, but the fate of KBTs remains still unclear because there was no validated method to monitor KBT production when the culturing experiments were conducted. Determination of KBT fate in *K. brevisulcata* cultures using the validated LC-MS method in the future will contribute to better understanding the inter-relationship between the two suites of biotoxins produced and enable bulk culturing under optimised conditions for production and isolation of these toxins.

Six BSXs were identified in extracts of *K. brevisulcata* cultures using LC-MS. Four of these BSXs have been isolated and purified for analytical, chemical and toxicological studies. However, the related studies for BSX-3 and BSX-6 were not conducted in this PhD project. Results of this research showed that BSX-6 is possibly an important parent compound in BSX metabolism. This compound may have the most similar structure to brevetoxin-1 amongst BSXs, and is potentially the most toxic. The isolation and purification of BSX-3 and BSX-6 will be valuable in the future for (i) establishment of more accurate analytical methods, (ii) structural determination, (iii) toxicity assessment and (iv) bio- or chemical- synthesis studies of BSXs.

Japanese collaborators have isolated and characterised KBT-F, KBT-G, KBT-H and KBT-I from the bulk extracts of *K. brevisulcata* produced at Cawthron. Four other large KBT-related compounds were identified in SPE extracts, but they have not been isolated and purified from mass cultures yet. My preliminary LC-MS studies suggested that some of these compounds (M2135, M2165, and M2181) were sulphated analogues of KBT-F, KBT-G and KBT-I respectively. They gave similar chemical characteristics to their parent KBTs in UV

and MS spectra. It would be useful to isolate and purify them for analytical, chemical and toxicological studies in the future.

Toxicological studies of BSXs, KBTs and C402 were carried out using several bioassays in this PhD study. BSXs are VGSC toxins similar to brevetoxins but with lower toxic potency. KBTs are unlikely to be either VGSC toxins or apoptosis inducers. The haemolytic activity and strong toxicity of KBTs suggested that the mode-of-action of KBTs may be similar to palytoxin or MTX, but further studies are required to confirm this. *In vitro* bioassays using P388 cells provided strong evidence that C402 is an apoptosis inducer similar to staurosporine, and involved caspase-3 activation. There is strong interest in novel apoptotic reagents for biomedical research. More experiments are required for further investigations of the activity and mode-of-action of C402 e.g. Annexin-V staining assay, TUNEL assay or DNA ladder electrophoresis, and mitochondrial assays.

The fish and larvae bioassays confirmed that *K. brevisulcata* is highly toxic to marine fish and invertebrates. KBTs rather than BSXs are more likely to be main toxic agents responsible for fish- and invertebrate larvae-killing. The toxic potency of individual KBTs to marine organisms has not been evaluated due to lack of sufficient materials. Detailed toxicity assessments for KBTs will be required. In addition to polycyclic ether toxins, *K. brevisulcata* may also produce ROS like *K. mikimotoi*. ROS were not investigated in this study, and will be valuable for future study to better understand the fish-killing mechanism of *K. brevisulcata* and other *Karenia* species.

Bioaccumulation of BSXs and KBTs in marine biota still remains unclear because no contaminated samples were collected from the *K. brevisulcata* bloom in 1998. In the future, to obtain contaminated samples, shellfish e.g. Greenshell<sup>TM</sup> mussel, oysters or cockle can be fed with low levels of *K. brevisulcata* for days to weeks under laboratory conditions. These samples can be extracted and analysed by the LC-MS/MS (MRM) method to assess potential risks of *K. brevisulcata* and its toxins to human health via the seafood chain.

In the case of *K. brevis*, several small ladder-frame polycyclic ethers were identified, isolated and purified by Prof. Satake, e.g. brevenal and brevisin (Satake *et al.*, 2008; Satake *et al.*, 2009). They can inhibit the binding of [<sup>3</sup>H]-BTX-3 to its binding site on the VGSC in rat brain synaptosomes and exhibit antagonism of the sodium channel activity of the brevetoxins. Related low molecular weight VGSC active compounds from *K. brevisulcata* were not investigated in this PhD project and may be an interesting topic for the future.

Nine strains of *K. mikimotoi* were also investigated by LC-MS in this PhD project and several novel polycyclic ether compounds have been identified in their cell pellets. Some of the compounds are cytotoxic to mammalian cells and possibly also toxic to marine biota. Isolation and purification of cytotoxic compounds in the future will be helpful to better understand the fish-killing mechanism of *K. mikimotoi*. The strains of this species appear to be unusually heterogeneous in their production of toxins and further studies on strain specificity and molecular genetics are required.

## 8.9 Summary of findings

A toxic dinoflagellate *K. brevisulcata* was isolated from the Wellington Harbour during a major bloom event in 1998, which caused mass mortalities of marine vertebrates and invertebrates (Chang, 1999a; Wear and Gardner 2001). The previous studies have revealed this novel species produces a toxin complex containing multiple toxins (Chang, 1999b; Keyzers, pers. comm.; Truman, 2007; Truman *et al.*, 2005). However, the previous toxin isolation work by Keyzers (pers. comm.) was incomplete due to the lack of sensitive and specific detection methods. *K. brevisulcata* produces two novel classes of toxins: BSXs and KBTs. BSXs are ladder polycyclic ether compounds with medium molecular weights (800-1000 Da). KBTs are complex polycyclic ethers with high molecular weights (1900-2200 Da).

A validated LC-MS (SIR) method was developed to quantitatively analyse BSXs in *K. brevisulcata* cultures, and isolate and characterise the toxin fractions (Holland *et al.*, 2012). After pure BSXs and KBTs were produced, a LC-MS/MS (MRM) method was developed for quantitative analysis of six BSXs and four KBTs. A preliminary validation of this method for BSXs and KBTs has been completed. The calibration for those toxins tested was highly linear with  $R^2 > 0.99$  over the concentration range of 5-200 ng mL<sup>-1</sup>. Recoveries for BSXs and KBTs from algal culture using algal extract/pure toxins were 46-102%. The MRM method precision was high for all toxins with RSDs 2-15%. The LOQs for BSXs and KBTs were ca. 2 ng mL<sup>-1</sup> (0.15 µg L<sup>-1</sup> culture), more sensitive than the SIR method, and showing potential for monitoring of seawater and contaminated samples of fish and shellfish.

In addition to quantitation methods, lack of sufficient crude materials limits studies on algal toxins and their accurate monitoring in the marine environment. In this study, *K. brevisulcata* was bulk cultured under different laboratory conditions for production of mg quantities of toxins (Beuzenberg *et al.*, 2012). The large volume automated photobioreactor shows great promise for further development to produce sufficient levels of toxins from

dinoflagellate cultures for structural characterisation, analytical standard production, investigation of mode-of-action, and subsequent pharmaceutical appraisals.

Six BSXs have been identified by LC-MS in extracts of *K. brevisulcata* cultures. Milligram quantities of BSX-1 and BSX-2 were isolated and purified from the acidic fractions sourced from a total of 1109 litres of unlabelled and  $^{13}\text{C}$ -labelled cultures using partitioning and multiple steps of chromatography (Holland *et al.*, 2012). Their lactone ring-closed derivatives BSX-4 ( $\text{C}_{49}\text{H}_{70}\text{O}_{15}$ ) and BSX-5 ( $\text{C}_{47}\text{H}_{66}\text{O}_{14}$ ) were produced by acidic catalysis from the ring-opened BSXs. Preliminary chemical studies on these BSXs (UV, MS/MS, NMR, micro-derivatisation) showed structural similarities to brevetoxin-1 but with some differences in the polyether rings and a longer, carboxylated side chain. Full structural elucidations by NMR are currently incomplete due to conformer effects on the spectra, presumably from a very flexible system of 7-, 8- plus 9-membered central polyether rings.

Toxicological studies based on these pure BSXs showed they are weakly toxic i.p. to mice and are VGSC agonists but weaker than brevetoxin-2 (Holland *et al.*, 2012). Culture extracts contain mainly BSX-1 and BSX-2 but the primary toxins produced by the cells are proposed to be BSX-4 and BSX-5, which are converted to the ring opened compounds by hydrolysis of the lactone when released from the cells to the culture medium. Similar but less substantial hydrolysis was observed for brevetoxins from *K. brevis*, confirming observations from Florida (Abraham *et al.*, 2006). In addition, two other BSXs (-3 & -6) were identified in SPE extracts of *K. brevisulcata* cultures by LC-MS. BSX-6, containing an unsaturated aldehyde side chain, is more similar to brevetoxin-1 in chemical structure than BSX-4, and may be an important intermediate in BSX metabolism.

Brevisulcenals (KBTs) are a complex of high molecular weight polycyclic ether toxins. LC-MS scanning studies indicated there are at least eight KBTs in SPE extracts of *K. brevisulcata* cultures (Holland *et al.*, 2012). Four KBTs have been isolated and purified at the University of Tokyo (Professor Masayuki Satake group) using the neutral fractions of large-scale *K. brevisulcata* cultures produced at Cawthron Institute. UV spectra and daughter ion MS suggest that KBT-F and KBT-G have some similarities to gymnocins, including a methyl butenal side chain, but KBTs are larger molecules and more toxic than gymnocin-B (Satake *et al.*, 2005). Structural elucidation of KBT-F ( $\text{C}_{107}\text{H}_{160}\text{O}_{38}$ ) by NMR and MS/MS (TOF-TOF) has resulted in the complex structure of this toxin being reported (Hamamoto *et al.*, 2012). Related studies on KBT-G, -H and -I are proceeding using NMR of  $^{13}\text{C}$ -enriched toxins isolated from cultures grown at Cawthron with added  $\text{NaH}^{13}\text{CO}_3$ . The preliminary data suggests that the structural difference between KBT-F and KBT-G (+ $\text{CH}_2\text{O}$ ) occurs in the

ether rings. KBT-H and KBT-I are the oxidative analogues of KBT-F and KBT-G respectively with hydroxylation of the  $\beta$ -methyl group on the side chain.

Toxicological studies with pure KBT-F and KBT-G revealed they are very toxic i.p. to mice, strongly haemolytic, and highly cytotoxic to P388, Vero and Neuro2a cells, but are unlikely to be VGSC agonists (Holland *et al.*, 2012). Further development of end-points for cytotoxicity assays revealed that damage to P388 cells by KBT-F involved effects on membranes but apoptotic mechanisms were not involved. Other KBT-related compounds (M2135, M2165 and M2181) have similar chemical characteristics to the isolated KBTs and are suggested to be the sulphated analogues of KBT-F, KBT-G and KBT-I respectively. Isolation and purification of these compounds in the future will contribute to better understanding of toxin production by *K. brevisulcata* and its overall toxicity.

*In vivo* bioassay studies with two fish species and larvae of five marine invertebrate species have confirmed observations during bloom events that *Karenia* species are toxic to marine biota and that the toxicity varies amongst both the algal species and test organisms (Shi *et al.*, 2012). *Karenia brevisulcata* has broad toxicity to fish and marine invertebrates and data is provided on the cell densities where harmful effects become pronounced. The chemical and ecotoxicological studies indicate that *K. brevisulcata* cells are very fragile and “leaky”, more so than *K. brevis*, and readily release BSXs and the more lethal KBTs into the surrounding seawater. *K. brevisulcata* is a high risk to coastal marine ecosystems, more so than *K. brevis* and *K. mikimotoi*, and poses a direct threat to aquaculture (fish and shellfish). This PhD study has provided preliminary analytical, chemical and toxicological investigations of *K. brevisulcata* and the toxins produced. The results will assist aquaculture, fish farmers and local governments by providing valuable information that can be applied to protection of shellfish aquaculture, cage fisheries and marine ecosystems from blooms of harmful *Karenia* species.

## References

- Aasen, J., Torgersen, T., & Aune, T. (2002, Jun 4–8). *Application of an improved method for detection of lipophilic amrine algal toxins (OA.DTXs, PTXs, YTXs AND AZAs) with LC/MS*. Paper presented at the 4<sup>th</sup> International Conference on Molluscan Shellfish Safety, Santiago de Compostella, Spain.
- Abraham, A., Plakas, S. M., Wang, Z. H., Jester, E. L. E., El Said, K. R., Granade, H. R. *et al.* (2006). Characterization of polar brevetoxin derivatives isolated from *Karenia brevis* cultures and natural blooms. *Toxicon*, 48(1), 104-115.
- Aebersold, R., & Mann, M. (2003). Mass spectrometry-based proteomics. *Nature*, 422(6928), 198-207.
- Alkhalaf, M., El-Mowafy, A., Renno, W., Rachid, O., Ali, A., & Al-Attyiah, R. (2008). Resveratrol-induced apoptosis in human breast cancer cells is mediated primarily through the caspase-3-dependent pathway. *Archives of Medical Research*, 39(2), 162-168.
- Amzil, Z., Pouchus, Y. F., Le Boterff, J., Roussakis, C., Verbist, J. F., Marcaillou-Lebaut, C. *et al.* (1992). Short-time cytotoxicity of mussel extracts: A new bioassay for okadaic acid detection. *Toxicon*, 30(11), 1419-1425.
- Anderson, D. M., Glibert, P. M., & Burkholder, J. A. M. (2002). Harmful algal blooms and eutrophication: nutrient sources, composition, and consequences. *Estuaries and Coasts*, 25(4), 704-726.
- APHA (1985). *Laboratory procedure for the examination of seawater and shellfish*: American Public Health Association.
- Arbab, A. S., Bashaw, L. A., Miller, B. R., Jordan, E. K., Lewis, B. K., Kalish, H. *et al.* (2003). Characterization of biophysical and metabolic properties of cells labeled with superparamagnetic iron oxide nanoparticles and transfection agent for cellular MR imaging. *Radiology*, 229(3), 838-846.
- Arzul, G., Gentien, P., Bodennac, G., Toularastel, F., Youenou, A., & Grassous, M. P. (1995). Comparison of toxic effects in *Gymnodinium cf. nagasakiense* polyunsaturated fatty acids. In Lassus, P. *et al.* (Eds.), *Harmful Marine Algal Blooms* (pp. 395-400). Paris: Lavoisier.
- Aune, T. (2008). Risk assessment of marine toxins. In Botana, L. M. (Ed.), *Seafood and Freshwater Toxins: Pharmacology, physiology and detection* (2nd ed.). Boca Raton: CRC Press
- Aune, T., & Berg, K. (1986). Use of freshly prepared rat hepatocytes to study toxicity of blooms of the blue-green algae *Microcystis aeruginosa* and *Oscillatoria agardhii*. *Journal of toxicology and environmental health*, 19(3), 325-326.
- Aune, T., Yasumoto, T., & Engeland, E. (1991). Light and scanning electron microscopic studies on effects of marine algal toxins toward freshly prepared hepatocytes. *Journal of Toxicology and Environmental Health*, 34(1), 1–9.
- Baden, D. G. (1989). Brevetoxins: unique polyether dinoflagellate toxins. *FASEB J.*, 3(7), 1807-1817.
- Baden, D. G., & Mende, T. J. (1982). Toxicity of two toxins from the Florida red tide marine dinoflagellate, *Ptychodiscus brevis*. *Toxicon*, 20(2), 457–461.
- Bellocci, M., Ronzitti, G., Milandri, A., Melchiorre, N., Grillo, C., Poletti, R. *et al.* (2008). A cytolytic assay for the measurement of palytoxin based on a cultured monolayer cell line. *Analytical Biochemistry*, 374(1), 48-55.
- Benson, J. M., Hahn, F. F., March, T. H., McDonald, J. D., Gomez, A. P., Sopori, M. J. *et al.* (2005). Inhalation toxicity of brevetoxin 3 in rats exposed for twenty-two days. *Environmental Health Perspectives*, 113(5), 626.

- Benson, J. M., Hahn, F. F., Tibbetts, B. M., Bowen, L. E., March, T. H., Langley, R. J. *et al.* (2002). Florida red tide: Inhalation toxicity of *Karenia brevis* extract in rats. *Harmful Algae*, 21–25.
- Bertrand, R., Solary, E., O'Connor, P., Kohn, K. W., & Pommier, Y. (1994). Induction of a common pathway of apoptosis by staurosporine. *Experimental Cell Research*, 211(2), 314-321.
- Beuzenberg, V., Mountfort, D., Holland, P. T., Shi, F., & MacKenzie, A. L. (2012). Optimization of growth and production of toxins by three dinoflagellates in photobioreactor cultures. *J. Appl. Phycol.*, *Accepted for publication*.
- Bidard, J. N., Vijverberg, H. P., Frelin, C., Chungue, E., Legrand, A. M., Bagnis, R. *et al.* (1984). Ciguatoxin is a novel type of Na<sup>+</sup> channel toxin. *Journal of Biological Chemistry*, 259(13), 8353-8357.
- Bignami, G. S. (1993). A rapid and sensitive hemolysis neutralization assay for palytoxin. *Toxicon*, 31(6), 817-820.
- Botes, L., Smit, A. J., & Cook, P. A. (2003). The potential threat of algal blooms to the abalone (*Haliotis midae*) mariculture industry situated around the South African coast. *Harmful Algae*, 2(4), 247-259.
- Briggs, L. (2008). *Reviews of cell-based cytotoxicity assays*. Hamilton, New Zealand: AgRes.
- Bulter, M. (Ed.). (2004). *Animal cell culture & technology* (2nd ed.). Oxon, UK: Bios Scientific Publishers.
- Cai, Y. Z., Xing, J., Sun, M., Zhan, Z. Q., & Corke, H. (2005). Phenolic antioxidants (hydrolyzable tannins, flavonols, and anthocyanins) identified by LC-ESI-MS and MALDI-QIT-TOF MS from *Rosa chinensis* Flowers. *Journal of Agricultural and Food Chemistry*, 53(26), 9940-9948.
- Camacho, F. G., Rodríguez, J. G., Mirón, A. S., García, M. C., Belarbi, E. H., Chisti, Y. *et al.* (2007). Biotechnological significance of toxic marine dinoflagellates. *Biotechnology advances*, 25(2), 176-194.
- Cardoso, S. M., Santos, S., Swerdlow, R. H., & Oliveira, C. R. (2001). Functional mitochondria are required for amyloid A $\beta$ -mediated neurotoxicity. *The FASEB Journal*, 15(8), 1439-1441.
- Carvalho, P. S., Catia, R., Moukha, S., Matias, W., & Creppy, E. (2006). Comparative study of domoic acid and okadaic acid induced - chromosomal abnormalities in the CACO-2 cell line. *International Journal of Environmental Research and Public Health*, 3(1), 4-10.
- Catterall, W. A. (1984). The molecular basis of neuronal excitability. *Science*, 223(4637), 653-661.
- Catterall, W. A. (2000). From ionic currents to molecular review mechanisms: the structure and function of voltage-gated sodium channels. *Neuron*, 26(1), 13-25.
- Catterall, W. A., Cest e, S., Yarov-Yarovoy, V., Yu, F. H., Konoki, K., & Scheuer, T. (2007). Voltage-gated ion channels and gating modifier toxins. *Toxicon*, 49(2), 124-141.
- Catterall, W. A., & Risk, M. (1981). Toxin T4<sub>46</sub> from *Ptychodiscus brevis* (formerly *Gymnodinium breve*) enhances activation of voltage-sensitive sodium channels by veratridine. *Molecular Pharmacology* 19(2), 345-348.
- Cembella, A. D., Milenkovic, L., Doucette, G., & Fernandez, M. (1995). In vitro Biochemical Methods and Mammalian Bioassays for Phycotoxins. In Hallegraeff, G. M. *et al.* (Eds.), *Manual on harmful marine microalgae*. Paris UNESCO.
- Chae, H., Kang, J., Byun, J., Han, K., Kim, D., Oh, S. *et al.* (2000). Molecular mechanism of staurosporine-induced apoptosis in osteoblasts. *Pharmacological Research*, 42(4), 373-381.

- Chan, A. T. (1980). Comparative physiological study of marine diatoms and dinoflagellates in relation to irradiance and cell size. II. relationship between photosynthesis, growth, and carbon/chlorophyll *a* ratio. *Journal of Phycology*, 16(3), 428-432.
- Chang, F. H. (1995). First records of *Gymnodinium* sp. nov. (cf. *breve*) (Dinophyceae) and other harmful phytoplankton species in the early 1993 blooms in New Zealand. In Lassus, P. *et al.* (Eds.), *Harmful Marine Algal Blooms* (pp. 27-32). Paris: Lavoisier Science Publishers.
- Chang, F. H. (1999a). *Gymnodinium brevisulcatum* sp. nov. (Gymnodiniales, Dinophyceae), a new species isolation from the 1998 summer toxic bloom in Wellington Harbour, New Zealand. *Phycologia*, 38(5), 377-384.
- Chang, F. H. (1999b). A new species of *Gymnodinium* that caused the 1998 summer human respiratory syndrome and decimation of marine life in Wellington Harbour, New Zealand. *Harmful Algae News*, 19(1), 3-4.
- Chang, F. H. (2003). Algal blooms wreak havoc in Hauraki Gulf. *Aquatic Biodiversity & Biosecurity* 3, 6-7.
- Chang, F. H. (2011). Toxic effects of three closely-related dinoflagellates, *Karenia concordia*, *K. brevisulcata* and *K. mikimotoi* (Gymnodiniales, Dinophyceae) on other microalgal species. *Harmful Algae*, 10(2), 181-187.
- Chang, F. H., Chiswell, S. M., & Uddstrom, M. J. (2001). Occurrence and distribution of *Karenia brevisulcata* (Dinophyceae) during the 1998 summer toxic outbreaks on the central east coast of New Zealand. *Phycologia*, 40(3), 215-222.
- Chang, F. H., MacKenzie, A. L., Till, D., Hannah, D. J., & Rhodes, L. (1995). The first toxic shellfish outbreaks and the associated phytoplankton blooms in early 1993 in New Zealand. In Lassus, P. *et al.* (Eds.), *Harmful marine algal blooms* (pp. 145-150). Paris: Lavoisier Science Publishing.
- Chang, F. H., & Ryan, K. G. (2004). *Karenia concordia* sp nov (Gymnodiniales, Dinophyceae), a new nonthecate dinoflagellate isolated from the New Zealand northeast coast during the 2002 harmful algal bloom events. *Phycologia*, 43(5), 552-562.
- Chang, F. H., Uddstrom, M. J., Pinkerton, M. H., & Richardson, K. A. (2008). Characterising the 2002 toxic *Karenia concordia* (Dinophyceae) outbreak and its development using satellite imagery on the north-eastern coast of New Zealand. *Harmful Algae*, 7(4), 532-544.
- Chang, F. H., Uddstrom, M. J., Pinkerton, M. H., Richardson, K. A., & Drury, J. (2002, November 22). *Recent Karenia/Gymnodinium blooms on the northeast coast of New Zealand and detection from satellite SST and ocean color images*. Paper presented at the Proceedings of the New Zealand Marine Biotoxin Science Workshop.
- Chang, F. H., Zeldis, J., Gall, M., & Hall, J. (2003). Seasonal and spatial variation of phytoplankton assemblages, biomass and cell size from spring to summer across the north-eastern New Zealand continental shelf. *Journal of Plankton Research*, 25(7), 737-758.
- Cheng, Y. S., Zhou, Y., Irvin, C. M., Pierce, R. H., Naar, J., Backer, L. C. *et al.* (2005). Characterization of marine aerosol for assessment of human exposure to brevetoxins. *Environmental Health Perspectives*, 113(5), 638-643.
- Chong, M. W. K., Gu, K. D., Lam, P. K. S., Yang, M., & Fong, W. F. (2000). Study on the cytotoxicity of microcystin-LR on cultured cells. *Chemosphere*, 41(1-2), 143-147.
- Christensen, M. L. M., Braunstein, T. H., & Treiman, M. (2008). Fluorescence assay for mitochondrial permeability transition in cardiomyocytes cultured in a microtiter plate. *Analytical Biochemistry*, 378(1), 25-31.
- Christian, B., & Lucas, B. (2008). Determination of marine biotoxins relevant for regulations: from the mouse bioassay to coupled LC-MS methods. *Analytical and Bioanalytical Chemistry*, 391(1), 117-134.



- Ciminiello, P., & Fattorusso, E. (2006). Bivalve molluscs as vectors of marine biotoxins involved in seafood poisoning. In Müller, W. E. G. (Ed.), *Molluscs: from chemoeological study to biotechnological application*. Berlin: Springer.
- Collins, J. A., Schandl, C. A., Young, K. K., Vesely, J., & Willingham, M. C. (1997). Major DNA fragmentation is a late event in apoptosis. *Journal of Histochemistry & Cytochemistry*, 45(7), 923-934.
- D'Amelio, M., Cavallucci, V., & Cecconi, F. (2010). Neuronal caspase-3 signaling: not only cell death. *Cell Death Differ*, 17(7), 1104-1114.
- da Silva, P. M., Hegaret, H., Lambert, C., Wikfors, G. H., Le Goic, N., Shumway, S. E. *et al.* (2008). Immunological responses of the Manila clam (*Ruditapes philippinarum*) with varying parasite (*Perkinsus olseni*) burden, during a long-term exposure to the harmful alga, *Karenia selliformis*, and possible interactions. *Toxicon*, 51(4), 563-573.
- Daranas, A. H., Norte, M., & Fernández, J. J. (2001). Toxic marine microalgae. *Toxicon*, 39(8), 1101-1132.
- Daugbjerg, N., Hansen, G., Larsen, J., & Moestrup, Ø. (2000). Phylogeny of some of the major genera of dinoflagellates based on ultrastructure and partial LSU rDNA sequence data, including the erection of three new genera of unarmoured dinoflagellates. *Phycologia*, 39(4), 302-317.
- Davidson, K., Miller, P., Wilding, T. A., Shutler, J., Bresnan, E., Kennington, K. *et al.* (2009). A large and prolonged bloom of *Karenia mikimotoi* in Scottish waters in 2006. *Harmful Algae*, 8(2), 349-361.
- Davis, C. C. (1948). *Gymnodinium brevis* sp. nov., a cause of discolored water and animal mortality in the Gulf of Mexico. *Botanical Gazette*, 109, 358-360.
- De Salas, M. F., Bolch, C. J. S., Botes, L., Nash, G., Wright, S. W., & Hallegraeff, G. M. (2003). *Takayama* gen. nov. (Gymnodiniales, Dinophyceae), a new genus of unarmored dinoflagellates with sigmoid apical grooves, including the description of two new species *Journal of Phycology*, 39(6), 1233-1246.
- Dechraoui, M.-Y., Naar, J., Pauillac, S., & Legrand, A.-M. (1999). Ciguatoxins and brevetoxins, neurotoxic polyether compounds active on sodium channels. *Toxicon*, 37(1), 125-143.
- Dechraoui, M.-Y., Tiedeken, J. A., Persad, R., Wang, Z., Granade, H. R., Dickey, R. W. *et al.* (2005). Use of two detection methods to discriminate ciguatoxins from brevetoxins: Application to great barracuda from Florida Keys. *Toxicon*, 46(3), 261-270.
- Dorantes-Aranda, J. J., Waite, T. D., Godrant, A., Rose, A. L., Tovar, C. D., Woods, G. M. *et al.* (2011). Novel application of a fish gill cell line assay to assess ichthyotoxicity of harmful marine microalgae. *Harmful Algae*, 10(4), 366-373.
- Dounay, A. B., & Forsyth, C. J. (2002). Okadaic Acid: The archetypal serine / threonine protein phosphatase inhibitor. *Current Medicinal Chemistry*, 9(22), 1939-1980.
- Dragunow, M., Trzoss, M., Brimble, M. A., Cameron, R., Beuzenberg, V., Holland, P. T. *et al.* (2005). Investigations into the cellular actions of the shellfish toxin gymnodimine and analogues. *Environmental Toxicology and Pharmacology*, 20(2), 305-312.
- Draisci, R., Palleschi, L., Giannetti, L., Lucentini, L., James, K. J., Bishop, A. G. *et al.* (1999). New approach to the direct detection of known and new diarrhoeic shellfish toxins in mussels and phytoplankton by liquid chromatography-mass spectrometry. *Journal of chromatography A*, 847(1-2), 213-221.
- EFSA (2009). *Marine biotoxins in shellfish – Summary on regulated marine biotoxins from* [http://www.efsa.europa.eu/EFSA/efsa\\_locale-1178620753812\\_1211902812884.htm](http://www.efsa.europa.eu/EFSA/efsa_locale-1178620753812_1211902812884.htm).
- Elmore, S. (2007). Apoptosis: A review of programmed cell death. *Toxicologic pathology*, 35(4), 495-516.
- Fairey, E. R., Bottein Dechraoui, M.-Y., Sheets, M. F., & Ramsdell, J. S. (2001). Modification of the cell based assay for brevetoxins using human cardiac voltage

- dependent sodium channels expressed in HEK-293 cells. *Biosensors and Bioelectronics*, 16(7-8), 579-586.
- Fairey, E. R., Edmunds, J. S., Deamer-Melia, N. J., Glasgow Jr, H., Johnson, F. M., Moeller, P. R. *et al.* (1999). Reporter gene assay for fish-killing activity produced by *Pfiesteria piscicida*. *Environmental Health Perspectives*, 107(9), 711.
- Fairey, E. R., & Ramsdell, J. S. (1999). Reporter gene assays for algal-derived toxins. *Natural Toxins*, 7(6), 415-421.
- Faulkner, D. J. (1996). Marine natural products. *Natural Product Reports*, 13(2), 75-125.
- FDA (2001). Guidance for industry: bioanalytical method validation. US Department of health and human services, US FDA. *Center for Drug Evaluation and Research, Rockville, MD, USA*.
- Fleming, L. E., Backer, L. C., & Baden, D. G. (2005a). Overview of aerosolized Florida red tide toxins: Exposures and effects. *Environmental Health Perspectives*, 113(5), 618-620.
- Fleming, L. E., Kirkpatrick, B., Backer, L. C., Bean, J. A., Wanner, A., Dalpra, D. *et al.* (2005b). Initial evaluation of the effects of aerosolized Florida red tide toxins (Brevetoxins) in persons with asthma. *Environmental Health Perspectives*, 113(5), 650-657.
- Fleming, L. E., Kirkpatrick, B., Backer, L. C., Bean, J. A., Wanner, A., Reich, A. *et al.* (2007). Aerosolized red-tide toxins (Brevetoxins) and asthma. *Chest*, 131(1), 187.
- Fossat, B., Porth é Nibelle, J., Sola, F., Masoni, A., Gentien, P., & Bodennec, G. (1999). Toxicity of fatty acid 18:5n3 from *Gymnodinium cf. mikimotoi*: II. intracellular pH and K<sup>+</sup> uptake in isolated trout hepatocytes. *Journal of Applied Toxicology*, 19(4), 275-278.
- Fux, E., McMillan, D., Bire, R., & Hess, P. (2007). Development of an ultra-performance liquid chromatography-mass spectrometry method for the detection of lipophilic marine toxins. *Journal of Chromatography A*, 1157(1-2), 273-280.
- Galluzzi, L., Zamzami, N., de La Motte Rouge, T., Lemaire, C., Brenner, C., & Kroemer, G. (2007). Methods for the assessment of mitochondrial membrane permeabilization in apoptosis. *Apoptosis*, 12(5), 803-813.
- Gardner, J. P. A., & Wear, R. G. (2006). Changes in subtidal macroinvertebrate community structure in Wellington Harbour (New Zealand) following a large-scale natural die-off. *New Zealand Journal of Marine and Freshwater Research*, 40(1), 29-42.
- Garthwaite, I. (2000). Keeping shellfish safe to eat: a brief review of shellfish toxins, and methods for their detection. *Trends in Food Science & Technology*, 11(7), 235-244.
- Gawley, R. E., Rein, K. S., Jeglitsch, G., Adams, D. J., Theodorakis, E. A., Tiebes, J. *et al.* (1995). The relationship of brevetoxin 'length' and A-ring functionality to binding and activity in neuronal sodium channels. *Chemistry & Biology*, 2(8), 533-541.
- Gentien, P., Lunven, M., Lazure, P., Youenou, A., & Crassous, M. P. (2007). Motility and autotoxicity in *Karenia mikimotoi* (Dinophyceae). *Philosophical Transactions of the Royal Society B-Biological Sciences*, 362(1487), 1937-1946.
- Glibert, P. M., Anderson, D. A., Gentien, P., Graneli, E., & Sellner, K. G. (2005). The global complex phenomena of harmful algal blooms. *Oceanography*, 18(2), 136-147.
- Grima, E. M., Aci é n Fern á ndez, F. G., Garc á Camacho, F., Camacho Rubio, F., & Chisti, Y. (2000). Scale-up of tubular photobioreactors. *Journal of Applied Phycology*, 12(3), 355-368.
- Grima, E. M., Aci é n Fern á ndez, J., Aci é n, F. G., & Chisti, Y. (2001). Tubular photobioreactor design for algal cultures. *Journal of Biotechnology*, 92(2), 113-131.
- Grima, E. M., Belarbi, E. H., Aci é n Fern á ndez, F. G., Robles Medina, A., & Chisti, Y. (2003). Recovery of microalgal biomass and metabolites: Process options and economics. *Biotechnology advances*, 20(7-8), 491-515.

- Guenoun-Lehmann, S., Fonseca, J. E., Horisberger, J. D., & Rakowski, R. F. (2007). Palytoxin acts on Na<sup>+</sup>,K<sup>+</sup>-ATPase but not nongastric H<sup>+</sup>,K<sup>+</sup>-ATPase. *Journal of Membrane Biology*, 216(2-3), 107-116.
- Guillard, R. R. L., & Hargraves, P. E. (1993). *Stichochris immobilis* is a diatom, not a chrysophyte. *Phycologia*, 32, 234-236.
- Habermann, E. (1989). Palytoxin acts through Na<sup>+</sup>, K<sup>+</sup>-ATPase. *Toxicon*, 27(11), 1171-1187.
- Hallegraeff, G. M. (1995). Harmful algal blooms: A global overview. In Hallegraeff, G. M. *et al.* (Eds.), *Manual on harmful marine microalgae* (pp. 1-22). Paris UNESCO.
- Hallegraeff, G. M., & Bolch, C. J. (1992). Transport of diatom and dinoflagellate resting spores in ship's ballast water: Implications for plankton biogeography and aquaculture. *J. Plankton Res.*, 14, 1067-1084.
- Hallegraeff, G. M., & Gollasch, S. (2006). Anthropogenic introductions of microalgae. *Ecology of Harmful Algae*, 379-390.
- Hamamoto, Y., Tachibana, K., Satake, M., Holland, P. T., Shi, F., & Beuzenberg, V. (2012). Brevisulcinal-F, a polycyclic ether toxin associated with massive fish-kills in New Zealand. *Journal of American Chemical Society*, 134(10), 4963-4968.
- Hashimoto, N., Aoyama, T., & Shioiri, T. (1981). Derivatization of carboxylic acids with diazomethane and trimethylsilyldiazomethane: Convenient methods and artifacts. *Chem Pharm Bull*, 29, 1475-1478.
- Haywood, A. J., Scholin, C. A., Marin, R., Steidinger, K. A., Heil, C., & Ray, J. (2007). Molecular detection of the brevetoxin-producing dinoflagellate *Karenia brevis* and closely related species using rRNA-targeted probes and a semiautomated sandwich hybridization assay. *Journal of Phycology*, 43(6), 1271-1286.
- Haywood, A. J., Steidinger, K. A., Truby, E. W., Bergquist, P. R., Bergquist, P. L., Adamson, J. *et al.* (2004). Comparative morphology and molecular phylogenetic analysis of three new species of the genus *Karenia* (Dinophyceae) from New Zealand. *Journal of Phycology*, 40(1), 165-179.
- Heil, C. A., Glibert, P. M., Al-Sarawi, M. A., Faraj, M., Behbehani, M., & Husain, M. (2001). First record of a fish-killing *Gymnodinium* sp. bloom in Kuwait Bay, Arabian Sea: chronology and potential causes. *Marine Ecology Progress Series*, 214, 15-23.
- Hess, P., McMahon, T., Slattery, D., Swords, D., Dowling, G., McCarron, M. *et al.* (2002, Jun 4–8). *Use of LC-MS testing to identify lipophilic toxins, to establish local trends and interspecies differences and to test the comparability of LC-MS testing with the mouse bioassay: An example from the Irish biotoxin monitoring programme 2001*. Paper presented at the 4<sup>th</sup> International Conference on Molluscan Shellfish Safety, Santiago de Compostella, Spain.
- Holland, P. T. (2008). Analysis of marine toxins – techniques, method validation, calibration standards and screening methods. In Botana, L. M. (Ed.), *Seafood and Freshwater Toxins: pharmacology, physiology and detection* (2nd ed., pp. 21-50). Boca Raton, FL: CRC Press.
- Holland, P. T., McNabb, P., Phodes, L. L., Selwood, A. I., & Neil, T. (2002, Jun 4–8). *Amnesic shellfish poisoning toxins in New Zealand shellfish: Detection of an unusual domoic acid isomer using a newly validated LC-MS/MS method*. Paper presented at the 4<sup>th</sup> International Conference on Molluscan Shellfish Safety, Santiago de Compostella, Spain.
- Holland, P. T., Shi, F., Satake, M., Hamamoto, Y., Ito, E., Beuzenberg, V. *et al.* (2012). Novel toxins produced by the dinoflagellate *Karenia brevisulcata*. *Harmful Algae*, 13(1), 47-57.
- Honjo, T. (1995). The biology and prediction of representative red tides associated with fish kills in Japan. *Japanese Reviews of Fisheries Science*, 2, 65 - 104.

- Hu, H., Chen, W., Shi, Y., & Cong, W. (2006). Nitrate and phosphate supplementation to increase toxin production by the marine dinoflagellate *Alexandrium tamarense*. *Marine Pollution Bulletin*, 52(7), 756-760.
- Hua, Y., & Cole, R. B. (1999). Solution reactivity of brevetoxins as monitored by electrospray ionization mass spectrometry and implications for detoxification. *Chem. Res. Toxicol.*, 12(12), 1268-1277.
- Huerta, S., Goulet, E. J., Huerta-Yepez, S., & Livingston, E. H. (2007). Screening and detection of apoptosis. *Journal of Surgical Research*, 139(1), 143-156.
- Hunt, I. (2006, Oct ). C-NMR Spectroscopy, from <http://www.chem.ucalgary.ca/courses/350/Carey5th/Ch13/ch13-cnmr-1.html>
- Hunt, L., Upadhyay, A., Jazayeri, J., Tudor, E., & White, J. (2011). Caspase-3, myogenic transcription factors and cell cycle inhibitors are regulated by leukemia inhibitory factor to mediate inhibition of myogenic differentiation. *Skeletal Muscle*, 1(1), 17.
- ICES (2006). *Report of the ICES-IOC Working Group on Harmful Algal Bloom Dynamics (WGHABD)* (No. ICES CM 2006/OCC:04). Gdynia, Poland: International Council for the Exploration of the Sea
- Ishida, H., Nozawa, A., Hamano, H., Naoki, H., Fujita, T., Kaspar, H. F. *et al.* (2004a). Brevetoxin B5, a new brevetoxin analog isolated from cockle *Austrovenus stutchburyi* in New Zealand, the marker for monitoring shellfish toxicity. *Tetrahedron Letters*, 45(1), 29-33.
- Ishida, H., Nozawa, A., Nukaya, H., Rhodes, L., McNabb, P., Holland, P. T. *et al.* (2004b). Confirmation of brevetoxin metabolism in cockle, *Austrovenus stutchburyi*, and greenshell mussel, *Perna canaliculus*, associated with New Zealand neurotoxic shellfish poisoning, by controlled exposure to *Karenia brevis* culture. *Toxicon*, 43(6), 701-712.
- Ishida, H., Nozawa, A., Nukaya, H., & Tsuji, K. (2004c). Comparative concentrations of brevetoxins PbTx-2, PbTx-3, BTX-B1 and BTX-B5 in cockle, *Austrovenus stutchburyi*, greenshell mussel, *Perna canaliculus*, and Pacific oyster, *Crassostrea gigas*, involved neurotoxic shellfish poisoning in New Zealand. *Toxicon*, 43(7), 779-789.
- Ishida, H., Nozawa, A., Totoribe, K., Muramatsu, N., Nukaya, H., Tsuji, K. *et al.* (1995). Brevetoxin B1, a new polyether marine toxin from the New Zealand shellfish, *Austrovenus stutchburyi*. *Tetrahedron Letters*, 36(5), 725-728.
- Ishimatsu, A., Oda, T., Yoshida, M., & Ozaki, M. (1996). Oxygen radicals are probably involved in the mortality of yellowtail by *Chattonella marina*. *Fish Sci.*, 62, 836-837.
- Issa, Y., Watts, D. C., Brunton, P. A., Waters, C. M., & Duxbury, A. J. (2004). Resin composite monomers alter MTT and LDH activity of human gingival fibroblasts in vitro. *Dental Materials*, 20(1), 12-20.
- Jantas-Skotniczna, D., Kajta, M., & Lason, W. (2006). Memantine attenuates staurosporine-induced activation of caspase-3 and LDH release in mouse primary neuronal cultures. *Brain Research*, 1069(1), 145-153.
- Jasperse, J. A. (1993). *Marine toxins and New Zealand shellfish*. Paper presented at the Proceedings of a workshop on research issues, June10-11, 1993.
- Jayaraj, R., Gupta, N., & Rao, P. V. L. (2009). Multiple signal transduction pathways in okadaic acid induced apoptosis in HeLa cells. *Toxicology*, 256(1-2), 118-127.
- Johannes, J. W., Wenglow, S., & Kishi, Y. (2005). Biomimetic macrocycle-forming Diels-Alder reaction of an iminium dienophile: synthetic studies directed toward gymnodimine. *Organic letters*, 7(18), 3997-4000.
- John, U., Quilliam, M., Medlin, L., & Cembella, A. D. (2000). Spirolide production and photoperiod-dependent growth of the marine dinoflagellate, *Alexandrium ostenfeldii*. In Hallegraeff, G. M. *et al.* (Eds.), *9th Harmful Algal Blooms*. Tasmania, Australia: Intergovernmental Oceanographic Commission of UNESCO.

- Katsuo, D., Kim, D., Yamaguchi, K., Matsuyama, Y., & Oda, T. (2007). A new simple screening method for the detection of cytotoxic substances produced by harmful red tide phytoplankton. *Harmful Algae*, 6(6), 790-798.
- Keyzers, R. A. (pers, comm.). The isolation of Wellington Harbour Toxin produced by the Dinoflagellate *Karenia brevisulcata*. Victoria University of Wellington.
- Kharrat, R., Servent, D., Girard, E., Ouanounou, G., Amar, M., Marrouchi, R. *et al.* (2008). The marine phycotoxin gymnodimine targets muscular and neuronal nicotinic acetylcholine receptor subtypes with high affinity. *Journal of Neurochemistry*, 107(4), 952.
- Kim, J., He, L., & Lemasters, J. J. (2003). Mitochondrial permeability transition: a common pathway to necrosis and apoptosis. *Biochemical and Biophysical Research Communications*, 304, 436-470.
- Kirkpatrick, B., Fleming, L. E., Squicciarini, D., Backer, L. C., Clark, R., Abraham, W. *et al.* (2004). Literature review of Florida red tide: implications for human health effects. *Harmful Algae*, 3(2), 99-115.
- Kita, M., & Uemura, D. (2005). Iminium alkaloids from marine invertebrates: Structure, biological activity, and biogenesis. *Chemistry Letters*, 34(4), 454-459.
- Kröger, K. (2008). *Recovery of subtidal benthic macroinvertebrate communities following natural and experimental disturbances*. Ph.D thesis, Victoria University of Wellington, Wellington.
- Kröger, K., Gardner, J., Rowden, A. A., & Wear, R. G. (2006). Long-term effects of a toxic algal bloom on subtidal soft-sediment macroinvertebrate communities in Wellington Harbour, New Zealand. *Estuarine, Coastal and Shelf Science*, 67(4), 589-604.
- Kruman, I., Guo, Q., & Mattson, M. P. (1998). Calcium and reactive oxygen species mediate staurosporine-induced mitochondrial dysfunction and apoptosis in PC12 cells. *Journal of Neuroscience Research*, 51(3), 293-308.
- Landsberg, J. H. (2002). The effects of harmful algal blooms on aquatic organisms. *Reviews in Fisheries Science*, 10(2), 113-390.
- Lang, G., Mitova, M. I., Ellis, G., van der Sar, S., Phipps, R. K., Blunt, J. W. *et al.* (2006). Bioactivity profiling using HPLC/microtiter-plate analysis: Application to a New Zealand marine alga-derived fungus, *Gliocladium* sp. *Journal of Natural products*, 69(4), 621-624.
- Larm, J. A., Beart, P. M., & Cheung, N. S. (1997). Neurotoxin domoic acid produces cytotoxicity via kainate- and ampa-sensitive receptors in cultured cortical neurones. *Neurochemistry International*, 31(5), 677-682.
- Lin, Y. Y., Risk, M., Ray, S. M., Van Engen, D., Clardy, J., Golik, J. *et al.* (1981). Isolation and structure of brevetoxin B from the "red tide" dinoflagellate *Ptychodiscus brevis* (*Gymnodinium breve*). *Journal of the American Chemical Society*, 103(22), 6773-6775.
- Loader, J. I., Hawkes, A. D., Beuzenberg, V., Jensen, D. J., Cooney, J. M., Wilkins, A. L. *et al.* (2007). Convenient large-scale purification of yessotoxin from *Protoceratium reticulatum* culture and isolation of a novel furanoyessotoxin. *Journal of Agricultural and Food Chemistry*, 55(26), 11093-11100.
- Lobner, D. (2000). Comparison of the LDH and MTT assays for quantifying cell death: validity for neuronal apoptosis? *Journal of Neuroscience Methods*, 96(2), 147-152.
- Loeblich, A. R. (1975). A seawater medium for dinoflagellates and the nutrition of *Cachonina Niei*. *Journal of Phycology*, 11(1), 80-86.
- Loeblich, A. R., & Smith, V. E. (1968). Chloroplast pigments of the marine dinoflagellate *Gyrodinium resplendens*. *Lipids*, 3, 5-13.
- Lombet, A., Bidard, J.-N., & Lazdunski, M. (1987). Ciguatoxin and brevetoxins share a common receptor site on the neuronal voltage-dependent Na<sup>+</sup> channel. *FEBS Letters*, 219(2), 355-359.

- López, A. M., Rodríguez, J. J. G., Mirón, A. S., Camacho, F. G., & Grima, E. M. (2011). Immunoregulatory potential of marine algal toxins yessotoxin and okadaic acid in mouse T lymphocyte cell line EL-4. *Toxicology Letters*, 207(2), 167-172.
- MacKenzie, L. (2008). The ecobiology of the brevetoxin, ciguatoxin and cyclic imine producers. In Botana, L. M. (Ed.), *Seafood and Freshwater Toxins: Pharmacology, physiology and detection* (2nd ed., pp. 433-467). Boca Raton, FL: CRC Press.
- MacKenzie, L., Haywood, A., Adamson, J., & Truman, P. (1996). Gymnodimine contamination of shellfish in New Zealand. In Yasumoto, T. *et al.* (Eds.), *Harmful and toxic algal blooms*. (pp. 97-100). Paris: Intergovernmental Oceanographic Commission of UNESCO.
- MacKenzie, L., Rhodes, L. L., Till, D., Chang, F. H., Kaspar, H., Haywood, A. *et al.* (1995). A *Gymnodinium* sp. bloom and the contamination of shellfish with lipid soluble toxins in New Zealand, Jan - April 1993. In Lassus, P. *et al.* (Eds.), *Harmful Marine Algal Blooms* (pp. 795-800). Paris: Lavoisier Science Publishers.
- MacKenzie, L., Smith, K. F., Rhodes, L., Brown, A., Langi, V., Edgar, M. *et al.* (in press). Mortalities of sea-cage salmon (*Oncorhynchus tshawytscha*) due to a bloom of *Pseudochattonella verruculosa* (Dictyochophyceae) in Queen Charlotte Sound, New Zealand. *Harmful Algae*, *Submission of publication*.
- Magaña, H. A., Contreras, C., & Villareal, T. A. (2003). A historical assessment of *Karenia brevis* in the western Gulf of Mexico. *Harmful Algae*, 2(3), 163-171.
- Manger, R. L., Leja, L. S., Lee, S. Y., Hungerford, J. M., Kirkpatrick, M. A., Yasumoto, T. *et al.* (2003). Detection of paralytic shellfish poison by rapid cell bioassay: antagonism of voltage-gated sodium channel active toxins in vitro. *Journal of AOAC International*, 86(3), 540-543.
- Manger, R. L., Leja, L. S., Lee, S. Y., Hungerford, J. M., & Wekell, M. M. (1993). Tetrazolium-based cell bioassay for neurotoxins active on voltage-sensitive sodium channels: Semiautomated assay for saxitoxins, brevetoxins, and ciguatoxins. *Analytical Biochemistry*, 214(1), 190-194.
- Marban, E., Yamagishi, T., & Tomaselli, G. F. (1998). Structure and function of voltage gated sodium channels. *The Journal of Physiology*, 508(3), 647-657.
- March, R. E. (1997). An introduction to quadrupole ion trap mass spectrometry. *Journal of Mass Spectrometry*, 32(4), 351-369.
- Marshall, J. A., Nichols, P. D., Hamilton, B., Lewis, R. J., & Hallegraeff, G. M. (2003). Ichthyotoxicity of *Chattonella marina* (Raphidophyceae) to damselfish (*Acanthochromis polycanthus*): the synergistic role of reactive oxygen species and free fatty acids. *Harmful Algae*, 2(4), 273-281.
- Marshall, J. A., Ross, T., Pyecroft, S., & Hallegraeff, G. (2005). Superoxide production by marine microalgae: II. Towards understanding ecological consequences and possible functions. *Marine Biology*, 147(2), 541-549.
- McFarren, E. F., Silva, F. J., Tanabe, H., Wilson, W. B., Campbell, J. E., & Lewis, K. H. (1965). The occurrence of a ciguatera-like poison in oysters, clams, and *Gymnodinium breve* cultures. *Toxicon*, 3(2), 111.
- McMaster, M. C. (2005). *LC/MS: A practical user's guide*. Hoboken, NJ: John Wiley & Sons, Inc.
- McNabb, P. (2008). Chemistry, metabolism, and chemical analysis of okadaic acid group toxins. In Botana, L. M. (Ed.), *Seafood and Freshwater Toxins: Pharmacology, physiology and detection* (2nd ed.). Boca Raton, FL: CRC Press.
- McNabb, P., Rhodes, L., Adamson, J., & Holland, P. (2006). Brevetoxin - an elusive toxin in New Zealand waters. *African Journal of Marine Science*, 28(2), 375-377.
- McNabb, P., Selwood, A. I., & Holland, P. T. (2005). Multiresidue method for determination of algal toxins in shellfish: Single-laboratory validation and interlaboratory study. *Journal of the Association of Official Analytical Chemists*, 88(3), 761-772.

- McNabb, P., Selwood, A. I., Munday, R., Wood, S. A., Taylor, D. I., Mackenzie, L. A. *et al.* (2010). Detection of tetrodotoxin from the grey sided-gilled sea slug - *Pleurobranchaea maculata*, and associated dog neurotoxicosis on beaches adjacent to the Hauraki Gulf, Auckland, New Zealand. *Toxicon*, 56(3), 466-473.
- Miles, C. O., Wilkins, A. L., Stirling, D. J., & MacKenzie, L. (2000). New Analogue of Gymnodimine from a *Gymnodinium* Species. *Journal of Agricultural and Food Chemistry*, 48(4), 1373-1376.
- Miles, C. O., Wilkins, A. L., Stirling, D. J., & MacKenzie, L. (2003). Gymnodimine C, an isomer of gymnodimine B, from *Karenia selliformis*. *Journal of Agricultural and Food Chemistry*, 51(16), 4838-4840.
- Mooney, B. D., Hallegraeff, G. M., & Place, A. R. (2010). Ichthyotoxicity of four species of gymnodinioid dinoflagellates (Kareniaceae, Dinophyta) and purified karlotoxins to larval sheepshead minnow. *Harmful Algae*, 9(6), 557-562.
- Mooney, B. D., Nichols, P. D., de Salas, M. F., & Hallegraeff, G. M. (2007). Lipid, fatty acid, and sterol composition of eight species of Kareniaceae (Dinophyta): Chemotaxonomy and putative lipid phycotoxins. *Journal of Phycology*, 43(1), 101-111.
- Morohashi, A., Satake, M., Murata, K., Naoki, H., Kaspar, H. F., & Yasumoto, T. (1995). Brevetoxin B3, a new brevetoxin analog isolated from the greenshell mussel *Perna canaliculus* involved in neurotoxic shellfish poisoning in New Zealand. *Tetrahedron Letters*, 36(49), 8995-8998.
- Morohashi, A., Satake, M., Naoki, H., Kaspar, H. F., Oshima, Y., & Yasumoto, T. (1999). Brevetoxin B4 isolated from greenshell mussels *Perna canaliculus*, the major toxin involved in neurotoxic shellfish poisoning in New Zealand. *Natural Toxins*, 7(2), 45-48.
- Mountfort, D., Beuzenberg, V., MacKenzie, L., & Rhodes, L. (2006). Enhancement of growth and gymnodimine production by the marine dinoflagellate, *Karenia selliformis*. *Harmful Algae*, 5(6), 658-664.
- Moyer, S. C., Cotter, R. J., & Woods, A. S. (2002). Fragmentation of phosphopeptides by atmospheric pressure MALDI and ESI/ion trap mass spectrometry. *Journal of the American Society for Mass Spectrometry*, 13(3), 274-283.
- Munday, R., Towers, N. R., Mackenzie, L., Beuzenberg, V., Holland, P. T., & Miles, C. O. (2004). Acute toxicity of gymnodimine to mice. *Toxicon*, 44(2), 173-178.
- Murata, K., Satake, M., Naoki, H., Kaspar, H. F., & Yasumoto, T. (1998). Isolation and structure of a new brevetoxin analog, brevetoxin B2, from greenshell mussels from New Zealand. *Tetrahedron*, 54(5-6), 735-742.
- Murata, M., Kumagai, M., Lee, J. S., & Yasumoto, T. (1987). Isolation and structure of yessotoxin, a novel polyether compound implicated in diarrhetic shellfish poisoning. *Tetrahedron Letters*, 28(47), 5869-5872.
- Murata, M., Legrand, A. M., Ishibashi, Y., Fukui, M., & Yasumoto, T. (1990). Structures and configurations of ciguatoxin from the moray eel *Gymnothorax javanicus* and its likely precursor from the dinoflagellate *Gambierdiscus toxicus*. *Journal of the American Chemical Society*, 112(11), 4380-4386.
- Murata, M., Naoki, H., Matsunaga, S., Satake, M., & Yasumoto, T. (1994). Structure and partial stereochemical assignments for maitotoxin, the most toxic and largest natural non-biopolymer. *Journal of the American Chemical Society*, 116(16), 7098-7107.
- Naoki, H., Murata, M., & Yasumoto, T. (1993). Negative-ion fast-atom bombardment tandemmass spectrometry for the structural study of polyether compounds: Structural verification of yessotoxin. *Rapid Communications in Mass Spectrometry*, 7, 179-182.
- Neely, T., & Campbell, L. (2006). A modified assay to determine hemolytic toxin variability among *Karenia* clones isolated from the Gulf of Mexico. *Harmful Algae*, 5(5), 592-598.

- Nicholson, D. W., Ali, A., Thornberry, N. A., Vaillancourt, J. P., Ding, C. K., Gallant, M. *et al.* (1995). Identification and inhibition of the ICE/CED-3 protease necessary for mammalian apoptosis. *Nature*, 376(6535), 37-43.
- Nor, Y. A., Sulong, N. H., Mel, M., Salleh, H. M., & Sopyan, I. (2010). The growth study of Vero cells in different type of microcarrier open access. *Materials Sciences and Applications*, 1, 261-266.
- Nozawa, A., Tsuji, K., & Ishida, H. (2003). Implication of brevetoxin B1 and PbTx-3 in neurotoxic shellfish poisoning in New Zealand by isolation and quantitative determination with liquid chromatography-tandem mass spectrometry. *Toxicon*, 42(1), 91-103.
- Núñez, O., Moyano, E., & Galceran, M. T. (2005). LC-MS/MS analysis of organic toxics in food. *Trends in Analytical Chemistry*, 24(7), 683-703.
- Obara, Y., Takahashi, M., Nakahata, N., & Ohizumi, Y. (1999). Maitotoxin-induced nerve growth factor production accompanied by the activation of a voltage-insensitive  $Ca^{2+}$  channel in C6-BU-1 glioma cells. *British Journal of Pharmacology*, 127(7), 1577-1582.
- Oda, T. S., Nakamura, A., Shikayama, M., Kawano, I., Ishimatsu, A., & Muramatsu, T. (1997). Generation of reactive oxygen species by raphidophycean phytoplankton. *Bioscience, Biotechnology, Biochemistry*, 61, 1658-1662.
- OECD (2001). OECD guideline for testing of chemicals 425. Acute oral toxicity—up and down procedure Retrieved 2 November 2007, from <http://www.epa.gov/oppfead1/harmonization/docs/E425guideline.pdf>
- Oshima, Y. (2007). *Chemical studies on cytotoxins produced by Karenia brevisulcata from New Zealand: Report to Cawthron Institute*: Graduate school of Life Science, Tohoku University, Japan.
- Oteri, G., Stamatii, A., Zampaglioni, F., & Zucco, F. (1998). Evaluation of the use of two human cell lines for okadaic acid and DTX 1 determination by cytotoxicity assays and damage characterization. *Natural Toxins*, 6(5), 197-209.
- Parrish, C. C., Bodennec, G., & Gentien, P. (1998). Haemolytic glycolipids from *Gymnodinium* species. *Phytochemistry*, 47(5), 783-787.
- Pawlak, J., Tempesta, M. S., Golik, J., Zagorski, M. G., Lee, M. S., Nakanishi, K. *et al.* (1987). Structure of brevetoxin A as constructed from NMR and mass spectral data. *Journal of the American Chemical Society*, 109(4), 1144-1150.
- Perez-Gomez, A., Garcia-Rodriguez, A., James, K. J., Ferrero-Gutierrez, A., Novelli, A., & Fernandez-Sanchez, M. T. (2004). The marine toxin Dinophysistoxin-2 induces differential apoptotic death of rat cerebellar neurons and astrocytes. *Toxicol. Sci.*, 80(1), 74-82.
- Perreault, F., Seleme Matias, M., Pedroso Melegari, S., de Carvalho Pinto, C. R. S., Creppy, E., Popovic, R. *et al.* (2011). Investigation of animal and algal bioassays for reliable saxitoxin ecotoxicity and cytotoxicity risk evaluation. *Ecotoxicology and Environmental Safety*, 74(4), 1021-1026.
- Pitois, S., Jackson, M. H., & Wood, B. J. B. (2001). Sources of the eutrophication problems associated with toxic algae: An overview. *Journal of Environmental Health*, 64(5), 25-33.
- Plakas, S. M., Wang, Z. H., El Said, K. R., Jester, E. L. E., Granade, H. R., Flewelling, L. *et al.* (2004). Brevetoxin metabolism and elimination in the Eastern oyster (*Crassostrea virginica*) after controlled exposures to *Karenia brevis*. *Toxicon*, 44(6), 677-685.
- Poli, M. A., Mende, T. J., & Baden, D. G. (1986). Brevetoxins, unique activators of voltage-sensitive sodium channels, bind to specific sites in rat brain synaptosomes. *Molecular pharmacology*, 30(2), 129-135.
- Prassopoulou, E., Katikou, P., Georgantelis, D., & Kyritsakis, A. (2009). Detection of okadaic acid and related esters in mussels during diarrhetic shellfish poisoning (DSP) episodes



- in Greece using the mouse bioassay, the PP2A inhibition assay and HPLC with fluorimetric detection. *Toxicon*, 53(2), 214-227.
- Promega (2009). Protocols and application guide: Cell viability from <http://www.promega.com/paguide/chap4.htm>
- Quick, J. A., & Henderson, G. E. (1974). Effects of *Gymnodinium breve* red tide on fishes and birds: a preliminary report on behavior, anatomy, hematology and histopathology. In Amborski, R. L. *et al.* (Eds.), *Proceedings of the Gulf Coast Regional Symposium on Diseases of Aquatic Animals, August 16-17, 1974* (pp. 85-113). Louisiana Sea Grant: Louisiana State University.
- Quilliam, M. A. (2003a). Marine phycotoxin structure chart: National Research Council Canada.
- Quilliam, M. A. (2003b). The role of chromatography in the hunt for red tide toxins. *Journal of Chromatography A*, 1000(1-2), 527-548.
- Ramsdell, J. S. (2008). The molecular and integrative basis to brevetoxin toxicity In Botana, L. M. (Ed.), *Seafood and Freshwater Toxins: Pharmacology, physiology and detection* (2nd ed.). Boca Raton, FL: CRC Press.
- Rao, P. V. L., Bhattacharya, R., Gupta, N., Parida, M. M., Bhaskar, A. S. B., & Dubey, R. (2002). Involvement of caspase and reactive oxygen species in cyanobacterial toxin anatoxin-a-induced cytotoxicity and apoptosis in rat thymocytes and Vero cells. *Archives of Toxicology*, 76(4), 227-235.
- Reguera, B., & Pizarro, G. (2008). Planktonic dinoflagellates that contain certain polyether toxins of the old "DSP" complex. In Botana, L. M. (Ed.), *Seafood and Freshwater Toxins: Pharmacology, physiology and detection* (2nd ed., pp. 257-283). Boca Raton, FL: CRC Press.
- Rein, K. S., Baden, D. G., & Gawley, R. E. (1994). Conformational analysis of the sodium channel modulator, brevetoxin A, comparison with brevetoxin B conformations, and a hypothesis about the common pharmacophore of the "Site 5" toxins. *The Journal of Organic Chemistry*, 59(8), 2101-2106.
- Renz, A., Berdel, W. E., Kreuter, M., Belka, C., Schulze-Osthoff, K., & Los, M. (2001). Rapid extracellular release of cytochrome c is specific for apoptosis and marks cell death in vivo. *Blood*, 98(5), 1542-1548.
- Reyzer, M. L., & Caprioli, R. M. (2007). MALDI-MS-based imaging of small molecules and proteins in tissues. *Current Opinion in Chemical Biology*, 11(1), 29-35.
- Rhodes, L., Munday, R., & Briggs, L. (2006). *Ostreopsis siamensis* and palytoxin-related compounds in New Zealand: A risk to human health? . In Moestrup, Ø. *et al.* (Eds.), *Proceedings of the 12<sup>th</sup> International Conference on Harmful Algae. ISSHA and International Commission of UNESCO, 2008* (pp. 326-329). Copenhagen.
- Riobó, P., Paz, B., Franco, J. M., Vázquez, J. A., Murado, M. A., & Cacho, E. (2008). Mouse bioassay for palytoxin. Specific symptoms and dose-response against dose-death time relationships. *Food and Chemical Toxicology*, 46(8), 2639-2647.
- Riss, T., & Moravec, R. A. (2004). Use of multiple assay endpoints to investigate the effects of incubation time, dose of toxin, and plating density in cell-based cytotoxicity ASSAY and Drug Development Technologies, 2, 51-62.
- Roberts, D., Davies, C., Mitchell, A., Moore, H., Picton, B., Portig, A. *et al.* (2004). Strangford Lough Ecological Change Investigation (SLECI). *Report to Environment and Heritage Service by the Queen's University, Belfast* Available online at: <http://www.ni-environment.gov.uk/print/0execsum.pdf>.
- Roth, P. B., Twiner, M. J., Wang, Z., Bottein Dechraoui, M.-Y., & Doucette, G. J. (2007). Fate and distribution of brevetoxin (PbTx) following lysis of *Karenia brevis* by algicidal bacteria, including analysis of open A-ring derivatives. *Toxicon*, 50(8), 1175-1191.

- Rzepa, H. S. (1995). Applications of  $^{13}\text{C}$  NMR., from [http://www.ch.ic.ac.uk/local/organic/nmr\\_13C.html](http://www.ch.ic.ac.uk/local/organic/nmr_13C.html)
- Satake, M., Bourdelais, A. J., Van Wagoner, R. M., Baden, D. G., & Wright, J. L. C. (2008). Brevisamide: An unprecedented monocyclic ether alkaloid from the dinoflagellate *Karenia brevis* that provides a potential model for ladder-frame initiation. *Organic Letters*, 10(16), 3465-3468.
- Satake, M., Campbell, A., Van Wagoner, R. M., Bourdelais, A. J., Jacocks, H., Baden, D. G. *et al.* (2009). Brevisin: An aberrant polycyclic ether structure from the dinoflagellate *Karenia brevis* and its implications for polyether assembly. *The Journal of Organic Chemistry*, 74(3), 989-994.
- Satake, M., Ishida, S., Yasumoto, T., Murata, M., Utsumi, H., & Hinomoto, T. (1995). Structural confirmation of maitotoxin based on complete  $^{13}\text{C}$  NMR assignments and the three-dimensional PFG NOESY-HMQC Spectrum. *Journal of the American Chemical Society*, 117(26), 7019-7020.
- Satake, M., Shoji, M., Oshima, Y., Naoki, H., Fujita, T., & Yasumoto, T. (2002). Gymnocin-A, a cytotoxic polyether from the notorious red tide dinoflagellate, *Gymnodinium mikimotoi*. *Tetrahedron Letters*, 43(33), 5829-5832.
- Satake, M., Tanaka, Y., Ishikura, Y., Oshima, Y., Naoki, H., & Yasumoto, T. (2005). Gymnocin-B with the largest contiguous polyether rings from the red tide dinoflagellate, *Karenia* (formerly *Gymnodinium*) *mikimotoi*. *Tetrahedron Letters*, 46(20), 3537-3540.
- Seki, T., Satake, M., Mackenzie, L., Kaspar, H. F., & Yasumoto, T. (1995). Gymnodimine, a new marine toxin of unprecedented structure isolated from New Zealand oysters and the dinoflagellate, *Gymnodinium* sp. *Tetrahedron Letters*, 36(39), 7093-7096.
- Seki, T., Satake, M., MacKenzie, L., Kaspar, H. F., & Yasumoto, T. (1996). Gymnodimine, a novel toxic imine isolated from the Foveaux Strait oysters and *Gymnodinium* sp. In Yasumoto, T. *et al.* (Eds.), *Harmful and Toxic Algal Blooms*. (pp. 495-498). Paris: Intergovernmental Oceanographic Commission of UNESCO.
- Selwood, A. I., Miles, C. O., Wilkins, A. L., Van Ginkel, R., Munday, R., Rise, F. *et al.* (2010). Isolation, structural determination, and acute toxicity of novel pinnatoxins E, F and G. *Journal of Agricultural and Food Chemistry*, 58(10), 6532-6542.
- Selwood, A. I., van Ginkel, R., Wilkins, A. L., Munday, R., Ramsdell, J. S., Jensen, D. J. *et al.* (2008). Semisynthesis of S-desoxybrevetoxin-B2 and brevetoxin-B2, and assessment of their acute toxicities. *Chemical Research in Toxicology*, 21(4), 944-950.
- Shanks, J. V. (2001). *In situ* NMR systems. *Current Issues in Molecular Biology*, 3(1), 15-26.
- Sheets, R. (2000). *History and characterization of the Vero Cell Line* (No. 5695): USPHS.
- Shi, F., McNabb, P., Rhodes, L., Holland, P., Webb, S., Adamson, J. *et al.* (2012). The toxic effects of three dinoflagellate species from the genus *Karenia* on invertebrate larvae and finfish. *New Zealand Journal of Marine and Freshwater Research, Publication online*.
- Shimizu, Y. (1993). Microalgal Metabolites. *Chemical Reviews*, 93, 1685-1698.
- Shimizu, Y. (2003). Microalgal metabolites. *Current Opinion in Microbiology*, 6(3), 236-243.
- Shimizu, Y., Chou, H. N., Bando, H., Van Duyne, G., & Clardy, J. (1986). Structure of brevetoxin A (GB-1 toxin), the most potent toxin in the Florida red tide organism *Gymnodinium breve* (*Ptychodiscus brevis*). *Journal of the American Chemical Society*, 108(3), 514-515.
- Shimojo, R. Y., & Iwaoka, W. T. (2000). A rapid hemolysis assay for the detection of sodium channel-specific marine toxins. *Toxicology*, 154(1-3), 1-7.
- Silke, J., O'Beirn, F., & Cronin, M. (2005). *Karenia mikimotoi: an exceptional dinoflagellate bloom in western Irish waters, summer 2005*. Galway: Marine Institute of Ireland.

- Slee, E. A., Adrain, C., & Martin, S. J. (2001). Executioner caspase-3, -6, and -7 perform distinct, non-redundant roles during the demolition phase of apoptosis. *Journal of Biological Chemistry*, 276(10), 7320-7326.
- Smith, K. F., Rhodes, L. L., Marfell, M. J., Zeewoldt, C. M., De Salas, M. F., Haywood, A. J. *et al.* (2007). Massive *Karenia mikimotoi* bloom in Northland, New Zealand: Use of traditional and molecular techniques for rapid identification of HAB species. *Harmful Algae News*, 1-3.
- Smith, P., Chang, F. H., & Mackenzie, L. (1993). *Toxic phytoplankton and algal blooms, summer 1992/93*. Paper presented at the Marine toxins and New Zealand shellfish, proceedings of a workshop on research issues, 10-11 June 1993.
- Sobel, J., & Painter, J. (2005). Illnesses caused by marine toxins. *Clinical Infectious Diseases*, 41(9), 1290-1296.
- Sola, F., Masoni, A., Fossat, B., Porthé-Nibelle, J., Gentien, P., & Bodennec, G. (1999). Toxicity of fatty acid 18:5n3 from *Gymnodinium cf. mikimotoi*: I. morphological and biochemical aspects on *Dicentrarchus labrax* gills and intestine. *Journal of Applied Toxicology*, 19(4), 279-284.
- Sournia, A., Chrdtiennot-Dinet, M. J., & Ricard, M. (1991). Marine phytoplankton: how many species in the world ocean? *Journal of Plankton Research*, 13(5), 1093-1099.
- Stirling, D. J. (2001). Survey of historical New Zealand shellfish samples for accumulation of gymnodimine. *New Zealand Journal of Marine and Freshwater Research*, 35, 851-857.
- Stivala, C. E., & Zakarian, A. (2009). Studies toward the synthesis of spirolides: assembly of the elaborated E-ring fragment. *Organic letters*, 11(4), 839-842.
- Suárez Korsnes, M., & Espenes, A. (2011). Yessotoxin as an apoptotic inducer. *Toxicon*, 57(7-8), 947-958.
- Suzuki, T., Beuzenberg, V., Mackenzie, L., & Quilliam, M. A. (2004). Discovery of okadaic acid esters in the toxic dinoflagellate *Dinophysis acuta* from New Zealand using liquid chromatography tandem mass spectrometry. *Rapid Communications in Mass Spectrometry*, 18(10), 1131-1138.
- Suzuki, T., Jin, T., Shiota, Y., Mitsuya, T., Okumura, Y., & Kamiyama, T. (2005). Quantification of lipophilic toxins associated with diarrhetic shellfish poisoning in Japanese bivalves by liquid chromatography-mass spectrometry and comparison with mouse bioassay. *Fisheries Science*, 71(6), 1370-1378.
- Tachibana, K., Scheuer, P. J., Tsukitani, Y., Kikuchi, H., Van Engen, D., Clardy, J. *et al.* (1981). Okadaic acid, a cytotoxic polyether from two marine sponges of the genus *Halichondria*. *Journal of the American Chemical Society*, 103(9), 2469-2471.
- Tang, E. P. Y. (1996). Why do dinoflagellates have lower growth rates? *Journal of Phycology*, 32(1), 80-84.
- Tatters, A., Muhlstein, H., & Tomas, C. (2009). The hemolytic activity of *Karenia selliformis* and two clones of *Karenia brevis* throughout a growth cycle. *Journal of Applied Phycology*, 22(4), 435-442.
- Terao, K., Ito, E., Igarashi, T., Aritake, S., Seki, T., Satake, M. *et al.* (1996). Effects of prymnesin, maitotoxin and gymnodimine on the structure of gills of small fish akahire, *Tanichthys albonubes* Lin. In Yasumoto, T. *et al.* (Eds.), *Harmful and Toxic Algal Blooms*. (pp. 479-481). Paris: Intergovernmental Oceanographic Commission of UNESCO.
- Tillmann, U., Elbrachter, M., Krock, B., John, U., & Cembella, A. (2009). *Azadinium spinosum* gen. et sp. nov. (Dinophyceae) identified as a primary producer of azaspiracid toxins. *European Journal of Phycology*, 44(1), 63-79.
- Toyofuku, H. (2006). Joint FAO/WHO/IOC activities to provide scientific advice on marine biotoxins (research report). *Marine Pollution Bulletin*, 52(12), 1735-1745.

- Trevino, C. L., Escobar, L., Vaca, L., Morales-Tlalpan, V., Ocampo, A. Y., & Darson, A. (2008). Maitotoxin: a unique pharmacological tool for elucidating  $\text{Ca}^{2+}$ -dependent mechanisms. In Botana, L. M. (Ed.), *Seafood and Freshwater Toxins: Pharmacology, Physiology and Detection*. (2nd ed.). Boca Raton: CRC Press.
- Truman, P. (2007). A cellular target for the lipophilic toxins from *Karenia brevisulcata*. *Toxicon*, 50(2), 251-255.
- Truman, P., Keyzers, R. A., Northcote, P. T., Ambrose, V., Redshaw, N. A., & Chang, H. F. (2005). Lipophilic toxicity from the marine dinoflagellate *Karenia brevisulcata*: use of the brevetoxin neuroblastoma assay to assess toxin presence and concentration. *Toxicon*, 46(4), 441-445.
- Truman, P., Stirling, D. J., Northcote, P. T., Lake, R. J., Seamer, C., & Hannah, D. J. (2002). Determination of brevetoxins in shellfish by the neuroblastoma assay. *Journal of AOAC International*, 85(5), 1057-1063.
- Tsujimoto, T., Ishihara, J., Horie, M., & Murai, A. (2002). Asymmetric construction of the azaspiro [5.5] undec-8-ene system towards gymnodimine synthesis. *Synlett*, 2002(3), 399-402.
- Tubaro, A., Dell'Ovo, V., Sosa, S., & Florio, C. (2010). Yessotoxins: A toxicological overview. *Toxicon*, 56(2), 163-172.
- Tubaro, A., Florio, C., Luxich, E., & Vertua, R. (1996). Suitability of the MTT-based cytotoxicity assay to detect okadaic acid contamination of mussels. *Toxicon*, 34(9), 965-974.
- Turrell, E. A., & Stobo, L. (2007). A comparison of the mouse bioassay with liquid chromatography-mass spectrometry for the detection of lipophilic toxins in shellfish from Scottish waters. *Toxicon*, 50(3), 442-447.
- Twiner, M. J., Dechraoui, M. Y. B., Wang, Z. H., Mikulski, C. M., Henry, M. S., Pierce, R. H. *et al.* (2007). Extraction and analysis of lipophilic brevetoxins from the red tide dinoflagellate *Karenia brevis*. *Analytical Biochemistry*, 369(1), 128-135.
- Twiner, M. J., Hess, P., Dechraoui, M. Y. B., McMahon, T., Samons, M. S., Satake, M. *et al.* (2005). Cytotoxic and cytoskeletal effects of azaspiracid-1 on mammalian cell lines. *Toxicon*, 45(7), 891-900.
- Ulrich, R. M., Casper, E. T., Campbell, L., Richardson, B., Heil, C. A., & Paul, J. H. (2010). Detection and quantification of *Karenia mikimotoi* using real-time nucleic acid sequence-based amplification with internal control RNA (IC-NASBA). *Harmful Algae*, 9(1), 116-122.
- Vale, C., & Botana, L. M. (2008). Marine toxins and the cytoskeleton: okadaic acid and dinophysistoxins. *FEBS Journal*, 275(24), 6060-6066.
- van Dolah, F. M. (2000). Marine algal toxins: Origins, health effects, and their increased occurrence. *Environmental Health Perspectives*, 108(Supplement 1), 133-141.
- van Engeland, M., Nieland, L. J. W., Ramaekers, F. C. S., Schutte, B., & Reutelingsperger, C. P. M. (1998). Annexin V-affinity assay: A review on an apoptosis detection system based on phosphatidylserine exposure. *Cytometry*, 31(1), 1-9.
- Walsh, J. G., Cullen, S. P., Sheridan, C., Lüthi, A. U., Gerner, C., & Martin, S. J. (2008). Executioner caspase-3 and caspase-7 are functionally distinct proteases. *Proceedings of the National Academy of Sciences*, 105(35), 12815-12819.
- Wang, D. Z. (2008). Neurotoxins from marine dinoflagellates: A brief review. *Marine Drugs*, 6(2), 349.
- Wang, Z. H., Plakas, S. M., El Said, K. R., Jester, E. L. E., Granade, H. R., & Dickey, R. W. (2004). LC/MS analysis of brevetoxin metabolites in the Eastern oyster (*Crassostrea virginica*). *Toxicon*, 43(4), 455-465.
- Waters (2005). *Waters Micromass Quattro Premier XE Mass Spectrometer: Operator's Guide*. Milford: Waters Corporation.

- Waters (2009). *Beginners guide to UPLC: Ultra-performance liquid chromatography*. Milford, MA: Waters Corporation.
- Waters, A. L., Hill, R. T., Place, A. R., & Hamann, M. T. (2010). The expanding role of marine microbes in pharmaceutical development. *Current Opinion in Biotechnology*, 21(6), 780-786.
- Waud, W. R. (2004). Murine L1210 and P388 leukemias. In Teicher, B. A. & P. A. Andrews (Eds.), *Anticancer drug development guide: Preclinical screening, clinical trials and approval* (Second ed.). Totowa, New Jersey: Humana Press Inc.
- Wear, R. G., & Gardner, J. P. A. (2001). Biological effects of the toxic algal bloom of February and March 1998 on the benthos of Wellington Harbour, New Zealand. *Marine Ecology Progress Series*, 218, 63-76.
- Xi, D., Van Dolah, F., & Ramsdell, J. (1992). Maitotoxin induces a calcium-dependent membrane depolarization in GH4C1 pituitary cells via activation of type L voltage-dependent calcium channels. *Journal of Biological Chemistry*, 267(35), 25025-25031.
- Xia, M., Huang, R., Witt, K. L., Southall, N., Fostel, J., Cho, M. H. *et al.* (2008). Compound cytotoxicity profiling using quantitative high-throughput screening. *Environmental Health Perspectives*, 116(3), 284-291.
- Yamasaki, Y., Kim, D., Matsuyama, Y., Oda, T., & Honjo, T. (2004). Production of superoxide anion and hydrogen peroxide by the red tide dinoflagellate *Karenia mikimotoi*. *Journal of Bioscience and Bioengineering*, 97(3), 212-215.
- Yang, C. Z., Albright, L. J., & Yousif, A. N. (1995). Oxygen-radical-mediated effects of the toxic phytoplankter *Heterosigma carterae* on Juvenile rainbow trout *Oncorhynchus mykiss*. *Disease of Aquatic Organisms*, 23, 101-108.
- Yasumoto, T., Oshima, Y., & Yamaguchi, M. (1978). Occurrence of a new type of shellfish poisoning in the Tohoku District. *Bulletin of the Japanese Society of Scientific Fisheries*, 44(11), 1249-1255.
- Yasumoto, T., & Satake, M. (1998). Bioactive compounds from marine microalgae. *Chimia*, 52(1-2), 63-68.
- Yasumoto, T., Undersal, B., Aune, T., Hormazabal, V., Skulberg, O. M., & Oshima, Y. (1990). Screening for hemolytic and ichthyotoxic components of *Chrysochromulina polylepis* and *Gyodinium aureolum* from Norwegian coastal waters. In Gran ėi, E. *et al.* (Eds.), *Toxic marine phytoplankton* (pp. 436-440). New York: Elsevier.
- Yue, T. L., Wang, C., Romanic, A. M., Kikly, K., Keller, P., DeWolf Jr, W. E. *et al.* (1998). Staurosporine-induced apoptosis in cardiomyocytes: A potential role of caspase-3. *Journal of Molecular and Cellular Cardiology*, 30(3), 495-507.
- Zhang, X. D., Gillespie, S. K., & Hersey, P. (2004). Staurosporine induces apoptosis of melanoma by both caspase-dependent and -independent apoptotic pathways. *Molecular Cancer Therapeutics*, 3(2), 187-197.
- Zou, Y., Yamasaki, Y., Matsuyama, Y., Yamaguchi, K., Honjo, T., & Oda, T. (2010). Possible involvement of hemolytic activity in the contact-dependent lethal effects of the dinoflagellate *Karenia mikimotoi* on the rotifer *Brachionus plicatilis*. *Harmful Algae*, 9(4), 367-373.
- Zucker, R. M., Hunter, E. S., & Rogers, J. M. (2000). Confocal laser scanning microscopy of morphology and apoptosis in organogenesis-stage mouse embryos. *Methods in Molecular Biology*, 135, 191-202.